



Mario REGNERI, MSc

**Modeling and multi-objective optimal control of integrated
wastewater collection and treatment systems in rural areas
based on fuzzy decision-making**

DISSERTATION

zur Erlangung des akademischen Grades

Doktor der technischen Wissenschaften

eingereicht an der

Technischen Universität Graz

Betreuer

Univ.-Prof. Dr.-Ing. Dirk Muschalla

Institut für Siedlungswasserwirtschaft
und Landschaftswasserbau

Prof. Peter A. Vanrolleghem, PhD., ing.
Université Laval, Département de génie civil et de génie des eaux

EIDESSTATTLICHE ERKLÄRUNG

AFFIDAVIT

Ich erkläre an Eides statt, dass ich die vorliegende Arbeit selbstständig verfasst, andere als die angegebenen Quellen/Hilfsmittel nicht benutzt, und die den benutzten Quellen wörtlich und inhaltlich entnommenen Stellen als solche kenntlich gemacht habe. Das in TUGRAZonline hochgeladene Textdokument ist mit der vorliegenden Dissertation identisch.

I declare that I have authored this thesis independently, that I have not used other than the declared sources/resources, and that I have explicitly indicated all material which has been quoted either literally or by content from the sources used. The text document uploaded to TUGRAZonline is identical to the present doctoral dissertation.

30/11/2014

Datum / Date



Unterschrift / Signature

Acknowledgement

The present project is supported by the National Research Fund, Luxembourg.

This doctoral thesis was realized over the last five years at the Resource Centre for Environmental Technologies of the Public Research Centre Henri Tudor in Luxembourg in cooperation with the Section of Engineering Hydrology and Water Management at Technische Universität Darmstadt, the Department of Civil Engineering and Water Engineering at Université Laval, and the Institute of Urban Water Management and Landscape Water Engineering at Graz University. During this time I additionally spent some weeks at the Department of Environmental Engineering, Technical University of Denmark.

Above all I want to thank Professor Dirk Muschalla who welcomed me at his Institute after the retirement of Professor Manfred Ostrowski from the Section of Engineering Hydrology and Water Management at Technische Universität Darmstadt. I want to equally thank Professor Manfred Ostrowski and especially Professor Peter Vanrolleghem for their supervision and Professor Dirk Muschalla and Professor Peter Vanrolleghem for the assessment of this work which I highly appreciate.

My most profound thanks go to Kai Klepiszewski who motivated me to do this PhD and supervised my work at the Resource Centre for Environmental Technologies.

A big thank you also to my colleagues at the Resource Centre for Environmental Technologies, the director Paul Schosseler and especially the ReseauSure2 project team, namely Steffi, Manu, Georges, David, Silvia and Hassanya for their support and discussions. In addition I would like to thank all my colleagues at the collaborating institutes.

Thanks to the staff of the Syndicat Intercommunal de Dépollution des Eaux résiduaires du Nord (SIDEN) for their great support during measurement campaigns and for providing the data for the case study catchment.

Special thanks to all my friends especially to the ones I lost sight of during finishing this work. You know who you are.

My work would not have been possible without the support and love of my family. Sincere thanks to you. This work is dedicated to you.

“The closer one looks at a real-world problem, the fuzzier becomes the solution.”

Zadeh, 1973

Abstract

Historically, sewer networks and wastewater treatment plants are designed and operated separately. Integrated control of urban wastewater collection and treatment systems is in the focus of research since the 1990s. Despite numerous scientific publications and some reports of implementations in practice showing increased system performance thanks to integrated control, the majority of operators are still cautious when it comes to the implementation of complex control approaches. The main cause for the missing acceptance among operators thereby is the fear of losing the ultimate control decision, especially when it comes to compromise multiple conflicting objectives. At the same time, especially in the case of small rural wastewater collection and treatment systems, treatment capacities often remain unused due to the lack of staff able to optimally adapt the operation to the current situation.

Due to this situation, the present thesis investigates the implementation of decision-making in system-wide control of integrated wastewater collection and treatment systems with a focus on rural catchments. Model predictive control is chosen to systematically investigate dynamics in the control of integrated rural systems. Fuzzy decision-making is used to compromise multiple conflicting objectives in system-wide control of integrated systems with a focus on specific goals and constraints of rural systems. The wastewater treatment plant capacity is determined simulation-based according to the predicted loading. For this purpose a Lagrangian model for time-dependent wastewater treatment plant load prediction had to be developed. A case study situated in Luxembourg is used to test the developed approach according to local rainfall time series and corresponding pollution loads. The reference model for simulation-based evaluation of the developed approach is calibrated according to the results of system-wide measurement campaigns. A phenomenological-deterministic reference model is proposed to consider the local variability of runoff from rainfall. Simulation results are compared to reference scenarios based on separated control of the sewer network and the wastewater treatment plant.

The simulation results of system-wide fuzzy predictive control of integrated rural systems during rain events show conflicting objectives predominantly according to stable wastewater treatment plant loading and combined sewer overflow reduction. At the wastewater treatment plant conflicting objectives predominantly consist of the wastewater treatment plant loading, total solids secondary settlement tank effluent concentrations and the optimization of the aeration according to efficient combined wet weather flow treatment and increased nitrification for simultaneous aerobic sludge stabilization. The comparison to the performance of the reference scenarios reveals potentials to reduce combined sewer overflow volumes and loads and increased aeration efficiencies according to the balance of multiple objectives.

Additionally, the developed tool for fuzzy predictive system-wide control adds transparency by visualizing the decision-making according to the chosen objectives of the operator.

Kurzfassung

Historisch betrachtet, werden Kanalnetze und Kläranlagen als separate System entworfen und betrieben. Die integrierte Steuerung urbaner Abwassersammel- und -behandlungssysteme befindet sich im Fokus der Forschung seit den 1990er Jahren. Trotz zahlreicher wissenschaftlicher Publikationen und einiger Berichte von Implementierungen in der Praxis, die erhöhte Systemleistungen durch integrierte Regelung belegen, sind die meisten Betreiber immer noch zurückhaltend, wenn es um die Implementierung komplexer Regelungsansätze geht. Die Hauptursache für die fehlende Akzeptanz unter Betreibern dabei ist die Befürchtung vor dem Verlust genereller Kontrollentscheidungen, insbesondere, wenn es um die Kompromissbildung mehrerer Zielkonflikte geht. Gleichzeitig, vor allem im Falle kleiner ländlicher Abwassersammel- und -behandlungssysteme, bleiben Behandlungskapazitäten oft ungenutzt aufgrund unzureichender Personalkapazitäten, um den Betrieb optimal an die aktuelle Situation anzupassen.

Aufgrund dieser Situation untersucht die vorliegende Arbeit die Anwendung der Entscheidungsfindung in der systemweiten Regelung integrierter Abwassersammel- und -behandlungssysteme mit dem Schwerpunkt ländlicher Einzugsgebiete. Dabei wird die modellprädiktive Regelung gewählt, um die Dynamik bei der Kontrolle integrierter ländlicher Systeme systematisch zu untersuchen. Fuzzy-Entscheidungsfindung wird für die Kompromissbildung mehrerer Zielkonflikte in der systemübergreifenden Regelung integrierter Systeme mit dem Fokus spezifischer Ziele und Randbedingungen ländlicher Systeme verwendet. Die Kläranlagenkapazität wird aufgrund von Frachtprädiktionen simulationsbasiert bestimmt. Dazu musste ein Lagrange-Modell zur zeitabhängigen Kläranlagenfrachtprädiktion entwickelt werden. Entwicklung und Test dieses Ansatzes erfolgt anhand einer luxemburgischen Fallstudie unter Verwendung örtlicher Niederschlagszeitreihen und entsprechender Schmutzfrachten. Die Kalibrierung des Referenzmodells für die simulationsbasierte Bewertung des entwickelten Ansatzes basiert auf Ergebnissen systemübergreifender Messkampagnen. Zur Berücksichtigung systemweiter Niederschlags-Abflussdynamiken wird ein phänomenologisch-deterministisches Referenzmodell vorgeschlagen. Die Simulationsergebnisse werden mit Referenzszenarien basierend auf separaten Regelungskonzepten für Kanalnetz und Kläranlage verglichen.

Die Simulationsergebnisse der systemweiten Fuzzy-prädiktiven Regelung integrierter ländlicher Systeme während Mischwassereignissen verdeutlichen Regelungskonflikte insbesondere zwischen der stabilen Beschickung der Kläranlage und der Reduzierung von Mischwasserentlastungen. Zielkonflikte auf der Kläranlage im Mischwasserbetrieb ergeben sich überwiegend aus der Kläranlagenbeschickung, zulässiger Ablaufkonzentrationen abfiltrierbarer Stoffe und der Optimierung der Belüftung bezüglich einer effizienten Schmutzfrachteliminierung und den Anforderungen an die erhöhte Nitrifikation für die simultan-aerobe Schlammstabilisierung. Der Leistungsvergleich mit Referenzszenarien zeigt potentielle Reduzierungen von Mischwasserentlastungsvolumen und -frachten sowie erhöhte Belüftungseffizienzen unter Berücksichtigung mehrerer Zielkonflikte.

Zusätzlich erhöht das entwickelte Werkzeug für die Fuzzy-prädiktive systemweite Regelung die Transparenz durch die Illustration der Entscheidungsfindung entsprechend den Zielvorgaben des Betreibers.

Contents

1. Introduction	22
1.1. Challenge	23
1.2. Aims, scope and hypothesis	26
1.3. Methodology	27
1.4. Structure	28
2. Integrated modeling of wastewater collection and centralized treatment systems with extended aeration in rural areas	30
2.1. Wastewater collection and centralized treatment systems in rural areas.....	30
2.2. Integrated modeling of wastewater collection and treatment systems	31
2.2.1. Hydraulic modeling	32
2.2.2. Pollutant flow modeling	34
2.3. Pollutant flows in wastewater collection and treatment systems in rural areas	38
3. System-wide control of centralized wastewater treatment systems	40
3.1. System-wide control.....	40
3.2. Control-related key terms.....	41
3.3. Sensors and actuators	43
3.3.1. Sensors	43
3.3.2. Actuators	43
3.4. Real-time control.....	44
3.4.1. Reactive real-time control	44
3.4.2. Predictive real-time control.....	45
4. Fuzzy multi-criteria decision-making.....	52
4.1. Decision making	52
4.1.1. A priori	53
4.1.2. A posteriori	54
4.1.3. Optimization problem	54
4.1.4. Satisficing	54
4.2. Fuzzy set theory	55
4.3. Decision-making with fuzzy objectives and fuzzy constraints	56
4.3.1. Membership functions.....	57
4.3.2. Aggregation	58
4.3.3. Weighting.....	60

5.	Development of a multi-objective fuzzy predictive controller for system-wide control of integrated wastewater collection and treatment systems in rural regions	61
5.1.	Fuzzy predictive control	61
5.2.	Process models	63
5.2.1.	Retention tanks with CSO structures	64
5.2.2.	WWTP	66
5.2.3.	Development of a discrete Lagrangian ISN observer model.....	66
5.2.4.	Power consumption	72
5.3.	Defining the fuzzy multi-criteria decision-making model	72
5.3.1.	Sewer networks	73
5.3.2.	Wastewater treatment plant	74
5.3.3.	System-wide control.....	75
5.4.	Hybrid fuzzy predictive control for plant-wide control.....	75
5.5.	Optimization.....	75
5.5.1.	Optimization of fuzzy objective functions.....	75
5.5.2.	Pattern search	76
6.	Wastewater pollutant flows and modeling in rural WCTSS.....	79
6.1.	Case study Haute-Sûre.....	81
6.1.1.	Sewer network	81
6.1.2.	Wastewater treatment plant Heiderscheidergrund	86
6.1.3.	Receiving waters	86
6.2.	Wastewater pollutant flows in rural WCTSS.....	87
6.2.1.	Monitoring and measurement campaigns	88
6.2.2.	Analysis	92
6.2.3.	Fractionation of COD and TKN	115
6.3.	Deterministic - phenomenological reference model.....	124
6.3.1.	Rainfall homogeneity evaluation	125
6.3.2.	Rainfall-runoff homogeneity evaluation	127
6.3.3.	Model description.....	135
6.3.4.	Model calibration.....	136
6.3.5.	Disturbance modeling	148
7.	Simulation-based evaluation of the integrated fuzzy predictive control approach	150
7.1.	Objectives of the integrated control.....	151
7.1.1.	Sewer network	152
7.1.2.	WWTP	153

7.2.	Controller	156
7.2.1.	Membership functions.....	156
7.2.2.	Fuzzy aggregation	159
7.2.3.	Horizons	159
7.3.	Performance analysis and discussion	161
7.3.1.	Choice of simulation periods.....	161
7.3.2.	Hydraulic calibration of the sewer network reference model.....	165
7.3.3.	Phenomenological rainfall runoff distribution model	168
7.3.4.	Exemplary analysis of event #1 of the rainfall time series of June 2012.....	170
7.3.5.	Summary of results August 2011	185
7.3.6.	Summary of results June 2012	193
8.	Comparison to static control scenarios and discussion of results	200
8.1.	Reference scenarios	201
8.2.	Performance analysis	202
8.2.1.	Integrated combined wastewater balance	202
8.2.2.	Combined sewer network.....	206
8.2.3.	Wastewater treatment plant	211
8.2.4.	Integrated system	223
9.	Conclusions and outlook	225
9.1.	Conclusions	225
9.2.	Outlook	226
10.	References.....	228

List of figures

Figure 3-1: Real-time control approach with feed-forward and feed-back control loop based on disturbance and process measurements (taken from Schütze et al. (2004), modified).....	44
Figure 3-2: Basic control loop	45
Figure 3-3: Model predictive control according to the RHOC approach.....	47
Figure 3-4: Time horizons in MPC and their relative sizes (according to Wolfgang Rauch and Harremoës (1999), modified).....	48
Figure 3-5: Supervisory MPC with online set-point optimization for PI/PID control (according to (Ostace et al. 2010), modified)	48
Figure 4-1: Common types of MFs (A) triangular, (B) trapezoidal, (C) Gaussian, (D) Z-type, (E) S-type	59
Figure 5-1: Conceptual illustration of FDM and its closed-loop implementation for FPC ...	62
Figure 5-2: Parameters in system-wide control of integrated WCTSs (Q_i = discharges, C_i = pollutant concentrations, RTs = retention tanks, RWs = receiving waters)	64
Figure 5-3: Simple ISN with a central WWTP. Nodes A, C and E are sub-catchments with retention tanks and CSO structures. Nodes B and D are conjunctions of different branches in the ISN.	71
Figure 5-4: Simple branch in an ISN where retention tank A describes an input and WWTP the output of a process model	71
Figure 5-5: Temporal tracking of discrete wastewater discharges from retention tanks to the WWTP according to a multiple of the constant control step size H_c	71
Figure 6-1: Haute-Sûre integrated WCTS for the final state (black border) and the state 2010 (red border and background).....	82
Figure 6-2: Specific retention tank volumes built in the catchment state 2010	85
Figure 6-3: Specific retention volume designed for the final state	85
Figure 6-4: Process diagram of one treatment lane of WWTP Heiderscheidergrund without tertiary treatment	86
Figure 6-5: Allocation of rain gauges operated by ASTA according to the Thiessen method. Background colors show the assignment (rain gauge Arsdorf: orange, rain gauge Eschdorf: green, rain gauge Esch/Sauer: purple, rain gauge Dahl: yellow)	89
Figure 6-6: 21 days moving minimum method for DWF analysis of the inflow at WWTP Heiderscheidergrund in the period of January 2012 to December 2012	93
Figure 6-7: 21 days moving minimum method for DWF analysis of the effluent at retention tank Dahl with pumping station in the period of January 2012 to December 2012.....	93
Figure 6-8: Boxplot evaluation of DWF per capita per day based on the 21 days moving minimum analysis for the period January 2010 to December 2012 at retention tanks with pumping station (DAH (black), NOC (red) and NOR (green)) and WWTP Heiderscheidergrund (blue).....	94

Figure 6-9: Variability of daily DWF hydrographs measured at (A) catchments and (B) the WWTP inlet	94
Figure 6-10: Daily mean DWF evaluation of TSS, conductivity, COD and BOD ₅ concentrations at retention tanks KAU and NOR	95
Figure 6-11: Daily mean DWF evaluation of TN, NH ₄ -N, NO _x -N and TKN concentrations at retention tanks KAU and NOR	96
Figure 6-12: Daily mean DWF evaluation of TP and PO ₄ -P concentrations at retention tanks KAU and NOR.....	96
Figure 6-13: Variability of the monitored COD DWF pollutographs for retention tanks (A) Kaundorf (gravity discharge to the WWTP) and (B) Nocher-Route (pumped discharge to the WWTP) according to mean concentrations and standard deviations	97
Figure 6-14: Daily mean DWF evaluation of TSS, COD and BOD ₅ concentrations at WWTP Heiderscheidergrund	98
Figure 6-15: Daily mean DWF evaluation of TN, NH ₄ -N, NO _x -N and TKN concentrations at WWTP Heiderscheidergrund	99
Figure 6-16: Daily mean DWF evaluation of PO ₄ -P concentrations at WWTP Heiderscheidergrund	99
Figure 6-17: Comparison of average DWF concentrations between catchment effluent and WWTP influent.....	101
Figure 6-18: System-wide volume balance between the sum of aggregated retention tank discharges to the WWTP (light blue line) and the aggregated inflow to the WWTP Heiderscheidergrund (dark blue line) for the year 2012	102
Figure 6-19: Double mass analysis of the system-wide volume balance for RDII estimation in the ISN for the year 2012.....	102
Figure 6-20: First flush analysis according to pollutant mass distribution versus volume (A = COD, B = BOD ₅ , C = S _{COD} , D = X _{COD} and E = TSS)	108
Figure 6-21: First flush analysis according to pollutant mass distribution versus volume (A = TKN, B = NH ₄ -N, C = NO _x -N, D = TP and E = PO ₄ -P)	109
Figure 6-22: First flush analysis according to mass first flush ratio (A = COD, B = BOD ₅ , C = S _{COD} , D = X _{COD} and E = TSS)	111
Figure 6-23: First flush analysis according to mass first flush ratio (A = TKN, B = NH ₄ -N, C = NO _x -N, D = TP and E = PO ₄ -P).....	112
Figure 6-24: Analysis of mean rainfall-runoff pollution contributions to CWWF loads.....	113
Figure 6-25: Inlet WWTP Heiderscheidergrund mean CWWF concentrations for TSS, COD and BOD ₅ from self-supervision	114
Figure 6-26: Inlet WWTP Heiderscheidergrund mean CWWF concentrations for TN, NH ₄ -N and NO _x -N from self-supervision	115
Figure 6-27: Comparison of wastewater fractionation results according to measurements from (A) the retention tank effluent and (B) the WWTP inlet .	121
Figure 6-28: Double sum analysis for pairwise spatial rainfall distribution analysis from 4 rain gauges in 2010	126
Figure 6-29: Double sum analysis for pairwise spatial rainfall distribution analysis from 4 rain gauges in 2011	126
Figure 6-30: Double sum analysis for pairwise spatial rainfall distribution analysis from 4 rain gauges in 2012	127

Figure 6-31: Principally retention tank water level oscillation during CSO ((Brombach et al. 1999), modified).....	128
Figure 6-32: Water level frequency analysis at retention tank Dahl for the evaluation of the critical water level causing CSO (dashed red line) based on continuous water level measurements in 2012 (A: frequency of water levels exceeding the critical water level, B: frequency of water levels equal to the critical water level, 1: total value range, 2: zoom).....	129
Figure 6-33: CSO illustration for the time series of measured water levels at the CSO weir (black line) and in the retention tank (grey line) at retention tank Dahl between July 2012 and January 2013 according to the critical water (dashed red line)	130
Figure 6-34: System-wide evaluation of RRCs according to measurement data in the period June 2010 to December 2012.....	131
Figure 6-35: System-wide evaluation of monthly RRC larger than one in the period from June 2010 to December 2012 state 2010	131
Figure 6-36: Time series of RRCs of the five catchments allocated to rainfall data from rain gauge Dahl	132
Figure 6-37: Time series of monthly mean RRCs related to rain gauge DAH (black dots) with standard deviation (red whiskers).	132
Figure 6-38: Mean monthly RRCs plotted against monthly precipitation depths for retention tanks allocated to rain gauge Dahl in the period June 2010 to December 2012	133
Figure 6-39: Comparison of aggregated monthly RRCs for sub-catchments allocated to rain gauge DAH for the period June to December considering the years (A) 2010, (B) 2011 and (C) 2012	134
Figure 6-40: Comparison of aggregated RRCs for sub-catchments allocated to rain gauge ESD (June 2011 to December 2012)	135
Figure 6-41: Comparison of aggregated RRCs for retention tanks DAH, KAU, ESD and HEI (June 2011 to December 2012)	135
Figure 6-42: Mean DWF hydrograph in the catchments.....	137
Figure 6-43: DWF pollutographs for COD and TKN.....	137
Figure 6-44: Results of the model calibration for accumulation and wash-off (A = KAU 12/07/2010, B = GOE 19/05/2011, C = GOE 31/05/2011, D = GOE 07/06/2011, E = GOE 22/06/2011; x.1 (left) showing COD, x.2 (right) showing TKN).....	140
Figure 6-45: DO-profile measurement setup.....	141
Figure 6-46: AST DO profile at WWTP Heiderscheidergrund 04/2011.....	142
Figure 6-47: WWTP effluent COD and TSS concentrations during DWF with continuous nitrification according to the average DWF pattern	143
Figure 6-48: WWTP effluent nitrogen concentrations during DWF with continuous nitrification according to the average DWF pattern	144
Figure 6-49: Hydraulic and pollutant peak loading during the CWWF campaign in 2010 ..	144
Figure 6-50: Effluent COD and TSS concentration calibration results during the CWWF campaign in 2010	144
Figure 6-51: Hydraulic loading during the DWF campaign in 2011	145

Figure 6-52: Effluent calibration results for the denitrification DWF campaign 2011.....	145
Figure 6-53: Correlation of $TSS_{measured} - TSS_{ASM1}$	146
Figure 6-54: Correlation of $COD_{measured} - TSS_{measured}$	146
Figure 6-55: Correlation of $BOD_{5,measured} - S_S + X_{S,ASM1}$	147
Figure 6-56: Correlation of $COD_{measured} - BOD_{5,measured}$	147
Figure 6-57: Correlation $NH_4-N_{measured} - S_{NH,ASM1}$	147
Figure 6-58: Correlation of $TKN_{measured} - NH_4-N_{measured}$	148
Figure 6-59: Evolution of tourism according to the monthly wastewater volume of camping site Bissen discharged to the WWTP in 2011	149
Figure 6-60 Wastewater temperature profile WWTP Heiderscheidergrund in the period 2010 to 2012	149
Figure 7-1: Control of discharges at retention tanks according to the WWTP reference load	153
Figure 7-2: Recommended aerated fraction of the activated sludge tank depending on the temperature (taken from DWA-A226 (DWA 2009), modified).....	155
Figure 7-3: Recommended activated sludge tank TS concentration depending on the temperature and the aerated part of the activated sludge tank (taken from ATV-A226 (DWA 2009), modified).....	156
Figure 7-4: Hybrid process model implementation	160
Figure 7-5: Correlation of monthly rainfall depth and corresponding mean antecedent DWF periods	162
Figure 7-6: Correlation of the monthly rainfall depth and the corresponding standard deviations (STD) of mean daily rainfall heights of rainfall data from rain gauges DAH,ESC, ESD and ARS	162
Figure 7-7: Correlation of monthly rainfall and monthly measured CWWF volume.....	163
Figure 7-8: Rainfall time series August 2011	163
Figure 7-9: Spatial variability of the rainfall time series August 2011 according to the double sum analysis	163
Figure 7-10: Rainfall time series June 2012.....	164
Figure 7-11: Spatial variability of the rainfall time series June 2012 according to the double sum analysis	164
Figure 7-12: Rainfall runoff model calibration results for the WWTP inlet hydrograph according to the rainfall time series of August 2011	167
Figure 7-13: Rainfall runoff model calibration results for the WWTP inlet hydrograph according to the rainfall time series of June 2012	168
Figure 7-14: Correlation analysis of CSO volumes (A) and loads (B) from system-wide FPC according to constant (RRCconst) and phenomenological (RRCphen) rainfall runoff distributions in June 2012.....	170
Figure 7-15: FDM results for the integrated WWTP capacity estimation and FPC during event #1 June 2012 (A) and statistical evaluation (B)	171
Figure 7-16: FDM results in the sewer network of CWWF event #1 of the rainfall time series of June 2012 (A) and statistical evaluation (B)	171
Figure 7-17: Lagrangian ISN observer model based hydrographs (A) and pollutographs (B through E) for CWWF event #1 of rainfall time series June 2012.	172

Figure 7-18: Comparison of WWTP influent prediction according to the WWTP capacity and WWTP loading according to sewer network FPC from reference model simulation for event #1 of the rainfall time series of June 2012.	174
Figure 7-19: Comparison of specific predicted WWTP AST parameters and corresponding reference simulation model parameters for event #1 of the rainfall time series of June 2012	175
Figure 7-20: Comparison of SST effluent predictions for WWTP capacity estimation and reference model simulation results for CWWF event #1 of the rainfall time series of June 2012.....	177
Figure 7-21: Comparison of the predicted hydraulic impact of CWWF event #1 of the rainfall time series of June 2012 on TSS concentrations in the SST and reference simulation model results from integrated FPC according the 1-dimensional model of Takács et al. (1991) (Layer 1 = top layer, layer 10 = bottom layer).	178
Figure 7-22: Linear correlation between MFs for hydraulic loading of the WWTP (MF6) and the SST effluent TSS concentration (MF1) for CWWF event #1 of the rainfall time series of June 2012.	179
Figure 7-23: Comparison of predicted and simulated SST effluent concentrations for CWWF event #1 of the rainfall time series of June 2012.....	179
Figure 7-24: WWTP multi-objective predictive hydraulic loading according to TKN influent load and SNHAST concentrations and corresponding DOAST set-point optimization for CWWF event #1 of the rainfall time series of June 2012	180
Figure 7-25: PLS-DA of MF results for DOAST set-point optimization (MF7) and effluent NH ₄ -N minimization (MF3), effluent TN minimization (MF4) and AST NH ₄ -N optimization (MF5) for CWWF event #1 of the rainfall time series of June 2012	181
Figure 7-26: FPC of retention tank #3 to minimize CSO during CWWF event #1 of the rainfall time series of June 2012	182
Figure 7-27: Comparison of the specific retention tank utilization of all retention tanks for different rainfall inputs according to the sewer network FPC approach for CWWF event #1 of the rainfall time series of June 2012	182
Figure 7-28: Correlation of MF results for total CSO volumes (MF1) and total COD CSO loads (MF2) and TKN CSO loads (MF3) for CWWF event #1 of the rainfall time series of June 2012	183
Figure 7-29: PLS-DA of MF results for ISN hydraulic homogenization (MF8 and MF9) and CSO volume minimization (MF1), retention tank use homogenization (MF5) resp. WWTP hydraulic loading homogenization (MF10) for CWWF event #1 of the rainfall time series of June 2012	184
Figure 7-30: PLS-DA of MF results for WWTP hydraulic loading (MF10) and WWTP COD loading (MF11) resp. WWTP TKN loading (MF12)) for CWWF event #1 of rainfall time series June 2012	184
Figure 7-31: FDM mean results and STDs of 5 CWWF events according to the rainfall time series of August 2011 for WWTP capacity estimation and control (A) and sewer network control (B)	185

Figure 7-32: Evaluation of MAPDs between model based WWTP capacity estimations and results from reference simulation based loading for the rainfall time series of August 2011 (A = WWTP loading, B = AST, C = SST effluent).....	187
Figure 7-33: Correlation of MF values for WWTP inflow and SST effluent TSS concentrations of 5 CWWF events according to the rainfall time series of August 2011	188
Figure 7-34: WWTP multi-objective predictive hydraulic loading according to TKN influent load and SNHAST concentrations and corresponding DOAST set-point optimization for 5 CWWF events according to the rainfall time series of August 2011	189
Figure 7-35: PLS-DA of MF results for DOAST set-point optimization (MF7) and effluent (A) NH ₄ -N minimization (MF3), (B) effluent TN minimization (MF4) and (C) AST NH ₄ -N optimization (MF5) for 5 CWWF events according to the rainfall time series of August 2011	190
Figure 7-36: Correlation of MF results for (A) total CSO volumes (MF1) and total COD CSO loads (MF2) and (B) TKN CSO loads (MF3) for 5 CWWF events according to the rainfall time series of August 2011	191
Figure 7-37: PLS-DA of MF results for ISN hydraulic homogenization (MF8 and MF9) and (A) CSO volume minimization (MF1), (B) retention tank use homogenization (MF5) and (C) WWTP hydraulic loading homogenization (MF10) for 5 CWWF events according to the rainfall time series of August 2011	192
Figure 7-38: PLS-DA of MF results for WWTP hydraulic loading (MF10) and (A) WWTP COD loading (MF11) and (B) WWTP TKN loading (MF12) for 5 CWWF events according to the rainfall time series of August 2011	193
Figure 7-39: FDM mean results and STDs of 11 CWWF events according to rainfall time series June 2012 for WWTP capacity estimation and control (A) and sewer network control (B).....	194
Figure 7-40: Evaluation of MAPDs between model based WWTP capacity estimations and results from reference simulation based loading for the rainfall time series of June 2012 (A = WWTP loading, B = AST, C = SST effluent	196
Figure 7-41: Correlation of MF values for WWTP inflow and SST effluent TSS concentrations of 11 CWWF events according to the rainfall time series of June 2012.....	196
Figure 7-42: WWTP multi-objective predictive hydraulic loading according to TKN influent load and SNHAST concentrations and corresponding DOAST set-point optimization for 11 CWWF events according to the rainfall time series of June 2012	197
Figure 7-43: PLS-DA of MF results for DOAST set-point optimization (MF7) and effluent NH ₄ -N minimization (MF3), effluent TN minimization (MF4) and AST NH ₄ -N optimization (MF5) for 11 CWWF events according to the rainfall time series of June 2012	197
Figure 7-44: Correlation of MF results for (A) total CSO volumes (MF1) and total COD CSO loads (MF2) and (B) TKN CSO loads (MF3) for 11 CWWF events according to the rainfall time series of June 2012	198

Figure 7-45: PLS-DA of MF results for ISN hydraulic homogenization (MF8 and MF9) and CSO volume minimization (MF1), retention tank use homogenization (MF5) and WWTP hydraulic loading homogenization (MF10) for 11 CWWF events according to the rainfall time series of June 2012	198
Figure 7-46: PLS-DA of MF results for WWTP hydraulic loading (MF10) and (A) WWTP COD loading (MF11) and (B) WWTP TKN loading (MF12) for 11 CWWF events according to the rainfall time series of June 2012.....	199
Figure 8-1: Event-specific (1) and total (2) ratios of CWWF treated at the WWTP and CSO for each scenario according to rainfall time series August 2011 (A: Volume, B: COD, C: TKN, D: NH ₄ -N).....	204
Figure 8-2: Event-specific (1) and total (2) ratios of CWWF treated at the WWTP and CSO for each scenario according to the rainfall time series of June 2012 (A: Volume, B: COD, C: TKN, D: NH ₄ -N)	206
Figure 8-3: Event-specific comparison of aggregated CSO volumes and event mean CSO concentrations for the rainfall time series of August 2011 (A: Vol, B: COD, D: TKN, E: NH ₄ -N)	208
Figure 8-4: Event-specific comparison of aggregated CSO volumes and event mean CSO concentrations for the rainfall time series of June 2012 (A: Vol, B: COD, D: TKN, E: NH ₄ -N)	208
Figure 8-5: Nonlinear regression between event-specific CSO volumes and CSO loads according to FPC	209
Figure 8-6: Nonlinear regression between event-specific CSO volumes and CSO loads according to reference scenarios (A) Ref1, (B) Ref2, (C) Ref3 and (D) Ref4.....	209
Figure 8-7: Event-specific scenario comparison of the WWTP CWWF performance according to the rainfall time series of August 2011 variant DO _{set,CWWF} = 0.7 g/m ³ (A = COD, B = NH ₄ -N, C = TN).....	213
Figure 8-8: Event-specific scenario comparison of the WWTP CWWF performance according to the rainfall time series of August 2011 variant S _{NHAST,CWWF} = 1.0 g/m ³ (A = COD, B = NH ₄ -N, C = TN).....	214
Figure 8-9: Event-specific scenario comparison of the WWTP CWWF performance according to the rainfall time series of June 2012 variant DO _{set,CWWF} = 0.7 g/m ³ (A = COD, B = NH ₄ -N, C = TN).....	215
Figure 8-10: Event-specific scenario comparison of the WWTP CWWF performance according to the rainfall time series of June 2012 variant S _{NHAST,CWWF} = 1.0 g/m ³ (A = COD, B = TN, C = NH ₄ -N).....	216
Figure 8-11: WWTP hydraulic capacity estimation according to rainfall time series (A) August 2011 and (B) June 2012 (1: correlation of S _{NHAST} , DO _{AST} and TSSEff, 2: frequency analysis).....	218
Figure 8-12: Comparison of WWTP aeration effort per wastewater load during CWWF events according to the rainfall time series of August 2011 (A: variant DO _{set,CWWF} = 0.7 g/m ³ , B: variant S _{NHAST,CWWF} = 1.0 g/m ³ ; 1: V _{Air} , 2: V _{air} /V _{Inf} , 3: V _{Air} /TKN _{Inf})	220
Figure 8-13: Correlations of aeration effort and TKN load during CWWF events according to rainfall time series August 2011 (A: variant DO _{set,CWWF} = 0.7 g/m ³ , B: variant S _{NHAST,CWWF} = 1.0 g/m ³).....	221

Figure 8-14: Comparison of WWTP aeration effort per wastewater load during CWWF events according to rainfall time series June 2012 (A: variant $DO_{set,CWWF} = 0.7 \text{ g/m}^3$, B: variant $S_{NHAST,CWWF} = 1.0 \text{ g/m}^3$; 1: V_{Air} , 2: V_{Air}/V_{Inf} , 3: V_{Air}/TKN_{Inf}) ..	221
Figure 8-15: Correlations of aeration effort and TKN load during CWWF events according to rainfall time series June 2012 (A: variant $DO_{set,CWWF} = 0.7 \text{ g/m}^3$, B: variant $S_{NHAST,CWWF} = 1.0 \text{ g/m}^3$) ..	222
Figure 8-16: System-wide performance comparison of TSS (A), COD (B) and BOD_5 (C) pollution loads from CSO and WWTP discharged to receiving waters according to rainfall time series August 2011 ..	223
Figure 8-17: System-wide performance comparison of nitrogen pollution loads from CSO and WWTP discharged to receiving waters according to rainfall time series August 2011 (A = TN, B = NH_4-N ; 1: $DO_{AST} = 0.7 \text{ g/m}^3$, 2: $S_{NHAST} = 1.0 \text{ g/m}^3$) ..	224
Figure 8-18: System-wide performance comparison of nitrogen pollution loads from CSO and WWTP discharged to receiving waters according to rainfall time series June 2012 (A = TN, B = NH_4-N ; 1: variant $DO_{AST} = 0.7 \text{ g/m}^3$, 2: variant $S_{NHAST} = 1.0 \text{ g/m}^3$) ..	224

List of tables

Table 2-1:	Definition of the level of integration for integrated urban water models (taken from (Bach et al. 2014), modified).....	31
Table 2-2:	Hydrologic and hydraulic processes in integrated models of WCTSS.....	32
Table 2-3:	Effects of sewage constituents on receiving waters	35
Table 2-4:	Daily mean DWF concentrations in rural catchments compared to urban concentrations	38
Table 4-1:	Common aggregation functions and their compensation effect.....	60
Table 6-1:	Abbreviations of catchments with combined sewer system.....	83
Table 6-2:	Catchment data state 2010.....	83
Table 6-3:	Catchment data final state	84
Table 6-4:	ISN data of the final state	85
Table 6-5:	Parameters monitored online at WWTP Heiderscheidergrund	90
Table 6-6:	Extent of the sewer network monitoring campaign.....	91
Table 6-7:	Mean DWF per capita per day resulting from 21 days moving minimum evaluations at retention tanks with pumping stations and at the WWTP for the period of January 2010 to December 2012	94
Table 6-8:	Evaluation of daily mean DWF concentrations for wastewater pollutants at retention tanks KAU and NOR and comparison to literature data on rural and urban systems	97
Table 6-9:	Evaluation of daily mean DWF pollution concentrations of the raw inflow at WWTP Heiderscheidergrund and comparison to the design assumptions	99
Table 6-10:	Mean DWF loading of WWTP Heiderscheidergrund, comparison of measurement data and design assumptions.....	100
Table 6-11:	Overview of monitored storm events and number of collected samples per event	103
Table 6-12:	Main hydraulic characteristics of the monitored storms and antecedent dry weather periods.....	103
Table 6-13:	Event mean concentrations measured at the effluent of retention tanks	104
Table 6-14:	Comparison of resulting event mean concentrations for combined wet weather flow to results from literature review and WWTP legal effluent limits	105
Table 6-15:	Nutrient event mean concentrations of storm water runoff from rural residential areas with agricultural land use observed by Lang et al. (2013)...	106
Table 6-16:	Monitored combined sewer overflow event mean concentrations at retention tanks	106
Table 6-17:	Comparison of typical event mean concentrations for combined sewer overflow	107
Table 6-18:	Statistical evaluation of the pollution load contribution from rainfall-runoff to the combined sewage load	114
Table 6-19:	Standard parameterization of COD, TSS and TKN fractionation	118
Table 6-20:	Results of DWF sum parameter fractionation at retention tanks according to ASM1	119

Table 6-21: Results of the DWF sum parameter fractionation at the WWTP according to ASM1	120
Table 6-22: Results of the CWWF sum parameter fractionation at retention tanks according to ASM1	122
Table 6-23: Results of CWWF sum parameter fractionation at the WWTP according to ASM1	123
Table 6-24: Comparison of the calibrated COD fractionation parameter sets according to ASM1	124
Table 6-25: Adapted system-wide concentration balance.....	138
Table 6-26: Calibration results of the accumulation and wash-off model according to calculated wash-off loads from measured CWWF loads and mean DWF loads for specific CWWF events	139
Table 6-27: Results of the parameter estimation for the accumulation and wash-off model and comparison to results from literature review	139
Table 6-28: Results of a clean water test to measure the real oxygen input and bottom flow rates.....	142
Table 7-1: Software components.....	150
Table 7-2: Linguistic description of sewer network objective functions for system-wide analysis and control of rural WCTSs.....	152
Table 7-3: Maximum throttle flows per retention tank.....	153
Table 7-4: Legal effluent concentration limits for WWTP Heiderscheidergrund.....	154
Table 7-5: Linguistic description of WWTP objective functions for capacity estimation, system-wide control and analysis of rural WCTSs during CWWF	155
Table 7-6: Specific triangular MFs used for sewer network control and analysis in system-wide FPC of integrated rural WCTSs.....	157
Table 7-7: Specific triangular MFs used for WWTP capacity estimation, control and analysis in system-wide FPC of integrated rural WCTSs	158
Table 7-8: Horizons chosen in the present FPC approach and their explanation	161
Table 7-9: Parameterization of the rainfall run-off model for impervious catchment surfaces.....	166
Table 7-10: Mean rainfall runoff model calibration results.....	166
Table 7-11: Comparison of CSO volumes and loads from system-wide FPC according to static and phenomenological rainfall runoff distribution June 2012.....	169
Table 7-12: MAPDs of hydro- and pollutographs for WWTP loading based on the Lagrangian ISN observer model for event #1 of the rainfall time series of June 2012.....	174
Table 7-13: MAPDs of the WWTP capacity estimation and loading according to the reference simulation model for selected AST parameters during CWWF event #1 of the rainfall time series of June 2012	175
Table 7-14: MAPDs of the WWTP capacity estimation and loading according to the reference simulation model for selected SST effluent parameters during CWWF event #1 of the rainfall time series of June 2012.....	176
Table 7-15: Summary of WWTP mean MF values and standard deviations for CWWF events of August 2011	186
Table 7-16: Summary of sewer network mean MF values and standard deviations for CWWF events of August 2011.....	186

Table 7-17: Summary of WWTP mean MF values and standard deviations for CWWF events of June 2012	194
Table 7-18 Summary of sewer network mean MF values and standard deviations for CWWF events of June 2012	195
Table 8-1: Variables and set-points of feedback controllers used in the reference scenarios	200
Table 8-2: Aggregation of CWWF events for the rainfall time series of June 2012.....	202
Table 8-3: Event-specific CWWF volumes and pollution loads according to the rainfall time series of August 2011	203
Table 8-4: Event-specific CWWF volumes and pollution loads according to the rainfall time series of June 2012	205
Table 8-5: Monthly pollutant loads treated at the WWTP during CWWF and corresponding mean effluent concentrations according to rainfall time series August 2011	213
Table 8-6: Monthly CWWF WWTP effluent loads and mean concentrations according to rainfall time series June 2012	215
Table 8-7: Results DO set-point optimization.....	219
Table 8-8: Comparison of the aeration effort during CWWF events according to rainfall time series August 2011	219
Table 8-9: Comparison of the aeration effort during CWWF events according to rainfall time series June 2012	222

List of abbreviations

AST	Activated sludge tank
BOD ₅	Biological oxygen demand after 5 days
BSM	Benchmark simulation model
COD	Chemical oxygen demand
CSO	Combined sewer overflow
CWWF	Combined wet weather flow
DO	Dissolved oxygen
DWF	Dry weather flow
EMC	Event mean concentration
FDM	Fuzzy decision making
FPC	Fuzzy predictive control
ISN	Interceptor sewer network
MAPD	Mean absolute percentage difference
MF	Membership function
MFF	Mass first flush ratio
MPC	Model predictive control
NH ₄ -N	Ammonium nitrate
NO _x -N	Nitrogen nitrate
PE	Population equivalent
PID	Proportional-Integral-Derivative
PLS-DA	Principle least square discriminant analysis
PO ₄ -P	Phosphate phosphorus
RDII	Rain derived inflow and infiltration
RHOC	Receding horizon optimal control
RRC	Rainfall runoff coefficient
RWF	Rain weather flow
SASS	Simultaneous aerobic sludge stabilization
SNH	Soluble ammonium nitrogen
SRT	Solid retention time
SST	Secondary settlement tank
TN	Total nitrogen
TP	Total phosphorus
TS	Total solids
TSS	Total suspended solids
WCTS	Wastewater collection and treatment system
WWTP	Wastewater treatment plant

1. Introduction

Integrated urban wastewater management is in the focus of research since the INTERURBA I conference (Lijklema *et al.* 1993) in 1993. Thereby, sewer network, wastewater treatment plant (WWTP) and receiving water are regarded as one system. While in conventional approaches each sub-system is designed and operated more or less isolated from each other, integrated approaches take interactions among sub-systems into account. Based on integrated modeling of urban water systems (IUWS), studies on integrated real-time control followed quickly showing significantly increased treatment capacities compared to their isolated implementation (Linde-Jensen 1993; Bauwens *et al.* 1996; Schilling *et al.* 1996; Vanrolleghem, Fronteau, *et al.* 1996; Schütze *et al.* 1999). A major benefit of integrated control approaches from the control engineering point of view thereby is that the number of disturbances decreases. Most important in the case of wastewater collection and treatment systems (WCTS) is that the inflow from the sewer network to the WWTP during combined wet weather flow (CWWF) is no longer a disturbance but a variable which can be controlled. Vice versa discharges from retention tanks in the sewer network to the WWTP are no longer constraints but become variables to be optimized according to e.g. the current capacity of the WWTP (Olsson and Jeppsson 2006). Generally known as “integrated urban drainage systems” (Rauch *et al.* 2005) or “integrated wastewater collection and treatment systems” (Benedetti *et al.* 2006) the latter will be used in the following since it draws the attention towards both the sewer network and the WWTP. Plenty of modeling studies on system-wide management and control of integrated WCTSs describe the benefits of such approaches. Schütze *et al.* (2004) give a comprehensive overview on the current state of real-time control of integrated WCTSs. Despite these promising benefits implementations of system-wide real-time control systems in practice are rather rare. Controllers found in WCTSs predominantly consist of simple approaches such as on-off controllers or reactive PID controllers and their derivatives for the control of constant discharges in sewer networks. At WWTPs simple control systems are omnipresent (e.g. reactive PID controllers for WWTP loading, TS or DO control in activated sludge tanks). Nevertheless, implementations of sophisticated real-time control approaches in WCTSs are rather rare even if reports from research and practice show promising results (Rauch *et al.* 2005).

Real-time control can be generally classified into reactive and predictive approaches (Capodaglio 1994). In reactive real-time control actuator actions solely result from feed-back by making adjustments according to monitored variables. In predictive real-time control actuator settings are chosen according to the forecast of the future behavior of the system to be controlled based to its current state and control actions. While in reactive real-time control set-points and control rules for actuator actions are defined offline, in predictive real-time control, better known as model predictive control (MPC), actuator settings are optimized online according to a specific goal, a so called objective function. Thereby, integrated modeling is the common method to develop and test system-wide control approaches for integrated WCTSs. Integrated models are always unique compositions according to the specific objective of the study they are built for. A comprehensive literature review on integrated models of urban water systems is given by Bach *et al.* (2014). Besides this, there are only a few modeling software packages available providing integrated modeling on their

own. These are SIMBA (IFAK 2007), WEST (Vanhooren *et al.* 2003), MIKE toolbox (DHI 2009), CITY DRAIN (Achleitner *et al.* 2007), MUSIC (eWater 2011) and Aquacycle (Mitchell 2005). Other approaches are based on customized data exchange protocols and sequential simulation.

1.1. Challenge

Despite the recommended need of system-wide control of integrated WCTs from science (Olsson and Jeppsson, 2006) in order to maximize the use of WWTP and sewer network retention tank capacities, practice-implementations are rather rare. One explanation for the missing acceptance of real-time control and especially MPC of integrated WCTs is the complexity and lacking transparency of such approaches (Schütze *et al.* 2004). From lessons learned Schütze *et al.* (2004) assume that acceptance among operators of integrated WCTs can be increased if the ultimate control decision is taken by operators themselves instead of computers using e.g. control assistance systems or operator-in-the-loop-approaches. Fuzzy logic control is well known for taking human decisions into account in real-time control (Babuška and Verbruggen 1996). Plenty of industrial disciplines benefit from this ability. Precup and Hellendoorn (2011) provide a comprehensive overview on fuzzy logic control in industrial applications. Fuchs *et al.* (1997) successfully adapt fuzzy logic control to real-time control of sewer networks reducing case specific CSO volume by 90%. Klepiszewski and Schmitt (2002) compare fuzzy logic control and conventional rule based control for a combined sewer system consisting of four retention tanks with combined sewer overflow (CSO) structures. Using the same simple rule base fuzzy logic control shows the same performance as the conventional rule based approach. Evaluating three different storm events their results show CSO reductions between zero and 20% for both approaches. Due to the nonlinear character of WWTPs the benefits of fuzzy logic control are widely explored. The list of examples from literature review ranges from first approaches for plant-wide automatic control based on fuzzy rules to mimic human control (Tong *et al.* 1980) to process specific fuzzy rule based approaches for e.g. nitrogen and phosphorous control (Kalker *et al.* 1999; Rammacher and Hansen 2000), secondary settlement tank (SST) sludge height control (Traoré *et al.* 2006) or step feed control (Zhu *et al.* 2009) to fuzzy logic rule based approaches for supervisory control of feedback controllers (Couillard and Zhu 1992; Belchior *et al.* 2012). Tränckner *et al.* (2007) successfully applied fuzzy rule based control for system-wide control of integrated WCTs with successful real-world implementations e.g. in the city of Chemnitz (Seggelke *et al.* 2008) or Wilhelmshaven (Seggelke *et al.*, 2013). Belonging to the category of reactive real-time control approaches the performance of fuzzy logic control approaches depends on the chosen rules and set-points which are usually derived offline from a limited set of data but also on the representativeness of the reference models chosen for performance evaluation (Weijers 2000). Due to the limited amount of data and the complexity of system-wide control, results strongly depend on the experience of persons responsible for the design of the control rules and set-points but necessarily do not reflect the optimal aggregation of operator decisions. Consequently, optimization cannot be guaranteed regarding the system's performance or for decision-making.

From a theoretical point of view optimal control (Lewis *et al.* 2012) is the best approach to compute the optimal control strategy for a given system. However, due to the unlimited temporal horizon, practicability is problematic because of large computational demands,

online implementability and the problem of local minima. For nonlinear systems (as in the present case) Michalska and Mayne (1989) show that at least theoretically the first two drawbacks can be overcome by transferring optimal control to receding horizon optimal control (RHOC) also known as MPC. In RHOC the prediction horizon is shifted forward with each sample instance to calculate the future set-point sequence according to a prediction model and states at each sample instance (Clarke *et al.* 1987). Details on MPC are provided in chapter 3. The risk of getting stuck in local minima concerning nonlinear optimization can be reduced by using global optimization approaches (Egea *et al.* 2007) but these are computationally demanding. Despite the limited number of implementations in practice sewer network MPC approaches have been proven to be practicable (Cembrano *et al.* 2004). Rare reports on practice implementations of MPC confirm benefits for WWTPs, too (O'Brien *et al.* 2011). But, studies on MPC of WWTPs reported in literature are limited to dry weather flow (DWF) situations where the hydraulic influence on the SST is negligible. In practice, especially during CWWF MPC of WWTP lacks state estimation of variables used in activated sludge and SST modeling (Vanrolleghem 1995). While for simulation reliable models for SST are available there is still a lack of robust prediction models for CWWF operation (Krebs 1995). Consequently, Lukasse and Keesman (1999) apply RHOC as a scientific method. They propose to design simple feed-back controllers by imitating the results of a RHOC to find the optimized operation and design of alternating activated sludge WWTPs for N-removal. Additionally, the method of RHOC analysis can also be used to derive rules for practicable reactive real-time control (Lukasse and Keesman 1999).

In system-wide control of integrated WCTSs the optimization problem usually pursues multiple objectives. Consequently, compromising decisions must be made. Decision-making can either be a-priori or a-posteriori. In the first approach decisions are made according to pre-assigned preferences while in the second approach decisions are chosen from a set of alternatives. In the case of computationally costly MPC approaches (as in the case of large nonlinear systems) decision-making usually is made a-priori (Tamura 1990). Therefore, the common approach in conventional MPC is to transfer the multi-objective problem into a single-objective one by aggregating the sub-goals and constraints. Thereby, decision-making is done by using multipliers for the weighting of sub-goals and constraints in the global objective function. Appropriate weighting scenarios are chosen offline either by trial-and-error or according to the analysis of the Pareto front (Fiorelli *et al.* 2013). To overcome this "piecemeal" approach Li *et al.* (2004) successfully investigate the use of fuzzy decision-making (FDM) in MPC to systematically solve the problem of a-priori decision-making also known as fuzzy predictive control (FPC) (da Costa Sousa and Kaymak 2001). Thereby, the aggregated objective function in MPC is replaced by a function for FDM.

The need of systematic and transparent decision-making approaches in system-wide control of integrated WCTSs is emphasized by (I) the complex and nonlinear character of the integrated system and (II) reports on the conflicting nature of certain objectives and constraints in the integrated system (Fu *et al.* 2008). While e.g. in sewer network control it is the aim to empty retention tanks as fast as possible to reduce CSO into receiving waters due to peak rain events in anticipation of future storms (Gelormino and Ricker 1994) the resulting hydraulic loading of the WWTP increases the risk of sludge wash-out in the SST (Leitão *et*

al. 2006). Another example for instance is the conflicting interest of WWTP loading during CWWF and energy minimization for aeration (Fu *et al.* 2008).

Most of the studies reported in literature are based on case studies of large urban catchments which are predominantly characterized by municipal and industrial wastewater and WWTPs with anaerobic sludge digestion. Case studies of rural catchments which are characterized by domestic and agricultural wastewater and WWTPs with simultaneous aerobic sludge stabilization (SASS)¹ are rare. Especially the simultaneous aerobic digestion of the activated sludge produced during the wastewater treatment process has significant influence on the control of the WWTP concerning solid retention time (SRT) and aeration. Consequently, this affects the composition of the activated sludge and the treatment capacity of the WWTP. Wiese *et al.* (2005) investigate real-time control approaches for integrated WCTSSs with sequencing batch reactors. Using a case study of a small system in a rural region they show benefits of additional CWWF treatment of about 50% compared to the separated control of sewer network and WWTP. Thereby, the study focuses predominantly on the increased loading of the sequencing batch reactor during CWWF and less on the consequences for sewer network control. Additionally, the authors do not address objectives and constraints for SASS. Moreover, the results are not transferable to WWTP with continuous inflow. Also using a rural system as case study Meirlaen (2002) does not address the issue of sludge treatment in the study focusing on immission based real-time control of integrated WCTSSs. Other studies on system-wide control of integrated WCTSSs found from literature focus on large systems and WWTPs with anaerobic sludge digestion (e.g. Seggelke *et al.* (2013)) reporting annual CSO reductions in the range of 25 to 85%. So far, quality aspects of waste activated sludge have only been considered in isolated WWTP control (Flores-Alsina *et al.* 2009) and system-wide operation of integrated WCTSSs (Vanrolleghem, Jeppsson, *et al.* 1996) but not in system-wide control of integrated WCTSSs.

At the moment the minimum design capacity of WWTP for profitable anaerobic sludge digestion in Germany is about 15000 PE (Gretzschel *et al.* 2012). Consequently, in rural regions the dominating approach to treat waste activated sludge from WWTPs is SASS. For example, in Luxembourg 25% of the wastewater is treated in WWTPs with SASS. From an energetic point of view such WWTPs suffer from extended aeration due to the stabilization process of activated sludge during the wastewater treatment process. Consequently, the energy remaining in the waste activated sludge from WWTPs with SASS is insufficient for further anaerobic sludge digestion. Therefore, it should be in the interest of operators of integrated rural WCTSSs to investigate additional treatment capacities during CWWF in order to compensate these deficits from an energetic point of view by optimizing the treatment volume and quality during CWWF and decreasing the impact of CSO on receiving waters.

Due to the computational effort, the complexity of IUWS models usually must be adapted to the objectives of the specific study (Meirlaen *et al.* 2001). Consequently, IUWS models are usually unique approaches. Additionally, calibration of IUWS models is rare due to insufficient monitoring data and measurement campaigns, especially for pollution load modeling of CWWF events. While in IUWS models WWTP sub-models benefit from the

¹ Simultaneous aerobic sludge stabilization is also known as extended aeration.

availability of online wastewater quality probes, sewer network sub-models often lack in adequate data due to scarce and costly wastewater quality monitoring campaigns (Vanrolleghem *et al.* 1999). Consequently, integrated monitoring and measurement campaigns are required by numerous studies in order to investigate and to improve the quality respectively the representativeness of integrated reference models for simulation-based control approach evaluations (Bach *et al.* 2014).

1.2. Aims, scope and hypothesis

Based on the challenges described in section 1.1 the aim of the present doctoral study is to investigate modeling and system-wide control of IUWTSs in rural regions with central WWTPs and SASS. Due to the common approach of simulation-based design of control approaches in integrated WCTSs research focuses on the one hand on the integrated modeling of such systems and on the other hand on multi-criteria decision-making in system-wide control.

Since qualitative information on case studies of rural catchments is rare the study has to provide detailed information on mass flows of pollutants and nutrients in integrated WCTSs in rural regions necessary for the simulation-based development of system-wide control approaches. The data gathered by integrated monitoring campaigns should provide insights into mass flows during DWF and especially during CWWF. Model calibration of a representative case study must be performed to provide detailed information on the quality of integrated models of wastewater treatment systems in rural regions.

The systematically implementation of a decision-making approach for multi-criteria control shall provide insights in conflicting objectives in system-wide control of IUWTSs in rural regions and central WWTPs with SASS. In combination with the systematically application of RHOC in FPC it is the aim to investigate the influence of multi-criteria decision making in optimized system-wide control. Concerning system-wide control of IUWTSs the present study will be limited to conceptual work. This is partly due to the chosen case study which was incomplete at the time of processing this study and hence only partly in operation.

Olsson and Jeppsson (2006) hypothesize that system-wide control of integrated WCTSs generally reduces emissions to receiving waters by the maximum use of WWTP and sewer network retention tank capacities. This hypothesis has been confirmed for large catchments with WWTP and anaerobic sludge digestion by e.g. Seggelke *et al.* (2013) and for rural catchments with continuous flow WWTPs by Meirlaen (2002) respectively sequencing batch reactor WWTPs by Wiese *et al.* (2005). Consequently, it is the aim of the present doctoral study to test the following hypothesis: System-wide control of integrated WCTSs in small rural catchments with central WWTPs and SASS generally reduces emissions to receiving waters.

Finally, the present work aims to provide a software tool to investigate system-wide control of IUWTSs. The methodical application of FPC will provide insights into conflicting objectives and constraints and systematically overcome problems of a-priori weighting based aggregated single-criteria optimization for multi-objective control (Li *et al.* 2004). Based on freely configurable fuzzy decision functions representing objectives and constraints of

operators the software tool should enable the investigation of decision-making in system-wide control. Additionally, the transparent approach of FPC should contribute to the acceptance of system-wide control of integrated WCTs. Due to the problems of MPC of WWTPs especially during CWWF (Vanrolleghem 1995; Weijers 2000) results can then be used to derive practicable reactive real-time control approaches for WWTPs (Lukasse and Keesman 1999) in system-wide control of IUWTSs.

1.3. Methodology

In order to reach the aims defined in section 1.2 the following methods must be applied to test the hypothesis.

A monitoring campaign shall provide information on the mass flow of nutrients and pollutants significant for the calibration of integrated reference models for model-based development of system-wide control approaches of integrated WCTs (Vanrolleghem *et al.* 1999). Results shall provide hydro- and pollutographs describing system dynamics during DWF and especially during CWWF. Important thereby is the influence of CWWF on WWTP performance and CSO emissions to receiving waters. Resulting pollutographs will be analyzed with data from literature in order to provide a comparison to urban systems.

Results of the system-wide monitoring campaign will be used to build and calibrate an integrated model of the chosen case study within the constraints of the chosen software. Especially the ability of computational parallelization has significant influence on the possible complexity of the reference model. Due to the large computational demand of integrated models of urban wastewater treatment systems, model reduction might be necessary (Meirlaen *et al.* 2001).

By replacing the objective function with a FDM function MPC approaches become FPC approaches (da Costa Sousa and Kaymak 2001). Based on the integrated reference model a system-wide FPC approach will be developed systematically applying RHOC and FDM. Consequently, RHOC will allow to investigate optimal control in nonlinear dynamic systems (Lukasse and Keesman 1999) as in the case of IUWTSs during CWWF, while FDM will allow to systematically investigate the influence of a-priori multi-criteria decision-making of conflicting objectives. Consequently, objectives and constraints of the operator for system-wide control must be transferred into fuzzy membership functions. Existing MPC for sewer networks is predominantly limited to hydraulic approaches. Consequently, for system-wide MPC of integrated WCTs taking the dynamic treatment capacity of the WWTP into account, it will be necessary to develop a practicable pollution-based prediction model for WWTP loading.

As integration calls for compromises (Olsson and Jeppsson 2006) the analysis of results from integrated fuzzy decision-making will provide insights into conflicting objectives of system-wide control of integrated WCTs in rural regions with central WWTPs and SASS. Additionally, the influence of excessive CWWF loading on the WWTP performance will be of interest.

Finally, the hypothesis will be tested by comparison of the developed approach to reference scenarios with no control.

1.4. Structure

The present doctoral study is structured as follows:

The study starts with the introduction in *chapter 1* where the challenges, aims, scope and hypothesis, and the methodology are described.

Chapter 2 provides a general overview on integrated modeling of urban wastewater systems with a focus on wastewater collection and centralized treatment systems with extended aeration in rural areas. Characteristics of such systems are described. The chapter provides an overview on the state of the art of integrated modeling of urban wastewater systems. It is commonly accepted that the IWA ASM are appropriate to simulate WWTPs (Gernaey *et al.* 2004). The literature review focuses on the requirements for integrated modeling of rural wastewater collection systems with centralized wastewater treatment. Additionally, the literature review focuses on characteristics of substance flows in rural WCTSSs.

Chapter 3 gives an introduction to real-time control of integrated WCTSSs. Key terms used in real-time control are explained. Based on this, an overview on the state of the art of real-time control of WCTSSs with the focus on integrated approaches is presented.

Chapter 4 provides the theoretical background of FDM necessary for the development of the presented FPC approach. The chapter gives an introduction both to fuzzy set theory which is the mathematical basis for FDM and decision-making. Deficits of conventional a-priori weighting approaches with multipliers for decision-making in aggregated objective functions for MPC are discussed.

Chapter 5 describes the development of the FPC approach for system-wide control of integrated WCTSSs. First an introduction to FPC is given. Then, process models for system-wide RHOC are discussed based on a literature review. A Lagrangian pollution load prediction model for the loading of WWTPs with decentralized retention tanks and wide-spread interceptor sewer networks (ISN) upstream of the WWTP is developed. Due to the method of system-wide RHOC this prediction model enables simulation-based estimation of WWTP capacities.

Chapter 6 presents the case study Haute-Sûre situated in the North of Luxembourg used to test the hypothesis. Here, structural data necessary to setup the integrated reference model is described. The chapter provides an overview on the existing monitoring equipment for hydraulic and wastewater quality data. The setup of system-wide complementary monitoring campaigns for model calibration and system-wide analysis of routine wastewater pollutants is presented. The monitoring data for DWF and CWWF is discussed in comparison to data from literature investigating differences between urban and rural catchments. The modelability of routine wastewater pollutants along the ISN is investigated based on chemical mass balance. A system-wide analysis of rainfall-runoff coefficients provides insights into disturbance and provides the basis of a combined deterministic-phenomenological

integrated reference model. Finally, the results of the reference model calibration according to the unfinished state of the integrated WCTSs is presented and discussed.

Chapter 7 presents the implementation of the approach developed in chapter 5 according to the objectives and constraints for system-wide FPC of the case study presented in chapter 6. Results are presented based on the simulation of two different months of local rainfall to investigate the general performance of the presented approach compared to static reference scenarios with isolated sewer network and WWTP control. The impact of disturbances investigated in chapter 6 is analyzed according to the deterministic-phenomenological reference model.

The hypothesis is tested based on the simulation results presented in chapter 7 and their discussion according to the comparison of simulation results with reference scenarios based on isolated static control in *chapter 8*. Results of different scenarios are compared according to their performance. FDM is used to analyze the capacity of the presented approach. Conclusions for the system-wide real-time control of integrated rural WCTSs with central WWTPs and SASS are drawn from the compromises according to the results of multi-criteria FDM.

Chapter 9 draws conclusions from these results and provides an outlook on possible further work.

2. Integrated modeling of wastewater collection and centralized treatment systems with extended aeration in rural areas

Integrated approaches in urban wastewater modeling are manifold. Bach et al. (2014) provide a comprehensive overview on IUWSs modeling. Most often such approaches consist of sub-models for sewer networks, WWTPs and receiving waters (Rauch *et al.* 2002). Due to large computational loads of such models the general modeling advice “as simple as possible, as complex as necessary” is of major importance. Specific objectives affect the possible complexity of the integrated model (Meirlaen *et al.* 2001). The following chapter provides an overview on integrated modeling of urban water systems with the focus on requirements of wastewater collection and centralized treatment systems with extended aeration in rural areas. Substances to be modeled are derived from necessities of model integration and primary impacts on receiving waters. A literature review provides information on substance flow differences between rural and urban catchments.

2.1. Wastewater collection and centralized treatment systems in rural areas

Wastewater treatment in rural areas can either be centralized or decentralized. While in decentralized treatment systems wastewater is treated next to the source, in centralized treatment systems wastewater is collected from a catchment and transported to one central WWTP. Libralato et al. (2012) provide a comprehensive overview on the variety of decentralized wastewater treatment approaches and discuss the decision-making between centralized and decentralized systems according to recent trends in wastewater treatment management. The authors conclude that none of the two treatment concepts can be excluded a-priori but decision-making is very case specific. Nevertheless a cost-benefit-analysis of appropriate treatment systems taking into account construction and lifetime operation costs must be part of the decision-making.

WCTSs with centralized treatment consist of sewer networks and WWTPs with capacities starting from 1000 PE. Integrated operation and management of WCTSs predominantly deals with the additional treatment of rainfall-runoff from combined sewer systems² at the WWTP. The digestion respectively stabilization of the waste activated sludge is linked to the size of the WWTP. The current economic lower limit for anaerobic digestion is about 15000 PE (Gretzschel *et al.* 2012). Sludge treatment at WWTPs below this size usually is simultaneously aerobic digestion based on extended aeration. Thereby, the activated sludge is respired during the wastewater treatment process in the bioreactor through extended aeration until the waste activated sludge is stabilized. Consequently, the energetic performance of such plants is affected by aeration on top of the nominal demand for wastewater treatment as it is the case at WWTP with anaerobic digestion of the waste activated sludge. In order to increase the endogenous respiration of the activated sludge the

² Separate sewer systems transport the sewage to the WWTP separately from the surface rainfall runoff. Combined sewer systems transport both sewage and surface rainfall runoff to the WWTP for combined treatment.

food/mass ratio is kept low through increased bioreactor volumes. Consequently, WWTPs with SASS, so called low loaded plants, do without primary clarifiers in order to guarantee denitrification. While wastewater treatment processes at WWTPs consist of biochemical conversion, physicochemical conversion and sedimentation, sewer networks are designed for collection, retention and transportation of wastewater to the WWTP. Characteristics of WCTSSs with centralized wastewater treatment in rural areas are:

- Strong load fluctuations at the inlet of the WWTP, inversely proportional to the connected catchment size (Boller 1997). Thereby, hydraulics and substance concentrations often fluctuate simultaneously, leading to strong load dynamics (Pujol and Lienard 1990).
- Densely populated widespread catchments with small local sewer networks but long and widespread ISNs. In order to avoid large pipe diameters in ISNs, the retention volume in the combined sewer network is often decentralized, leading to numerous small retention tanks and CSO structures with long and heterogeneous transportation times in the ISN (Boller 1997). Consequently, pipe diameters in the ISN can be designed according to the superposed throttle flows from all retention tanks.

2.2. Integrated modeling of wastewater collection and treatment systems

According to Rauch et al. (2002) integrated models of urban water systems consist of at least two sub-models of the urban water cycle. The set of possible combinations is manifold and linked to the aim of the study. The majority is composed of sub-models for the drainage system (including rainfall-runoff models), the WWTP and the receiving water. Bach et al. (2014) provide a comprehensive review on integrated modeling of urban water systems. They classify these models according to their level of integration which is linked to their specific objectives. This classification is described in Table 2-1.

Table 2-1: Definition of the level of integration for integrated urban water models (taken from (Bach et al. 2014), modified)

Level of Integration	Class	Definition
1	Integrated Component-based Models	Represent the lowest level of integration and focuses on the integration of components within the local urban water sub-system (e.g. coupling several treatment processes within a wastewater treatment plant) analogous to plant-wide models, generalized to also refer to other urban water sub-systems (e.g. pipe network or a natural water body).
2	Integrated Urban Drainage Models or Integrated Water Supply Models	Integrate sub-systems of either the urban drainage (wastewater and/or storm water depending on location in the world) or water supply streams, particularly treatment and transport processes best described as system-wide models.
3	Integrated Urban Water Cycle Models	Link IUDMs and IWSMs into a common framework known as the total urban water cycle.
4	Integrated Urban Water System Models	Are the highest level of integration that combine different urban water infrastructures (institutional or physical) and disciplines (e.g. climate, economics, actor behavior, etc.) of the total urban water cycle.

Integrated modeling of wastewater collection and centralized treatment systems with extended aeration in rural areas

The level of integration increases with the diversity of sub-systems taken into account. According to this classification integrated models for system-wide control of sewer networks and WWTPs belong to the group of integrated urban drainage models also known as system-wide models (level 2). A specific review on integrated urban drainage models is given by Rauch et al. (2005). For further information on IUWS modeling the reader is referred to Bach et al. (2014).

2.2.1. Hydraulic modeling

Table 2-2 presents hydrologic and hydraulic processes of sub-systems occurring in integrated WCTSSs. Ideally, integrated reference models for design and testing of system-wide control approaches should take all of these processes into account. The range of available hydrologic and hydraulic approaches in urban water modeling is manifold. Approaches in hydraulic sewer network modeling range from simple hydrologic approaches based on constant translation to hydrodynamic approaches based on the Saint Venant equations. Hydrodynamic approaches are predominantly used to model complex hydraulic effects such as backflow. Hydrologic approaches considering backwater effects such as the pipe-combiner-splitter approach by Solvi et al. (2005) provide comparable results with less computational effort. Zoppou (2001) provides a comprehensive review on most common software packages and models. Many of these software tools are still appropriate today but the list could easily be extended according to recent developments and national preferences. Nevertheless, the presented modeling approaches are still state of the art. The selection of the appropriate model depends on the problem at hand. Thereby, the ideal complexity is the simplest one that solves the questions to be answered (Rauch *et al.* 2002).

Table 2-2: Hydrologic and hydraulic processes in integrated models of WCTSSs

Sub-system	Process
Catchment	DWF discharge
	Rainfall runoff formation
	Rainfall runoff concentration
Sewer system	Translation
	Retention
	Backflow
	Displacement
	Separation
WWTP	Displacement

2.2.1.1. Catchment

Urban drainage modeling distinguishes between DWF and rain weather flow (RWF). DWF is usually generated according to daily patterns of wastewater production per PE. For domestic wastewater production, drinking water consumption per PE is usually taken as a reference. While wastewater production from industry in rural regions usually is very small, influences of tourism or agriculture are more important (Pujol and Lienard 1990).

In combined sewer systems CWWF is composed of DWF and RWF. Rainfall-runoff modeling consists of models for runoff formation and concentration. The process of runoff formation describes the effective amount of rainfall leading to runoff. Two different approaches have

been established in urban hydrology. In the North American area the SCS approach is the predominant approach while in Europe the loss rates approach is the established one. Details on these models are given in Beven (2011). Runoff concentration describes the period between rainfall and runoff at the outlet of the sub-catchment. A common approach is the model of Kirpich (1940). Comprehensive reviews on hydrologic urban storm water models are given by Zoppou (2001) and Elliott and Trowsdale (2007). These reviews also provide information on respective models used for rain derived infiltration and runoff from pervious catchment surfaces.

2.2.1.2. Sewer network

Sewer systems can be classified in local and interceptor sewers. Local sewers collect the domestic and / or industrial sewage on the sub-catchment level. Subsequently, it is transported by interceptor sewers to the central WWTP. Due to the small sizes of rural villages hydraulic modeling on sub-catchment level can be simply described by the concentration time according to the approach of Kirpich (1940). ISNs play an important role in centralized rural WCTs due to the usually large distances between sub-catchments and the WWTP. Hydraulic models describe the transportation through the pipes. A general distinction can be made between hydrologic and hydrodynamic approaches. By solving the one-dimensional Saint Venant equations hydrodynamic approaches are appropriate when complex hydraulic effects such as backwater effects are of importance while hydrologic models are predominantly used for continuous studies when such effects are negligible and computational effort is to be limited because of long term simulation. Hydrologic approaches describe the in-pipe flow only in one direction through translation. A common approach is the reservoir cascade approach. Ambitious approaches additionally consider retention within the process of transportation such as the Kalinin-Miljukov approach. Details on hydrologic approaches for sewer network modeling can be found in Zoppou (2001). In combined sewer networks the interface between local sewer networks and the ISN often consists of retention tanks providing additional retention volume for sewage during CWWF. In case of exceeding this extra retention volume CSO structures help to avoid hydraulic overloading of the WWTP during CWWF by releasing water to the receiving water. It is the aim of system-wide control approaches of integrated WCTs to coordinate the controlled release from these tanks according to the capacity of the WWTP. Hydraulic modeling of these tanks is usually based on mass balance equations for the specific retention volume. Backwater effects due to characteristics of the tank inlet can be considered either by hydrodynamic modeling approaches in the upstream sewer pipe, virtual tanks upstream the real tank or by distributing parts of the overflow back to the upstream sewer network (Solvi *et al.* 2005). A comprehensive review of urban storm water models is given by Zoppou (2001).

2.2.1.3. WWTP

Conventional hydraulic models for WWTPs in continuous operation are based on the principle of displacement which means that the same amount of wastewater which enters the WWTP at the inlet must leave the WWTP at the outlet. Besides this simplified approach, transient system behaviors such as time delays and flow damping can be modeled according to n-th order differential equations and variable volume tanks as proposed by De Clercq *et al.* (1999). In contrast to WWTPs with continuous flow, hydraulic models of WWTPs in batch operation can be described as a retention tank which must be filled or

emptied according to the current phase of operation. Details on sequencing batch reactor WWTPs can be found in Wiese *et al.* (2005). Integrated control of WWTPs and combined sewer networks is very sensitive to the capacity of the WWTP during CWWF operation. Especially the SST is sensitive to hydraulic shock loadings (Carstensen *et al.* 1998). The performance of the SST and hence the effluent quality of the WWTP is based on the process of sedimentation of the activated sludge and its separation from the soluble phase. The most commonly used model to simulate this process in SSTs is the one-dimensional sedimentation model developed by Takács *et al.* (1991) based on solid-flux theory. Its capability to reasonably approximate the sludge balance and shifts of the sludge blanket level makes it appropriate for integrated modeling studies. Nevertheless, several phenomena at real SSTs cannot be considered by one-dimensional models such as the influence of the SST geometry, inlet outlet arrangements, short-circuit flows or the sludge removal process (Holenda *et al.* 2006). Consequently, they fail in realistically predicting the dynamics of the sludge blanket and effluent concentrations. This is a drawback for practical implementations in MPC (Krebs 1995). Another approach which is able to model sludge blanket dynamics are models based on computational fluid dynamics for SST. Although they show better results than models based on solid-flux theory their large computational demand makes them impracticable for applications in modeling of IUWSs (Krebs 1995). Despite recent advances in model development (e.g. Watts *et al.* (1996), Diehl and Jeppsson (1998), Bürger *et al.* (2005), Plósz *et al.* (2007) or De Clercq *et al.* (2008)) the Takács-model remains the standard in modeling-practice (Plósz *et al.* 2011).

2.2.2. Pollutant flow modeling

Pollutant flows necessary to describe the operation of WCTs are defined by the models used to describe each unit process of the system. Pollutants affecting the receiving water quality define the complexity of the integrated model. In principal, two integrated modeling approaches are possible:

- One general model describes all substances and processes in the overall system. Advantage of this approach is the unified description of all substances. The use of lumped variables is not necessary. Major drawback is the computational demand due to the number of parameters used in the total model.
- Specific sub-models describe respective processes for each sub-system. Sub-models are reduced according to specific demands. Advantage of this approach is the adapted computational demand (Meirlaen *et al.* 2001). Major drawback is the incompatibility of state variables, processes and parameters of the sub-models (Fronteau *et al.* 1997).

In principal, both approaches must guarantee a system-wide continuous mass-balance (Vanrolleghem *et al.* 2005). The integration of specific sub-models is the most applied approach.

2.2.2.1. Substances

IWA ASM 1 and 3 which are predominantly used for activated sludge WWTP modeling (Gernaey *et al.* 2004) principally describe the treatment of wastewater by mass balances of carbon and nitrogen according to biological and chemical processes based on the growth and decay of biomass in the wastewater-activated sludge-suspension. The degradation of organic carbon is described according to its COD. COD represents the amount of oxygen-

depleting substance in the wastewater. Nitrogen fractions in the wastewater are calculated from TKN. TKN represents the organically bound nitrogen in the wastewater. In raw wastewater nearly all of the nitrogen is present as TKN. ASM2d (Henze *et al.* 1999) and ASM3bioP (Rieger *et al.* 2001) extend the approach by the fate of phosphorus. Consequently, sewer network models must cover at least COD and TKN to feed with the WWTP model. Details on the fractionation of COD and TKN for model integration of sewer networks and WWTPs are given e.g. in Koch *et al.* (2001). Examples for model interfaces between WWTPs and receiving waters are given by Benedetti *et al.* (2004) and Schütze *et al.* (2011).

The principal objective of wastewater treatment is to minimize the effects from wastewater discharges into receiving waters (EC 1991). Harmful sewage constituents can be grouped according to their effects on receiving water as described in Table 2-3. The objective of the EU Water Framework Directive (EC 2000) is the good ecological status of natural water courses. Its adoption in 2000 caused a paradigm shift from emission-based verification procedures for urban wastewater treatment structures to immission-based approaches (Blumensaat *et al.* 2012). Simplified verification approaches like for instance the German guideline ATV-A 128 (DWA 1992a) for CSO structures which is based on annual COD discharge loads are replaced by immission-based approaches taking additional parameters into account. The German guidelines ATV-M 3 (BWK 2001) resp. 7 (BWK 2008) for instance now demand verifications of annual excess frequencies for hydraulic stress, ammonia and TSS from the receiving water point of view. Ammonia plays an important role due to its pH depending balance with ammoniac which is highly toxic to fish. TSS causes turbidity and is partly organic.

Table 2-3: Effects of sewage constituents on receiving waters

Group	Constituent	Effect on receiving water
Oxygen consuming (organic) substances	BOD ₅ COD	Affect the oxygen balance
Nutrients	N P	Cause excessive algae growth
Toxic substances	Heavy metals	Poisoning of organisms
Endocrine substances	Xenobiotica Synthetic hormones etc.	Affect like hormones

Modeling of other toxic and endocrine substances is out of the scope of this work.

Consequently, integrated models for WCTSSs must predominantly describe the flux of TSS, organics and nutrients from the source of wastewater generation in the catchment, its transport to the WWTP and its treatment according to the available treatment steps. For immission-based evaluation, the fate of substances in receiving waters must be modeled too. For emission-based approaches CSO and WWTP effluent concentrations are sufficient.

Integrated modeling of wastewater collection and centralized treatment systems with extended aeration in rural areas

2.2.2.2. Catchment

Models to simulate processes at catchment level can be classified according to approaches for DWF and RWF. DWF models simulate the generation of domestic, municipal and industrial wastewater usually as daily patterns either according to means of local measurement campaigns or Fourier series (Rodríguez *et al.* 2013). Ambitious approaches distinguish between weekdays and the weekend or take seasonal variations into account (see e.g. Insel *et al.*, 2005). In rural areas wastewater from domestic sources is dominating while wastewater from industrial sources is rather rare.

Quality models at the catchment level for RWF describe the buildup of pollution on the impervious catchment surface and its wash-off due to rainfall-runoff. While the simplest approaches only consider constant concentrations in rainfall-runoff sophisticated approaches model the buildup process based on the length of the preceding dry weather period and model wash-off according to rain intensity (Obropta and Kardos 2007). However, this process is not very well understood. Functions to describe the accumulation of matter are linear, power, exponential or Michaelis-Menten. The most common approach is the simple exponential relationship. Although the unreliability of this function is known there is still a lack of data to investigate alternative approaches (Zoppou 2001). Wash-off is usually modeled as first-order decay functions (Obropta and Kardos 2007).

2.2.2.3. Sewer network

Common approaches to model water quality in sewer systems are (I) routing assuming complete mixing and (II) routing assuming advection-dispersion. Additionally, the following processes can be considered (Obropta and Kardos 2007):

- Sedimentation and erosion,
- Biochemical degradation processes.

Uncertainty in calibration of these models increases with growing model complexity. More complex models do not guarantee more accurate results (Meirlaen *et al.* 2001). In their review on urban storm water models Obropta and Kardos (2007) conclude that storm water quality models are the weak point in integrated modeling approaches since they are less developed than activated sludge models or river water quality models. They base this on two arguments:

- Sewer quality modeling is based on hydraulic modeling. Unless the flow in the sewer is not modelled adequately, quality modeling will not be reliable (Zoppou 2001).
- The lack of field data for model development hindered model development so far. Continuous monitoring comparably to the standard at WWTPs would contribute to model improvement.

Interceptor sewer network

In order to simplify models for pollutants build-up on the catchment surface and sedimentation in the sewer it is a common approach to lump both models especially if the hydraulic model is a hydrologic approach and information for sedimentation and erosion in the sewer is missing. Biochemical degradation processes in sewer networks are difficult to identify and hence to calibrate. Consequently, most of all applications from literature review are assuming the pollutants to be conservative.

Retention tanks

Pollution removal is modelled by first-order decay coupled with complete mixing or plug-flow, sedimentation dynamics or removal as a function of the hydraulic residence time (Obropta and Kardos 2007).

2.2.2.4. Wastewater treatment plant

Due to their design, the food to biomass ratio of WWTPs with SASS is smaller than at WWTPs with anaerobic waste activated sludge digestion. Because of this WWTPs with SASS are designed without primary clarifiers. Hence, primary treatment of the wastewater only consists of screens for coarse particles and sand traps for inorganic particles. The present PhD study focusses on continuously fed WWTPs with SASS. Popular models are the IWA ASM 1-3 (Gernaey *et al.* 2004). In the following the scope of these models is described.

Activated Sludge Model No. 1 (Henze *et al.* 1987) is the most popular model for dynamic wastewater treatment plant simulation. It balances COD and N by modeling 8 biological processes (3 growth processes, 2 decay processes, 2 hydrolysis processes and ammonification). It considers 13 fractions; 8 fractions for COD, 4 fractions for N and alkalinity.

Activated Sludge Model No. 2d (Henze *et al.* 1999) additionally balances P. The model consists of 21 processes (5 growth processes, 5 decay processes, 3 digestion processes, 3 hydrolysis processes, 3 processes for phosphate storage and 2 for chemical precipitation of phosphate). It considers 19 fractions; 10 fractions for COD, 3 fractions for N, 2 fractions for P, 3 fractions for the dry matter content and alkalinity.

Activated Sludge Model No. 3 (Gujer *et al.* 1999) balances COD and N. It adds the process of organic substrate storage. Overall the model describes 12 processes (3 growth processes, 6 decay processes, 2 storage processes and 1 hydrolysis process) and considers 13 fractions; 8 for COD, 3 for N as well as 1 fraction for the dry matter content and alkalinity.

Activated Sludge Model No. 3bioP (Rieger *et al.* 2001) adds the balances for biological and chemical P treatment to ASM3. Therefore, 4 additional fractions are necessary. The original 12 processes of ASM3 are adapted and 11 processes are added to describe the P balance.

Despite recommendations by IWA to use ASM3, ASM1 is still the most popular model (Gernaey *et al.* 2004). ASM2d and ASM3bioP are appropriate when P must be modeled. ASM3 is able to model substrate storage. Additionally, some drawbacks of ASM1 are corrected. For details on each model the reader is either referred to each original publication or the review of Gernaey *et al.* (2004).

2.3. Pollutant flows in wastewater collection and treatment systems in rural areas

WWTP operation usually distinguishes between DWF and CWWF operation. While during DWF wastewater entering the WWTP usually is only slightly diluted, wastewater pollutant concentrations during CWWF strongly depend on (I) the process of accumulation and wash-off of pollutants in the catchment and sewer network and (II) the subsequent dilution by rainfall runoff (Lang *et al.* 2013). Due to the missing primary clarifier at low loaded WWTPs for SASS the first flush load is directly passed to the activated sludge tank (AST) followed by a subsequent feeding period with lower concentrations until DWF conditions are reached again. Consequently, energy saving potentials result from adaptation of the DO set-points to dynamic load conditions (Lukasse and Keesman 1999).

Studies on wastewater substance flows in rural catchments are rare. Pujol and Lienard (1990) investigate wastewater from small communities in France. They conclude that the scale of variation in flow and concentrations varies inversely with the size of the community. Additionally, infiltration water has a significant influence on volumes and concentrations due to the length and conditions of the sewer network. They monitor average DWF concentrations of raw wastewater but do not compare them to concentrations of urban wastewater. Heip *et al.* (1997) investigate wastewater from a typical rural Flemish catchment with the aim to set up a sewer flow quality model. They compare daily mean DWF concentrations of rural catchments to daily mean DWF concentrations of urban catchments. The results are shown in Table 2-4 and compared to daily mean DWF concentrations in urban catchments. The data from Heip *et al.* (1997) shows clear differences for per capita flow and TKN. According to the authors, the production of wastewater in rural regions is much smaller and TKN concentrations are much higher. In comparison to Pujol and Lienard (1990) their results for COD and BOD are nearly double the size. Larger nitrogen concentrations in rural catchments are explained by agriculture in these catchments. Dairy farms can also contribute to increased N concentrations (Longhurst *et al.* 2000). The results of Heip *et al.* (1997) show very low concentrations for S_{COD} and S_{BOD} which are not explained by the authors.

Table 2-4: Daily mean DWF concentrations in rural catchments compared to urban concentrations

Parameter	Concentrations			
	Pujol and Lienard (1990)	Heip <i>et al.</i> (1997)		ATV-DVWK (1992b)*
Catchment	Rural	rural	urban	urban
Per capita flow [l]	150 ± 50	87	136	185
TSS [mg/l]	250 ± 30	463	350	n.a.
COD [mg/l]	700 ± 100	1511	1372	647
S_{COD} [mg/l]	n.a.	221	132	383
BOD [mg/l]	300 ± 65	713.6	682.3	n.a.
S_{BOD} [mg/l]	n.a.	53.6	32.3	n.a.
TN [mg/l]	80 ± 20	n.a.	n.a.	n.a.
TKN [mg/l]	n.a.	74.0	47.9	59.3
TP [mg/l]	35	9.29	6.59	13.5

* 85% values

Integrated modeling of wastewater collection and centralized treatment systems with extended aeration in rural areas

Studies on pollutant flows in rural catchments during RWF are also rare. Mallin et al. (2009) investigate the impact of storm water runoff on the water quality of an urban, a suburban and a rural stream. Their results show that urban streams suffer the highest BOD, TSS and ortho-Phosphate concentrations during RWF while rural streams show the highest total organic carbon concentrations. Lang et al. (2013) describe increased nutrient concentrations in runoff from rural catchments with agricultural use.

3. System-wide control of centralized wastewater treatment systems

Control of sewer networks and WWTPs is complex and seldom straightforward. Conflicting objectives in integrated approaches additionally increase the complexity. The aim of the present PhD study is to investigate system-wide control approaches with the help of FPC. The systematic application of FPC is based on MPC, in particular RHOC. The following chapter describes the principles of MPC with focus on urban wastewater treatment systems. An overview on examples both of isolated and integrated control approaches illustrates the development in this field from the first approach to the current state of the art in research and engineering practice.

3.1. System-wide control

System-wide control of integrated WCTs is the approach of combined control and operation of sewer networks and WWTPs that extends the initial idea of plant-wide control of WWTPs to combine different control units to increase performance and robustness. By integrating control approaches former external disturbances become internal variables (Olsson and Jeppsson 2006). In the case of conflicting variables the integration creates additional degrees of freedom in the optimization process for finding the best compromise. At the level of the WWTP classic examples for such compromises from plant-wide control are:

- The interaction between the aerator and the settler controlled by the return sludge flow.
- The interactions between anoxic zones in pre-denitrifying WWTPs and the nitrifying reactor.

Plant-wide control approaches at the level of the WWTP for example expand the control of the effluent quality for instance to the demands of sludge settle-ability in the SST (Flores-Alsina et al., 2009) or to the demands of the anaerobic digestion process of the excess sludge (Pires *et al.* 2006).

Initial system-wide control approaches extend the integrated wastewater treatment system by adapting discharges of the sewer network to a reference value defined by the WWTP capacity. This can either be a static reference or the current capacity of the WWTP. First attempts of system-wide control evolved in the late 1990s (for example Nyberg et al. (1996)). Slowly, the approach is gaining access into engineering practice (for example Erbe et al. (2002), Pleau et al. (2005) or Seggelke et al. (2013)).

Historically, sewer networks and WWTPs are designed and operated separately (Rauch *et al.* 2005). In Germany, for instance, the inflow to the WWTP during CWWF initially was commonly limited to twice the 85-percentile of the DWF hourly peak flow Q_s plus the extraneous water flow Q_e (Seggelke *et al.* 2005). Thanks to the results of many research studies initiated by pioneering work done at the first INTERURBA workshop in 1992 (Lijklema *et al.* 1993) and successful implementations, the acceptance of an integrated operation of sewer network and WWTP increased. For example, in Germany this led to the

increase of inflow limitations for WWTP during CWWF according to their size (DWA 2003). Despite these results and successful installations the vast majority of sewer network and WWTP operators still has a very cautious attitude towards dynamic control approaches (Heusch 2011). Consequently, Schütze et al. (2004) assume from lessons learned that acceptance among operators of WCTSs can only be increased if the ultimate control decision remains to be taken by operators themselves instead of computers using e.g. control assistance systems or operator-in-the-loop-approaches.

Brdys et al. (2008) state that one major difficulty in integrating predictive control approaches of WCTSs lies in the wide range of process dynamics present in the integrated system. While retention tanks in sewer systems fill within the range of minutes, wastewater transport to the WWTP is often in the range of hours. At WWTP the range of dynamics is even bigger. While biochemical processes take place in the range of minutes, the time scale of the sludge household is in the range of days. Disregarding these dynamics in MPC might endanger the robustness of the approach.

Usually, design guidelines try to compensate these dynamics by using fixed safety factors in the design process. For example the German design guideline ATV-DVWK-A 198 (DWA 2003) proposes a factor to consider the hydraulic influence of rain water discharge during combined sewage treatment at activated sludge WWTPs in the range of three to nine times the average annual amount of DWF depending on the size of the WWTP. From an integrated urban wastewater management point of view this is an improvement for the receiving water quality since this increases the freedom of action of the WCTS operator to reduce CSO by increasing the CWWF load to the WWTP. On the other hand efficiency decreases with increasing design safety coefficients. Consequently, studies on integrated modeling of WCTSs show increased performance through optimal control by considering these dynamics (e.g. Butler and Schütze (2005)).

3.2. Control-related key terms

In the following the most important key terms of real-time control of WCTSs will be explained:

Actuators are hardware components which influence the process according to instructions of the controller. Actuators in WCTSs are listed in section 3.3.2.

In *closed-loop control systems* actuator settings are processed according to the difference of a feedback signal to the output signal, the so called error.

Controllers are software components which process information from sensors in a system to be automated and carry out instructions for actuators.

In control systems *disturbances* are any undesirable or uncontrollable impacts on the process to be controlled. Disturbances can be either internal or external. Internal disturbances are process related (e.g. failures of sensors or actuators). External disturbances describe external impacts on the system which cannot be controlled (e.g. infiltration water in sewer networks).

System-wide control of centralized wastewater treatment systems

Errors are computed according to the difference of measured signals and set-point values. When errors are detected the controller processes instruction for the actuator to adapt the output signal to the set-point value.

Feedback control is a control approach that uses information from sensors to manipulate a variable (a measured signal to be controlled) to achieve a desired reference value (set-point).

In *feed forward control* (also called anticipative control) process disturbing parameters are measured to derive corrective actions concerning predicted effects in order to achieve desired results. Control-variable adjustments are not error-based but model-based. Knowledge about disturbance measurements must be available. Control signals once sent cannot be further adjusted. This must be considered in the control approach.

Fuzzy-logic control systems are based on fuzzy logic where variables take on continuous values between zero and one instead of discrete values of either zero or one. Fuzzy logic control is predominantly used to implement linguistic variable values into control in order to represent expert knowledge in complex systems. Details on fuzzy logic are given in section 4.2.

On-off controllers, also known as bang-bang or hysteresis controllers are feedback controllers that switch between two states.

In *open-loop control systems* only input signals are used to actuate on outputs. There is no adjustment to measured errors.

A *proportional-integral-derivative (PID) controller* (and its simplifications P, PI and PD) is a standard feedback controller for continuously variable actuator settings. Its signal to the actuator is a function of the difference between the measured signal and the desired value.

Robustness or *stability* describes the ability of a control approach to deal with uncertainty.

Sensors are hardware components which measure the process evolution. Sensors can be physical or software-based. Sensors in WCTSs are listed in section 3.3.1.

A *set-point* (or reference value) is the desired value of a process variable.

Supervisory control describes the control of many individual controllers or control loops for different states of the system under control. The approach is illustrated in Figure 3-5.

In control systems a *variable* is a measured signal to be manipulated according to a certain reference value (set-point).

A comprehensive introduction to control theory is given e.g. by Lewis et al. (2012).

3.3. Sensors and actuators

Sensors and actuators are of major importance in control. In the following common sensors and actuators in integrated WCTs are presented. Comprehensive overviews and discussions on equipment for real-time control of urban wastewater systems are given by Schütze et al. (2004) and Campisano et al. (2013).

3.3.1. Sensors

Hydrologic monitoring: Rainfall now-casting is based on rain gauges such as tipping gauges, weighing gauges, drop counters and radar data. The prediction of rainfall run-off improves the efficiency of real-time control approaches (Gaborit *et al.* 2013). Uncertainty increases with the length of the forecast horizon.

Hydraulic monitoring: Hydraulic measurements consist of water level measurements and flow measurements. For sewer network control information on the outflow of retention tanks is crucial. Flow rates can be measured with weirs, gates, flumes or orifices based on level-flow converting relationships. These approaches lead to measurement errors between two and five percent. Digital alternative approaches are electromagnetic meters for completely filled pipes (measurement errors less than one percent) or ultrasonic meters (Doppler meters or transient time meters) for partially filled pipes. Here, measurement errors are about five percent. Water level measurement can be done by capacity probes, pressure sensors, ultrasonic probes or microwave sensors. Water level data provides information on filling degrees of retention tanks. In combination with effluent measurements the inflow to retention tanks can be calculated (Hansen *et al.* 2011).

Quality monitoring: Available sensors for online water quality monitoring consists of the following variables: temperature, pH⁺, turbidity, dissolved oxygen, oxidation reduction potential⁺, suspended solids*, organic carbon*, chemical oxygen demand*, electrical conductivity, ammonia⁺, nitrogen and nitrate*. Monitoring of variables with * are based on UV/VIS spectra analysis, variables with + are done with ion selective electrodes (He *et al.* 2011; Campisano *et al.* 2013). While online monitoring of quality parameters is standard at WWTPs it is still rare in sewer networks (Olsson 2012). Approaches for real-time control now find their way into practice. Hoppe et al. (2011) for example use on-line TSS measurements for the control of a sewer network.

3.3.2. Actuators

Actuators for real-time control of urban wastewater treatment systems consist of:

Hydraulic actuators: These are aggregates to manipulate the flow in the WCTs e.g. by pumps (preferably frequency controlled for variable flows), gates, weirs, valves or flow splitters.

Chemical dosing devices: Chemical dosing devices are aggregates that adjust conditions in reactors to achieve aspired performances, e.g. adding readily biodegradable COD to enhance denitrification, pH control or addition of polymers to enhance sedimentation in SST.

Aeration devices: Aerators are essential aggregates for aerobic wastewater treatment. On the one hand artificial input of oxygen enhances the process of organic matter oxidation and nitrification and on the other hand the process of SASS demands additional aeration for endogenous respiration. Artificial aeration is predominantly done by mechanical surface aerators or more cost effective by turbine blowers creating fine bubbles. Aeration is energy intensive and is the main cost factor in wastewater treatment (Devisscher *et al.* 2006).

Details on actuators in integrated wastewater treatment systems are given in Campisano *et al.* (2013).

3.4. Real-time control

Control systems are referred to as real-time control if process variables are monitored online in the system and (almost) in real-time this data is used to operate actuators. Figure 3-1 depicts the control loop approach. A comprehensive review on real-time control of wastewater systems is given by Schütze *et al.* (2004). Real-time control can either be reactive or predictive (Lukasse and Keesman 1999).

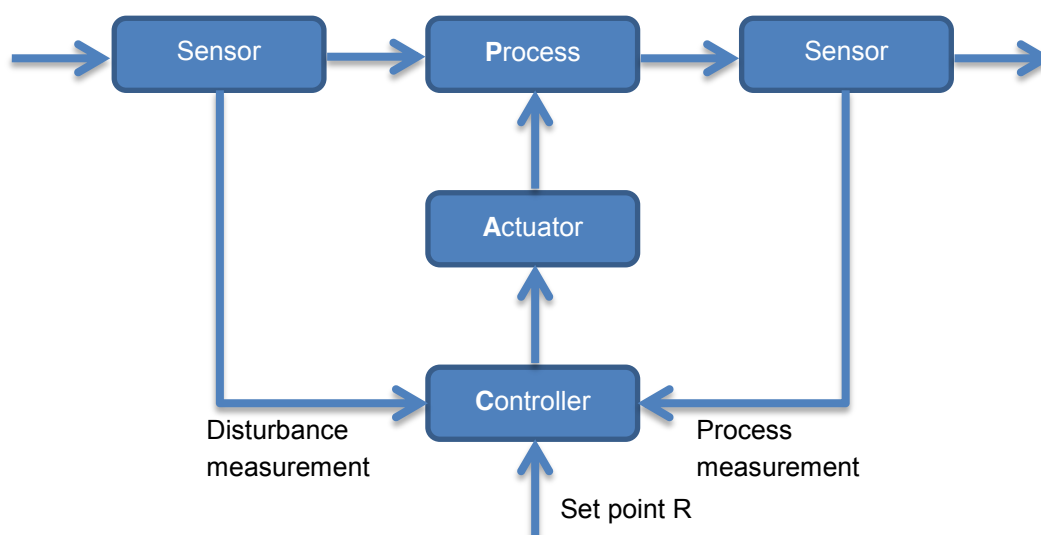


Figure 3-1: Real-time control approach with feed-forward and feed-back control loop based on disturbance and process measurements (taken from Schütze *et al.* (2004), modified)

3.4.1. Reactive real-time control

In reactive real-time control, control occurs in a feedback loop based on set-points for the variables of interest. Aim of the controller is to minimize the difference between the monitored process variables and desired set-points. Figure 3-2 depicts the general basic control loop approach. Established reactive real-time control approaches are on-off controllers and proportional-integral-derivative (PID) controllers (and their simplifications P, PI and PD). Equation 3-1 describes the general mathematical formulation.

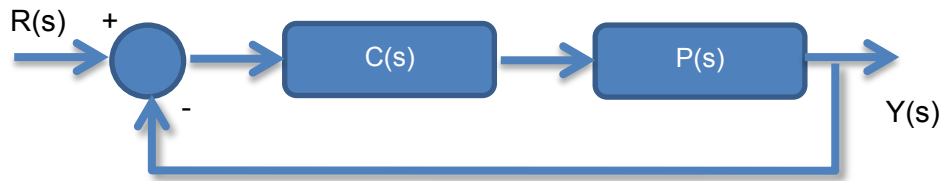


Figure 3-2: Basic control loop

$$C(s) = k_p \left(a + \frac{1}{T_i s} + b \frac{T_d}{\frac{T_d}{N} s + 1} \right) R(s) - k_p \left(1 + \frac{1}{T_i s} + \frac{T_d}{\frac{T_d}{N} s + 1} \right) Y(s) \quad \text{Equation 3-1}$$

with: k_p ... the controller proportional gain, T_i ... the integral time, T_d ... the derivative time, N ... the derivative filter, a , b ... the set-point weightings for proportional and derivative actions respectively, $R(s)$... the reference or set-point, $P(s)$... the process and $Y(s)$... the measured signal.

According to this, the following most popular controller concepts with their decision variables can be derived:

- PI: $\theta_{PI} = [k_p, T_i]$
- PD: $\theta_{PI} = [k_p, T_d]$
- PID: $\theta_{PI} = [k_p, T_i, T_d]$

Reynoso-Meza et al. (2014) provide a comprehensive introduction to the design of proportional controllers and their tuning. Popular applications in sewer networks are load control respectively DO control at WWTPs (e.g. Wahab et al. (2009)). The approach of Wahab et al. (2009) has shown to be robust but due to static set-points it is inappropriate for online optimization.

3.4.2. Predictive real-time control

Predictive real-time control is also known as MPC or RHOC. In the following, the term MPC is preferably used. In MPC control decisions for actuator settings are calculated online in parallel to the process. MPC systems have three major characteristics:

- Feed-back and feed-forward according to the receding horizon approach.
- Use of a process resp. prediction model for the evaluation of possible controller actions.
- An objective function to mathematically describe goals and constraints.
- Optimal actuator settings are calculated with the help of optimization algorithms.

The process model describes the development of the state variables according to actuator settings. Prediction models can be linear or nonlinear. Equation 3-2 to Equation 3-10 present the general mathematical description of linear and nonlinear MPC for a finite horizon.

$$\min_{\mathbf{u}(\tau)} J(\mathbf{x}(\tau), \mathbf{u}(\tau), t_c, t_p) \quad \text{Equation 3-2}$$

with:

- for the linear case

$$J(\mathbf{x}(\tau), \mathbf{u}(\tau), t_c, t_p) = \sum_t^{t+t_p} F(\mathbf{x}(\tau), \mathbf{u}(\tau)) \quad \text{Equation 3-3}$$

- for the nonlinear case

$$J(\mathbf{x}(\tau), \mathbf{u}(\tau), t_c, t_p) = \int_t^{t+t_p} F(\mathbf{x}(\tau), \mathbf{u}(\tau)) d\tau \quad \text{Equation 3-4}$$

$$F = (\mathbf{x} - \mathbf{x}_s)^T \mathbf{Q}(\mathbf{x} - \mathbf{x}_s) + (\mathbf{u} - \mathbf{u}_s)^T \mathbf{R}(\mathbf{u} - \mathbf{u}_s) \quad \text{Equation 3-5}$$

subject to:

$$\dot{\mathbf{x}}(\tau) = \mathbf{f}(\mathbf{x}(\tau), \mathbf{u}(\tau)), \forall \tau \in [t, t + t_p] \quad \text{Equation 3-6}$$

$$\mathbf{u}(\tau) \in \mathbf{U}, \forall \tau \in [t, t + t_p] \quad \text{Equation 3-7}$$

$$\mathbf{u}(\tau) = \mathbf{u}(\tau + t_c), \forall \tau \in [t + t_c, t + t_p] \quad \text{Equation 3-8}$$

$$\mathbf{x}(\tau) \in \mathbf{X}, \forall \tau \in [t, t + t_p] \quad \text{Equation 3-9}$$

$$\mathbf{x}(\tau) \in \mathbf{X}_f, \forall \tau \in [t, t + t_p] \quad \text{Equation 3-10}$$

with: $\dot{\mathbf{x}}$ representing the dynamic system in the form of differential equations or algebraic equations, \mathbf{x} ... the state variables, \mathbf{u} ... the control variables, t_c and t_p ... respectively the control and the prediction horizon, \mathbf{X}_f ... the terminal set, t ... the independent variable, τ ... the process family, J ... the objective or cost function, \mathbf{Q} and \mathbf{R} ... weight matrices.

Zhu et al. (2000) demonstrate the integration of linear and nonlinear MPC for plant-wide control by hybrid MPC.

The choice of appropriate solvers for mathematical optimization is case dependent and is predominantly based on the process model. An overview on and discussion of appropriate algorithms for MPC of wastewater treatment systems is given in Schütze et al. (2002) and with focus on sewer networks in Heusch (2011). While for offline control controller decisions are derived from predefined scenarios one major advantage of MPC is the calculation of optimal actuator settings based on the current and predicted state of the system. Figure 3-3 shows the RHOC approach for MPC. The receding horizon approach describes the consecutive optimization at each control step in MPC solving a finite horizon control problem. The optimization yields an optimal sequence of actuator settings for the objective functions and constraints for the evaluation. Only settings for the current control step are executed. Subsequently, the horizon moves on by the length of the control step and states are updated in the feedback loop. Thereby, the horizons for online optimization (control -, evaluation -, and prediction horizon) are consecutively updated according to passed control steps. Aim of the control approach is to minimize the difference between projected outputs

and their reference values by manipulating variables through actuator settings. Figure 3-4 shows the different time horizons in MPC and their relative sizes.

The *control horizon* is the period of time for which a set of control settings has to be computed with the help of an optimization algorithm. For control horizons shorter than the forecast horizon (also known as prediction horizon) control decisions must be extrapolated.

The *control step* (T_s) is the fixed step size during which controller actions are kept constant. Optimization is done for every T_s . After the elapse of T_s the control horizon moves on by the length of T_s according to the receding horizon approach.

The *evaluation horizon* is the period of time for which the computed controller actions are evaluated according to a process model.

The *forecast horizon* (also known as prediction horizon) is the period of time for which assumptions on the system input (e.g. flow or loads) can be done based on a forecast model. While simple approaches use constant inflow equal to the current inflow during the forecast horizon (Fiorelli *et al.* 2013) sophisticated approaches are based on rainfall now-casting (Liguori *et al.* 2012). For forecast horizons shorter than the prediction horizon assumptions on system input must additionally be defined (e.g. no inflow).

Figure 3-5 illustrates the principle of MPC for supervisory control. Hereby, MPC is used for online optimization of set-points for PI resp. PID controllers. This is often used at WWTPs for the online optimization of set-points such as reference values for DO control (e.g. Ostace *et al.* (2010)).

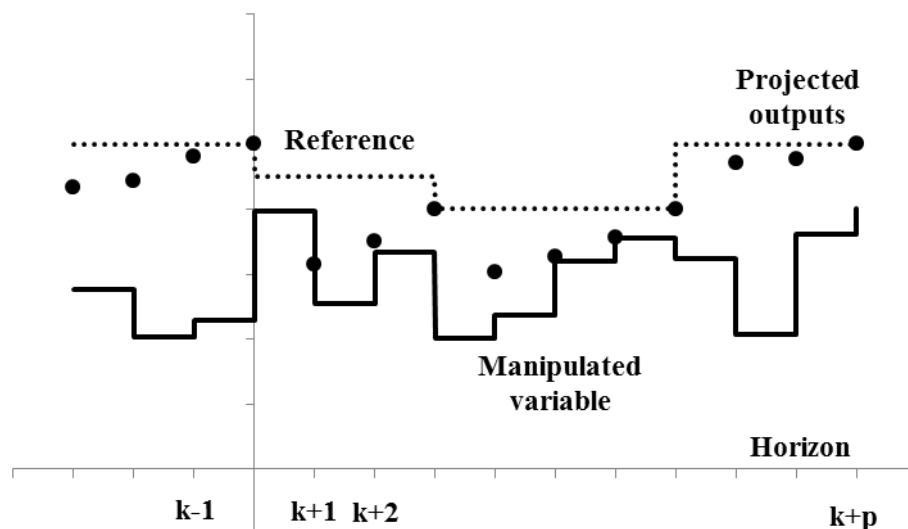


Figure 3-3: Model predictive control according to the RHOC approach

In process control the general goal is to maintain a variable from a specific process in a desired range. While in conventional reactive control compensational adjustments are made on the manipulated variable due to differences between a measured variable and a set point, in MPC controller actions are based on dynamic models of the process. These models can

be either linear or nonlinear. The ideas of RHOC and MPC can be tracked back to the 1960s (García *et al.* 1989). First fields of application were within the chemical and oil refinement industry and later in power system balancing systems (Xi *et al.* 2013). The advantage over responsive controllers such as PID controllers is the ability to predict future conditions and hence prepare control actions in advance. This is especially of advantage in systems with large time delays and high-order dynamics as it is the case in integrated WCTSs. Nevertheless, the choice of the control approach is always linked to the specific system and process to be controlled. A comprehensive introduction in MPC is given e.g. by Morari and Lee (1999).

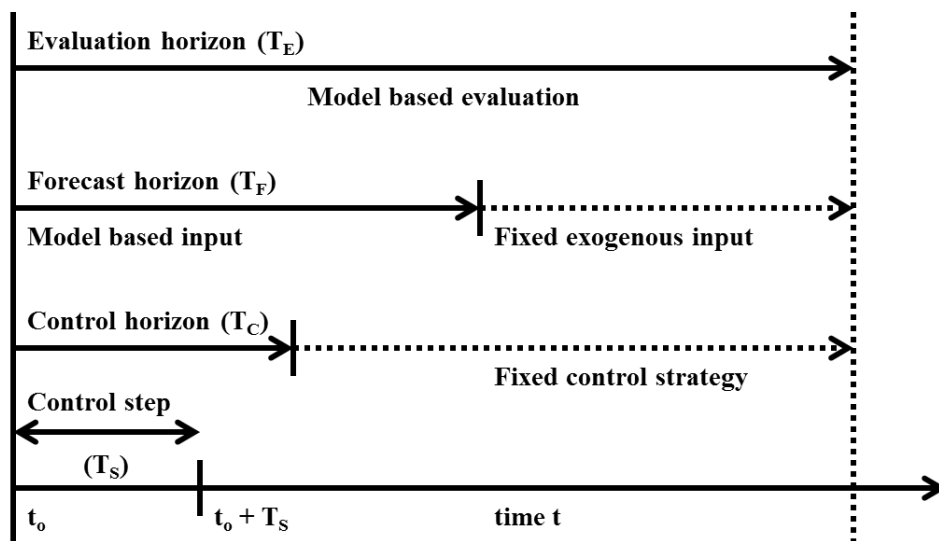


Figure 3-4: Time horizons in MPC and their relative sizes (according to Wolfgang Rauch and Harremoës (1999), modified)

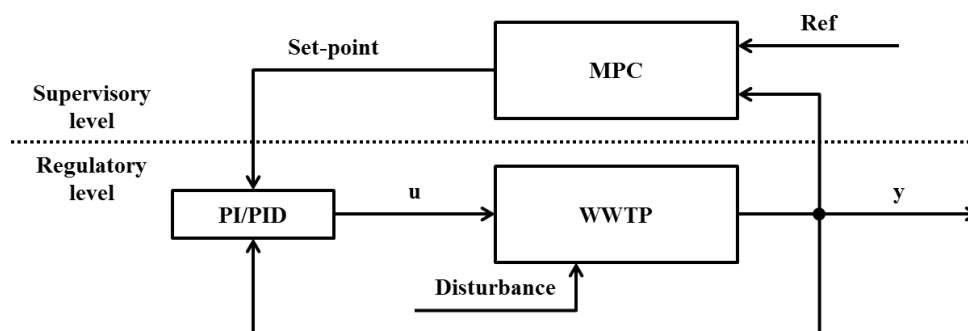


Figure 3-5: Supervisory MPC with online set-point optimization for PI/PID control (according to (Ostace *et al.* 2010), modified)

3.4.2.1. MPC of sewer networks

Traditionally, sewer networks and WWTPs are operated and controlled separately and often it is still the case (Schütze *et al.* 2004). Sewer network control evolved in the USA in the 1960s (Schilling *et al.* 1996). The main objective of combined sewer network control is to minimize CSO volume and frequency. Common additional objectives are e.g. (Marinaki and Papageorgiou 2005):

- fast emptying of retention tanks,

- constant inflow to the WWTP,
- minimization of actuator actions.

MPC of sewer networks attracts the scientific community for two decades now. While early publications investigated the general benefit of MPC of sewer networks (Beeneken *et al.* 2013) more recent studies predominantly study different approaches for prediction models and optimizers. Investigated prediction models range between linear approaches based on simple hydraulic translation with constant flow times (e.g. Fiorelli *et al.* (2013)), nonlinear approaches based on hydrodynamic models (e.g. Heusch *et al.* (2012)) and hybrid approaches based on piece-wise linear prediction models (e.g. Ocampo-Martinez and Puig (2010)). Computational effort is still the major problem for nonlinear prediction models in practical installations (Heusch *et al.* 2012). Due to this, prediction models for MPC of sewer networks are predominantly linear. Consequently, hydrodynamic prediction models are limited to rule-based real-time control approaches (Fuchs and Beeneken 2005). Optimization approaches are strongly linked to the objective function and hence to the prediction model. In the case of nonlinear functions or models derivative free optimization algorithms are needed such as genetic algorithms (e.g. Rauch and Harremoës (1999)) or pattern search algorithms (e.g. Leirens *et al.* (2010)). The advantage of linear optimization algorithms is their speed and robustness (Fiorelli *et al.* 2013).

Studies on water quality based approaches such as turbidity are still limited to rule-based real-time control approaches due to the nonlinearity of their prediction models (e.g. Hoppe *et al.* (2011), Weinreich *et al.* (1997)).

Reports on successful installations of sewer network real-time control are still rare compared to the number of research publications. Examples are Bordeaux – France (Kopečný *et al.* 2000); Montreal – Canada (Fradet *et al.* 2010); Québec – Canada (Pleau *et al.* 2001); Paris – France, Louisville – USA, Wilmington – USA (Colas *et al.* 2004); Bogota – Columbia (Zamora *et al.* 2010); Barcelona – Spain (Cembrano *et al.* 2004); Seattle – USA (Gelormino and Ricker 1994); Copenhagen – Denmark (Grum *et al.* 2011) or Haute-Sûre – Luxembourg (Fiorelli *et al.* 2013).

Comprehensive additional information on MPC of sewer networks is given in Heusch (2011) and Ocampo-Martinez (2010).

3.4.2.2. MPC of wastewater treatment plants

MPC of WWTPs has been investigated since the end of the 1990s. The main objective in wastewater treatment is the elimination of pollution contained in the influent to the WWTP according to legal effluent concentration limits. Consequently, effluent concentration limits are no set-points but constraints. Due to rising energy costs and a general increasing awareness of sustainability energy efficiency is also in the focus of WWTP operators. Hence, minimization of treatment costs is the second objective in MPC of WWTPs (Holenda *et al.* 2008).

Studies can be classified into approaches for (I) feedback control replacing conventional PI or PID controllers (e.g. Chotkowski *et al.* (2005)) and (II) supervisory feedback MPC

approaches where the aim is to find optimal set-points (Ostace *et al.* 2010). Both of these particular applications show good results. While modeling studies can make use of full IWA ASM 1-3 installations with dynamic SST models (e.g. Shen *et al.* (2008), Stare *et al.* (2007) and Ostace *et al.* (2011)) the main challenge in practical installations of MPC of WWTPs based on simplified prediction models are robustness problems caused by model mismatches (Weijers 2000). Successful implementations of MPC of WWTPs for DWF operation show real energy reductions of up to 25 percent (e.g. (O'Brien *et al.* 2011)).

A comprehensive discussion on MPC of WWTPs is given by Weijers (2000). Further details on MPC of WWTPs can be found in Vanrolleghem (1995) and Rauch and Harremoës (1999).

3.4.2.3. System-wide MPC of integrated wastewater treatment systems

System-wide control of integrated wastewater treatment systems describes the combined control and operation of sewer networks and WWTPs (Olsson and Jeppsson 2006). Translating this to MPC the inflow to the WWTP is no longer an external disturbance but an internal variable and vice versa (Olsson and Jeppsson 2006). Beside simplified prediction models for ASMs a major challenge is to find such models for the dynamic sedimentation process of SSTs (Diehl and Farås 2012). A possibility to overcome this problem is the continuous measurement of the sludge level in the SST with fixed set-points for critical states (Seggelke *et al.* 2005). Sludge level measurement approaches are only practicable if there is a retention tank for influent control upstream just in front of the WWTP and reactions towards hydraulic overloading of the SST are quickly possible. Due to decentralized retention tanks and long transport times in ISNs this is seldom the case in rural WCTSs. Consequently, MPC of rural sewer networks with central wastewater treatment is feed-forward. Thereby, system-wide MPC approaches are “ballistic” since actuator settings for sewer network control cannot be revised.

Studies on integrated MPC are rare. Rauch and Harremoës (1999) investigated the potential of integrated MPC. Their results show the increase of performance according to the treatment potential of the WWTP. Fu *et al.* (2008) investigated the potential of multi-objective optimal control based on genetic algorithms with focus on receiving waters. Meirlaen (2002) investigated system-wide real-time control of integrated WCTSs from an immission-based point of view. Tränckner *et al.* (2007) used a simple prediction model for the nitrification capacity of the WWTP based on steady state assumptions. The approach especially shows benefits for small and medium events. Brdys *et al.* (2008) investigated supervisory MPC of integrated wastewater treatment systems with a focus on temporal resolutions of the different processes.

Integrated real-time control studies predominantly focus on offline optimized rule-based approaches (e.g. Seggelke *et al.* (2005)). Especially immission-based approaches highlight the interactions between real-time control and receiving water quality (e.g. Langeveld *et al.* (2013)). Practical implementations are reported for instance for the cities of Québec, Canada (Pleau *et al.* 2005), Wilhelmshafen, Germany (Seggelke *et al.* 2013) or Copenhagen, Denmark (Grum *et al.* 2011).

3.4.2.4. Decision-making in system-wide control of centralized wastewater treatment systems

As shown before sub-goals in system-wide control can be conflicting. When conflicting, the MPC problem becomes a multi-criteria optimization problem. Thereby, optimal solutions are a trade-off between the conflicting objectives. For the case of non-conflicting objectives optimal solutions per sub-goal can be derived in parallel (Olsson and Jeppsson 2006). For optimal control, we usually seek Pareto-optimal solutions for each control step (Miettinen 1999) where all objectives have been improved until further improvements only lead to trade-offs between conflicting objectives. This set of optimal solutions is called Pareto-front.

Definition 3-1. *Pareto Optimal: A point $x^* \in X$, is Pareto optimal if there does not exist another point, $x \in X$, such that $F(x) \leq F(x^*)$, and $F_i(x) < F_i(x^*)$ for at least one objective function.*

For control, operators have to choose a preferable one from this set of alternatives which resembles decision-making (Reynoso-Meza *et al.* 2014). Consequently, decision-making in the conventional MPC approach resembles the tuning of objectives and constraints in the objective by the help of weighting matrices Q and R in Equation 3-5. Descriptive examples of this process in control approaches of urban WCTs can be found for instance in Seggelke *et al.* (2005) or Fiorelli *et al.* (2013). Seggelke *et al.* (2005) describe the tuning of the WWTP loading during CWWF. Fiorelli *et al.* (2013) illustrate the tuning of specific objectives of a MPC approach for a sewer network. If this tuning is done by trial-and-error the Pareto-front stays unknown. Offline tuning is not straight-forward, computational expensive (Reynoso-Meza *et al.* 2014) and limited to the chosen range of data for simulation-based evaluation. Consequently, parameter tuning is rare in practice. Additionally, the chosen set of weights is aggregated according to the testing data and not event specific based on the aggregation of operator preferences.

4. Fuzzy multi-criteria decision-making

A different approach to the conventional decision-making respectively tuning of weights in MPC presented in section 3.4.2.4 is FPC. By replacing the cost function to be optimized within the RHOC approach by a function for fuzzy multi-criteria decision-making FPC dynamically considers decision-making according to the preferences of the operator in each control step. Thereby, decision-making is done according to the aggregation of the single objectives consisting of goals and constraints. The approach thereby mimics human decision-making by compromising conflicting objectives according to their preferences in the ranges between total acceptance and total rejection described by their fuzzy membership functions. The following chapter describes the principles of multi-criteria decision-making with fuzzy membership functions.

4.1. Decision making

Decision-making can be described as the choice of an action from a discrete set of alternatives. The science of decision-making distinguishes two main fields (Sousa and Kaymak 2002):

- Descriptive decision-making
- Normative decision-making.

In descriptive decision-making the aim is to study the cognitive process that leads to the selection of actions among alternatives which resembles the information processing process. In contradiction normative decision-making considers the choice of the best action as a rational process and is hence comparable to an optimization process. This allows the following mathematical formulation of the rational decision-making process (Equation 4-1):

$$a^* = \max_{a \in A} D(\kappa(a)) \quad \text{Equation 4-1}$$

with: a^* ... the best decision alternative, A ... the set of alternatives, D ... the decision function and $\kappa(a) = [\kappa_1(a), \dots, \kappa_n(a)]^T$... vector for n different decision criteria.

In control engineering practice normative decision-making is the favorite approach (Sousa and Kaymak 2002). In engineering decision-making is predominantly applied as a planning process. This process can involve many aspects, depending on the objectives of the decision-maker. Consequently, classification of decision problems is manifold. Sousa and Kaymak (2002) present the following main types of classification:

- **Multi-stage vs. single-step decisions:** Decisions can either be made within one single step or decision-making may include several steps due to complexity.
- **Multi-person vs. individual decisions:** Decisions can be made either by one person or can include several people.
- **Multi-criteria vs. simple optimization decisions:** Due to the complexity of the decision problem the process includes either several conflicting objectives or is rather simply structured.
- **Operational vs. exploratory decisions:** While operational decision problems are clearly defined, exploratory decision problems are ill-defined in the beginning. In such cases the decision-making process usually consists of a number of iterations which

decrease uncertainty consecutively. This finally leads to the specification of decision goals and constraints.

- **Probabilistic vs. deterministic decisions:** Sophisticated decision-making approaches additionally take uncertainties into account.

In control decision-making usually is operational since the goals and constraints are known beforehand. Predominantly, a single controller makes decisions. In feed-back control decisions predominantly can be made in a single step while in MPC the system's future behavior is considered usually taking several control steps into account. Consequently, these are multi-stage, multi-criteria, individual, operational decisions. While conventional decision-making predominantly is deterministic, fuzzy approaches can take vagueness and non-probabilistic uncertainties into account (Sousa and Kaymak 2002).

As described in section 3.4.2 MPC is an optimization problem. Due to the mathematical formulation of optimization problems as decision-making problems, a wide range of weighting approaches for decision aid exist. Mattson and Messac (2005) distinguish two main approaches for the treatment of multi-objective problems in optimization: Aggregate objective function approaches for a priori decision-making and generate-first choose-later approaches for a posteriori decision-making. The premier describes the decision-making in advance of the optimization process. In the second case the optimal solution is chosen after the multi-criteria optimization from the Pareto-front of optimal solutions respectively from a population of alternatives (Muschalla 2009). Marler and Arora (2004) provide a comprehensive overview on multi-objective optimization approaches for engineering classified according to a priori and a posteriori articulation of preferences.

For further information on multi-criteria decision-making the interested reader is referred for instance to Zopounidis and Doumpos (2002). Ribeiro (1996) additionally provides a comparison to classical discrete decision-making approaches.

4.1.1. A priori

A priori decision-making in multi-criteria optimization is done by the weighting of preferences in an aggregated objective function. Main advantage of a priori decision-making approaches in control is the reduction of the multi-objective optimization problem to a single-objective one. Consequently, the optimization approach is no more limited to those able to deal with multi-objective ones. As mentioned before the weighted sum approach is predominantly used in a priori decision-making approaches in MPC (Equation 4-2).

- Weighted sum method

$$U = \sum_{i=1}^k w_i F_i(x)$$

Equation 4-2

with: x ... the vector of design variables, F ... the vector of objective functions, w ... the vector of weighting coefficients, k ... the number of objective functions and U ... the aggregated objective function (also known as cost function).

In the framework of sewer network applied MPC Fiorelli and Schutz (2009) for instance investigate the influence of different a priori weighting scenarios on the global performance

of a linear MPC approach for CSO minimization for a small number of characteristic rain events based on the weighted sum approach.

For Pareto-optimal solutions the Pareto front must be investigated offline via multi-criteria optimization of the weighting coefficients (Fiorelli *et al.* 2013). The illustration of the Pareto front provides helpful information on the impact of different weighting coefficient scenarios (Mattson and Messac 2005). Due to the computational effort tuning is predominantly reduced to trial-and-error approaches in real implementations (Garriga and Soroush 2010).

4.1.2. A posteriori

In a posteriori decision-making an optimal solution is chosen from the generation of semi equal alternatives, the so called Pareto front. Consequently, all variants must be simulated. For this purpose Pareto optimization approaches are necessary. Details on such approaches can be found in Fu *et al.* (2008) and Marler and Arora (2004). Due to their computational effort a posteriori approaches are limited to offline optimization. They are seldom feasible in MPC of IUWTS where online optimization is needed (Muschalla 2009).

4.1.3. Optimization problem

As seen before the decision-making process can be formulated as an optimization problem. The standard formulation of an optimization problem is in terms of minimization (Equation 4-3) (Rao 2009):

$$\min_X f(X) \tag{Equation 4-3}$$

Subject to the constraints

$$\begin{aligned} g_i(X) &\leq 0, & i &= 1, 2, \dots, m \\ h_j(X) &= 0, & j &= 1, 2, \dots, n \end{aligned} \tag{Equation 4-4}$$

with: X ... the n -dimensional design vector, $f(X)$... the objective function, $g_i(X)$... the inequality constraints and $h_j(X)$... the equality constraints.

Depending on the problem optimization problems can be stated with or without constraints. Maximization is formulated through the inversion of minimization. By solving more than one objective function the problem becomes multi-objective. In the case of conflicting objectives the result will be the Pareto set which is a set of trade-offs where each objective cannot be improved without worsening another objective. Multi-objective optimization can be handled either single-modal or multi-modal. In the first case the objective functions are aggregated into one objective function. Decision-making must be done a priori through weighting of the single objectives (Fiorelli and Schutz 2009). In the latter case the decision-making is based on the Pareto set a posteriori. Popular solving algorithms are for example evolutionary algorithms. For further details on multi-modal optimization the reader is referred to (Muschalla 2009). Details on the variety of optimization approaches are provided for example by (Fletcher 2013) or (Rao 2009).

4.1.4. Satisficing

In contrast to optimal decision-making where the best decision is Pareto-optimal the approach of satisficing aims at finding solutions which satisfy a set of constraints until an acceptable threshold is met. Especially in real-time control this is often necessary when

decisions must be done in a limited time frame while the optimization problem is non-convex (Chen *et al.* 2003). The satisficing problem can be stated in an analogous way to the decision-making problem.

4.2. Fuzzy set theory

Fuzzy set theory was first introduced by Zadeh (1965) in 1965. Based on his work the foundations of fuzzy set theory will be described in the following. Fuzzy set theory is an extension of the classical definition of sets. The classical “crisp” set theory is based on the principle of binarity where elements either belong or do not belong to the set – their membership is either 1 (member) or 0 (non-member). In contradiction, in fuzzy set theory the membership of elements to the set is expressed gradually by a function usually in the real unit interval [0 1]. The advantages of this are used whenever problems are difficult to be expressed by classical sets such as in linguistics or decision-making. For further details the reader is referred to the works of, for instance, Zimmermann (2001).

Definition 4-1. *Membership: The membership of an element x to a subset A of the universal set U is described by:*

$$\mu_A(x) = \begin{cases} \mathbf{1} & \text{if } x \in A \\ \mathbf{0} & \text{otherwise} \end{cases}$$

For conventional sets the valuation set is $\{0, 1\}$. By replacing it with the closed set $[0, 1]$, a fuzzy set A is defined.

Definition 4-2. *Fuzzy set: A set A is called a fuzzy set if each element of x of A is characterized by a membership function which associates each element a real number in the interval $[0, 1]$.*

$$A = \{[x, \mu_A(x)]: x \in U, \mathbf{0} \leq \mu_A(x) \leq \mathbf{1}\}$$

Definition 4-3. *Support: The set $\{x \in A \mid \mu_A(x) > \mathbf{0}\}$ is called support of (A, μ) .*

Definition 4-4. *Core: The set $\{x \in A \mid \mu_A(x) = \mathbf{1}\}$ is called core of (A, μ) .*

The basic operations for fuzzy sets are defined similar to the ones for conventional sets. Hence, for 2 fuzzy sets A and B on the universe X and a given element x of the universe the following definitions of fuzzy operations are given according to Zadeh (1965):

Definition 4-5. *Union resp. fuzzy-OR:*

$$\mu_{A \cup B}(x) = \mu_A(x) \vee \mu_B(x) \equiv \max_{x \in X} \{\mu_A(x), \mu_B(x)\}$$

Definition 4-6. *Intersection resp. fuzzy-AND:*

$$\mu_{A \cap B}(x) = \mu_A(x) \wedge \mu_B(x) \equiv \min_{x \in X} \{\mu_A(x), \mu_B(x)\}$$

Definition 4-7. *Complement resp. fuzzy-NOT:*

$$\mu_{\bar{A}}(x) = \mathbf{1} - \mu_A(x)$$

Definition 4-8. *Empty set ϕ :*

$$\mu(\phi) = 0$$

Definition 4-9. *Entity X :*

$$\mu(X) = 1$$

Likewise, De Morgan's laws also hold for fuzzy sets:

$$\overline{A \cap B} = \overline{A} \cup \overline{B} \quad \text{Equation 4-5}$$

$$\overline{A \cup B} = \overline{A} \cap \overline{B} \quad \text{Equation 4-6}$$

Since fuzzy sets can overlap, the definition of the excluded middle operation is different from conventional sets.

Definition 10: Excluded middle

$$A \cup \overline{A} \neq X$$

$$A \cap \overline{A} \neq \phi$$

4.3. Decision-making with fuzzy objectives and fuzzy constraints

In FDM the fuzziness of the system is modeled by fuzzy goals, fuzzy constraints and fuzzy decisions. The approach was first introduced by Bellman and Zadeh in 1970. FDM is proposed to deal with non-probabilistic uncertainty and vagueness in the particular case (Sousa and Kaymak 2002).

In decision-making the set of alternatives A cannot always be expressed explicitly but is often defined implicitly by constraints (Equation 4-8). These constraints define the search space. Due to the clear distinction between the goals represented by the objective function and constraints, this decision model is called an asymmetric model. By replacing the crisp goals and constraints with their fuzzy equivalents the conventional decision-making becomes a fuzzy one. Due to Bellman and Zadeh (1970) a fuzzy goal G is defined as a fuzzy set on a set of alternatives A characterized by its membership function describing the degree of satisfaction to the specified decision (Equation 4-7).

$$\mu_G : A \rightarrow [0, 1] \quad \text{Equation 4-7}$$

Further, Bellman and Zadeh (1970) define the fuzzy constraint C as a fuzzy set on a set of alternatives A characterized by its membership function describing the fuzzy region within the set of possible solutions (Equation 4-8).

$$\mu_C : A \rightarrow [0, 1] \quad \text{Equation 4-8}$$

The support of a fuzzy constraint determines the set of possible alternatives for the decision-making problem. The support defines the crisp constraints while the solution set adds possible violation to the constraints.

Since a decision should satisfy both goals and constraints Bellman and Zadeh (1970) propose the fuzzy decision Z as the fuzzy set resulting from the intersection of a fuzzy goal G and a fuzzy constraint C (Equation 4-9).

$$Z = G \cap C \quad \text{Equation 4-9}$$

The corresponding membership function characterizes the fuzzy decision (Equation 4-10):

$$\mu_Z(x) = \min[\mu_G(x), \mu_C(x)] \quad \text{Equation 4-10}$$

The optimal decision λ^* is the maximum value of the membership function μ_Z , also called the maximizing decision (Equation 4-11).

$$\mu_Z(x) = \lambda^* = \max_{x \in Z} [\mu_Z(x)] \quad \text{Equation 4-11}$$

It is important to state that fuzzy goals and fuzzy constraints are treated equally in FDM. In comparison to crisp decision-making fuzzy goals and fuzzy constraints also quantify the degrees to which the objectives are reached and hence make the decision-making process more transparent.

Nevertheless, crisp constraints can be considered in FDM by incorporating crisp equivalents (Sasikumar and Mujumdar 1998). This is for instance necessary in the case of mass balances for minimum effluent concentrations at WWTPs. For the set of crisp constraints $g_h(X) \leq 0$, $h = 1, 2, \dots, n_G$, the FDM problem becomes (Equation 4-12):

$$\begin{aligned} \max \quad & \lambda && \text{Equation 4-12} \\ \text{subject to} \quad & \mu_Z(X) \geq \lambda \quad \forall y \\ & g_h(X) \leq 0 \quad \forall h \\ & 0 \leq \lambda \leq 1 \end{aligned}$$

4.3.1. Membership functions

A membership function for a fuzzy set A on the universe of discourse X maps each element of X to a value between zero and one, the membership value. Hence, this value describes the degree of membership of the element X to the fuzzy set Z (Zadeh 1965) resembling the degree of preference in the decision-making process (Equation 4-13). Thereby the value of one is equal to absolute preference and zero equals absolute rejection.

$$\mu_Z : X \rightarrow [0, 1] \quad \text{Equation 4-13}$$

In principle any continuous function can be used as a fuzzy membership function. Usually, simple functions are preferred, such as:

- Triangular membership functions (Equation 4-14 resp. Figure 4-1A)

$$\mu_Z(x) = \begin{cases} 0, & x \leq a \\ \frac{x-a}{m-a}, & a < x \leq m \\ \frac{b-x}{b-m}, & m < x < b \\ 0, & x \geq b \end{cases} \quad \text{Equation 4-14}$$

and

- Trapezoidal membership functions (Equation 4-15 resp. Figure 4-1B)

$$\mu_Z(x) = \begin{cases} 0, & x \leq a \\ \frac{x-a}{b-a}, & a < x \leq b \\ 1, & b \leq x \leq c \\ \frac{d-x}{d-c}, & c \leq x \leq d \\ 0, & d \leq x \end{cases} \quad \text{Equation 4-15}$$

Case specific alternatives are especially for emphasizing certain ranges in the MF:

- R or Z type membership functions (Equation 4-16 resp. Figure 4-1D)

$$\mu_Z(x) = \begin{cases} 1, & x \leq a \\ 1 - 2 \cdot \left(\frac{x-a}{b-a}\right)^2, & a \leq x \leq \frac{a+b}{2} \\ 2 \cdot \left(\frac{x-b}{b-a}\right)^2, & \frac{a+b}{2} \leq x \leq b \\ 0, & x \geq b \end{cases} \quad \text{Equation 4-16}$$

- L or S type membership functions (Equation 4-17 resp. Figure 4-1E)

$$\mu_Z(x) = \begin{cases} 0, & x \leq a \\ 2 \cdot \left(\frac{x-a}{b-a}\right)^2, & a \leq x \leq \frac{a+b}{2} \\ 1 - 2 \cdot \left(\frac{x-b}{b-a}\right)^2, & \frac{a+b}{2} \leq x \leq b \\ 1, & x \geq b \end{cases} \quad \text{Equation 4-17}$$

- Gaussian membership functions (Equation 4-18 resp. Figure 4-1C)

$$\mu_Z(x) = e^{-\frac{(x-c)^2}{2\sigma^2}} \quad \text{Equation 4-18}$$

Figure 4-1 illustrates the described membership functions (MF). The choice and design of appropriate membership functions is always case-dependent.

4.3.2. Aggregation

In FDM multi-objective decision-making is made a priori by aggregating the single objectives to one objective function (Equation 4-19). Bellman and Zadeh (1970) propose the fuzzy-MIN operator for aggregation. The aggregation of single objectives according to AND-conjunctions does not allow any compensation within the aggregation of single objectives. Dependent on the specific case, this is not always wanted. Table 4-1 gives an overview of common aggregation functions and their characteristics relating to compensational effects (Rommelfanger 1994).

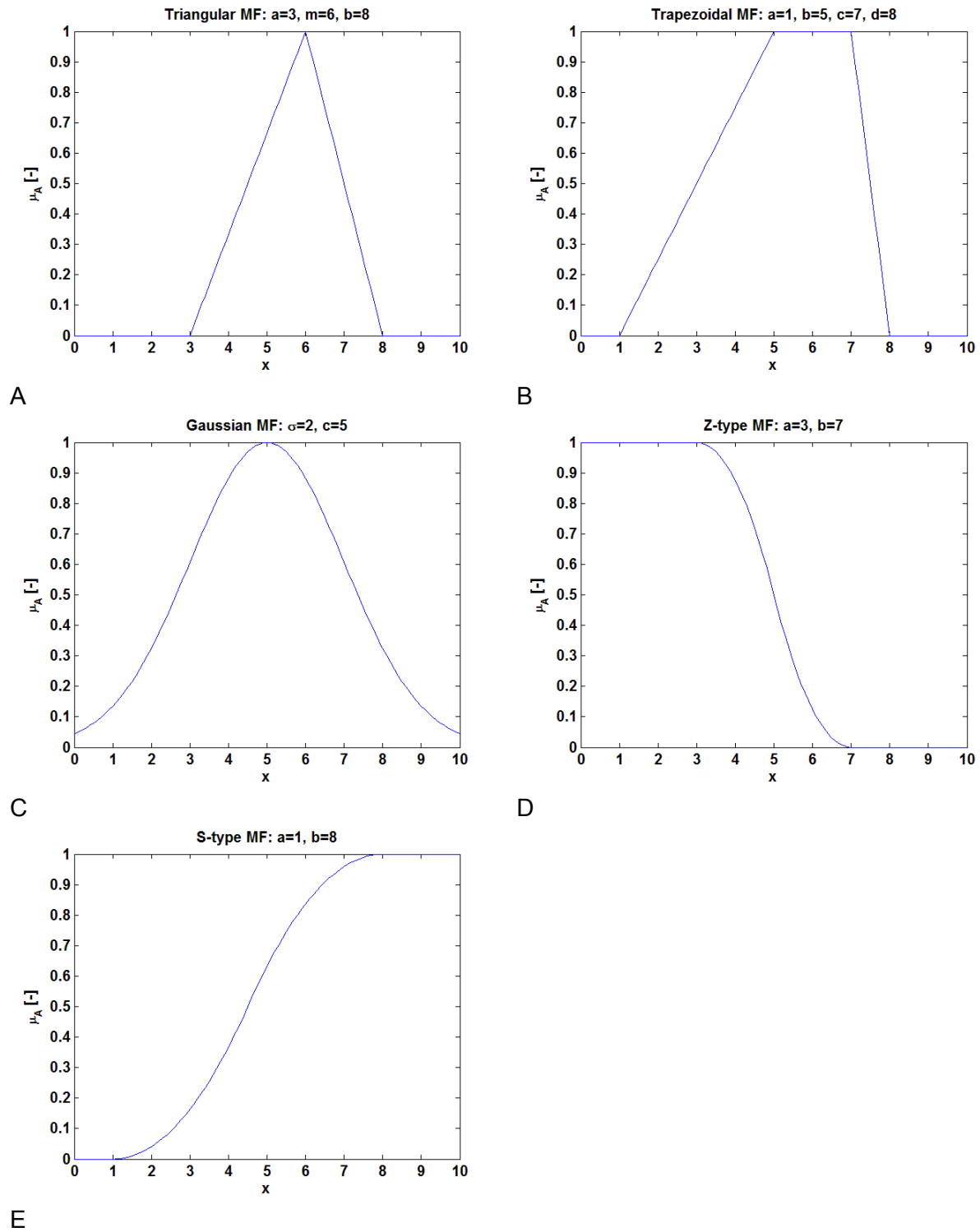


Figure 4-1: Common types of MFs (A) triangular, (B) trapezoidal, (C) Gaussian, (D) Z-type, (E) S-type

For simplification Dubois and Prade (1984) present a general notation for FDM without the explicit naming of conjunctions (Equation 4-19).

$$\mu_Z(x) = h(\mu_1(x), \dots, \mu_N(x))$$

Equation 4-19

Table 4-1: Common aggregation functions and their compensation effect

Operator	Function	Compensation
Algebraic product	$\mu_A \cdot \mu_B$	Unwanted
MIN	$\min(\mu_A, \mu_B)$	↑
Geometric mean	$\sqrt{\mu_A \cdot \mu_B}$	
Arithmetic mean	$0.5 \cdot (\mu_A + \mu_B)$	↓
MAX	$\max(\mu_A, \mu_B)$	
Algebraic mean	$\mu_A + \mu_B - \mu_A \cdot \mu_B$	Wanted

4.3.3. Weighting

Without weighting all objectives in the FDM function have equal impact on the decision-making. Similar to conventional decision-making a priori weighting of sub-goals is possible. Conventional approaches are:

- Weighted sum

$$\mu_D(x) = \sum_{i=1}^N \alpha_i \cdot \mu_i(x) \quad \text{Equation 4-20}$$

with: $\sum_{i=1}^N \alpha_i \equiv 1$

- Modifiers

$$\mu_{mod}(x) \equiv \mu^\gamma(x), \quad \gamma > 0 \quad \text{Equation 4-21}$$

- Multipliers

$$\mu_D(x) = h(\lambda_1 \cdot \mu_1(x), \dots, \lambda_N \cdot \mu_N(x)), \quad 0 \leq \lambda_i \leq 1, \quad i = 1, \dots, N \quad \text{Equation 4-22}$$

The selection of an appropriate weighting function is case specific. Specific influences have been studied in several works. Further details are given for example in Dubois and Prade (1984), Kaymak and Sousa (2003) or Mendonça et al. (2006). In the present study FDM will be used to illustrate conflicting objectives in the system-wide control of IUWTS. Consequently, no additional a priori weighting will be used.

5. Development of a multi-objective fuzzy predictive controller for system-wide control of integrated wastewater collection and treatment systems in rural regions

The ability of human operators to control complex, nonlinear or partially unknown systems often outperforms conventional linear or partial-linear control approaches (da Costa Sousa and Kaymak 2001). Fuzzy logic control is an established technique to implement human expert knowledge into the control of technical systems. It is established in many industrial branches. A comprehensive overview on industrial applications is given for instance by Precup and Hellendoorn (2011). Considering applications in WCTSSs, approaches have been investigated for sewer networks (for instance by Klepiszewski and Schmitt (2002), Hou and Ricker (1992), Fuchs et al. (1997) and Tamaki (1994)), for WWTPs (for instance by Ruano et al. (2010), Traoré et al. (2006), Tsai et al. (1994), Rammacher and Hansen (2000), Couillard and Zhu (1992), Belchior et al. (2012), Kalker et al. (1999) and Tong et al. (1980)) and for the integrated control of sewer network and WWTP (for instance by Seggelke et al. (2013)). Reported results are predominantly positive. The number of studies especially related to WWTPs and the reported benefits confirm the practicability of fuzzy logic control for the control of highly nonlinear systems (Jeppsson 1995). As described in section 3.4, reactive real-time control considered on its own is not suitable for predictive optimization. Consequently, it is the aim of the present PhD study to transfer the positive features of fuzzy logic control to MPC by implementing FDM as described in the previous chapter for FPC. System-wide FPC will be systematically used to investigate interactions of subsystems due to the integrated control of WCTSSs in rural catchments. The present chapter describes the principles of FPC and its implementation for system-wide control of WCTSSs in rural catchments. The choice and development of appropriate process models for MPC is discussed. Thereby, the system-wide control of sewer network discharges and WWTP loading according to the actual capacity is based on the development of a novel Lagrangian wastewater tracking model.

5.1. Fuzzy predictive control

FPC combines conventional MPC and fuzzy multi-criteria decision-making. Thereby, MPC objectives consisting of goals and constraints are described by MFs according to fuzzy set theory (see section 4.2) and FDM (see section 4.3) as introduced by Bellman and Zadeh (1970). Assuming a control problem described by $i = 1 \dots q$ goals G_i and $l = 1 \dots r$ constraints C_l μ_{G_i} and μ_{C_l} are the MFs that represent the satisfaction of the fuzzy goals respectively fuzzy constraints by mapping from the space of goals G_i respectively the space of constraints C_l to the interval $[0,1]$. Fuzzy objectives can be defined for the domain of control actions, system's outputs, state variables or for any other suitable domain. Usually, fuzzy constraints are defined in the domain of control actions and fuzzy goals in the domain of state space variables (da Costa Sousa and Kaymak 2001). In the predictive control scheme all the chosen objectives must be evaluated at each sample time within the prediction horizon. For multiple-input-multiple-output systems a policy π of control actions is defined according to Definition 5-1 (da Costa Sousa and Kaymak, 2001).

Development of a multi-objective fuzzy predictive controller for system-wide control of integrated wastewater collection and treatment systems in rural regions

Definition 5-1. Policy: A policy π is a sequence of control actions for the entire prediction horizon H_p in MPC.

$$\pi = \mathbf{u}(k), \dots, \mathbf{u}(k + H_p - 1), \pi \in \Omega$$

with: Ω ... set of alternatives, H_p ... prediction horizon, u ... control variable

The decision per control step is derived from the MF μ_π for the policy π according to a decision function. A variety of aggregation functions for decision-making is presented in section 4.3.2 and discussed in Table 4-1. Equation 5-1 generally describes the aggregation process.

$$\mu_\pi = \varphi(\mu_{G_1} \dots \mu_{G_q}, \mu_{C_1} \dots \mu_{C_r}) \quad \text{Equation 5-1}$$

with: φ ... the decision function that aggregates the objectives, μ ... membership function, G ... goals and C ... constraints

The aim of the presented approach is to find the maximum satisfaction of the aggregated MF. Consequently, the optimum policy π^* is found by the maximization of μ_π :

$$\pi^* = \underset{\mathbf{u}(k), \dots, \mathbf{u}(k+H_p-1)}{\operatorname{argmax}} \mu_\pi \quad \text{Equation 5-2}$$

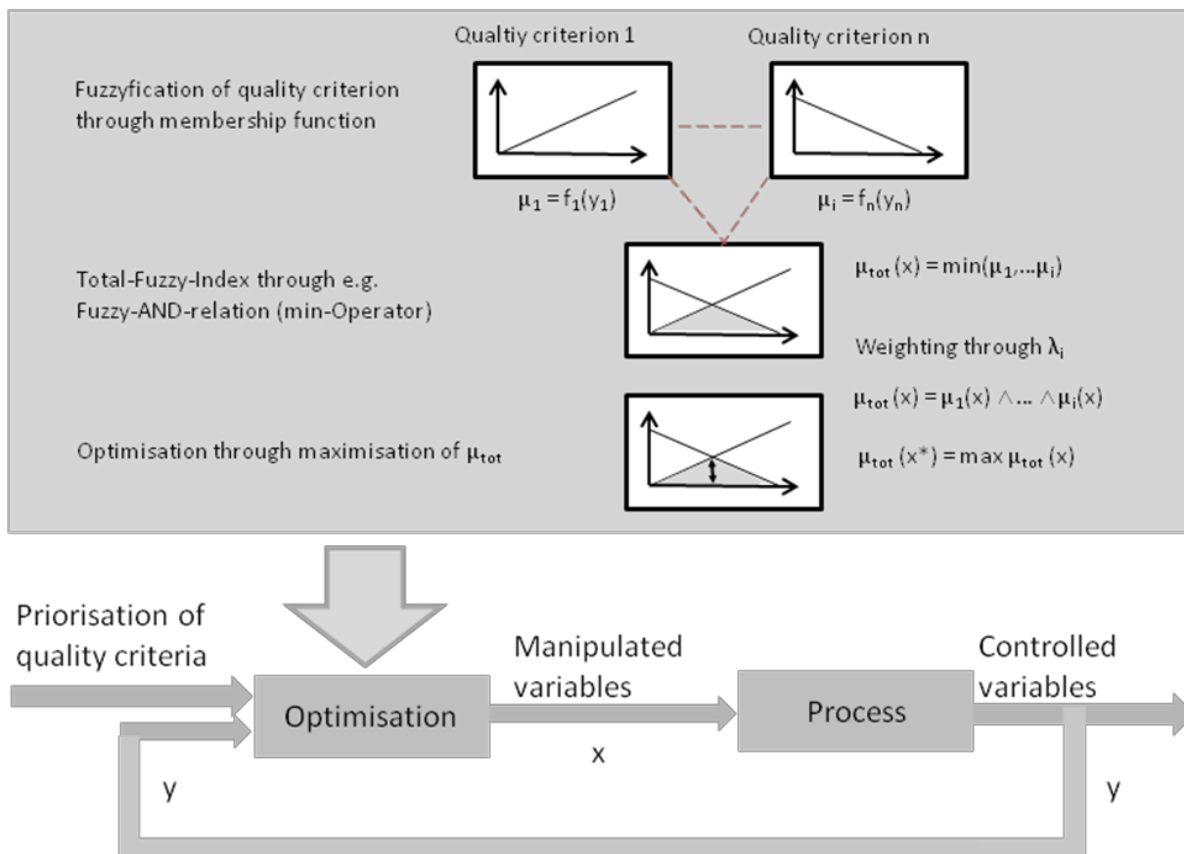


Figure 5-1: Conceptual illustration of FDM and its closed-loop implementation for FPC

Additional preferences can be made by the weighting of specific goals or constraints. Several approaches are presented in section 4.3.3 and discussed in Table 4-1. Since it is the aim of the present PhD study to investigate the influence of conflicting objectives on each other the opportunity of additionally weighting will not be used. Figure 5-1 illustrates the approach of FPC and its implementation in a continuous feed-back control loop. The latter is similar to conventional MPC approaches. From the description of FPC the following major differences to conventional MPC can be specified (Kaymak *et al.* 1997):

- FPC uses soft instead of hard descriptions of control objectives. Thereby goals and constraints are described by MFs specifying compromises between conflicting objectives in the decision-making process.
- FPC resembles multi-stage online decision-making for control while in conventional MPC decision-making is limited to a global, offline tuning of the trade-off between conflicting objectives.
- According to the process of decision-making in FPC goals and constraints are treated equally while in conventional MPC penalty functions are used to respect hard constraints.

Thereby, a major benefit of the approach is the description of operator goals and constraints for control in a transparent and illustrative way (Kaymak *et al.* 1997). The approach has been successfully implemented into systems with both discrete and continuous states (Kaymak *et al.* 1997).

5.2. Process models

Similar to conventional MPC, process models are used to predict future states in the system under control according to controller settings. Preferably, process models are linear or piecewise linear in closed loops in order to make MPC approaches robust (Belarbi and Megri 2007) and fast (Kaymak *et al.* 1997). However, strong process nonlinearities justify the use of nonlinear MPC (Camacho and Bordons 2007). Thanks to the nonlinear character of many control tasks the popularity of nonlinear MPC is consequently increasing. In sewer network MPC linear process models are popular. Nonlinear deterministic approaches are not practicable due to their computational effort especially in complex systems (Heusch 2011). In the case of WWTP MPC, linear process models lack robustness due to large model uncertainties (Weijers 2000). Stochastic process models based on neural networks or fuzzy neural models have shown to be appropriate both for sewer networks (e.g. Darsono and Labadie (2007)) and WWTPs (O'Brien *et al.* 2011). Neural network models must be trained according to representative measurement data. Due to the lack of appropriate data at the WWTP, integrated process models based on neural networks are not an option in the present case. The use of nonlinear process models for MPC affects the choice of numerical optimization algorithms (Grüne and Pannek 2011).

MPC can be either used to replace feed-back controllers (see e.g. Han *et al.* (2014)) or for supervisory control. In the latter, the control approach determines optimized set-points for feed-back controllers (see e.g. Vega *et al.* (2014)). In the present approach FPC is used for supervisory control. Figure 5-2 illustrates the process parameters involved in the present integrated FPC approach. The integrated system consists of numerous retention tanks with

Development of a multi-objective fuzzy predictive controller for system-wide control of integrated wastewater collection and treatment systems in rural regions

CSO structures which are connected to the WWTP by an ISN. Parameters consist of measured states, predicted loadings and actuator settings. According to the aim of system-wide control approaches of integrated WCTs to reduce CSO emissions by increasing the WWTP loading, actuators are:

- aggregates for controlling the outflow of retention tanks such as throttles or pumps and
- aggregates for controlling the inflow to the WWTP such as pumps or screw elevators.

Additional objectives of the present integrated FPC of system-wide control of rural WCTs are the optimization of aeration according to SASS by extended aeration and treatment cost minimization. Thereby, about 60 percent of treatment costs at WWTPs based on activated sludge are related to aeration. Consequently, blowers are actuators in the supervisory control of optimal DO concentrations during CWWF treatment at the WWTP.

Both for linear and nonlinear approaches process models are often simplifications of real-world processes especially in the case of WCTs. Consequently, prediction errors occur due to uncertainties (Bahakim and Ricardez-Sandoval 2014). Model-uncertainties can either be reduced by increasing the complexity of process models or by reducing control and prediction horizons in the closed-loop (Morari and Lee 1999).

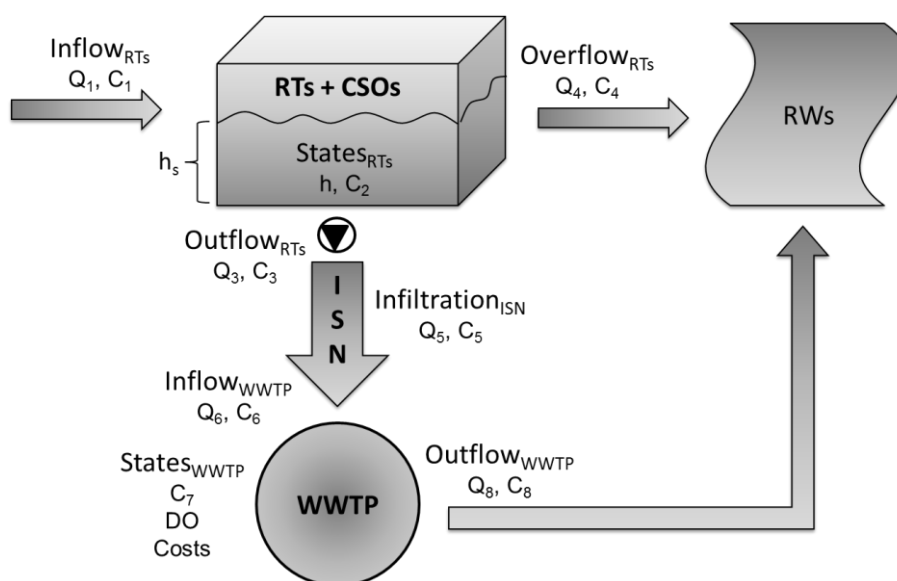


Figure 5-2: Parameters in system-wide control of integrated WCTs (Q_i = discharges, C_i = pollutant concentrations, RTs = retention tanks, RWs = receiving waters)

5.2.1. Retention tanks with CSO structures

In the following the hydraulic and pollution load process model to predict future states of retention tanks in the integrated WCTs is described. Based on feed-back loops the process model considers current states, predicted loads and actuator settings at each retention tank. States of retention tanks consist of the inflow at the current time step including pollutant concentrations, the filling degree and pollutant concentrations in the retention tank and

overflow to receiving waters (see Figure 5-2). Due to the results of Heusch (2011) of nonlinear deterministic sewer network MPC a linear approach is chosen.

5.2.1.1. Hydraulic model

Retention tanks are modeled according to the balance of their volume (Equation 5-3) within the constant time step Δt .

$$V(t + \Delta t) = V(t) + Q_{in}(\Delta t) - Q_{out}(\Delta t) - Q_{over}(\Delta t) \quad \text{Equation 5-3}$$

with: $V(t)$... current volume of wastewater in a retention tank, Q_{in} ... inflow to a retention tank, Q_{out} ... outflow of a retention tank, Q_{over} ... combined sewer overflow at a retention tank, Δt ... constant prediction step equal to the control step H_c and t ... current simulation time.

Q_{in} is assumed to be constant during Δt . Continuous measurements of Q_{out} and water level h in each retention tank enable a closed loop approach. The filling degree of each retention tank can be estimated from the water level h according to water level – volume relations specific for each retention tank. Additional rainfall now-casting can improve the prediction (Achleitner *et al.* 2009; Gaborit *et al.* 2013). Sewer overflow is calculated from (Equation 5-4) as exceedance of the specific maximum volume.

$$Q_{over}(\Delta t) = (V(t) + dV(\Delta t) - V_{max})/\Delta t \quad \text{Equation 5-4}$$

with: dV ... change of wastewater in the retention tank, $V(t)$... current volume of wastewater in the retention tank, Q_{over} ... combined sewer overflow at the retention tank, V_{max} ... maximum volume of the retention tank, Δt ... constant prediction time step equal to the control step H_c and t ... current simulation time.

5.2.1.2. Pollution load model

Retention tanks with CSO are modeled as completely mixed tanks. Mixing of concentrations is calculated according to (Equation 5-5). The process model for pollution loads describes the change of concentrations for COD and TKN at retention tanks with CSO structures during CWWF. Transformation and sedimentation of pollutants within the sewer network and retention tanks are assumed to be insignificant. Although these effects have been studied by several authors (for instance Jiang *et al.* (2009) for the first or Kutzner *et al.* (2007) for the latter) these deterministic models often lack transferability (Kutzner *et al.* 2007). It is assumed that concentrations only change because of mixing.

$$C_i(t + \Delta t) = \frac{C_i(t) \cdot V(t) + C_{i,in}(t) \cdot V_{in}(\Delta t) - C_i(t) \cdot V_{out}(\Delta t)}{V(t) + V_{in}(\Delta t) - V_{out}(\Delta t)} \quad \text{Equation 5-5}$$

with: i ... pollutant COD or TKN, C ... concentration of COD or TKN, $V(t)$... current wastewater volume in the retention tank, V_{in} ... wastewater inflow to the retention tank during Δt , V_{out} ... wastewater outflow of the retention tank during Δt , $C_{i,in}$... concentration of COD and TKN in the retention tank inflow assumed to be constant during Δt , Δt ... constant prediction step equal to the control step and t ... current simulation time

Development of a multi-objective fuzzy predictive controller for system-wide control of integrated wastewater collection and treatment systems in rural regions

5.2.2. WWTP

Due to their nonlinearity, studies on MPC of WWTPs can be distinguished according to the use of process models:

- Nonlinear approaches using deterministic models. These approaches are predominantly based on ASM1 (Henze *et al.* 1987) and the double-exponential settling velocity model for SST proposed by Takács *et al.* (1991) according to the Benchmark Simulation Model (BSM) 1 (Copp 2001) or BSM2 (Jeppsson *et al.* 2007) WWTP configurations. These studies mainly focus on the optimization of WWTP control, based on the systematic use of MPC (see e.g. Shen *et al.* (2008), Ostace *et al.* (2010), Stare *et al.* (2007) or Holenda *et al.* (2008)).
- Linear approaches according to classic MPC using mechanistic models. These approaches are limited to DWF control due to the nonexistence of linear replacement models for the dynamic prediction of sludge levels in SSTs (see e.g. Smets *et al.* (2003), Cruz Bournazou *et al.* (2012) or Kim *et al.* (2000)).
- Black box models based on neural networks or fuzzy neural models (see e.g. El-Din and Smith (2002), Ráduly *et al.* (2007), Han *et al.* (2012) or (Han *et al.* 2014) for approaches based on neural networks and e.g. Yoo *et al.* (2003) for approaches based on fuzzy modeling). These models have in common that they must be trained by reference data. Although reported findings show excellent results in reproducing mechanistic models uncertainties concerning extrapolation of training data is often unclear.

According to the aim of the present PhD study to investigate the influence of conflicting objectives and intrinsic dynamics in system-wide control of integrated WCTs in rural regions the chosen models must consider these characteristics. Consequently, state-of-the-art simulation models are chosen for WWTP process modeling as proposed by BSM1 (Copp 2001) which is a simulation environment defining a plant layout, simulation models, influent loads, test procedures and evaluation criteria. Proposed simulation models are ASM1 (Henze *et al.* 1987) for ASTs and the double-exponential settling velocity model for SSTs according to Takács *et al.* (1991). The primary objective of BSM1 and BSM2 is to provide a framework to develop and compare real-time control approaches for WWTPs (Gernaey *et al.* 2008). The WWTP layout proposed by BSM1 consists of two anoxic ASTs followed by three aerated ASTs (Copp 2001). In the present case this plant layout must be adapted to the optimal structure found for WWTP model calibration according to section 6.3.4.2 guaranteeing coherence between the reference model and process model for FPC.

5.2.3. Development of a discrete Lagrangian ISN observer model

Transportation systems such as sewer networks are usually very large in size. In WCTs the ISN forms the link between sub-catchments with their local sewer networks and retention tanks with CSO structures at the one end and the central WWTP at the other hand. Due to the characteristics of rural WCTs with central wastewater treatment (see section 2.1) retention tanks for combined sewage storage are often arranged decentralized, close to their sub-catchment. If not explicitly designed for integrated operation, additional balancing retention tanks for controlled WWTP loading during CWWF operation usually are missing.

Figure 5-3 illustrates the resulting control problem according to a simple example of a WCTS consisting of three sub-catchments where all local retention tanks are connected in parallel to the central WWTP³. In such cases, retention tank discharges on sub-catchment level must be used to control the loading of the WWTP during CWWF according to a reference value given by the WWTP operator. Due to usually inhomogeneous retention tank filling degrees and specific transportation times to the WWTP during CWWF MPC of rural sewer networks for simultaneous CSO minimization and constant WWTP loading is a multi-criteria optimization problem (Fiorelli and Schutz 2009). While in sewer network MPC the WWTP capacity is a constraint, in integrated MPC approaches it is a variable. Using ASM1 (Henze *et al.* 1987) for AST process modeling and the double-exponential settling velocity model according to Takács *et al.* (1991) for SST process modeling to determine the current WWTP capacity the system-wide MPC approach becomes nonlinear (Shen *et al.* 2008). Consequently, the current WWTP capacity cannot be calculated explicitly (Tränckner *et al.* 2007a) but must be derived according to simulation-based evaluations. This corresponds to the approach of MPC. Thereby, the objective of FDM in the present FPC approach is to continuously derive hydro- and pollutographs to optimize the WWTP loading according to its current capacity and to minimize CSO at retention tanks simultaneously. Besides specific goals and constraints especially compromises according to multi-criteria optimization of conflicting objectives are described by MFs within the FDM. FPC then derives corresponding actuator settings at retention tanks and at the WWTP. Due to different specific transportation times of discharged wastewater from each retention tank to the WWTP the hydro- and pollutograph resulting from throttle flows at retention tanks must be tracked in the ISN in order to respect dynamic trajectories for optimized WWTP loading during CWWF within the RHOC approach. According to the operation of ISNs hydro- and pollutograph tracking for integrated WWTP capacity determination and sewer network control, input-output models are recommended. General information about such models can be found e.g. in Rabitz *et al.* (1999). Additionally, the ISN hydro- and pollutograph tracking provides a continuous system-wide feed-back loop implementation. Since the WWTP performance evaluation is based on time series the ISN hydro- and pollutograph tracking model needs a temporal reference. According to the chosen control horizon for sewer network control the ISN tracking model should be discrete corresponding to the control step size. Zierolf *et al.* (1998) use a Lagrangian input-output model to backtrack chlorine in drinking water distribution networks. Input-output models are established quantitative approaches for model-based fault detection, mapping the input and output data of a system (Venkatasubramanian *et al.* 2003). Due to the promising results of Zierolf *et al.* (1998) a Lagrangian discrete wastewater input-output tracking model for system-wide control of WCTSs in rural regions will be developed and described in the following.

Lagrangian models are popular approaches for particle tracking. They are established in many disciplines such as atmospheric modeling (a comprehensive review is given by Wilson and Sawford (1996)), open water modeling (e.g. Miranda *et al.* (1999)), hydrologic modeling (such as storm rainfall forecasting (Burlando *et al.* 1996) or quantitative precipitation

³ Retention tanks can also be arranged in series which means that the discharge of an upstream retention tank feeds a downstream retention tank.

nowcasting (Zahraei *et al.* 2012)) but also in engineering such as transport engineering (e.g. MPC of transport networks (Negenborn *et al.* 2008) or real-time train timetabling (Caprara *et al.* 2006)) or integrated power systems scheduling (e.g. (Yan and Luh 1997)). While Eulerian models discretize the modeling space in both time and space Lagrangian models discretize in time only for tracking objectives at fixed points within the model space (Laird *et al.* 2003). Lagrangian models are applicable when the individual movements of objects are used to characterize spatial behavior (Doyle and Ensign 2009). In contrast to Eulerian models where the reference frame is a spatially bounded room, in Lagrangian models the reference frame is based on the tracking of specific identifiable objects through time. Transferring this to ISNs the Lagrangian input-output model must track each discharge from every retention tank per discrete control step to the WWTP. Due to discrete control steps each wastewater discharge resembles a water parcel with a certain volume and pollutant concentrations. Since flow in ISNs is predominantly longitudinal the tracking of discrete discharge parcels can be reduced to a 1-D problem. Each wastewater parcel discharged to the ISN is assumed to have the following initial characteristics:

- Event independent total transport time $t_{f,0,i}$
- Volume V_i
- $C_{COD,i}$
- $C_{TKN,i}$

Considering the ISN branch in Figure 5-4 node *A* is a retention tank with CSO structure upstream of a WWTP. H_c is the constant control horizon, $q_i(n)$ the retention tank discharge during control step n and t_f the event independent specific flow time from retention tank *A* to the WWTP. The basic idea of the presented approach is the assumption that each discrete wastewater flow discharged at retention tanks into ISNs can be tracked according to the current control step n . The approach is depicted for one ISN branch respective retention tank in Figure 5-5. From a literature review on sewer network MPC (see section 3.4.2.1) it can be seen that hydraulic prediction models predominantly consist of approaches based on translation neglecting additional effects such as retention and diffusion. These effects are predominantly modeled according to the nonlinear St. Venant differential equations. Due to the computational demand, MPC approaches considering such sophisticated process models are not practicable (Heusch 2011). Concluding from literature research on sewer network MPC (see section 3.4.2.1) and with respect to the complexity of system-wide FPC of integrated WCTSS ISN hydraulics during CWWF for MPC are described by constant flow times from each retention tank i to the WWTP (Equation 5-8).

The first assumption made to track discrete volumetric flows q according to throttle flows from retention tanks in ISNs for constant control steps H_c during CWWF is to describe the position and movement x of wastewater discharges according to their residual flow time t_{res} to the WWTP (Equation 5-6). Backwater effects are neglected.

$$\frac{dq(x, t_{res})}{dt} + v \frac{dq(x, t_{res})}{dx} = q(x, t_{res}) \quad \text{Equation 5-6}$$

where

$$dt = H_c = \text{const.} \quad \text{Equation 5-7}$$

with: q ... volumetric flow, t_{res} ... residual flow time of a discrete volumetric flow i to the WWTP, x ... spatial position in the ISN and v ... wastewater velocity

Thereby, flow velocities v during CWWF in the ISN are assumed to be constant. Consequently, total flow times $t_{f,0j}$ become constant, specific for each retention tank j (Equation 5-8).

$$t_{f,0j} = \text{const.} \quad \text{Equation 5-8}$$

with: $t_{f,0j}$... constant total flow time from retention tank j to the WWTP

A flow time test with discrete discharges from retention tanks in a rural ISN (see section 6.1.1) confirms the practicability of this approach (Regneri *et al.* 2012). Thereby, hydraulic impulses created from throttle flows of impended DWF in retention tanks were tracked at the WWTP. The test confirmed the assumed transportation times in the ISN for system-wide MPC. Note that in the case of rural systems these times are usually in the range of minutes to hours and often inhomogeneously distributed.

Assuming the total flow times from each retention tank to the WWTP being multiples of the constant control horizon H_c , the movement of discrete hydraulic throttle flows according to actuator settings from retention tanks within the ISN and hence their arrival at the WWTP can be described according to the number of control steps n .

$$n = \frac{t_{f,0j}}{H_c}, \quad n \in \mathbb{N} \quad \text{Equation 5-9}$$

with: n ... number of control steps for a specific wastewater discharge parcel to flow from its retention tank to the WWTP and H_c ... chosen control horizon

In the following each discrete volumetric throttle flow q_i within the ISN can be tracked according to its residual flow time to the WWTP which is updated each control step H_c . For each discrete volumetric throttle flow q_i the temporal tracking is initiated with the corresponding specific total flow time $t_{f,0j}$.

$$t_{res,i,k+1} = t_{res,i,k} - H_c \quad \text{Equation 5-10}$$

with: $t_{res,i,k}$... current temporal position of each parcel i in the ISN on its way to the WWTP corresponding to the residual flow time and k ... current time step multiple of the control step size H_c

The volume V_i of a specific discrete volumetric throttle flow q_i discharged during one control step H_c is equal to their product (Equation 5-11).

$$V_i = q_i \cdot H_c \quad \text{Equation 5-11}$$

Development of a multi-objective fuzzy predictive controller for system-wide control of integrated wastewater collection and treatment systems in rural regions

For the predictive composition of the WWTP inflow hydrograph Q , all discrete volumetric throttle flows q_i in the ISN are aggregated according to their residual flow time $t_{res,i}$ calculated from Equation 5-10. This creates a vector of n elements sorted according to the residual flow time t_{res} (Equation 5-12).

$$Q(n) = \sum_{i \in t_{res,i}} q(t_{res,i}) \quad \text{Equation 5-12}$$

with: $Q(n)$... n th element of a vector describing the total volumetric flow in the ISN

Discrete volumetric flows arriving at the WWTP, which corresponds to a residual flow time $t_{res,i}$ equal to zero, are taken out of the ISN input-output process model and transferred to the WWTP process model for FPC.

For the simulation-based estimation of the current WWTP capacity the predicted hydrograph according to Equation 5-12 must be extended by corresponding pollutographs for COD and TKN. In order to track pollutant flows within ISNs similar to volumetric flows biochemical transformations within the ISN are expected to be negligible. Hence, concentrations of each pollutant l in discrete volumetric throttle flows q_i discharged at retention tanks j during constant control steps H_c are assumed to stay constant (Equation 5-13).

$$\frac{dC_l}{dt} = \text{const.} \quad \text{Equation 5-13}$$

with: l ... COD resp. TKN

Consequently, concentrations of COD and TKN are tracked together with their corresponding discrete hydraulic flows q_i according to Equation 5-14.

$$\frac{dC_l(x, t_{res})}{dt} + \frac{dC_l(x, t_{res})}{dx} = C_l(x, t_{res}) \quad \text{Equation 5-14}$$

where

$$dt = H_c = \text{const.} \quad \text{Equation 5-15}$$

with: C ... concentration of pollutant l of a discrete volumetric flow q_i to the WWTP, t_{res} ... residual flow time of a discrete volumetric flow q_i to the WWTP and x ... the spatial position in the ISN

The pollutographs for COD and TKN corresponding to the hydrograph (see Equation 5-12) are calculated according to Equation 5-16 assuming complete mixing when aggregating discrete wastewater throttle flows according to similar residual flow times.

$$C_l(n) = \frac{\sum_{i \in t_{res,i}} C_{i,l} \cdot V_i}{\sum_{i \in t_{res,i}} V_i} \quad \text{Equation 5-16}$$

with: $C_l(n)$... n th element of a vector describing the total pollutograph in the ISN and j ... pollutant COD resp. TKN

Development of a multi-objective fuzzy predictive controller for system-wide control of integrated wastewater collection and treatment systems in rural regions

Dispersion is considered by complete mixing in a small virtual tank just in front of the WWTP. The Lagrangian ISN process model forms the link between local retention tanks with CSO structures and the WWTP. Together with the process models presented in section 5.2.1 and 5.2.2 they form an integrated process model for system-wide FPC according to fuzzy goals and fuzzy constraints used to describe the decision-making in the case of conflicting objectives in multi-objective optimization problems.

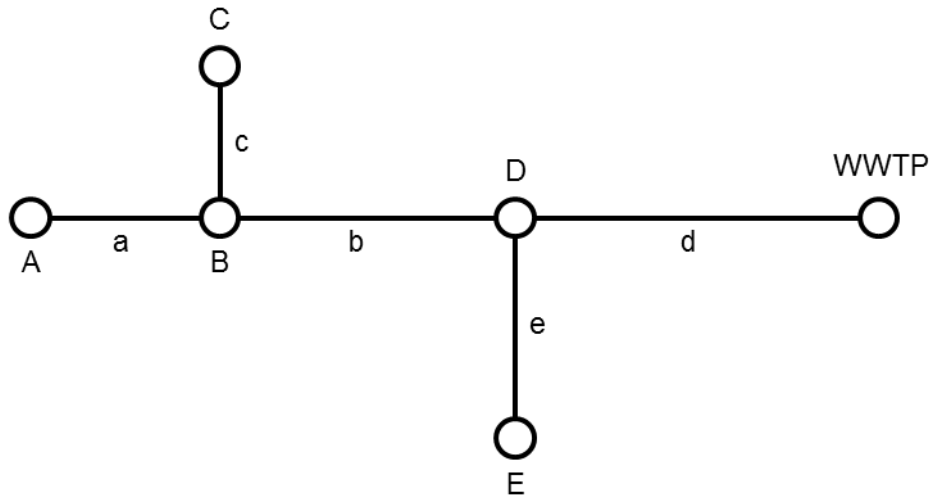


Figure 5-3: Simple ISN with a central WWTP. Nodes A, C and E are sub-catchments with retention tanks and CSO structures. Nodes B and D are conjunctions of different branches in the ISN.

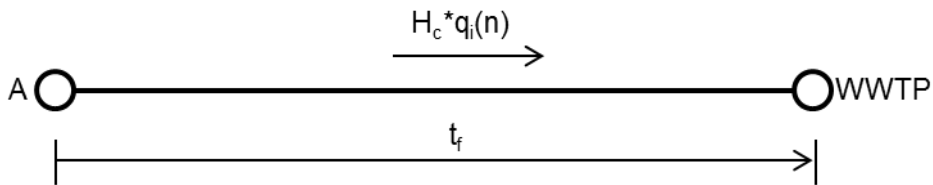


Figure 5-4: Simple branch in an ISN where retention tank A describes an input and WWTP the output of a process model

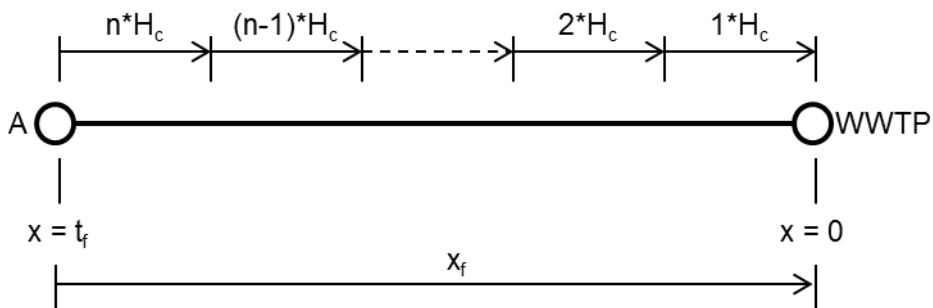


Figure 5-5: Temporal tracking of discrete wastewater discharges from retention tanks to the WWTP according to a multiple of the constant control step size H_c

Development of a multi-objective fuzzy predictive controller for system-wide control of integrated wastewater collection and treatment systems in rural regions

Due to mean total flow times in rural ISNs during CWWF in the range of hours, system-wide control problems of integrated WCTs especially in rural systems are feed-forward.

5.2.4. Power consumption

Power consumption for pumping at retention tanks and in the ISN is not taken into account since it is the major goal of integrated WCTs to adapt the WWTP loading to its treatment capacity. Treatment costs will only be minimized by increasing treatment efficiency. It is shown by many studies that aeration is the major part of energy consumption in municipal wastewater treatment based on activated sludge (Kroiss and Svardal 2009). Consequently, energy minimization at WWTPs is limited to aeration. In conventional multi-objective control approaches conflicting goals and constraints are translated to monetary references (see e.g. BSM1 (Copp 2001)). Thanks to the ability of FDM to treat goals and constraints equally (da Costa Sousa and Kaymak 2001), in the present FPC the injected air volume according to Equation 5-17 can be used directly to evaluate the aeration effort according to multi-criteria optimization.

$$\dot{S}_{O,B} = k_{La} \cdot (S_{O,sat} - S_O) \quad \text{Equation 5-17}$$

with: $S_{O,B}$... oxygen increment per time step, k_{La} ... specific oxygen supply, $S_{O,sat}$... oxygen saturation concentration and S_O ... current oxygen concentration

5.3. Defining the fuzzy multi-criteria decision-making model

As described before, the aggregation of MFs for goals and constraints defines the fuzzy multi-criteria decision-making model and thus provides the opportunity to describe compromises between conflicting objectives in multi-criteria optimization as illustrated in Figure 5-1. It is the general aim of multi-objective decision-making approaches to find one solution which is the best compromise of all conflicting goals and constraints according to the specific preferences of the decision maker. Due to this method of compromise it is natural to describe both goals and constraints as fuzzy relations in order to find the best agreement amongst conflicting objectives. During the process of fuzzyfication, both, goals and constraints are normalized by degrees of preference for decision-making according their membership functions within a common codomain of [0, 1]. Consequently, goals and constraints are treated equally in fuzzy multi-criteria decision-making. This replaces the step of parameter scaling for comparative purposes. For instance, in control performance evaluation with BSM1 (Jeppsson and Pons 2004) WWTP effluent concentrations of various parameters are weighted differently in order to make their specific effects on receiving waters comparable.

Fuzzy goals represent the specific preferences of the decision maker. They are described by membership function values equal to one representing absolute preference and diminishing values according to the degree of deviation from the optimum. Constraints are omnipresent in technical systems. Unlike goals which are optional, constraints have crisp limits which must be complied with. Penalization due to violation is done by membership function values equal to zero while perfect agreement with the crisp constraint gives a membership function value of one. Acceptable values have membership values according to the degree of their

compromise. Thereby, the aggregation function plays a crucial role. Due to the character of the chosen function (see Table 4-1) violations are compensated more or less.

Defining decisions a priori is not straightforward but is a case-dependent and partly subjective process depending on specific preferences of the decision-maker. Consequently, there is no general receipt for the design of MFs for goals and constraints. Thereby, expert knowledge is of crucial importance. This is reflected by three facts:

- Due to the mapping of process variable values and their equivalent MF values reflecting the degree of preference in the decision-making process the codomain of each variable must be known a priori. While overestimated codomains distort the course of MFs and make them less sensitive, underestimated codomains can lead to unwanted rejections due to variable values exceeding the range defined by MFs.
- The type of MF defines the course of the function. Consequently, it describes the compromise in the case of conflicting objectives. Triangular or trapezoidal MFs, which are the most popular ones, describe a linear relation between variable values and their degree of preference in the decision-making process. Functions with a non-linear course allow for certain preferences in the decision-making process by bending the preferred range either to one or to zero. However, using nonlinear MFs affects the range of algorithms appropriate to solve the optimization problem.
- The choice of the aggregation function defines the degree of compromises made between conflicting objectives. If compromises are unwanted, additional weighting of objectives in the aggregated fuzzy multi-criteria decision-making function can be added to express preferences.

It is hence the objective of the fuzzy multi-criteria decision-making model to translate this expert knowledge and operator preferences into a logic which can be implemented into MPC.

Generally speaking, fuzzy multi-criteria decision-making provides the opportunity to describe objectives in a more detailed way than just by specifying hard goals and constraints as is the case for conventional MPC (Kaymak *et al.* 1997).

In the following, popular goals and constraints in system-wide control of WCTSs are listed from literature. The list shows the variety of objectives according to case-specific aims of most of the reported studies. Consequently, examples of MFs for objectives in system-wide control of WCTSs will only be given in chapter 7 for the present case study.

5.3.1. Sewer networks

Schütze *et al.* (2004) provide a substantial overview on combined sewer network control objectives. The main goal is to minimize the impact of CSO on receiving waters by minimizing CSO volume and pollutant load. Approaches can be distinguished between emission and immission based approaches. Considering pollutant concentrations additional to hydraulic information, sewer network control approaches can additionally reduce pollutant loads to receiving waters or adapt pollutant CSO loads to different receiving water states

Development of a multi-objective fuzzy predictive controller for system-wide control of integrated wastewater collection and treatment systems in rural regions

(Meirlaen 2002). Thereby, the use of retention tank volume in combined sewer networks can be optimized through different actions which must be expressed as goals to be optimized:

- empty retention tanks as fast as possible,
 - according to their filling degree,
 - according to their risk of overflow,
 - according to their degree of pollution,
- homogenize the use of retention tank volume in the sewer network.

The goals to be implemented strongly depend on the information used for prediction.

Besides goals, constraints are of equal importance in MPC. In the case of sewer systems these mostly arise from:

- hydraulic capacities of bottlenecks in interceptor sewer pipes,
- hydraulic capacities of pumps at retention tanks and within the ISN,
- receiving water sensitivity classes,
- the current WWTP treatment capacity.

While the choice of goals predominantly depends on the specific aims of the controller constraints to be taken into account strongly depend on the specific structure. Consequently, the constellation of goals and constraints is rather case-specific.

5.3.2. Wastewater treatment plant

Primary objective in wastewater treatment is the cleaning of wastewater according to legal effluent concentration limits for the primary constituents BOD₅, COD, TN, NH₄-N, TSS and TP (EC 1991). It is well known that the activated sludge wastewater treatment is an energy expensive process due to artificial aeration with mechanical surface aerators or blowers. Hence, the minimization of energy consumption has become the second main objective in modern wastewater treatment. The combination of these conflicting objectives leads to process efficiency. MFs must be used to describe the objectives for the optimization of the treatment process by preferring lower effluent concentrations for the required parameters and penalizing violations through exceeding legal effluent limits. The process-related power consumption in activated sludge wastewater treatment is dominated by the aeration process. Other energy consumers are either:

- comparably small and hence negligible (e.g. pumping for phosphate precipitation),
- not a process variable (e.g. mixing) or
- indispensable (e.g. internal wastewater or sludge pumping).

A third objective in WWTP control is the treatment of the excess sludge which is often related to a certain SRT. At WWTPs with SASS SRTs of about 25 days are common practice in order to mineralize the activated sludge during the wastewater treatment process in the AST. At WWTPs where WAS is anaerobically digested, much smaller SRT are preferred for energy recovery which is in the case of such plants an additional goal in the optimization scheme. In the case of SASS the SRT of 25 days together with minimum concentrations for DO during aeration form an additional objective representing process stability which must additionally be translated into fuzzy goals and constraints.

5.3.3. System-wide control

Popular integrated real-time control approaches to increase the total performance of WCTSS during CWWF are:

- control of the hydraulic load to the WWTP according to the current sludge level in the SST (e.g. Seggelke et al. (2013)),
- control of the load to the WWTP according to the current pollution treatment capacity (e.g. Tränckner et al. (2007b)),
- bypass of WWTP process units according to the degree of pollution of the sewage (e.g. Ahnert et al. (2009)),
- aeration tank settling (Nielsen *et al.* 2000),
- controlled CSO according to the current state of the receiving water (e.g. Hoppe et al. (2011)),
- immission based real-time control (Meirlaen 2002).

Thereby, approaches three and four introduce extra WWTP treatment concepts to increase capacities during CWWF.

In the framework of the present study it is the goal to investigate the impact of the current treatment capacity of WWTPs with SASS on the system-wide control of WCTSS. Thereby, the impact on system-wide control is considered by an integrated FPC approach describing the optimization problem in the receding horizon using integrated fuzzy goals and constraints.

5.4. Hybrid fuzzy predictive control for plant-wide control

The process models presented are partly linear (retention tanks with CSO structures, Lagrangian ISN tracking model) and partly nonlinear (WWTP). Combining these models for system-wide FPC a hybrid model is created. Examples for hybrid MPC are rare. Comparable to the present case Zhu et al. (2000) report on a hybrid MPC approach for system-wide control. They propose to decompose complex systems into linear and nonlinear sub-systems with respect to their appropriate MPC technology. Thereby, the main objective of their work is to guarantee a system-wide mass balance for bidirectional mass and energy transfer. Their results demonstrate principal applicability of hybrid MPC approaches.

5.5. Optimization

5.5.1. Optimization of fuzzy objective functions

The choice of appropriate numerical solvers is case-dependent and linked to the complexity of the objective function to be minimized (Fletcher 2013). Schütze et al. (2002) provide an overview on numerical optimization approaches.

In FPC the objective function is composed on the one hand of the model used for the prediction of future states of the system under control and on the other hand of the chosen MFs and aggregation function for fuzzy multi-criteria decision-making. Both can either be linear or nonlinear. Consequently, the chosen functions determine the appropriate method for optimization.

5.5.2. Pattern search

It is shown that in the present case the system-wide process model used for future state prediction is hybrid, partly linear and partly nonlinear. The prediction model is incorporated in the aggregated fuzzy multi-criteria decision-making function. Hence, an optimization problem is formed which is nonlinear and non-differentiable with hidden constraints⁴. Additionally, the formulated optimization problem is non-smooth leading to many local minima (Leirens *et al.* 2010). In practice the computation time is limited to the control step size k_c which is in the case of sewer network MPC in the range of several minutes. Within this available period of time a solution has to be found that is as good as possible. Since information on the gradient and Hessian is not available for the integrated optimization problem, elaborated quasi-Newton optimization methods for nonlinear problems are not appropriate (Lewis *et al.* 2000). There are various approaches available to solve unconstrained optimization techniques that do not explicitly use derivatives. These methods can be categorized according to deterministic and probabilistic approaches. While deterministic methods or so-called local search methods tend to converge to local minima, probabilistic methods for global optimization are computationally expensive and non-convergent. Especially for computationally expensive cost functions stochastic optimization algorithms can only run for a limited number of iterations which decreases the probability of finding the global minimum (Wetter and Wright 2004). In the case of MPC of wastewater treatment systems studies on stochastic optimization algorithms are rare and limited to small numbers of degrees of freedom (see e.g. Rauch and Harremoës, (1999)). Hence, they are not yet applicable to complex systems. In the case of sewer networks pattern search algorithms have proven to be applicable for solving nonlinear MPC problems (Leirens *et al.* 2010; Heusch 2011) even for objective functions with many local minima (Giraldo *et al.* 2010). Additionally, Herrera *et al.* (2013) have successfully investigated the use of pattern search approaches for the control of irrigation systems. Based on this review pattern search approaches are investigated for the present system-wide FPC of integrated WCTs.

Pattern search was introduced by Robert Hooke and T.A. Jeeves in 1961 (Hooke and Jeeves 1961). The method belongs to the group of direct search approaches for optimization. This category of optimization approaches is called derivative-free since these methods neither compute nor approximate derivatives. They distinguish from other derivative-free approaches such as evolutionary algorithms or simulated annealing algorithms since they do not require numerical function values but only relatively rank the objective values within a countable set. They quickly became very popular mainly because they are easy to implement and convergent. In recent years they have been replaced by more sophisticated approaches to a large extent. Nevertheless they persist since they work well in practice even when elaborated approaches fail. Therefore, direct search approaches are often used as a starting point for the use of more sophisticated methods. They are divided into three basic categories according to their search approach: *pattern search methods*, *simplex methods* and methods with *adaptive sets of search directions* (mesh adaptive direct search). Further details are given e.g. by Lewis *et al.* (2000).

⁴ Constraints are considered as objectives in FDM (Sousa and Kaymak 2002).

Pattern search is an iterative approach. In each iteration s a set of solutions X_s is replaced by a new solution X^+ if $f(X^+) < f(X_s)$. X^+ is selected from a discrete set of candidates in \mathbb{R}^n . This set is called mesh M_s which is constructed around the current solution X_s according to the mesh size $\Delta_s \in \mathbb{R}^+$ (Leirens *et al.* 2010). A pattern is a set of vectors $\{v_i\}$ used to determine the search direction at each iteration which is determined by the number of independent variables and the positive basis set. In the generalized form of pattern search 2 basis sets are commonly used, the maximal basis with $2N$ vectors and the minimal basis with $N + 1$ vectors with each fixed directions. The following example illustrates the approach for 3 independent variables in the objective function:

- $2N$ basis set

$$\begin{array}{lll} v_1 = [1 \ 0 \ 0] & v_2 = [0 \ 1 \ 0] & v_3 = [0 \ 0 \ 1] \\ v_4 = [-1 \ 0 \ 0] & v_5 = [0 \ -1 \ 0] & v_6 = [0 \ 0 \ -1] \end{array}$$

- $N + 1$ basis set

$$\begin{array}{lll} v_1 = [1 \ 0 \ 0] & v_2 = [0 \ 1 \ 0] & v_3 = [0 \ 0 \ 1] \\ v_4 = [-1 \ -1 \ -1] & & \end{array}$$

For each iteration the *mesh* is constructed by multiplying each pattern vector v_i by the mesh size Δ_s . Then the mesh is centered on the current solution X_s by adding it to the mesh. The algorithm polls the mesh by computing its objective function values. If an improved solution X^+ is found the poll was successful and $X_{s+1} := X^+$. After polling the mesh size is changed according to the result. If polling was successful the mesh size is increased by $\Delta_{s+1} = \varepsilon \Delta_s$, with a constant expansion factor $\varepsilon > 1$, else the mesh size is decreased by $\Delta_{s+1} = \gamma \Delta_s$, with a constant contraction factor $\gamma \in [0, 1]$ for the following iteration.

While with the general pattern search approach the step size is fixed, with the mesh adaptive direct search approach the pattern set is randomly selected. Hence the search step gets very flexible by allowing the algorithm to generate trial points anywhere on the mesh. This increases the exploration of the space of variables (Audet *et al.* 2008). Consequently the convergence speed increases and the risk to get stuck in local minima decreases compared to GPS algorithms (Audet *et al.* 2010). Iteration stops according to the satisfaction stopping criteria such as:

- the mesh size falls below a given tolerance,
- the number of objective function evaluations exceeds a given maximum or
- the objective function value improvement falls below a given tolerance.

A comprehensive overview and additional information is given by Rios and Sahinidis (2012).

To overcome the local minima problem in direct search approaches Latin hypercube sampling is added to the pattern search approach. Latin hypercube sampling is a form of stratified sampling commonly used to reduce the number of runs in Monte Carlo simulation. Combined with the pattern search approach, the codomain per iteration is divided into k equal sub-spaces according to the number of variables. Then, within each sub-space a random point is selected. Serving as starting points for the pattern search approach, Latin hypercube sampling effectively samples the search space but provides the necessary

Development of a multi-objective fuzzy predictive controller for system-wide control of integrated wastewater collection and treatment systems in rural regions

randomness to overcome local minima. Details on the integrated Latin hypercube sampling – pattern search approach are given in Davey (2008).

6. Wastewater pollutant flows and modeling in rural WCTSS

Conventionally, complex control approaches such as those investigated in this PhD study are developed and tested based on simulations. Reference models are used to mimic the real system to be controlled. Their representativeness is of crucial importance to guarantee a subsequent successful implementation (Langergraber *et al.* 2004). In control, benchmarking is increasingly used to evaluate and compare different approaches. Thereby, performance is evaluated according to the process and to economic aspects. Benchmark simulation model (BSM) number 1 (Copp 2001) provides platform-independent simulation procedures for WWTPs defined around a simulation model, a plant layout, realistic influent loads and a test protocol that provide an objective measure of performance (Vanrolleghem and Gillot 2002). BSM number 2 extends the approach to anaerobic sludge digestion (Jeppsson *et al.* 2007). In some cases, the plant layout (e.g. Han *et al.*, 2012; Holanda *et al.*, 2008; Ostace *et al.*, 2011; Stare *et al.*, 2007; Vallerio *et al.*, 2014) and influent disturbance scenarios (e.g. Shen *et al.*, 2009, 2008; Traoré *et al.*, 2006; Vega *et al.*, 2014) provided by the benchmark (Gernaey *et al.* 2006) are used for the simulation-based development of WWTP MPC approaches. When applied to real case studies, especially the provided plant layout must be adapted to the specific situation in order to provide a calibrated reference model. Due to this, Abusam *et al.* (2002) needed to adapt the benchmark plant layout to the specifications of the oxidation ditch WWTP of the city of Rotterdam in order to develop and evaluate adequate nitrogen control strategies. Vanrolleghem and Gillot (2002) discussed the transferability of benchmark-based control approaches to deviating plant layouts proposing additional robustness and economic measures in order to overcome this problem. While already established for WWTPs, an extension for BSM2 to consider sewer networks for integrated control schemes was only recently proposed by (Saagi *et al.* 2014). Benchmarking methodologies for sewer network real-time control have been proposed e.g. by Borsanyi *et al.* (2008).

As shown by the literature review in section 2.3, data on system-wide flow of wastewater pollutants in rural WCTSS is rare. Available data indicates comparably larger pollution loads to be expected. Especially pollution load modeling in the sewer network during CWWF lags behind WWTP modeling due to the scarcity of corresponding measurement data (Rauch *et al.* 2005). Consequently, further investigations of pollutant flows in IUWSs are proposed by many researchers (Bach *et al.* 2014). Characteristics and the fate of pollutant flows as well as the contribution of rainfall-runoff in rural WCTSS are investigated based on event mean concentrations (EMC), first flush and chemical mass balance analysis. Results are compared to data from literature for rural and urban systems. Due to complexity and corresponding computational effort, sewer network pollution load models are often reduced to the sum parameters COD and TKN (see section 2.2.2). Fractionation models convert sum parameters to the fractions necessary in WWTP models. Additionally, a fraction model must be used to evaluate the controller performance concerning TSS, BOD₅ or NH₄-N CSO loads. The fractionation model is calibrated according to investigated wastewater pollutants at retention tanks and at the WWTP both during DWF and CWWF. Additionally, fractionation

model results are compared to results from regression analysis and used to investigate appropriate approaches in the present case of rural WCTSS.

Consequently, a real case study typically for rural WCTSS is used in the present PhD study:

- to investigate the fate of wastewater pollutants in comparison to urban systems and
- to calibrate a reference model for simulation-based evaluation of the system-wide FPC approach developed in chapter 5.

The chosen WCTS is situated around the Haute-Sûre storage lake in a natural park in the north of Luxembourg. The system is operated by the “Syndicat Intercommunal de Dépollution des Eaux résiduaires du Nord” (SIDEN). The artificial storage lake is Luxembourg’s main drinking water reservoir serving about 70% of the country. According to the national importance of the local water quality it was decided to rebuild the wastewater treatment system for centralized wastewater treatment. A first part is in operation since fall 2009 (see Figure 6-1). Due to this situation two different states of the WCTS must be distinguished:

- a) state 2010, which describes the state during the monitoring and measurement campaign done for the present work. This system state is used for model calibration. The degree of expansion did not change during the processing period of this study.
- b) final state, which describes the state of the finished WCTS used for the evaluation of the presented approach.

The following chapter starts with the description of the case study and the necessary data to build the reference model for the simulation-based evaluation of the proposed FPC approach. In MPC robustness describes the capability of the controller to deal with noises, disturbances and errors. In the following these effects are referred to as disturbances. Taking them into account contributes to the representativeness of the reference model. In sewer network modeling deviations from the real system occur predominantly due to:

- conceptual modeling approaches (Wagener *et al.* 2003)
- given active drainage surface data (Freni *et al.* 2009),
- hydraulic measurement errors (Campisano *et al.* 2013),
- rain-gauge measurement errors (Bertrand-Krajewski *et al.* 2003) and
- non-representative rainfall-inputs (Vaes *et al.* 2005).

In WWTP modeling deviations from the real system are mainly due to:

- conceptual model approximations (Gernaey *et al.* 2004),
- influent load dynamics (Gernaey *et al.* 2011),
- influent temperature dynamics (Gernaey *et al.* 2006) and
- sensor measurement errors (Rosen and Olsson 1998).

The consideration of disturbances should contribute to the performance of MPC both of sewer networks and WWTPs due to the adaptation to increased dynamics. The expected effectiveness of sewer network MPC is derived from the heterogeneity of the system to be controlled (Zacharof *et al.* 2004). At WWTPs, simulation results are too optimistic if disturbances are not taken into account, due to insufficient excitement of the system (Ráduly *et al.* 2007).

Due to the limited spatial and temporal resolution of rainfall data, runoff from rainfall can be considered as the major disturbance in sewer network real-time control (Cembrano *et al.* 2004). At the WWTP the resulting CWWF is also considered as a major disturbance in WWTP real-time control (Gernaey *et al.* 2006). In the present case study, rainfall data is limited to four rain gauges for 24 sub-catchments. Since these sub-catchments show similar characteristics concerning rainfall-runoff influencing parameters in hydrological modeling, retention tank filling at sub-catchments allocated to the same rain gauge (see Figure 6-5) would be the same. In section 6.3.2 it will be shown that the evaluation of rainfall-runoff from retention tank discharge measurements reveals additional spatial dynamics compared to the corresponding evaluation of rainfall time series limited to four rain gauges. Due to the described importance to consider disturbances in simulation-based real-time control evaluations, the influence of this additional information of spatial rainfall-runoff dynamics on system-wide FPC of integrated WCTSS will be investigated by incorporating this information into the integrated deterministic reference model using lumped random coefficients to consider disturbances according to the measured rainfall-runoff variability. The phenomenological consideration of the measured system-wide rainfall-runoff variability is assumed to additionally contribute to the performance evaluation of the proposed integrated FPC approach.

Due to the under-loaded situation at the WWTP, the calibration of the associated reference model is limited to the model layout appropriate to simulate the dynamics of low loaded oxidation ditches and the corresponding oxygen input.

6.1. Case study Haute-Sûre

The final state of the Haute-Sûre WCTS consists of 37 sub-catchments of the size of villages, single houses and settlements including 3 camping sites connected to the WWTP Heiderscheidergrund for central biological wastewater treatment. The catchment is situated in the rural north of Luxembourg. Land-use is residential and agricultural with significant tourism in summer. Due to tourism population equivalents nearly double during the summer months. The catchment is situated around the Haute-Sûre storage lake in the Luxembourg Ardennes. Because of the hilly landside 26 pumping stations are situated in the final sewer network to transport the wastewater to the central WWTP.

6.1.1. Sewer network

Combined sewer networks dominate the local drainage systems in the sub-catchments. Only 12 sub-catchments of the final system drain rainfall-runoff in separate systems. Consequently, during CWWF the inflow to the WWTP is diluted by rainfall-runoff and CSO is affected by domestic sewage. Figure 6-1 shows the state of the catchment as connected to the WWTP Heiderscheidergrund in 2010 (red background) and the final state (total figure). For illustrative reasons abbreviations are used for the sub-catchments with local combined sewer networks according to Table 6-1. Table 6-2 lists the main characteristics of the catchment in 2010. Retention tanks with CSO structures are designed according the German design guideline ATV-A 128 (ATV-DVWK, 1992a) based on the impervious catchment surface A_{is} making use of the possibility to reduce retention tank volume in rural regions. A_{is} is assumed to be equal to the hardened catchment surface A_{red} if details on A_{is} are missing, as in the present case. Due to the residential and agricultural land use in rural

regions the catchment area connected to the sewer network is more than twice the size of the hardened area which is assumed to be impervious. Uncertainty related to input data availability, especially concerning runoff coefficients, increases (Schaarup-Jensen *et al.* 2005). Typically for WCTSS in rural regions retention tank volume for combined sewage treatment is organized decentralized on sub-catchment level (Boller 1997). The touristic influence is reflected in the doubling of PE during the summer holiday season. The specific retention tank volume V_{spec} describes the retention tank volume per impervious catchment surface A_{is} . All retention tanks are designed according to the German design guideline ATV-A 128 (ATV-DVWK, 1992a). Figure 6-2 and Figure 6-3 show the analysis of V_{spec} respective A_{is} and A_{CA} built in 2010 respectively for the final state. The analysis reveals noticeable differences in specific volumes for both states. Given the relevance of the total amount and distribution of retention volume for sewer network real-time control (Zacharof *et al.* 2004) this heterogeneity should be beneficial for system-wide FPC.

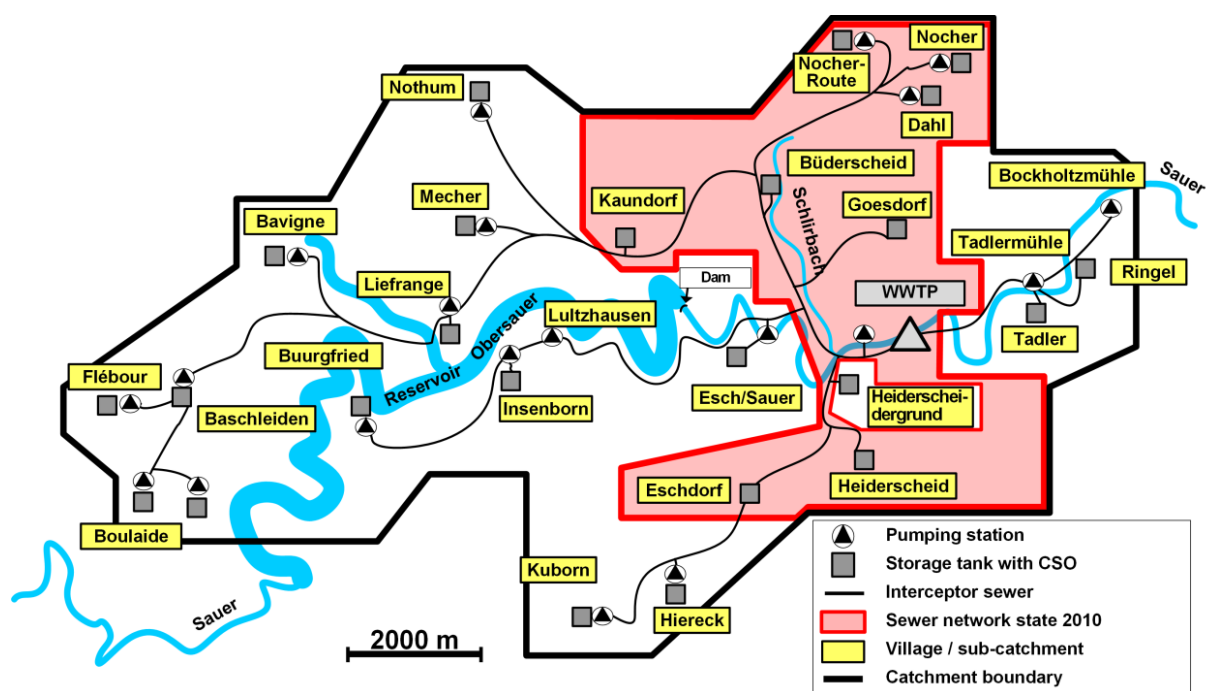


Figure 6-1: Haute-Sûre integrated WCTSS for the final state (black border) and the state 2010 (red border and background)

Table 6-1: Abbreviations of catchments with combined sewer system

Catchment	Abbreviation	Catchment	Abbreviation
Baschleiden	BAS	Heiderscheidergrund	HEG
Boulaide Bauschelbusch	BAU	Hiereck	HIE
Bavigne	BAV	Insenborn	INB
Boulaide Boellerbuch	BOE	Kaundorf	KAU
Buederscheid	BUE	Kuborn	KUB
Buurgfried	BUU	Liefrange	LIE
Dahl	DAH	Mecher	MEC
Esch/Sûre (Sauer)	ESC	Nocher	NOC
Eschdorf	ESD	Nocher-Route	NOR
Flèbour	FLE	Nothum	NOT
Goesdorf	GOE	Ringel	RIN
Heiderscheid	HEI	Tadler	TAD

Table 6-2: Catchment data state 2010

Catchment	Sewer	Surface		Retention tank		Population Equivalents	
		A _{red} [ha]	A _{CA} [ha]	V [m ³]	V _{spec} [m ³ /ha]	Winter [-]	Summer [-]
BUE	combined	6.0	16.5	90	15	126	251
Camping Bissen	separate					0	394
Camping LeMoulin	separate					0	392
DAH	combined	6.0	19.0	270	45	234	262
ESD east	combined	6.4	12.8	330	18.9	148	218
ESD west	combined	11.1	22.2			445	654
GOE	combined	11.4	24.7	190	16.7	229	550
HEI	combined	13.6	30.0	220	16.2	487	518
Hotel Bissen	Separate					18	70
KAU	combined	11.0	22.0	180	16.4	218	367
NOC	combined	4.2	16.2	166	39.5	187	336
NOR	combined	5.2	18.6	157	30.2	135	146
TOTAL		74.9	182.1	1603	21.4	2227	4158

Table 6-3 and Table 6-4 summarize the characteristics of the catchments and the ISN for the final state describing the minimum information for approximate models used for long-term hydrological simulations. Flow times from each retention tank to the WWTP during CWWF are calculated according Equation 6-1 to Equation 6-3 assuming completely filled pipes and gravity flow which is the desired state during CWWF operation of the sewer network.

$$Q = \frac{\pi \cdot d^2}{4} \cdot \left(-2 \cdot \lg \left[\frac{2.51 \cdot \nu}{d \cdot \sqrt{2g \cdot d \cdot J_E}} + \frac{k_b}{3.71 \cdot d} \right] \cdot \sqrt{2g \cdot d \cdot J_E} \right) \quad \text{Equation 6-1}$$

with: Q ... the discharge in a completely filled sewer pipe with gravity flow, d ... the pipe diameter, ν ... the kinematic viscosity of wastewater equal to $1.31 \cdot 10^{-6} \text{ m}^2/\text{s}$, g ... the gravity of earth equal to 9.81 m/s^2 , J_E ... the energy slope line and k_b ... the operational roughness.

$$v = \frac{Q}{A}$$

Equation 6-2

with: v ... the flow velocity, Q ... the discharge for complete filling and gravity flow and A ... the cross-section of the sewer pipe.

Table 6-3: Catchment data final state

Catchment	Sewer	Surface [ha]		Retention tank		Population Equivalents	
		A _{red} [ha]	A _{CA} [ha]	V [m ³]	V _{spec} [m ³ /ha]	Winter [-]	Summer [-]
BAS	combined	6.2	16.8	225	12.0	390	599
BAU	combined	4.2	11.8	120	28.6	364	532
BAV	combined	8.0	16.0	102	12.8	210	285
Bockholtzmühle	Separate					25	105
BOE	combined	7.7	23.3	100	13.0	364	822
BUE	combined	6.0	16.5	90	15.0	164	289
BUU	combined	0.2	0.4	1	5.0	8	18
Camping Bissen	Separate					0	394
Camping Moulin	Separate					0	392
Camping Esch	Separate					0	400
DAH	combined	6.1	19.3	270	44.3	423	460
ESC	combined	5.6	11.2	95	17.0	435	803
ESD east	combined	20.6	41.2	330	16.0	640	940
ESD west	combined						
FLE	combined	0.7	2.6	32	45.7	59	89
Fuussefeld	Separate					0	15
GOE	combined	11.4	24.7	190	16.7	428	752
HEI	combined	13.6	30.0	220	16.2	628	676
HEG	combined	3.0	6.0	26	8.7	113	189
HIE	combined	1.5	3.0	20	13.3	48	48
Hotel Bissen	Separate					18	70
INB	combined	6.7	13.4	90	13.4	312	667
Insenborn Strand	Separate					0	30
KAU	combined	14.0	28.0	180	12.9	251	400
KUB	combined	5.5	11.0	70	12.7	126	156
LIE	combined	8.0	16.0	150	18.8	140	451
Lultzenhausen	Separate					222	589
MEC	combined	4.0	8.0	51	12.8	110	163
NOC	combined	4.2	16.2	166	39.5	397	422
NOR	combined	5.2	18.6	157	30.2	244	260
NOT	combined	19.0	38.0	242	12.7	399	467
RIN	combined	1.9	7.0	100	52.6	58	88
Rommwiss	Separate					0	15
SEBES	Separate					17	27
TAD	combined	1.7	4.9	100	58.8	83	104
Tadlermühle	Separate					0	292
Zillenhatt	Separate		16.8			11	33
TOTAL		165.0	383.9			6687	12042

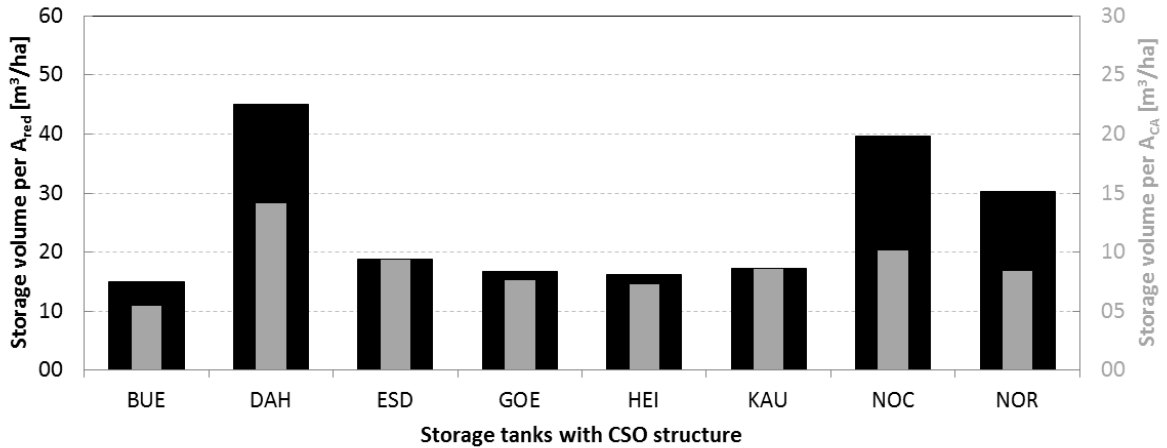


Figure 6-2: Specific retention tank volumes built in the catchment state 2010

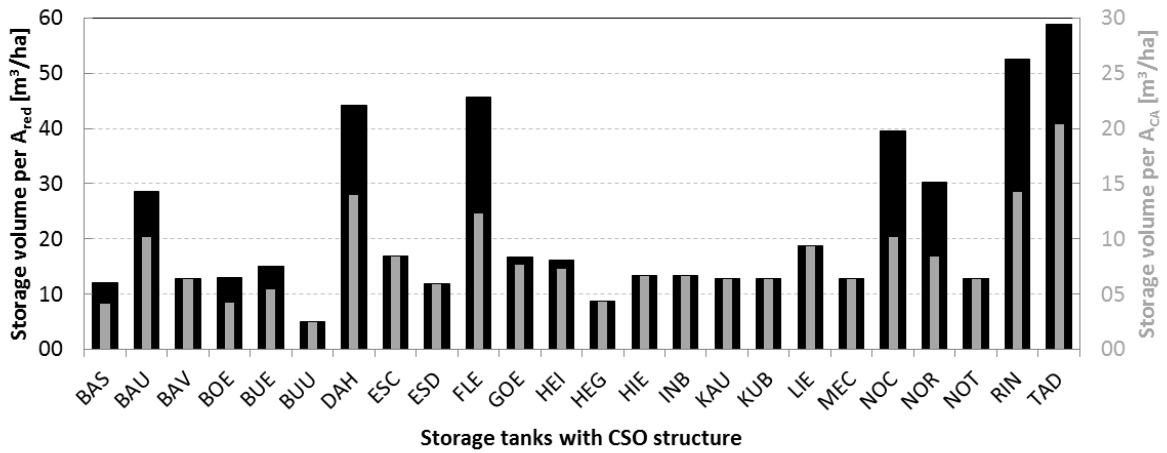


Figure 6-3: Specific retention volume designed for the final state

Table 6-4: ISN data of the final state

Catchment	Interceptor sewer network		Catchment	Interceptor sewer network	
	Length [m]	Ø Flow time [min]		Length [m]	Ø Flow time [min]
BAS	16799	104	HEG	700	10
BAU	18163	115	HIE	4164	33
BAV	14988	93	INB	8193	41
BOE	17736	107	KAU	7628	61
BUE	4580	42	KUB	7848	36
BUU	10968	44	LIE	11559	85
DAH	8230	69	MEC	10316	69
ESC	3017	22	NOC	8061	65
ESD	3570	24	NOR	8508	67
FLE	17197	105	NOT	11761	73
GOE	3853	31	RIN	4726	18
HEI	2667	18	TAD	4326	17

$$t_f = \frac{v}{l}$$

Equation 6-3

with: t_f ... the flow time in a sewer pipe section, v ... the flow velocity and l ... the length of the sewer pipe section.

6.1.2. Wastewater treatment plant Heiderscheidergrund

WWTP Heiderscheidergrund is a low loaded activated sludge type plant in continuous operation. The design treatment capacity is equal to 12 000 PE. Typically for its size the ASTs are built as oxidation ditches with intermittent aeration enabling nitrification and denitrification in the same tank. Fine bubble blowers provide the oxygen necessary for aerobic wastewater treatment and SASS by extended aeration. Due to SASS mechanical pre-treatment only consists of coarse and fine screens and an aerated sand trap without primary clarifier. The SSTs are horizontal type tanks. Tertiary treatment includes UV disinfection and sand filtration but this is not part of the presented FPC approach. The excess sludge is stabilized simultaneously by mineralization during the wastewater treatment process given the SRT of 25 days and extended aeration for endogenous respiration. The WWTP consists of two identical lanes, one only used for winter operation and both for summer operation. Figure 6-4 shows one treatment lane without the tertiary treatment. The WWTP is designed according to the German design guidelines ATV-A 131 for single-stage activated sludge plants (ATV-DVWK, 1992b) and DWA-A 226 concerning principles for wastewater treatment in activated sludge plants with SASS (DWA 2009). Each oxidation ditch has a volume of 2810 m³ which is close to the design volume of 2720.6 m³. The design surface per SST is 168.2 m² with a depth of 4.54 m. The constructed surface is 269.7 m² and a depth of 3 m. This reduces the design sludge volume surface loading from 500 to 297 l/(m²*h) and the surface loading rate from 1.32 to 0.825 m/h. Consequently, the SST capacity increases significantly.

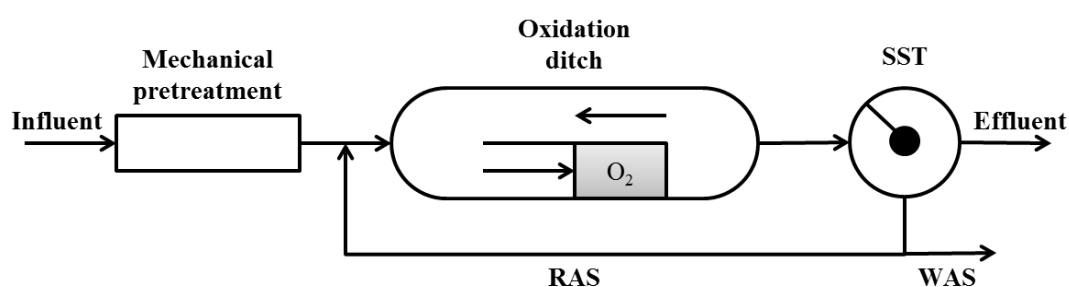


Figure 6-4: Process diagram of one treatment lane of WWTP Heiderscheidergrund without tertiary treatment

6.1.3. Receiving waters

The WCTS is situated around the Haute-Sûre storage lake which is a drinking water reservoir in the North of Luxembourg serving about 70% of the country's population. WWTP effluent and CSO from 25 retention tanks is drained into 18 different natural receiving waters. While the eastern part and the WWTP discharge downstream of the storage lake, the western part of the system discharges either directly into the reservoir or into receiving waters upstream the lake. Figure 6-1 illustrates the system.

6.2. Wastewater pollutant flows in rural WCTSS

In this PhD study system-wide data from online monitoring and offline measurement campaigns is used:

- to analyze pollutant flows of wastewater pollutants in integrated WCTSS in rural regions and
- to calibrate an integrated reference model to apply the proposed system-wide FPC approach.

To this end, data was collected between January 2010 and December 2012. The data consists of online monitoring data and complementary monitoring campaigns in the sewer network and at the WWTP. Objective of the integrated monitoring campaign is a system-wide hydraulic and pollutant flow analysis in order to investigate the behavior of wastewater pollutants in WCTSS and to analyze the impact of the ISN on the WWTP influent. Based on the equipment for hydraulic control of the retention tanks in the combined sewer network a system-wide volume balance can be made. The critical weir crest level for CSO at each retention tank currently in operation was estimated according to the approach of Brombach *et al.* (1999) based on the frequency analysis of water levels in the tank. The sum of all retention tank effluents is balanced with the continuous flow measurement at the WWTP inlet. This allows a detailed analysis of rain derived inflow and infiltration (RDII) in the ISN. Due to problematic online quality monitoring data at the WWTP Heiderscheidergrund a continuous analysis of the pollutants balance along the ISN was not possible and was limited to the data from supplementary measurement campaigns and data for WWTP self-supervision. Sampling for self-supervision at WWTP Heiderscheidergrund is limited to daily averages based on 24h composite samples. With this temporal resolution data on CWWF concentrations at the WWTP are insufficient to calculate EMCs. Additionally, pollution loads from rainfall-runoff are very case-specific. In fact, eroded mass is predominantly affected by the accumulation during dry weather periods preceding rain-events and the intensity of the specific rain event (Bertrand-Krajewski *et al.* 1998). Despite intensive investigations of appropriate modeling approaches, the modeling uncertainties are still quite large (Rossi *et al.* 2005). Overall, varying contributions of domestic sewage, rainfall-runoff and eroded sewer deposits contribute to the large variability of pollutant concentrations during CWWF (Gromaire *et al.* 2001). Due to this nonlinear behavior, system-wide pollutant balances should be based on simultaneous input-output measurements (for instance Kafi *et al.* (2008)). In the case of sequential measurement campaigns at retention tanks and the WWTP, the flux of wastewater pollutants in the WCTS is analyzed based on differentiated processes during DWF and CWWF. Zawilski and Brzezińska (2009) investigated differences of WWTP inflow compositions between DWF and CWWF based on a fractionation model. Inspired by this approach, measurement data from the present study at the retention tank outlets (representing an inlet of the ISN) and the WWTP inlet (representing the outlet of the ISN) of different events were used to investigate the impact of the ISN, the continuity of pollutant flux along the ISN and its modeling by extending the fractionation analysis to the catchment according to the following method:

1. DWF analysis
 - a. Hydraulic balance analysis according to system-wide flow measurements at retention tanks and at the WWTP inlet during DWF.

- b. System-wide balance of pollutant concentrations during DWF and regression analysis based on correlation analysis and fractionation models for the sum parameters COD and TKN (Henze 1992) both at retention tanks and at the WWTP inlet.
 - c. Assessment of pollutant transformation processes during DWF according to the comparison of hydraulic and pollutant concentration balances and corresponding results of fractionation model calibrations.
2. CWWF analysis
 - a. Hydraulic balance according to system-wide flow measurements at retention tank outlets and at the WWTP inlet during CWWF to assess the impact of RDII.
 - b. As described before, the comparison of mean CWWF concentrations based on different rain events is not effective for investigating the fate of pollutants along ISNs. Consequently, the investigation is limited to regression analysis based on the fractionation of sum parameters similar to the DWF analysis and additional correlation analysis.
 3. Comparison of fractionation models for DWF and CWWF to assess the impact of ISNs during CWWF due to nonlinear relations between sum parameters and single fractions for system-wide continuous modeling of routine wastewater fractions.

Additionally, results from the measurement campaigns were used to investigate mean DWF concentrations, EMCs and the contribution of rainfall runoff to pollutant concentrations during CWWF. The latter was derived from chemical mass balances of mean dry weather wastewater concentrations and combined wastewater concentrations which would help to characterize wastewater pollutants in rural WCTSS. The results were compared to literature data for rural and urban catchments.

6.2.1. Monitoring and measurement campaigns

6.2.1.1. Rain

The ASTA (Administration des services techniques de l'agriculture) Luxembourg maintains a nationwide network of meteorological stations. Precipitation data is available offline in a resolution of mm per 10 minutes⁵. Four of these meteorological stations are situated within the catchment or close to it (Arisdorf). Each sub-catchment is assigned to one of these rain gauges according to the Thiessen-method (Thiessen 1911). Spatial variability of rainfall is beneficial for the efficiency of sewer network control (Schütze *et al.* 2008). In the present case rainfall data is based on four rain gauges each feeding four to nine sub-catchments. Assuming system-wide homogenous rainfall-runoff characteristics in the reference model, retention tank fillings within each rain gauge allocation would only differ according to their specific retention tank volumes. In order to adapt the filling variability in the reference model to the monitored real behavior of the system during CWWF rainfall runoff coefficients (RRC)s of all retention tanks are investigated and used as a tracer for additional information on rainfall-runoff variability within each rain gauge allocation group.

⁵ The meteorological data is available at www.agrimeteo.lu.

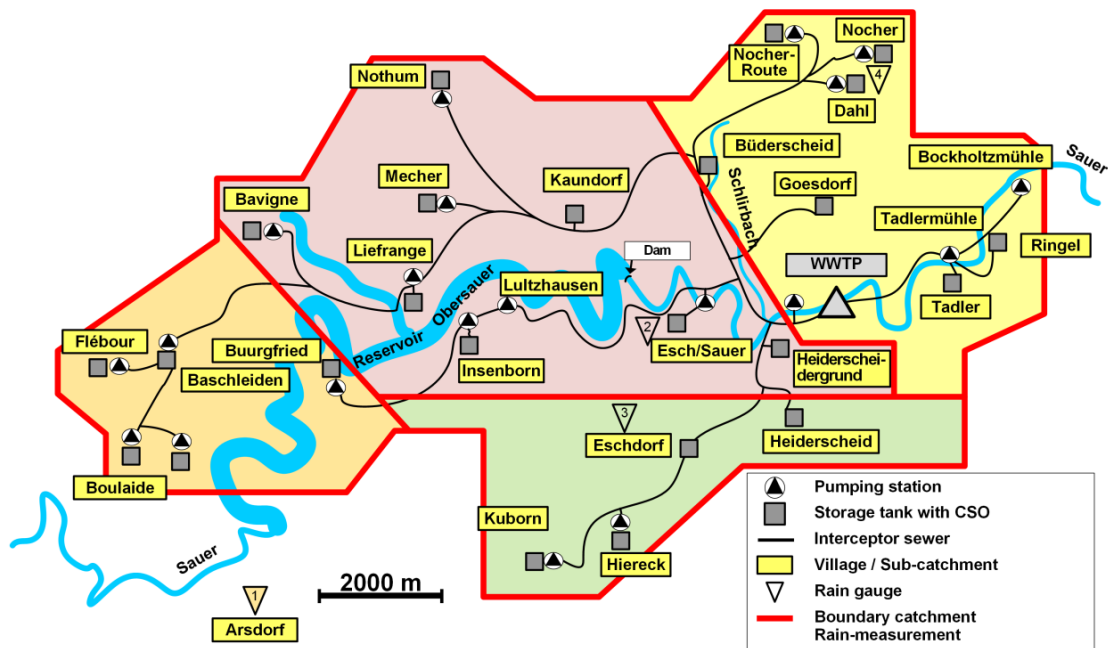


Figure 6-5: Allocation of rain gauges operated by ASTA according to the Thiessen method. Background colors show the assignment (rain gauge Arsdorf: orange, rain gauge Eschdorf: green, rain gauge Esch/Sauer: purple, rain gauge Dahl: yellow)

6.2.1.2. Online monitoring

Online monitoring equipment is essential for control. Measurement signals are used to trigger control actions and to adapt monitored variables to their reference values. While hydraulic measurement equipment is quite robust wastewater quality monitoring is rather sensitive and requires regular calibration (Campisano *et al.* 2013). In the following the system-wide measurement equipment installed in the case study is briefly described.

Sewer network

Each retention tank is equipped with an inductive flow measurement device for variable discharge control. According to the specific geographic situation retention tanks are either equipped with frequency controllable throttles or frequency controllable pumps for hydraulic based MPC. In the case of gravity flow partial filled inductive flow measurement devices are installed. Retention tanks with pumping stations are equipped with pressure flow inductive measurement devices. Additionally, each tank is equipped with pressure based water level meters. Measurement data is stored at 30 second intervals. Additional information on the sewer network and the installed equipment is given in Fiorelli and Schutz (2009). Analysis of online data of retention tanks with gravity flow to the WWTP showed that the installed partial filled inductive flow measurement devices are not able to measure DWF in the present small range (ca. one l/s) due to the focus on reliable measurement during CWWF.

WWTP

Table 6-5 illustrates the parameters monitored online at WWTP Heiderscheidergrund. Data is stored at 30 second intervals. A comprehensive data analysis considering outliers, drifts and trends according to recommendations of Rieger *et al.* (2013) showed that only online values for Q, DO, TS, temperature and conductivity were within reliable ranges. Wastewater

quality data for COD, NH₄-N and NO₃-N showed large uncertainty due to frequent drifts into ranges which are not process conform. Mismatch between laboratory measurements and online monitoring data due to drifts is a well-known problem at WWTPs (Rieger *et al.* 2004). This stresses the crucial importance of periodic sensor calibration. Continuous monitoring of the blower frequency in combination with a clear water aeration test done prior to the startup of the WWTP is used to characterize the oxygen input into the oxidation ditch.

Table 6-5: Parameters monitored online at WWTP Heiderscheidergrund

Location	Parameter
Intake pumping station	Q _{in}
	h _{PS}
Aerated sand trap outlet	pH
	Temperature
	Conductivity
	TCOD
Oxidation ditch	DO*
	TS
	NH ₄ -N
	NO _x -N
	PO ₄ -P
Secondary settlement tank outlet	Temperature
	COD
	TP

*DO sensor is situated right after the aeration field
(see **Figure 6-45**)

6.2.1.3. Self-supervision WWTP Heiderscheidergrund

As described before the present online wastewater quality data at WWTP Heiderscheidergrund showed large uncertainties. Alternatively, the measurement data for self-supervision of the WWTP is used for the routine wastewater pollutants flow analysis along the ISN. Self-supervision measurement data of WWTP Heiderscheidergrund was provided by the operator SIDEN. The laboratory data consists of 24h composite samples representing daily mean values for TSS, COD, BOD₅, TN, NH₄-N, NO_x-N and TP measured at the WWTP influent and effluent. The data was filtered for DWF respectively CWWF according to rain data and daily hydraulic loads.

6.2.1.4. Complementing measurement campaigns

Complementing measurement campaigns were performed in the sewer network and at the WWTP in 2010, 2011 and 2012:

- to complement the hydraulic sewer network data with data on wastewater parameters for system-wide pollutants flow analysis and
- to investigate the pollution load variations for the calibration of the integrated reference model.

Sewer network

Additional monitoring campaigns were performed at three retention tanks with CSO structures in order to determine DWF hydro- and pollutographs and to investigate concentration profiles during rain events as foundation for the subsequent calibration of the reference model. For both DWF and rain events the following parameters were measured: TSS, COD, S_{COD} , BOD_5 , TN, $\text{NH}_4\text{-N}$, $\text{NO}_x\text{-N}$, TP, $\text{PO}_4\text{-P}$, pH and conductivity. Grab and composite sampling with subsequent VIS spectral photometry analysis in the laboratory was chosen because:

- small wastewater flows during DWF (one to two l/s) are insufficient to continuously cover the sensors of online probes and
- online measurement of BOD_5 , TN, TP and $\text{PO}_4\text{-P}$ is limited to analyzers.

DWF sampling was based on 2h-composite samples taken at 10min-intervals. CWWF event sampling was based on grab samples in staggered intervals of 2, 5, 10 and 30 to 60 minutes. CWWF event sampling was triggered by the water level in the retention tank. Small intervals in the beginning of the event shall guarantee to cover first flush effects. The main disadvantage of the approach is the limited number of samples per event and consequently the uncertainty of covering the characteristic information of an event by defining the sampling time series in advance of the event. Concentrations were measured with HACH-LANGE cuvette tests based on VIS spectral photometry. Soluble fractions were measured after filtration using 0.45 micron pore size filters. TSS was measured from the residue after drying at 105°C. BOD_5 was measured according to the pressure caused by microbial oxygen respiration after five days in incubation bottles (WTW OxiTop®). X_{COD} was calculated from the difference between COD and S_{COD} , TKN from the difference between TN and $\text{NO}_x\text{-N}$. Table 6-6 summarizes the extent of the sewer network monitoring campaign.

Table 6-6: Extent of the sewer network monitoring campaign

Sub-catchment	Retention tank type	Period	Number of events	
			DWF	CWWF
Kaundorf	Offline bypass	06/2010 – 08/2010	4	3
Nocher-Route	Online bypass with pumping station	03/2011 – 04/2011 08/2011	3	1
Goesdorf	Online bypass	04/2011 – 06/2011	-	12

Additionally, a flow time test was conducted to validate transportation times for discrete hydraulic discharges in the sewer network calculated from the given design data. To this end during DWF wastewater was stored in all retention tanks. The coordinated emptying of all retention tanks created peak discharges which were recorded at the inlet of the WWTP. The allocation of inflow peaks to the respective retention tank discharges allowed to calibrate the hydraulic reference simulation model of the ISN and to validate the corresponding constant flow times assumed for MPC. A detailed description of the test and the model calibration is given by Regneri *et al.* (2012).

WWTP

Since the self-supervision data of WWTP Heiderscheidergrund only consists of daily composite samples two additional measurement campaigns were performed at the WWTP

to investigate the diurnal dynamics for DWF and one CWWF event. 2-h-composite sampling based on pumped grab samples was done for COD, S_{COD} , TN, $\text{NO}_x\text{-N}$, $\text{NH}_4\text{-N}$ and TP both at the inlet and the outlet of the plant. Grab samples for TSS, VSS and alkalinity completed the campaigns. Sampling both the WWTP inlet and the effluent of the aerated sand trap the effect of the sand trap on particulate fractions could be estimated. The sand trap retains about 10% of the particulate COD. Effects on TKN were not noticeable. VSS was measured according to ignition of the TSS residue at a temperature of 550°C. Alkalinity was measured by the amount of sulfuric acid needed to bring the wastewater sample to a pH of 4.2. Additionally, an oxygen profile was measured along one oxidation ditch during continuous aeration in order to derive an appropriate model layout.

6.2.2. Analysis

6.2.2.1. DWF

Wastewater flow

In combined sewer systems wet weather flow from the catchment to the WWTP consists of a base flow of domestic sewage which is measurable during DWF and runoff from rainfall or snow melt. In the present case domestic wastewater is assumed to include wastewater from farms and small workshops. Wastewater discharges at retention tanks show large differences between DWF and CWWF. In the present case DWF from the small villages is in the range of about one liter per second. During CWWF discharges increase dramatically. In combined sewer network operation they must be throttled at retention tanks according to the reference capacity of the WWTP. In order to improve accuracy during control the flow sensitive measurement range is optimized for the specific control range. Consequently, measurement quality outside this range as for example during DWF suffers. Due to this, DWF at retention tanks with gravity flow to the WWTP could not be measured in the present case. Since discharge during pumping is constant, the system-wide hydraulic analysis during DWF was limited to the effluent of retention tanks with pressure flow to the WWTP. Daily volumes were integrated according to pumping intervals at dry weather days which were derived from the 21 days moving minimum method (De Bénédittis and Bertrand-Krajewski 2005). Thereby at least one dry weather day in a 21 days interval is assumed. Wastewater production per capita was calculated from the given data for PE.

Figure 6-6 and Figure 6-7 exemplary illustrate the approach for WWTP Heiderscheidergrund resp. retention tank DAH for the year 2012. The boxplot evaluation according to Figure 6-8 reveals the dynamics of small rural WCTSSs due to seasonal effects and catchment size-related sensitivity towards temporal effects such as weekends or holidays (Pujol and Lienard 1990). Despite reduced rainfall in winter the 21 days moving minimum discharges quadruple in December 2012. Ellis (2001) mentioned hydraulic leakage into sewers from increased groundwater levels particularly after rain events as a major source for sewer infiltration. Thereby, decay rates in the surrounding water table are much slower than in the sewer network. Consequently, infiltration continues long after the rain event has ceased. Seasonal variations of groundwater levels increase infiltration, especially in winter (Weiß *et al.* 2002). Additionally, delayed runoff from snow melt might also contribute to increased runoff during winter month (Valeo and Ho 2004). Further investigations are out of the scope of the present work. Nevertheless, the analysis illustrates the catchment size-related sensitivity of small

rural systems towards RDII. Table 6-7 summarizes the resulting mean DWF discharges per capita and day. The results are quite close to each other and show no outliers. Standard deviations are about one third of the means illustrating the dynamics in DWF in small rural WCTs. In average the mean daily per capita sewage production is 0.150 m^3 which is close to the German assumption of $0.185 \text{ m}^3/\text{PE}/\text{d}$ for designing municipal WWTPs (DWA 1992b). Differences to the daily mean per capita DWF of $0.175 \text{ m}^3/\text{d}$ measured at the WWTP inlet can be related to:

- uncertainties in the given PE data for each sub-catchment,
- infiltration of groundwater in the ISN and
- hydraulic measurement uncertainties.

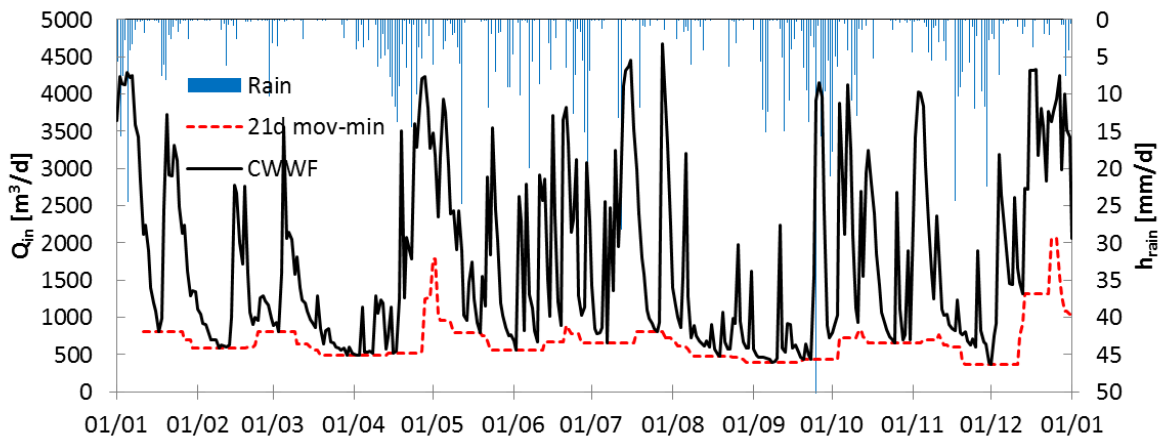


Figure 6-6: 21 days moving minimum method for DWF analysis of the inflow at WWTP Heiderscheidergrund in the period of January 2012 to December 2012

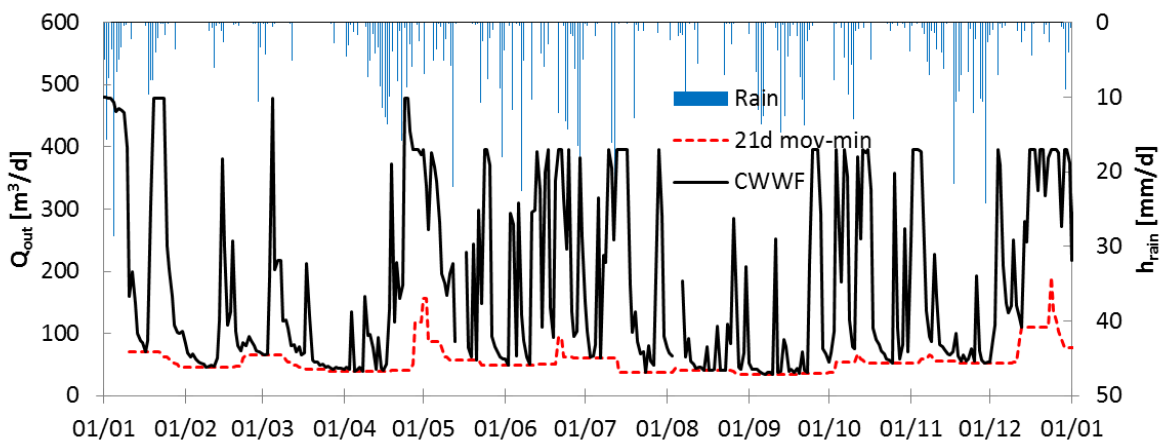


Figure 6-7: 21 days moving minimum method for DWF analysis of the effluent at retention tank Dahl with pumping station in the period of January 2012 to December 2012

The subsequent system-wide pollutants flow investigation during DWF will help to answer this question.

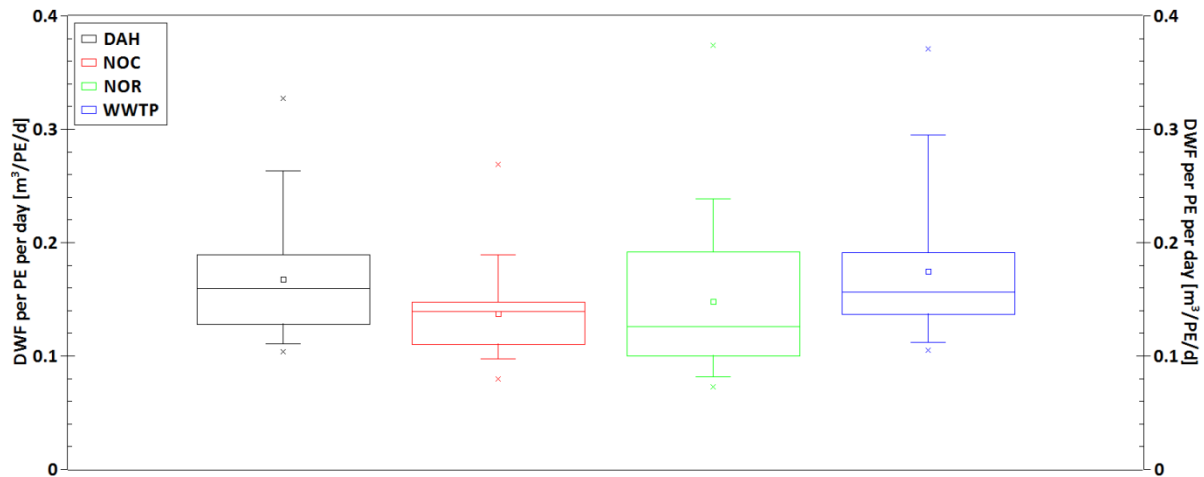


Figure 6-8: Boxplot evaluation of DWF per capita per day based on the 21 days moving minimum analysis for the period January 2010 to December 2012 at retention tanks with pumping station (DAH (black), NOC (red) and NOR (green)) and WWTP Heiderscheidergrund (blue).

Table 6-7: Mean DWF per capita per day resulting from 21 days moving minimum evaluations at retention tanks with pumping stations and at the WWTP for the period of January 2010 to December 2012

	Per capita DWF [m ³ /d]			
	DAH	NOC	NOR	WWTP
MEAN	0.168	0.137	0.148	0.175
STD	0.052	0.036	0.064	0.059

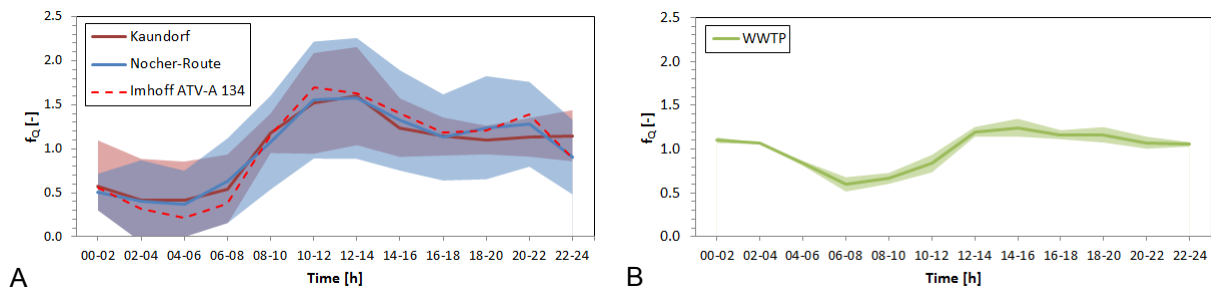


Figure 6-9: Variability of daily DWF hydrographs measured at (A) catchments and (B) the WWTP inlet

Figure 6-9 (A) shows the variability of the DWF hydrographs monitored at both catchments under investigation. The results correspond to the variability described by Pujol and Lienard (1990) and Heip et al. (1997). In average the monitored DWF hydrographs on catchment level correspond to the reference DWF hydrograph for residential catchments according to (DWA 2000). The average DWF hydrograph measured at the WWTP inlet illustrated in Figure 6-9 (B) is flattened according to different specific transport times from retention tanks to the WWTP.

Wastewater pollutants

Catchment

Due to the hilly catchment geomorphology of the chosen case study about 50 percent of the retention tanks must be operated with pumping stations in order to transport the wastewater to the WWTP. During DWF wastewater is pumped in intervals to the WWTP according to the retention tank threshold water levels chosen to activate pumping. Besides the hydrograph, the mixing of impounding wastewater during DWF according to the resulting pumping intervals affects the pollutographs of DWF discharged to the WWTP. In order to simplify the sewer network reference simulation model during DWF it was decided to consider the effect of impounded DWF from retention tanks with pumping stations according to measured hydro- and pollutographs instead of the detailed modeling of pumping intervals at each retention tank with pumping station. Thereby, the chosen approach additionally considers the impact of particulate matter accumulation in the wet well and effects on the composition of raw dry weather sewage according to changing aerobic/anaerobic conditions. These processes have been studied by e.g. Hvitved-Jacobsen et al. (1999). Detailed modeling of these processes in retention tanks with pumping stations is out of the scope of the present work. Consequently, for wastewater quality monitoring one retention tank with gravity flow to the WWTP and one with a pumping station were chosen in order to equally consider the impact of retention tank discharges with gravity and pressure flow to the WWTP when using one average daily DWF hydro- and pollutograph for DWF catchment effluents. Figure 6-10 to Figure 6-12 show the resulting boxplots from the DWF measurement campaigns at retention tanks KAU and NOR. The variability of the COD concentration is predominantly caused by the variability of particulate COD.

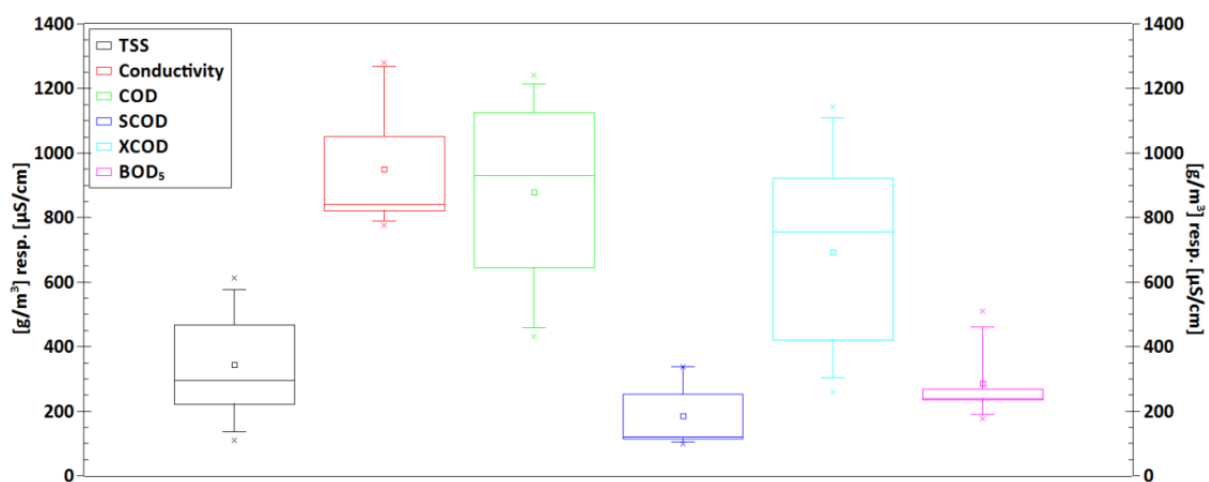


Figure 6-10: Daily mean DWF evaluation of TSS, conductivity, COD and BOD₅ concentrations at retention tanks KAU and NOR

The variability of the COD concentrations is exceptional high and predominantly caused by the variability of particulate COD. This leads to a COD to BOD₅ ratio of 3.1 to 1 which exceeds the common ratio of 2 to 1 for domestic wastewater. The COD to TSS ratio of 2.6 also exceeds the common ratio of 1.4 - 1.0 to 1 indicating increased amounts of organic particulate matter. VSS could give additional information on the inorganic content of the

particulate matter. Unfortunately, this parameter was not measured. Figure 6-13 illustrates the variability of the monitored daily COD DWF pollutographs according to average 2h-mean concentrations and corresponding standard deviations differentiated according to the retention tank effluent (A) Kaundorf with gravity flow to the WWTP and (B) Nocher-Route with a pumping station. While the Kaundorf pollutograph shows a distinctive concentration variability with common peak concentrations around noon and 8 pm, the Nocher-Route pollutograph shows high mean COD concentrations caused by the mixing of impounded DWF in the wet well of the pumping station. The high mean concentration probably results from the accumulation of particulate matter, noticeable especially after rainfall events. In order to correspond to both ratios particulate COD must be predominantly slowly biodegradable. Despite similar standard deviations for TSS, S_{COD} and BOD_5 the latter shows a much smaller interquartile range. Nitrogen and TKN are dominated by NH_4-N . NO_x-N concentrations are negligible. PO_4-P variability is in a comparable range. Variability of total phosphorous is dominated by particulate phosphorous related to particulate matter.

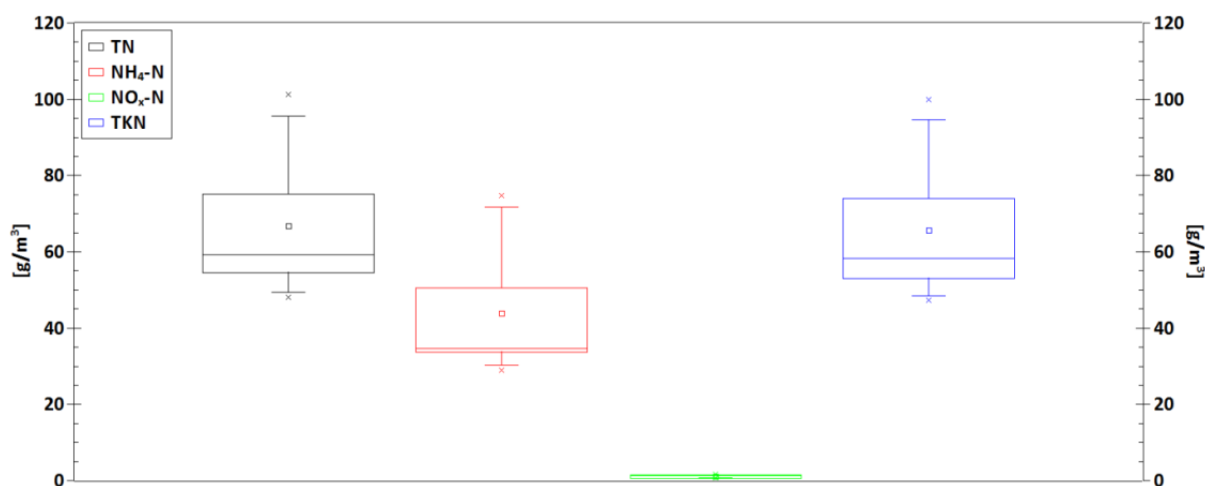


Figure 6-11: Daily mean DWF evaluation of TN, NH_4-N , NO_x-N and TKN concentrations at retention tanks KAU and NOR

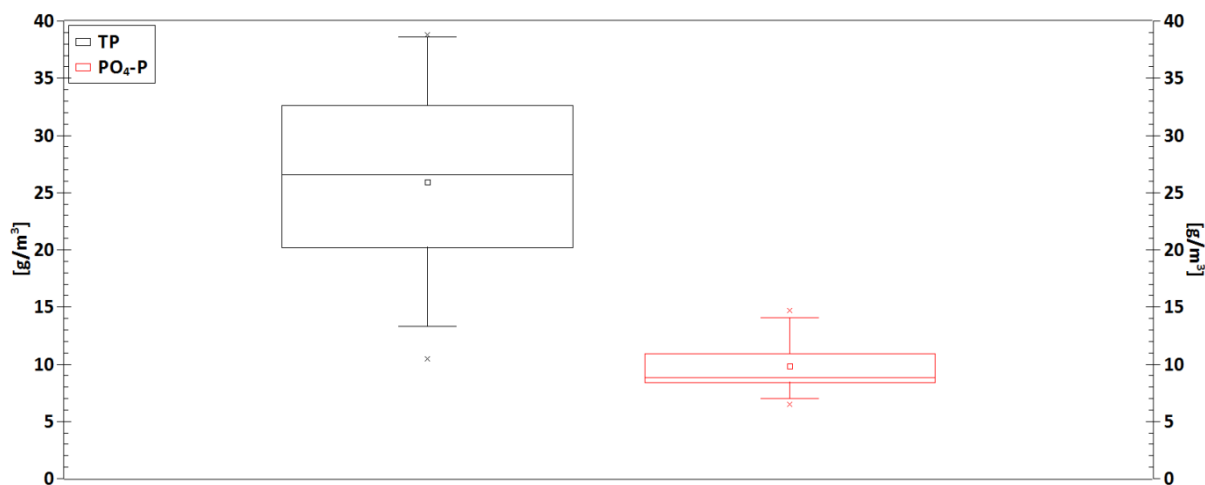


Figure 6-12: Daily mean DWF evaluation of TP and PO_4-P concentrations at retention tanks KAU and NOR

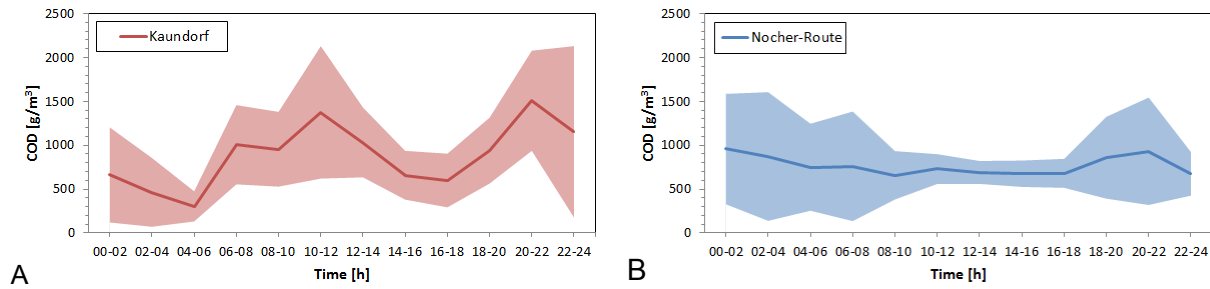


Figure 6-13: Variability of the monitored COD DWF pollutographs for retention tanks (A) Kaundorf (gravity discharge to the WWTP) and (B) Nocher-Route (pumped discharge to the WWTP) according to mean concentrations and standard deviations

The wide range of concentrations confirms the variability of pollution loads from rural catchments as stated by Pujol and Lienard (1990). Due to the small numbers of PE per catchment the resulting pollutographs is less homogenized according to the mixing of individual wastewater production patterns.

Table 6-8 summarizes the results from the measurement campaign for DWF concentrations of routine wastewater parameters as daily mean values and their standard deviations.

Table 6-8: Evaluation of daily mean DWF concentrations for wastewater pollutants at retention tanks KAU and NOR and comparison to literature data on rural and urban systems

Parameter	Haute-Sûre* ¹	Pujol and Lienard (1990)* ¹	Heip et al. (1997)	Brombach et al. (2005)	Gasperi et al. (2008)	Tchobanoglous et al. (2004)* ²	ATV-DVWK (1992b)* ³
Catchment	Rural	Rural	Rural	Urban	Urban	General	General
Flow [l/PE]	151 ± 51	150 ± 50	87	n.a.	n.a.	n.a.	185
TSS [g/m ³]	344 ± 179	250 ± 30	463	n.a.	198	120 – 370	378
COD [g/m ³]	878 ± 315	700 ± 100	1511	403	388	260 – 900	647
S _{COD} [g/m ³]	186 ± 106	n.a.	221	n.a.	n.a.	n.a.	383
X _{COD} [g/m ³]	692 ± 335	n.a.	n.a.	n.a.	n.a.	n.a.	264
BOD ₅ [g/m ³]	287 ± 130	300 ± 65	714	178	181	120 – 380	324
TN [g/m ³]	67 ± 19	80 ± 20	n.a.	34	n.a.	20 – 70	n.a.
NH ₄ -N [g/m ³]	44 ± 18	60	n.a.	n.a.	n.a.	n.a.	n.a.
NO _x -N [g/m ³]	1 ± 0.4	n.a.	n.a.	n.a.	n.a.	0	n.a.
TKN [g/m ³]	66 ± 19	n.a.	74	n.a.	36	20 – 45	59.3
TP [g/m ³]	26 ± 10	35	n.a.	n.a.	n.a.	n.a.	n.a.
PO ₄ -P [g/m ³]	10 ± 3	30	9	4.5	n.a.	4 – 12	13.5

*¹ mean value with standard deviation

*² min and max values

*³ 85-percentile

The comparison to literature data for rural and urban catchments confirms the findings of studies by Pujol and Lienard (1990) and Heip et al. (1997) that concentrations of pollutants are higher in rural catchments compared to urban catchments. Per capita DWF is equal to the findings of Pujol and Lienard (1990) but larger than the data given by Heip et al. (1997). Most striking difference to the average concentrations according to the German design

guideline ATV-A 131 (ATV-DVWK, 1992b) is the low S_{COD} concentration. Heip et al. (1997) confirm these findings for rural catchments. However, their TCOD concentrations cannot be confirmed by the present findings. This might be linked to the smaller per capita wastewater flows of their observations. Compared to the general range of DWF concentrations presented by Tchobanoglous et al. (2004) the present results are situated at the upper limits for most of the parameters, except for TKN which is clearly exceeding. Especially larger nutrient concentrations are typically for rural catchments due to the dominating contribution of domestic wastewater (Heip *et al.* 1997). Additionally, agricultural wastewater from dairy farms might contribute to increased nitrogen concentrations (Longhurst *et al.* 2000). Altogether, the present concentrations are comparable to the assumptions used for the design of the WWTP Heiderscheidergrund (DWA 1992b) except for the ratio of soluble to particular COD which affects the amount of non-degradable, easily and slowly degradable soluble COD and consequently the WWTP performance and dynamics. It must be taken into account that the design concentrations relate to the 85-percentiles.

WWTP

Mean DWF concentrations are derived from the SIDEN self-supervision data for the years 2010 to 2012. DWF days are filtered according to rainfall and mean daily DWF volumes. The data is completed by DWF data from complementary measurement campaigns to gather supplementary information on daily patterns of hydro- and pollutographs. Figure 6-14 to Figure 6-16 show the resulting boxplots from the DWF measurement campaigns at WWTP Heiderscheidergrund. Table 6-9 summarizes the daily mean values and their standard deviations.

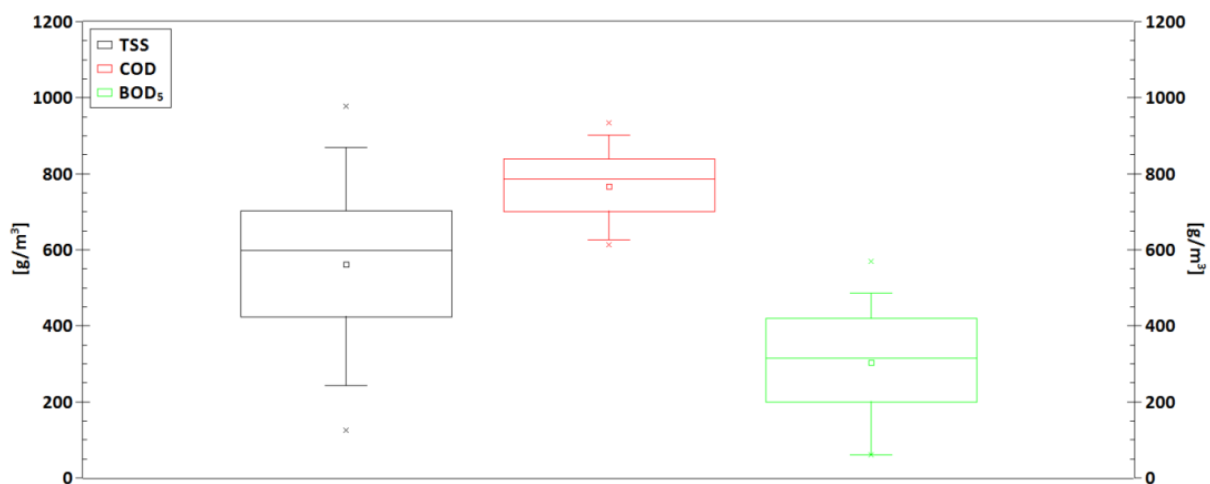


Figure 6-14: Daily mean DWF evaluation of TSS, COD and BOD₅ concentrations at WWTP Heiderscheidergrund

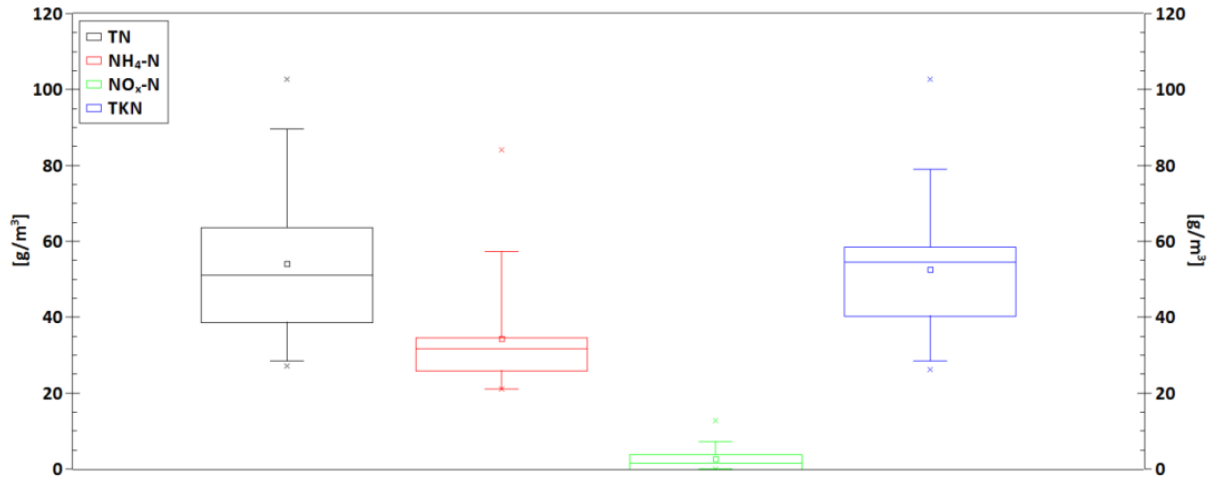


Figure 6-15: Daily mean DWF evaluation of TN, NH₄-N, NO_x-N and TKN concentrations at WWTP Heiderscheidergrund

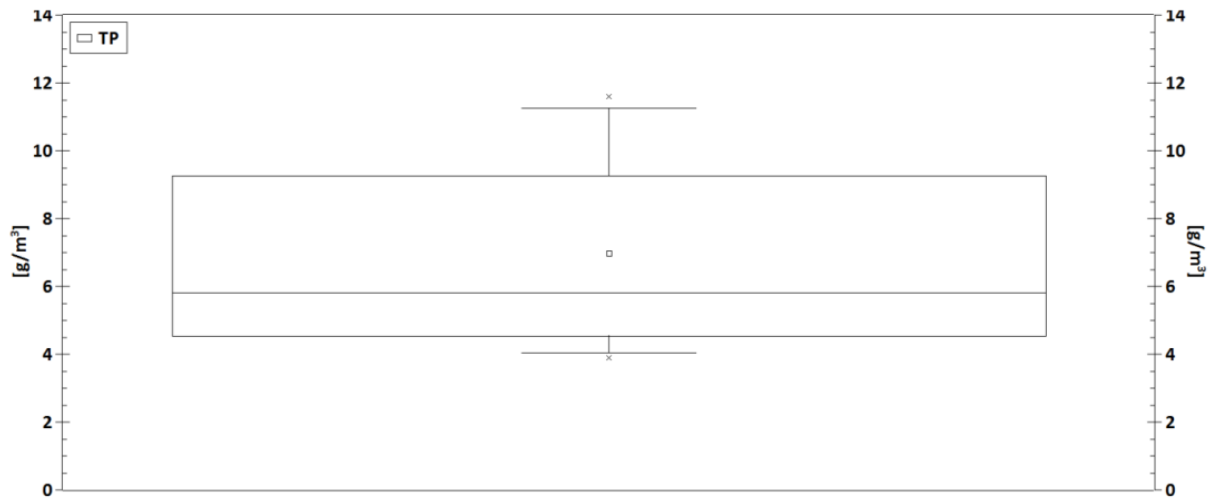


Figure 6-16: Daily mean DWF evaluation of PO₄-P concentrations at WWTP Heiderscheidergrund

Table 6-9: Evaluation of daily mean DWF pollution concentrations of the raw inflow at WWTP Heiderscheidergrund and comparison to the design assumptions

		TSS	COD	BOD ₅	TN	NH ₄ -N	NO _x -N	TKN	TP
		[g/m ³]							
Monitoring	MEAN	561.4	767.1	343.5	55.2	34.4	2.6	52.5	7.0
	STD	214.0	94.9	111.6	19.7	15.1	3.3	18.5	2.8
Design*		378.0	647.0	324.0	-	-	0.0	59.3	13.5

* 85-percentile

The mean nutrient ratio COD : TKN : TP⁶ is 110 : 7.5 : 1 and thus close to the ideal ratio of 100 : 5 – 10 : 1. The COD to BOD₅ ratio of 2.2 is only slightly above the present design

⁶ Total phosphate

assumption of 2.0 for domestic wastewater according to ATV-A 131 (ATV-DVWK, 1992b). The COD to TSS ratio of 1.4 is at the upper limit of the common range of 1.0 to 1.4 indicating a high content of organic particulate matter. The design guideline ATV-A 131 (ATV-DVWK, 1992b) even assumes a COD to TSS ratio of 1.7. Overall, the comparison of COD to TSS ratios and COD to BOD₅ ratios between wastewater analyzed at the chosen retention tanks and the WWTP inlet shows a change of ratios towards common values for raw wastewater. Since during the monitoring campaign the number of retention tanks with pumping stations was only three of eight the influence on both the COD to TSS ratio and COD to BOD₅ ratio is still noticeable at the WWTP inlet but in a much smaller extent compared to the results investigated at the retention tanks. Since the number of retention tanks with pumping stations in the final system will be nearly the same as the number of retention tanks with gravity flow to the WWTP the investigated DWF profiles will be considered as representative. The other pollutant mean DWF concentrations and standard deviations correspond to the values measured at the chosen retention tanks. The resulting daily DWF loads correspond to the design assumptions according to the German design guideline ATV-A 131 (ATV-DVWK, 1992b) (see Table 6-10) except for S_{COD}⁷ and TP showing significantly lower values for both parameters. The calibration of a fractionation model in section 6.2.3 will show details about differences in modeling TSS, soluble and particulate COD, BOD₅, NH₄-N and N_{org} from the sum parameters COD and TKN at retention tanks and at the WWTP inlet.

Table 6-10: Mean DWF loading of WWTP Heiderscheidergrund, comparison of measurement data and design assumptions

Parameter	WWTP Heiderscheidergrund	ATV-A 131
PE	12042	12000
Per capita flow [m ³ /d]	0.171	0.185
TCOD [kg/d]	1580	1440
SCOD [kg/d]	335*	853
BOD ₅	707	720
TSS [kg/d]	1156	840
TKN [kg/d]	108	132
PO4-P [kg/d]	14	30

* calculated according to the relation of SCOD to TCOD measured at retention tanks during DWF presented in Table 6-8

System-wide analysis

Sewage quality changes due to transport in sewer networks have been investigated by many researchers. According to the availability of oxygen in the sewer different processes have been investigated and modelled:

- transformation of nitrogen compounds (Pai *et al.* 2013),
- organic matter removal (Baban and Talinli 2009) and
- hydrogen sulfide oxidation (Hvitved-Jacobsen *et al.* 1999).

⁷ Due to missing self-supervision measurement data S_{COD} was derived from the sewer network assuming a constant ratio of S_{COD} and X_{COD} corresponding to the measurements at the retention tanks.

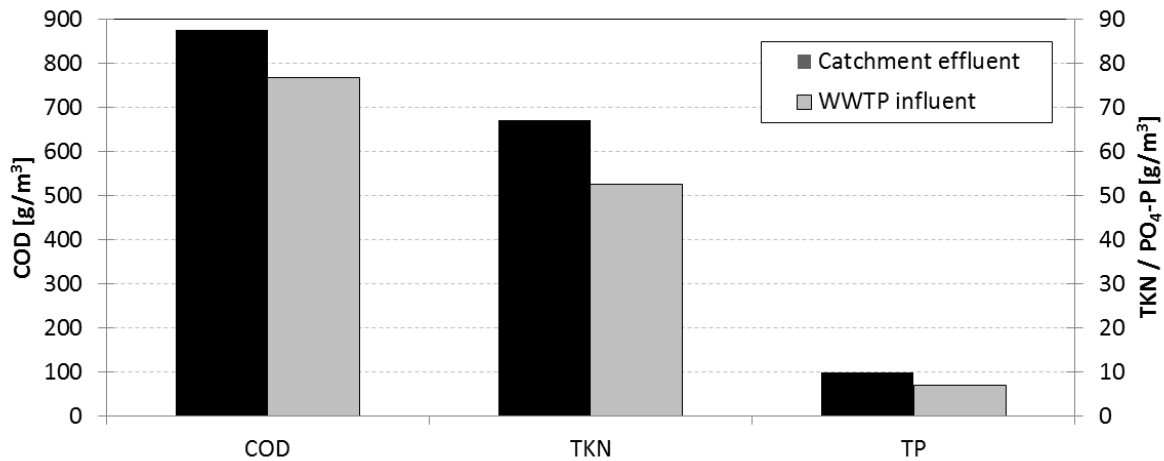


Figure 6-17: Comparison of average DWF concentrations between catchment effluent and WWTP influent

Consequently, the influence of transport in the ISN on sewage pollutants during DWF is analyzed by comparing the mean concentrations at catchment outlets and at the WWTP inlet. According to the necessities of integrated models for WCTSS (see section 2.2.2) the model of the ISN must consider at least the fate of the sum parameters COD, TKN and TP (if phosphate removal is considered at the WWTP). The results of the system-wide comparison of these parameters are shown in Figure 6-17. The mean decrease in concentrations is 21%. This corresponds to the mean increase of DWF per capita of 16% in the ISN hydraulic balance according to Table 6-7. Since the reduction of $\text{NH}_4\text{-N}$ and TN according to Table 6-8 and Table 6-9 is 22% resp. 17% the investigated decrease in concentrations in the ISN during DWF can be predominantly related to dilution. Consequently, transformation processes due to sewer biofilm processes (see e.g. Jiang et al. (2009)) can be neglected in the present case. The increase of TSS by 62% according to Table 6-8 and Table 6-9 can be explained by the accumulation of solid matter during CWWF in the pump well of the WWTP inlet (Chebbo *et al.* 1995). Further investigations of TSS accumulation during DWF and its composition is out of the scope of the present study.

6.2.2.2. CWWF

Combined wastewater is composed of domestic wastewater and rainfall-runoff. In the present case domestic wastewater consists of sewage from households, farms and small workshops. The contribution of rainfall-runoff and wastewater to CWWF and pollution loads is calculated from chemical mass balance, similar to studies by Gromaire et al. (2001), Soonthornnonda and Christensen (2008) or Gasperi et al. (2010).

Wastewater flow

RDII water can have a significant impact on the WWTP load during CWWF (Zhang 2007). If not taken into account, the hydraulic loading of the WWTP is underestimated, consequently causing emergency CSO at the WWTP in order to avoid sludge wash-out at the SST. There are several model-based approaches for estimating sewer network infiltration. Thanks to the system-wide installation of inductive flow measurement devices for sewer network real-time control RDII can be measured in the studied system. In the ISN RDII is calculated from the hydraulic balance between the WWTP inflow and the sum of retention tank outflows during

CWWF. Figure 6-18 shows the comparison between the sum of aggregated retention tank discharges to the WWTP (light blue line) and the aggregated inflow to the WWTP Heiderscheidergrund (dark blue line) exemplary for the year 2012. The drifting parallel form of both lines indicates a linear correlation. Figure 6-19 confirms the linear behavior of RDII in the ISN with a coefficient of determination of 0.9987. The slope of the linear correlation function describes the percentage of RDII of about 15 percent. Weiß et al. (2002) observed 34 German combined sewer systems during a four year period. Their results showed in average 35% of infiltration water. The comparably small RDII in the present case demonstrates the quality of the newly built ISN.

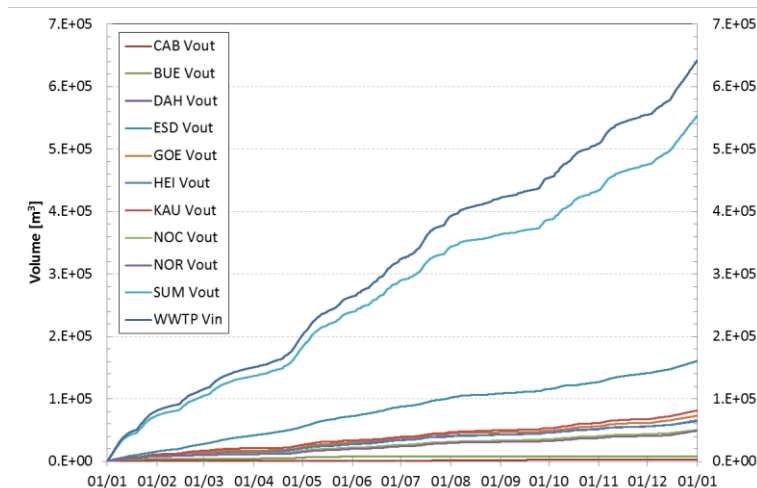


Figure 6-18: System-wide volume balance between the sum of aggregated retention tank discharges to the WWTP (light blue line) and the aggregated inflow to the WWTP Heiderscheidergrund (dark blue line) for the year 2012

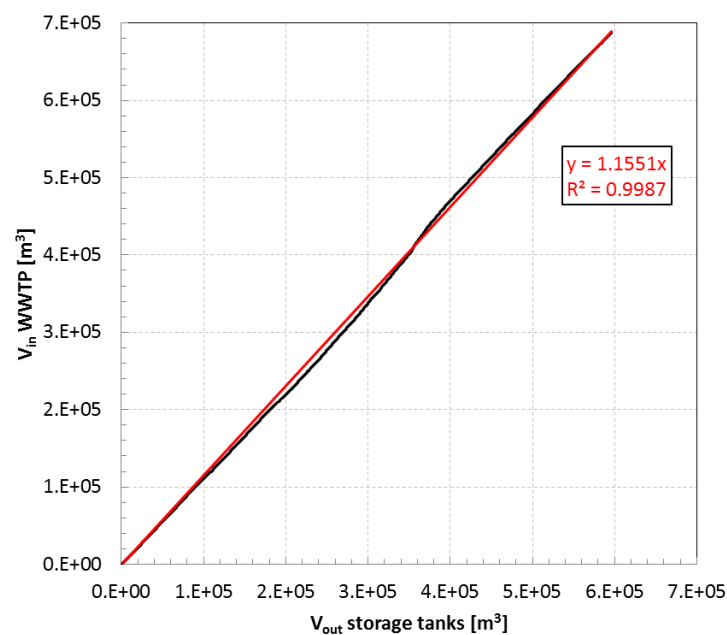


Figure 6-19: Double mass analysis of the system-wide volume balance for RDII estimation in the ISN for the year 2012

Wastewater pollutants**Catchment**

In the framework of this PhD study 14 rain events were sampled at the outflow and overflow of the retention tanks Kaundorf, Nocher-Route and Goesdorf based on grab samples (see Table 6-11). Thereby, three CSO events were sampled according to the method presented in section 6.2.1.4. Table 6-12 describes the corresponding hydrologic and hydraulic characteristics.

Table 6-11: Overview of monitored storm events and number of collected samples per event

Event no.	Date [dd/mm/yyyy]	Retention tank	Collected samples	
			Outflow	Overflow
1	12/07/2010	KAU	16	
2	23/07/2010	KAU	15	
3	04/08/2010	KAU	16	
4	16/08/2010	KAU		14
5	03/04/2011	NOR	24	
6	28/04/2011	GOE	11	
7	19/05/2011	GOE	10	
8	31/05/2011	GOE	36	2
9	05/06/2011	GOE	13	
10	06/06/2011	GOE	6	
11	07/06/2011	GOE	9	
12	18/06/2011	GOE	10	
13	19/06/2011	GOE	6	
14	22/06/2011	GOE	13	7

Table 6-12: Main hydraulic characteristics of the monitored storms and antecedent dry weather periods

Event no.	Rainfall length [min]	Rainfall depth [min]	Observed volume [m ³]	Max flow rate [m ³ /h]	Runoff coefficient [-]	Antecedent dry period [d]
1	20	2.4	85	758	0.32	1.4
2	60	0.7	57	304	0.74	1.7
3	120	2.9	112	620	0.35	1.8
4	3030	27.2	1292	2961	0.43	0.8
5	686	10.0	141	180	0.33	2.5
6	210	2.6	43	75	0.22	0.5
7	40	3.8	168	910	0.58	4.2
8	820	21.1	907	1801	0.57	8.9
9	460	5.6	104	252	0.24	0.6
10	5	2.5	60	472	0.32	0.4
11	90	4.8	142	581	0.39	1.2
12	90	1.6	58	110	0.48	0.3
13	930	5.4	61	257	0.15	0.2
14	220	7.9	314	770	0.52	0.2

Retention tank inflows are calculated from the outflow and the change of water level inside the retention tank. The resulting is balanced with the measured outflow. Uncertainties regarding maximum flow rates are quite high due to the complex nonlinear water level – volume relation of the tanks and the sensitivity of pressure based water level meters. This also affects the pollution load model calibration presented in section 6.3.4.1.

The analysis shows a wide range of rain events and antecedent dry weather periods providing a differentiated foundation for the calibration of a pollution load model for rainfall-runoff based on accumulation and wash-off.

- **Event mean concentration (EMC)**

A common approach to describe the pollutant loads of rainfall events in combined sewer systems is the EMC (Equation 6-4).

$$EMC = \frac{\sum Q_i c_i \Delta t_i}{\sum Q_i \Delta t_i} \quad \text{Equation 6-4}$$

with: Q_i ... the discharge during time interval i , c_i ... the concentration of pollutant j during time interval i and Δt_i ... the length of time interval i .

Table 6-13 summarizes the EMC of the investigated wastewater pollutants measured in the effluent of retention tanks for each rain event. The results show a wide range of EMCs. This emphasizes the need for pollution load models for rainfall runoff during CWWF based on accumulation and wash-off. All EMCs exceed permit limits for WWTP discharges to receiving waters (EC 1991). Consequently, AST bypass control of highly diluted combined sewage for increasing the treatment capacity of the WWTP during CWWF treatment as proposed by (Ahnert *et al.* 2009) is inadequate in the present case.

Table 6-13: Event mean concentrations measured at the effluent of retention tanks

Event no.	EMC [g/m ³]										
	TSS	COD	S _{COD}	X _{COD}	BOD ₅	TN	TKN	NH ₄ -N	NO _x -N	TP	PO ₄ -P
1	280	396	102	294	128	15	12	3.3	2.5	9.3	n.a.
2	135	240	54	186	87	10	8	2.8	1.7	6.0	n.a.
3	85	139	35	104	54	11	9	2.8	1.5	4.4	n.a.
4	207	359	147	212	114	29	27	15.1	1.6	4.2	2.6
5	295	561	123	438	182	43	39	20.7	4.1	5.2	3.2
6	427	458	80	378	207	27	25	6.9	1.8	4.0	1.0
7	279	204	47	157	67	13	10	4.0	3.5	3.3	1.3
8	543	519	80	439	214	32	30	8.7	2.6	5.3	2.7
9	165	172	52	120	64	13	11	5.1	2.2	1.7	0.9
10	1636	931	53	879	280	28	24	3.5	3.3	4.7	2.1
11	285	193	47	146	73	14	11	4.2	2.9	2.7	1.0
12	76	125	45	80	47	9	8	3.2	1.6	1.3	0.7
13	169	248	41	207	88	15	13	6.7	2.0	2.4	1.2
14	78	79	18	61	31	11	9	3.2	2.1	1.0	0.5

Table 6-14 shows the comparison of the present findings to data from a literature review on EMCs for combined sewer systems in rural (urban with low population density and high degree of pervious surface) and urban catchments. The present results confirm the results of Lee and Bang (2000) of increased EMCs of particulate pollutants due to the increased contribution from pervious catchment surfaces. Additionally, the data shows increased ammonium EMCs indicating surface runoff from agricultural land fertilized with manure from animal farming as investigated by (Pierson *et al.* 2001).

Table 6-14: Comparison of resulting event mean concentrations for combined wet weather flow to results from literature review and WWTP legal effluent limits

Parameter		EMC CWWF						EC (1991)
		Haute-Sûre	Tchobanoglous et al. (2004)	Choe et al. (2002)	Lee and Bang (2000)	Kafi et al. (2008)*	Brombach et al. (2005) ⁺	
Catchment		Rural	General	Urban	Rural	Urban	General	General
TSS [g/m ³]	Min	76	270	-	22.0	144	-	
	Max	1636	550	-	1413.1	495	-	
	Mean	333	-	278.8	346.2	275	174.5	< 30
BOD ₅ [g O ₂ /m ³]	Min	31	60	-	24.3	108	-	
	Max	280	220	-	217.1	290	-	
	Mean	117	-	123.4	106.5	171	60.0	< 15
COD [g O ₂ /m ³]	Min	79	260	-	50.1	281	-	
	Max	931	480	-	726.0	737	-	
	Mean	330	-	312.9	239.1	431	141.0	< 75
TN [g N/m ³]	Min	9	-	-	-	-	-	
	Max	43	-	-	-	-	-	
	Mean	19	-	-	-	-	-	< 15
TKN [g N/m ³]	Min	8	4	-	0.5	13	-	
	Max	39	17	-	24.7	39	-	
	Mean	17	-	8.45	11.5	25	-	-
NH ₄ -N [g N/m ³]	Min	2.8	-	-	-	-	-	
	Max	20.7	-	-	-	-	-	
	Mean	6.4	-	-	-	-	1.94	< 3
NO _x -N [g N/m ³]	Min	1.5	-	-	0.04	-	-	
	Max	4.1	-	-	0.94	-	-	
	Mean	2.4	-	-	0.47	-	1.13	-
TP [g P/m ³]	Min	1.0	1.2	-	3.7	-	-	
	Max	9.3	2.8	-	22.4	-	-	
	Mean	4.0	-	1.98	10.3	-	-	-
PO ₄ -P [g P/m ³]	Min	0.5	-	-	1.35	-	-	
	Max	3.2	-	-	6.44	-	-	
	Mean	1.6	-	-	3.93	-	1.25	< 1

* Percentiles D10, D90 and Median

⁺ Median

Literature review on pollutant flow analysis in sewer networks is predominantly restricted to TSS and COD which are the most common pollutants in studies on CSO. Detailed

investigations of nutrients during CWWF especially in rural catchments are rare. Lang et al. (2013) analyzed runoff nutrient loads in a residential catchment in China with intensive agricultural land use in order to investigate the influence on runoff concentrations. Their findings are summarized in Table 6-15 showing especially increased mean nitrate concentrations resulting from fertilizers. In comparison, nitrate EMC from the present monitoring campaigns are about half as high but still significantly higher than EMCs investigated by Brombach *et al.* (2005) or Lee and Bang (2000). In contradiction observations concerning TSS, PO₄-P and NH₄-N by Lang *et al.* (2013) show significantly smaller EMCs compared to the present investigations.

Table 6-15: Nutrient event mean concentrations of storm water runoff from rural residential areas with agricultural land use observed by Lang *et al.* (2013)

Statistics	Nutrients EMC for Storm Water Runoff			
	TSS [g/m ³]	PO ₄ -P [g P/m ³]	NH ₄ -N [g N/m ³]	NO ₃ -N [g N/m ³]
Min	94	0.11	0.02	2.03
Max	649	0.52	0.57	10.30
Mean	288	0.32	0.26	4.18

Due to limited retention tank capacities combined sewer networks discharge sewage through CSO structures into receiving waters when the available retention tank volume is exceeded. Thereby CSO events cause hydraulic stress to the receiving water and discharge pollutants. Table 6-16 summarizes the mean CSO concentrations observed during the measurement campaigns of this PhD study showing comparably low concentrations. Only TSS and BOD₅ concentrations exceed the legal WWTP effluent limits. Table 6-17 compares these results to mean CSO concentrations from CSO monitoring studies found in literature. The present concentration findings are much smaller than the comparison data from literature. Thereby, retention tank design for first flush events plays an important role (Sztruhár *et al.* 2002). The larger the retention tank is the smaller are CSO frequencies and EMCs. For rural catchments e.g. the German design guideline ATV-A 128 for retention tanks (DWA 1992a) proposes reduced retention tank volumes according to the assumption of a reduced influence of DWF concentrations during CWWF.

Table 6-16: Monitored combined sewer overflow event mean concentrations at retention tanks

Event no.	CSO EMC [g/m ³]										
	TSS	COD	S _{COD}	X _{COD}	BOD ₅	TN	TKN	NH ₄ -N	NO _x -N	TP	PO ₄ -P
4	14	38	16	21	16	4.1	2.9	0.7	1.2	1.6	0.5
8	136	76	22	54	25	5.2	4.3	0.7	1.0	2.4	0.8
14	162	40	13	27	10	5.4	4.8	0.8	0.6	0.5	0.2

Table 6-17: Comparison of typical event mean concentrations for combined sewer overflow

Parameter		CSO EMC					
		Haute-Sûre	Sztruhár et al. (2002)	Suárez and Puertas (2005)	Díaz-Fierros et al. (2002)	Brombach et al. (2005) ⁺	EC (1991)
TSS [g/m ³]	Min	14	-	229	160	-	
	Max	162	-	733	411	-	
	Mean	104	430	512	282	174.5	< 30
BOD ₅ [g O ₂ /m ³]	Min	10	-	166	71	-	
	Max	25	-	389	171	-	
	Mean	17	175	316	123	60.0	< 15
COD [g O ₂ /m ³]	Min	38	-	293	134	-	
	Max	76	-	834	540	-	
	Mean	40	445	587	329	141	< 75
TN [g N/m ³]	Min	4.1	-	-	-	-	
	Max	5.4	-	-	-	-	
	Mean	4.9	16.8	-	-	12.6	< 15
TKN [g N/m ³]	Min	2.9	-	-	13.2	-	
	Max	4.8	-	-	33.0	-	
	Mean	4.0	-	-	22.8	-	-
NH ₄ -N [g N/m ³]	Min	0.7	-	-	5.2	-	
	Max	0.8	-	-	12.8	-	
	Mean	0.7	6.21	-	8.7	1.94	< 3
NO _x -N [g N/m ³]	Min	0.6	-	-	-	-	
	Max	1.2	-	-	-	-	
	Mean	0.9	1.38	-	-	1.13	-
TP [g P/m ³]	Min	0.5	-	-	0.5	-	
	Max	2.4	-	-	4.6	-	
	Mean	1.5	2.63	-	2.2	1.25	-
PO ₄ -P [g P/m ³]	Min	0.2	-	-	-	-	
	Max	0.8	-	-	-	-	
	Mean	0.5	0.63	-	-	-	< 1

⁺ Median

- **First flush analysis**

Often, initial parts of runoff volumes from rain events contain a significant portion of pollution load of the event. This phenomenon is known as the first flush (Bertrand-Krajewski *et al.* 1998). Despite extensive research by plenty of researchers still no consistent definition or approach to quantify the phenomenon exists (Bach *et al.* 2010). The most convenient approach of first flush investigation is based on the visual analysis of pollutant mass distribution versus volume (Bertrand-Krajewski *et al.* 1998). Arbitrary definitions are then used to interpret the presence of first flush effects. Strict definitions such as those by Bertrand-Krajewski *et al.* (1998) demand 70-80% of the pollution load to be transported within the first 20% of the runoff volume. This definition makes first flush effects from a theoretically point of view very rare (Bach *et al.* 2010). Figure 6-20 and Figure 6-21 show the results for the collected data. Superior curves (progressions above the bisector) describe increased pollutant concentrations in the beginning of the event.

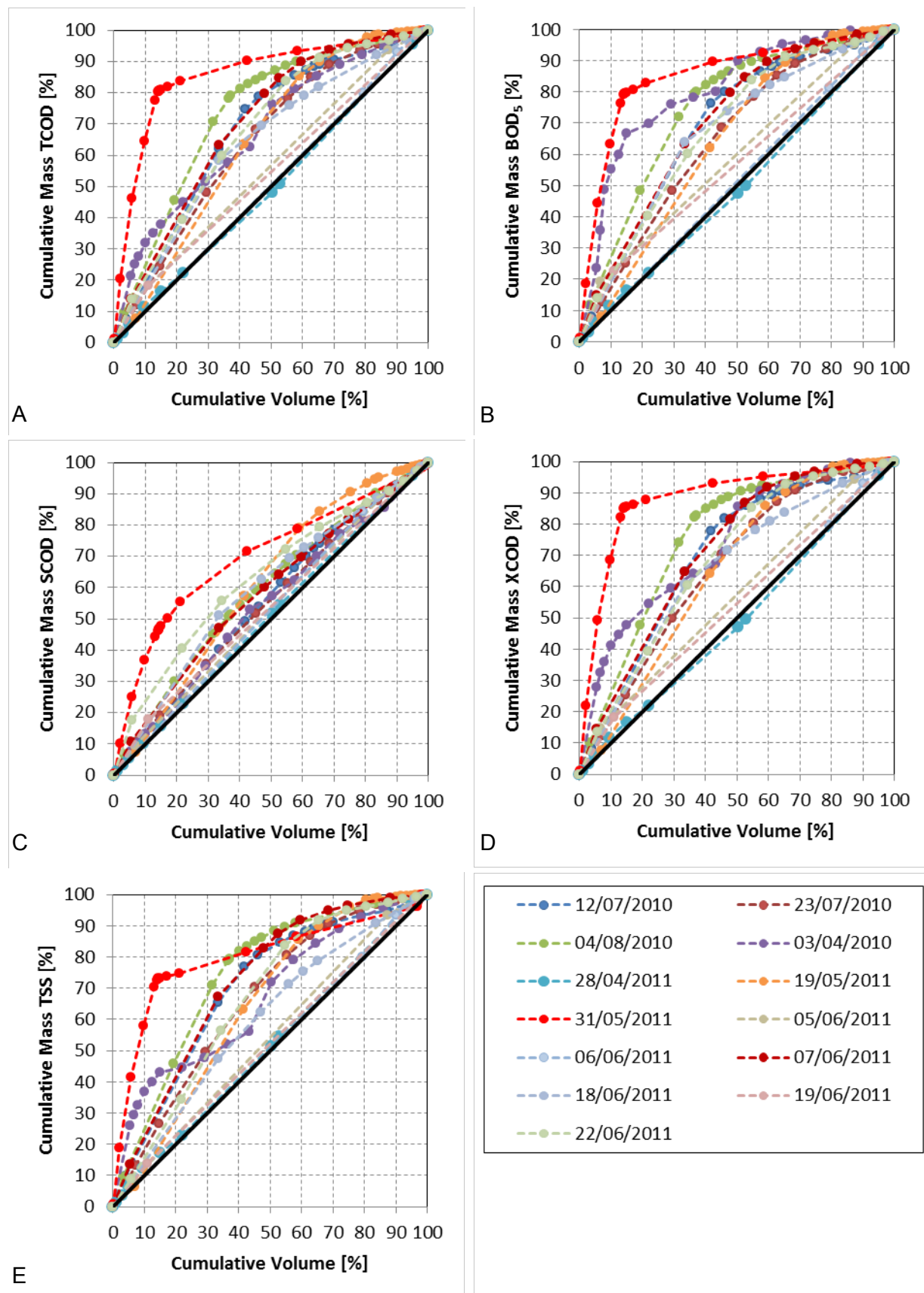


Figure 6-20: First flush analysis according to pollutant mass distribution versus volume (A = COD, B = BOD₅, C = S_{COD}, D = X_{COD} and E = TSS)

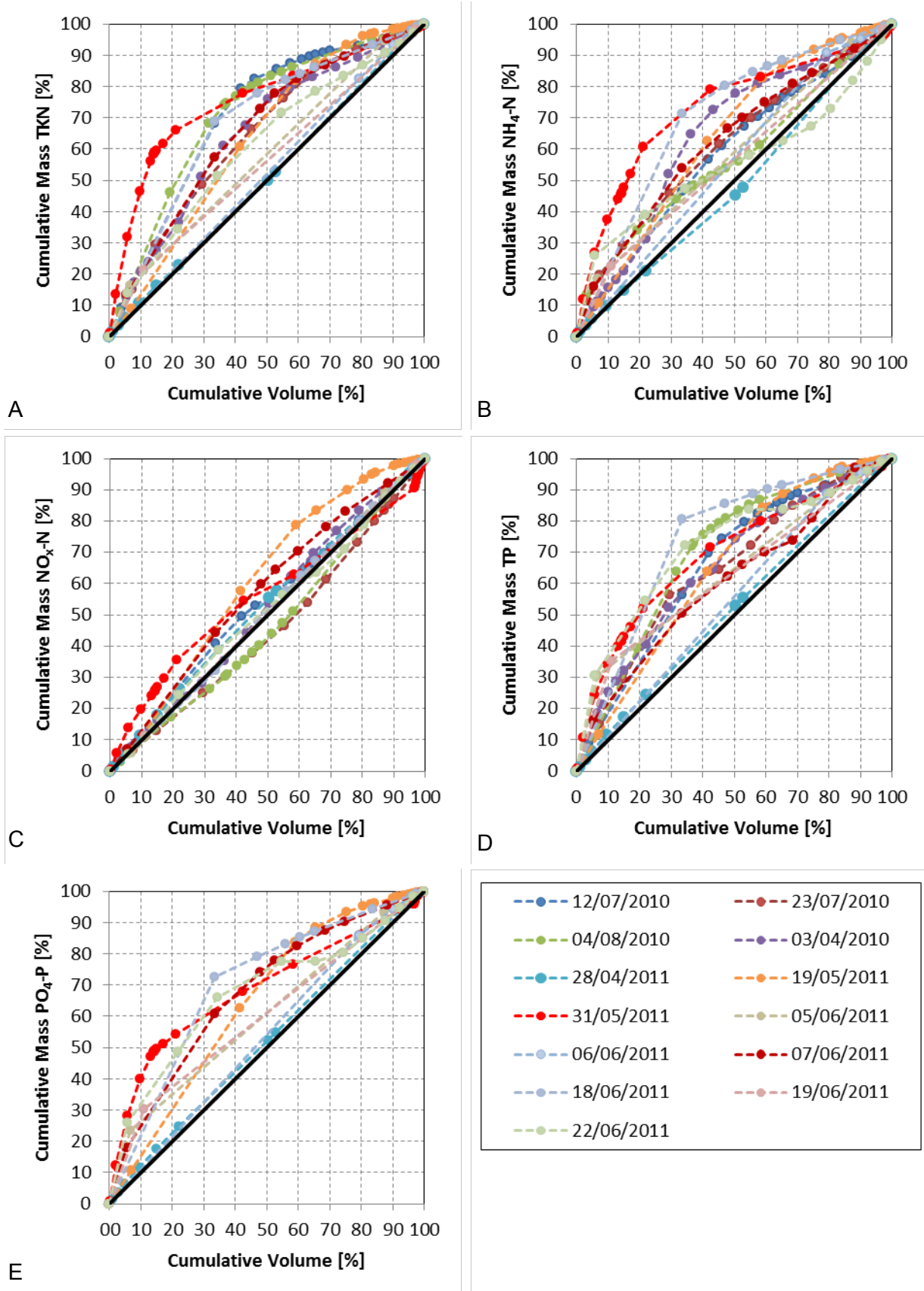


Figure 6-21: First flush analysis according to pollutant mass distribution versus volume (A = TKN, B = NH₄-N, C = NO_x-N, D = TP and E = PO₄-P)

Inferior curves (progressions below the bisector) describe dilution in the beginning of an event. Even for specific pollutants curve progressions are always event specific (Bertrand-Krajewski *et al.* 1998). According to the definition of Bertrand-Krajewski *et al.* (1998) only event 31/05/2011 shows first flush effects. Event 03/04/2010 shows a first flush effect only for BOD₅. Nevertheless most of the curves are superior, even for soluble pollutants. This effect has been explained according to wave theory by Krebs *et al.* (1999).

Han *et al.* (2006) propose a mass first flush ratio (MFF) in order to quantify the first flush effect. By definition the MFF is equal to zero in the beginning and equal to one at the end of an event. Values greater than one within the curve progression indicate first flush (Barco *et al.* 2008).

$$MFF_n = \frac{\int_0^{T_1} c(t)q(t)dt}{\frac{M}{\int_0^{T_1} q(t)dt}} \quad \text{Equation 6-5}$$

with: n ... the point in time of the storm event corresponding to the percentage of runoff ranging between 0% and 100%, M ... the total mass of the pollutant, V ... the total runoff volume, $c(t)$... the pollutant concentration as a function of time and $q(t)$... the runoff as a function of time

Figure 6-22 and Figure 6-23 show the application of MFF to the present data. Every event shows at least small first flush effects. The maximum value of MFF shows the magnitude of the first flush effect. As to be expected, particulate fractions show the largest values. Interestingly, the results for 31/05/2011 show significant first flush effects for each fraction, even for NO_x-N and PO₄-P indicating contributions by runoff from agricultural catchments. Unfortunately, the approach does not quantify the contribution of pollution load from rainfall-runoff to the combined sewage load.

Bach *et al.* (2010) criticize that conventional approaches for first flush investigations in combined sewer systems do not take the background load into account. They propose to quantify the first flush according to the runoff volume needed to reduce the stormwater pollutant concentration to background concentrations. This clearly distinguishes pollutographs into a first section where concentrations are dominated by the wash-off of pollutants followed by a section of dilution. Instead of quantifying the effect according to a dimensionless fraction of the total runoff volume the event specific volume which causes increased runoff concentrations is considered. This is coherent to approaches used for pollution load modeling based on accumulation and wash-off (see section 2.2.2.2). The approach requires continuous sampling before and after the event in order to quantify the background concentration which is practically different for TN, TP and PO₄-P where online probes are not available (see section 3.3.1). Alternatively, information about the mean background concentration must be used as derived in section 6.2.2.1. Due to the illustrated variability of background concentrations for rural WCTSS robustness problems occur because of underestimated background concentrations. From a modeling point of view it is important to quantify the contribution of wash-off from rainfall-runoff to the combined load.

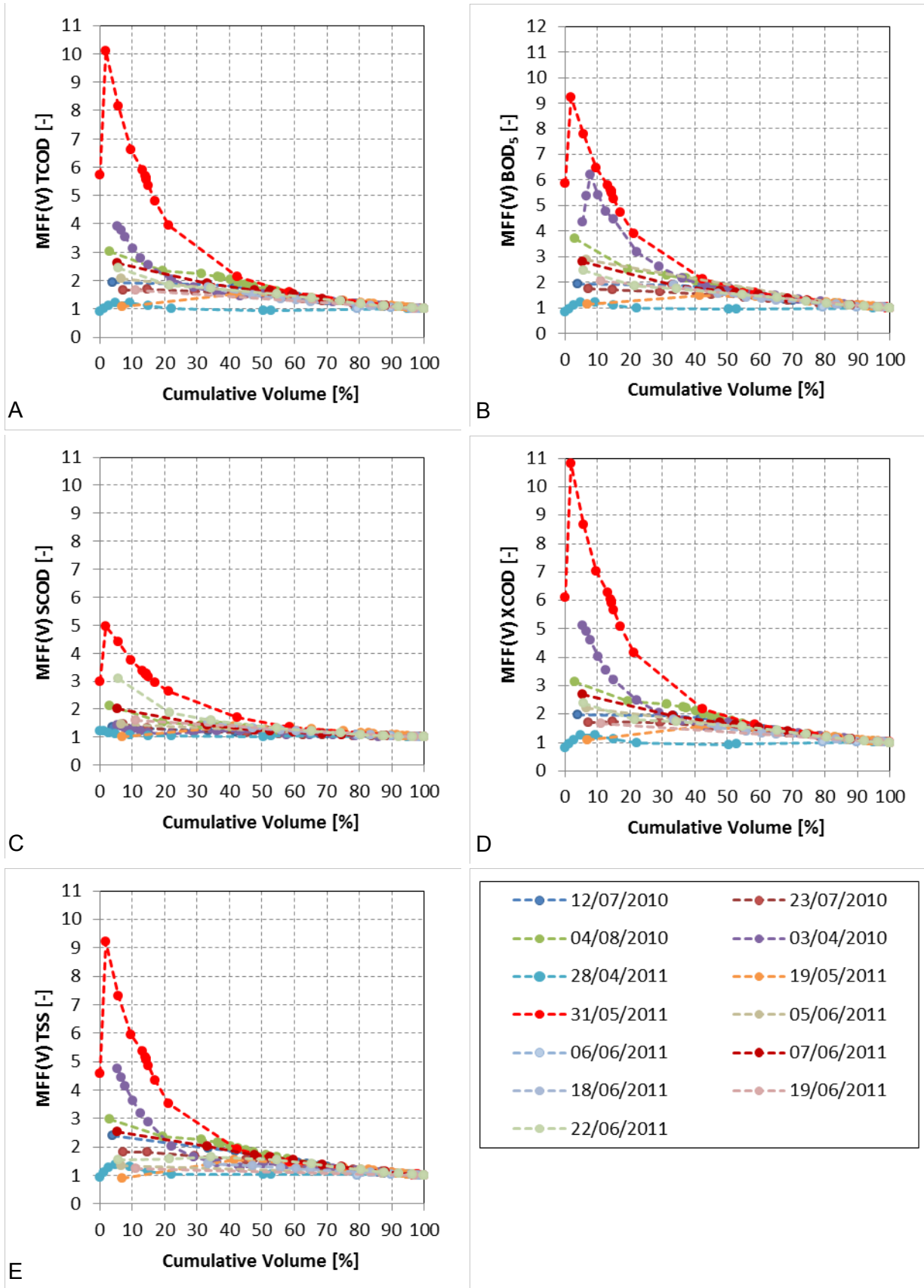


Figure 6-22: First flush analysis according to mass first flush ratio (A = COD, B = BOD₅, C = S_{COD}, D = X_{COD} and E = TSS)

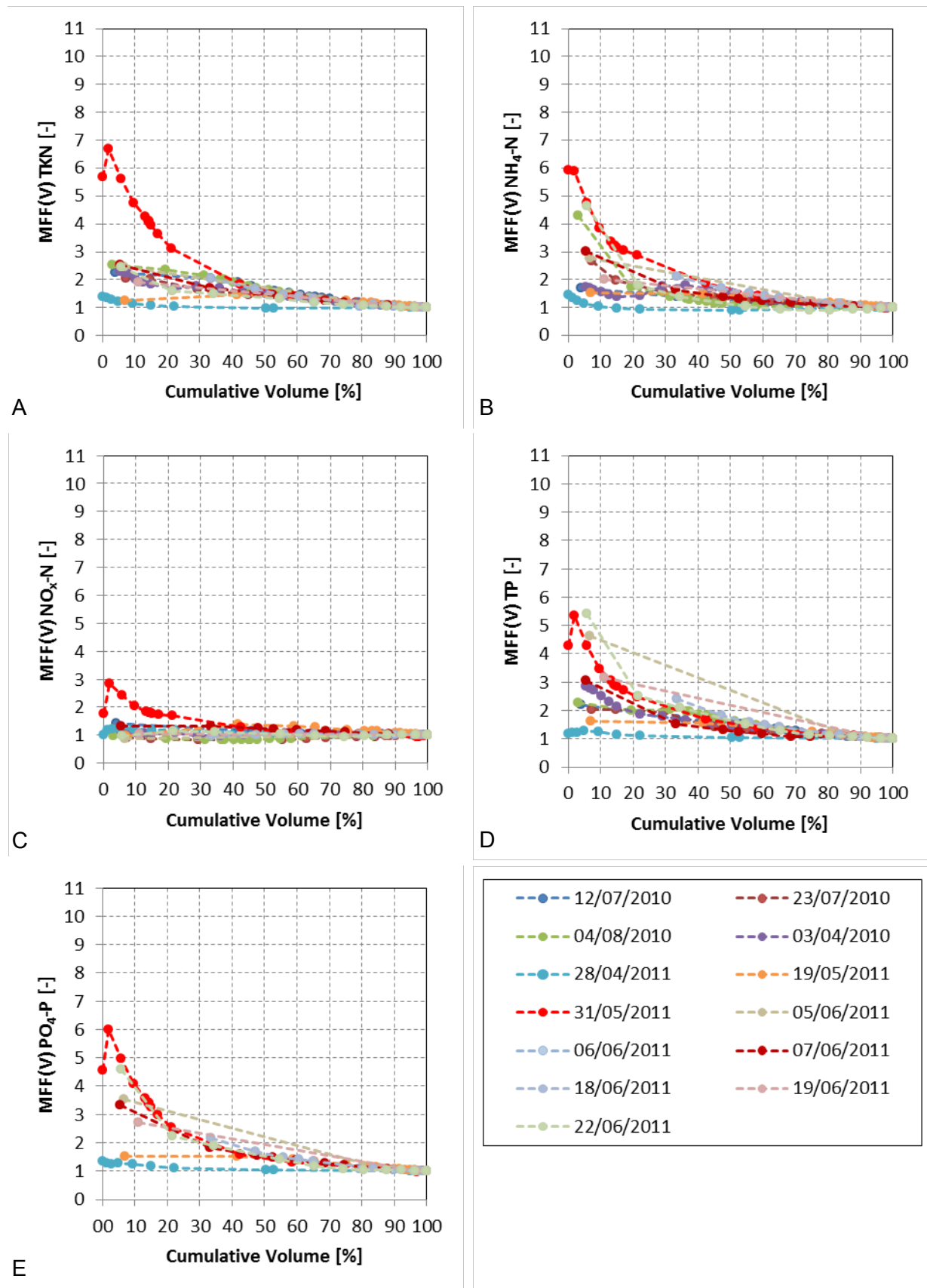


Figure 6-23: First flush analysis according to mass first flush ratio (A = TKN, B = NH₄-N, C = NO_x-N, D = TP and E = PO₄-P)

Therefore, the approach proposed by Bach et al. (2010) is reduced to a steady CWWF chemical pollution load balance in order to quantify the contribution of pollution load from rainfall-runoff to the combined sewage load per event according to Equation 6-6 and Equation 6-7. Similar approaches have been proposed for instance by Gasperi et al. (2010) to quantify the contribution of rainfall-runoff and sewer deposits to combined sewer flow loads. Due to sequential monitoring in the present case, input-output balances to quantify sewer deposits are not possible.

$$M_{PC} = M_{PD} + M_{PR} \tag{Equation 6-6}$$

with: M_{PC} ... the pollution mass in the combined wastewater, M_{PD} ... the pollution mass in the domestic wastewater and M_{PR} ... the pollution mass in the rainfall-runoff.

$$M_{PD} = \int c_i \cdot Q dt \tag{Equation 6-7}$$

with: C_i ... the concentration of pollutant i and Q ... the domestic wastewater flow.

Results are presented in Figure 6-24 and Table 6-18. $\text{NO}_x\text{-N}$ shows the largest relative contribution from rainfall-runoff to the combined sewage indicating loads from catchments with agricultural land use. Nevertheless, the total load both during DWF and CWWF is quite small. Rainfall-runoff contribution for TSS is in average 80% ranging between 50 and 99%. $\text{NH}_4\text{-N}$ and $\text{PO}_4\text{-P}$ show the lowest mean contributions from runoff during CWWF. Nevertheless, large value ranges show event-specific contributions through rainfall-runoff. This is confirmed by corresponding cumulative mass versus volume distributions.

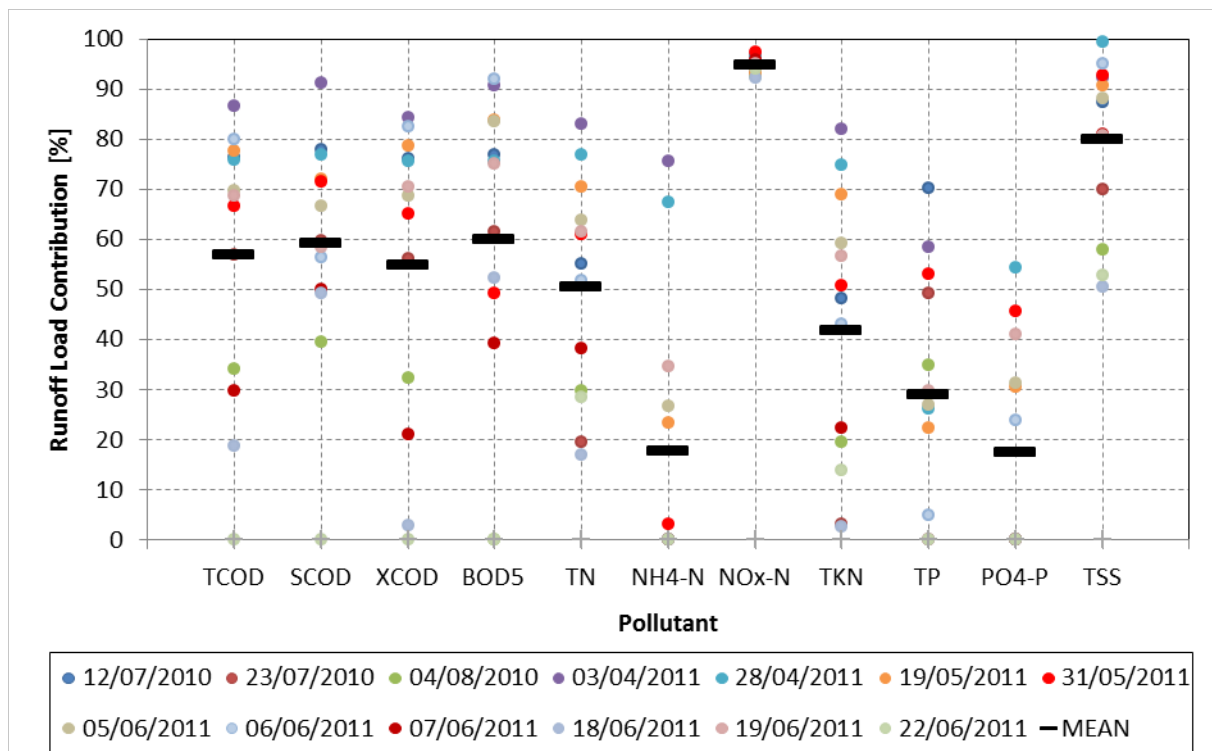


Figure 6-24: Analysis of mean rainfall-runoff pollution contributions to CWWF loads

Table 6-18: Statistical evaluation of the pollution load contribution from rainfall-runoff to the combined sewage load

Fraction	Runoff Load Contribution [%]						
	MEAN	STD	MIN	Q1	MEDIAN	Q3	MAX
COD	57	26	0	32	69	77	86
S _{COD}	59	22	0	50	60	74	91
X _{COD}	55	29	0	27	69	77	84
BOD ₅	60	30	0	44	75	84	92
TN	50	21	17	29	55	67	83
NH ₄ -N	18	26	0	0	0	31	76
NO _x -N	95	2	92	93	95	96	97
TKN	42	26	3	17	48	64	82
TP	29	23	0	2	27	51	70
PO ₄ -P	17	20	0	0	0	36	54
TSS	80	16	50	64	87	93	99

Average load contributions of COD fractions and BOD₅ larger than 50% demonstrate significant contributions from rainfall-runoff, even for S_{COD}. Mean contributions for total N and TKN are slightly smaller caused by organic N and NH₄-N. In general the evaluation demonstrates a significant and event-specific load contribution for COD and TKN from rainfall-runoff. This argues for pollution load models based on accumulation and wash-off in rural WCTSSs.

WWTP

Self-supervision data at WWTP Heiderscheidergrund consisted of 24-h-composite samples. Such data is not adequate to calculate EMCs. Mean concentrations presented in Figure 6-25 and Figure 6-26 qualitatively correspond to the EMC observed in the catchment according to Table 6-13. In the following differences in combined sewage composition between the catchment and the WWTP inlet will be investigated based on the fractionation of sum parameters and the expected influence on the integrated model will be discussed.

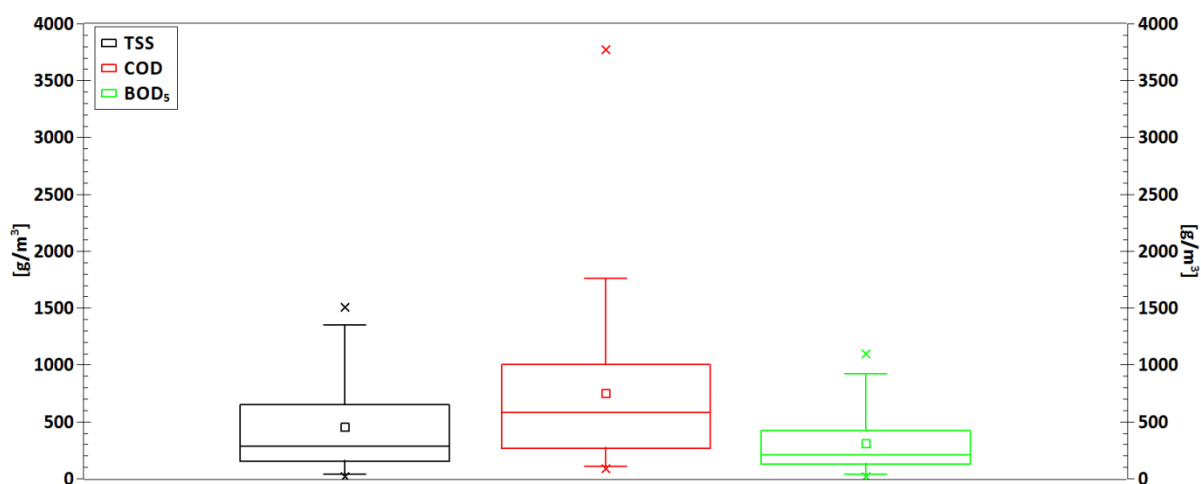


Figure 6-25: Inlet WWTP Heiderscheidergrund mean CWWF concentrations for TSS, COD and BOD₅ from self-supervision

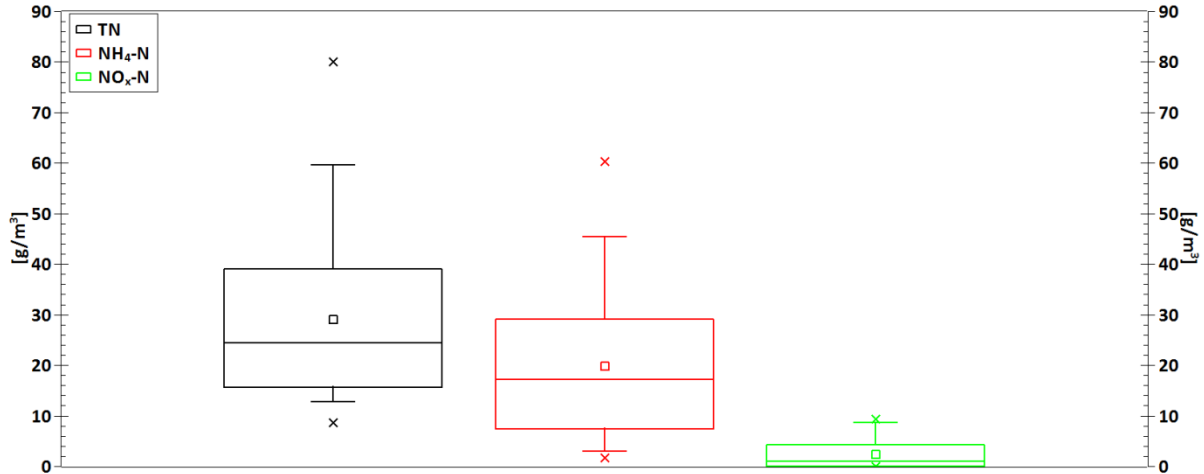


Figure 6-26: Inlet WWTP Heiderscheidergrund mean CWWF concentrations for TN, NH₄-N and NO_x-N from self-supervision

6.2.3. Fractionation of COD and TKN

When integrating the sewer network model, consisting of the sum parameters COD and TKN in the present case, with the WWTP model, consisting of 13 fractions using ASM1 (Henze *et al.* 1987) in the present case, a fractionation model describes the modeling of the ASM1 fractions from the sum parameters COD and TKN. In wastewater treatment the sum parameter COD describes the organic matter content consisting of soluble and particulate inert and biodegradable fractions (Henze 1992). Equation 6-8 to Equation 6-21 describe the fractionation of COD and TKN for the ASM1 according to the German design guideline ATV-DVWK-A131E (DWA 1992b) and BSM1 (Copp 2001). Table 6-19 shows the model parameters and presents corresponding common values. Equation 6-8 shows the general fractionation of COD according to soluble and particulate COD which both can be biodegradable and inert. The fraction of soluble inorganic COD i_{SI} can be approximated from the WWTP SST effluent. The production of S_I during wastewater treatment (Henze *et al.* 1987) is assumed to be insignificant. S_I is assumed to be constant and hence transferable to the wastewater in the catchment.

$$COD = S_S + S_I + X_S + X_I \quad \text{Equation 6-8}$$

with: COD ... the total organic matter in the wastewater described as COD, S_S ... the soluble easily biodegradable fraction, S_I ... the soluble inert fraction, X_S ... the particulate slowly biodegradable fraction and X_I ... the particulate inert fraction

$$S_I = COD \cdot i_{SI} \quad \text{Equation 6-9}$$

TSS is assumed to be a constant fraction of the total COD (Equation 6-10). From the results of the presented measurement campaigns the fraction of TSS to COD $i_{XTSS,COD}$ can be calculated.

$$X_{TSS} = i_{XTSS,COD} \cdot COD \quad \text{Equation 6-10}$$

with: X_{TSS} ... the total concentration of suspended solids

Filterable solids consist of organic and inorganic fractions. The fraction B of nonvolatile TSS quantifies the inorganic fraction. The value of B ranges between 0.2 for wastewater from primary settlers and 0.3 for raw wastewater (70 – 80% organic X_{COD}). B is taken from the results of the supplementary measurement campaign at the WWTP inlet. According to DWA (1992b) the organic dry matter in the WWTP inflow has $i_{COD,VSS} = 1.45$ g COD per g organic SS. This was confirmed by many measurements and is hence adopted in the present fractionation model calibration. These assumptions allow the calibration of particulate COD according to Equation 6-11.

$$X_{COD} = i_{COD,VSS} \cdot (1 - B) \cdot X_{TSS} \quad \text{Equation 6-11}$$

with: X_{COD} ... the sum of slowly biodegradable and inert particulate fraction of the chemical oxygen demand

The biodegradable COD is calculated from the difference of total COD and inert COD assuming the particulate inert COD to be constant (Equation 6-12). Depending on the type of wastewater and retention time in the primary settling tank the fraction A of inert COD from particulate COD can be assumed to be in the range of 0.2 to 0.35 (ATV-DVWK, 1992b).

$$C_{COD,Bio} = COD - i_{SI} \cdot COD - X_{COD} \cdot A \quad \text{Equation 6-12}$$

with: $C_{COD,Bio}$... the sum of soluble and particulate biodegradable COD fractions

The fraction of soluble easily biodegradable COD is calculated from the total biodegradable COD (Equation 6-13).

$$S_S = i_{SS,COD,Bio} \cdot C_{COD,Bio} \quad \text{Equation 6-13}$$

The heterotrophic (Equation 6-14) and autotrophic biomass (Equation 6-15) is necessary to calculate the fraction of particulate slowly biodegradable COD from the mass balance of the total biodegradable COD (Equation 6-16).

$$X_{BH} = i_{BH,COD,Bio} \cdot C_{COD,Bio} \quad \text{Equation 6-14}$$

with: X_{BH} ... the heterotrophic biomass

$$X_{BA} = 0.0001 \quad \text{Equation 6-15}$$

with: X_{BA} ... the autotrophic biomass

The particulate slowly biodegradable biomass is balanced with the total biodegradable biomass (Equation 6-29).

$$X_S = C_{COD,Bio} - S_S - X_{BH} - X_{BA} \quad \text{Equation 6-16}$$

Inorganic TSS is calculated from the measured fraction B of nonvolatile TSS (Equation 6-17).

$$X_{TSS,Inorg} = B \cdot X_{TSS} \quad \text{Equation 6-17}$$

with: $X_{TSS,Inorg}$... the inorganic fraction of TSS

Organic TSS is calculated from the total sum of particulate matter (Equation 6-18).

$$X_{TSS,Org} = i_{TSS,XI} \cdot X_I + i_{TSS,XS} \cdot X_S + i_{TSS,XB} \cdot (X_{BH} + X_{BA}) \quad \text{Equation 6-18}$$

with: $X_{TSS,Org}$... the sum of organic particulate fractions, $i_{TSS,XI}$... the fraction of TSS from particulate inert COD, $i_{TSS,XS}$... the fraction of TSS from particulate soluble COD and $i_{TSS,XB}$... the fraction of TSS from biomass

Total TSS is calculated from the inorganic and organic TSS (Equation 6-19)

$$X_{TSS} = X_{TSS,Inorg} + X_{TSS,Org} \quad \text{Equation 6-19}$$

Biodegradable organic nitrogen is calculated from the corresponding fractions of organic matter (Equation 6-20 and Equation 6-21).

$$S_{ND} = S_S \cdot i_{N,SS} \quad \text{Equation 6-20}$$

with: $i_{N,SS}$... the fraction of N from soluble biodegradable COD

$$X_{ND} = X_S \cdot i_{N,XS} \quad \text{Equation 6-21}$$

with: $i_{N,XS}$... the fraction of N from particulate biodegradable COD

Equation 6-22 describes the calculation of ammonium according to the fractional composition of TKN corresponding to ASM1 (Henze *et al.* 1987).

$$S_{NH} = TKN - (i_{N,SS} \cdot S_S + i_{N,XS} \cdot X_S + i_{N,SI} \cdot S_I + i_{N,XI} \cdot X_I + i_{N,XB} \cdot (X_{BH} + X_{BA})) \quad \text{Equation 6-22}$$

with: S_{NH} ... the fraction of soluble ammonia nitrogen, TKN ... the total Kjeldahl nitrogen, S_{ND} ... the fraction of soluble biologically degradable organic nitrogen, S_{NI} ... the fraction of soluble biologically inert organic nitrogen, X_{ND} ... the fraction of particulate biologically degradable organic nitrogen, X_{NI} ... the fraction of particulate inert organic nitrogen, $i_{N,SS}$... the fraction of N from soluble biodegradable COD, $i_{N,XS}$... the fraction of N from particulate biodegradable COD, $i_{N,SI}$... the fraction of N from soluble inert COD, $i_{N,XI}$... the fraction of N from particulate inert COD and $i_{N,XB}$... the fraction of N from biomass

Calibration of these parameters according to measurement data improves the fractionation. However, the measurability of many fractions is limited. Henze (1992) and Petersen *et al.* (2003) provide a comprehensive overview of available methods. From the present measurement data only $i_{XTSS,COD}$, B and i_{SI} are measurable. While $i_{COD,VSS}$ is adopted from DWA (1992b) the remaining model parameters A, $i_{SS,COD,Bio}$ and $i_{BH,COD,Bio}$ are modified by trial-and-error to calibrate the mass balance of COD according to X_{COD} and S_{COD} resulting from the measurement campaigns with respect to their investigated min, mean and max concentrations.

Due to the fact that in activated sludge modeling uncertainty concerning model calibration increases with the degree of freedom (Rieger *et al.* 2013) the fractionation of TKN and the calibration of TSS must be treated differently. While in the case of COD the balance between the number of variables and the number of parameters is good, the fractionation of TKN and the modeling of TSS from COD are quite imbalanced (five parameters for two variables in the case of TKN and 6 parameters for one variable in the case TSS). Consequently, the standard parameterization according to Table 6-19 is kept to investigate the performance of the fractionation model to model especially $\text{NH}_4\text{-N}$ and TSS from the sum parameters COD and TKN at retention tanks at the WWTP inlet. The investigation of a detailed TKN and TSS fractionation model calibration is out of the scope of the present work.

Table 6-19: Standard parameterization of COD, TSS and TKN fractionation

Parameter		Value
$i_{COD,VSS}$	Fraction of COD to VSS	1.45 ¹⁾
$i_{XTSS,COD}$	Fraction of TSS to COD	250/620 ²⁾
B	Fraction of nonvolatile TSS	0.20 – 0.30 ¹⁾
i_{SI}	Fraction of inert soluble COD	0.05 – 0.10 ¹⁾
A	Fraction of inert COD from particulate COD	0.20 – 0.35 ¹⁾
$i_{SS,COD,Bio}$	Fraction of S_S from biodegradable COD	0.25 ²⁾
$i_{BH,COD,Bio}$	Fraction of biomass from biodegradable COD	0.18 ²⁾
$i_{TSS,XI}$	Fraction of TSS from particulate inert COD	0.75 ³⁾
$i_{TSS,XS}$	Fraction of TSS from particulate biodegradable COD	0.75 ³⁾
$i_{TSS,XB}$	Fraction of TSS from biomass	0.90 ³⁾
$i_{TSS,Inorg}$	Fraction of TSS from particulate mineralic material	1.00 ³⁾
$i_{N,XB}$	Fraction of nitrogen from biomass	0.08 ³⁾
$i_{N,XI}$	Fraction of nitrogen from particulate inert COD	0.045 ³⁾
$i_{N,SI}$	Fraction of nitrogen from soluble inert COD	0.02 ³⁾
$i_{N,SS}$	Fraction of nitrogen from soluble biodegradable COD	0.03 ³⁾
$i_{N,XS}$	Fraction of nitrogen from particulate biodegradable COD	0.03 ³⁾

¹⁾ ATV-A 131 (DWA 1992b)

²⁾ SIMBA manual (ifak 2009)

³⁾ BSM1 (Copp 2001)

Zawilski and Brzezińska (2009) investigated different fractionation parameterizations necessary to model DWF and CWWF in an integrated model for a WCTS and compare their results to data from literature on similar studies. Their literature review reveals a wide range of parameterizations for DWF found from different studies. Their investigations based on fractionation model calibration reveals a clear increase of inert matter at the WWTP inlet during CWWF. In order to investigate the impact of rainfall-runoff on the composition wastewater along the ISN in the present case, fractionation model calibration is done in the following for DWF and CWWF both at retention tanks and at the WWTP inlet. Fractionation at retention tanks is necessary to model wastewater parameters for the emission-based evaluation of simulation results additionally to the sum parameters COD and TKN used in the sewer network model such as TSS, BOD_5 or $\text{NH}_4\text{-N}$. Fractionation model calibration results for DWF and CWWF at the retention tanks and at the WWTP are presented in the following sections.

6.2.3.1. DWF

Table 6-20 shows the calibration results of the ASM1 fractionation of the sum parameters at retention tanks during DWF based on mass balances for each fraction. In order to show the resulting modeling quality for the total concentration range results are differentiated according to minimum, mean and maximum concentrations. Corresponding percentage values show the agreement between the modeled fractions and results from the measurement campaigns. The calibrated fractionation model parameters are compared in Table 6-24 and discussed in section 6.2.3.3. Since the model is balanced according to the total COD mean calibration results for COD show a perfect agreement. Modeled concentrations of S_{COD} and X_{COD} also show a good agreement with the measured values over the whole range. While calibration results for S_{COD} range between 92% in lower concentration ranges and 78% in higher concentration ranges, concentration results for X_{COD} are 131% for lower concentration ranges and 86% for higher concentration ranges. Using the default fractionation, TSS is clearly overestimated especially at lower concentration ranges. Measured N_{org} is calculated from the difference of TKN and $\text{NH}_4\text{-N}$ measurement data. Due to the balance with particulate organic matter N_{org} is overestimated while ammonium is underestimated. This under- and overestimation can be explained by the high nitrogen concentrations in the observed data which obviously does not correspond to the default fractionation parameterization according to Table 6-19. From the receiving water point of view the underestimation of $\text{NH}_4\text{-N}$ is more critical than the overestimation of N_{org} due to the toxicity of $\text{NH}_4\text{-N}$.

Table 6-20: Results of DWF sum parameter fractionation at retention tanks according to ASM1

Parameter Name	Value	Fract.	Concentrations								
			Min			Mean			Max		
			Meas.	Model	[%]	Meas.	Model	[%]	Meas.	Model	[%]
			[g/m ³]	[g/m ³]	[%]	[g/m ³]	[g/m ³]	[%]	[g/m ³]	[g/m ³]	[%]
i_{SI}	0.019	S_I		8.2			16.7			23.6	
$i_{SS,COD,Bio}$	0.220	S_S		83.2			169.5			239.7	
		S_{COD}	99.5	91.4	92	185.6	186.2	100	338.5	263.3	78
A	0.250	X_I		44.5			90.7			128.2	
$i_{BH,COD,Bio}$	0.180	X_S		226.9			462.3			653.7	
$i_{COD,VSS}$	1.450	X_{COD}	259.4	339.5	131	692.2	691.7	100	1141.8	978.0	86
		COD	430.9	430.9	100	877.9	877.9	100	1241.3	1241.3	100
B	0.272	TSS	110.4	294.8	267	343.6	600.7	175	613.6	849.4	138
$i_{XTSS,COD}$	0.391										
$i_{TSS,XI}$	0.750										
$i_{TSS,XS}$	0.750										
$i_{TSS,XB}$	0.900										
$i_{TSS,Inorg}$	1.000										
$i_{N,SS}$	0.030	S_{NH}	29.0	21.8	75	43.9	31.2	71	74.7	51.2	69
$i_{N,XS}$	0.030	N_{org}	18.4	16.9	92	21.8	34.5	158	25.3	48.7	193
$i_{N,SI}$	0.020										
$i_{N,XI}$	0.045										
$i_{N,XB}$	0.080										

Table 6-21 shows the calibration results of the ASM1 fractionation of the sum parameters at the WWTP inlet during DWF. In comparison to the calibration results at retention tanks during DWF (Table 6-20) lower S_{COD} concentrations are fairly overestimated while higher S_{COD} concentrations are underestimated. With calibration results between 107 and 90% modeling results show comparably better results for particulate COD over the whole range than at the retention tanks. This corresponds to the investigated different COD to TSS ratios. TKN fractionation improves at the WWTP inlet according to the standard parameterization. Nevertheless, ammonium is still underestimated especially in lower concentration ranges due to the overestimation of particulate matter which increases the modeled organic nitrogen concentrations.

Table 6-21: Results of the DWF sum parameter fractionation at the WWTP according to ASM1

Parameter		Fract.	Concentrations								
Name	Value		Min			Mean			Max		
			Meas.	Model		Meas.	Model		Meas.	Model	
			[g/m ³]	[%]	[g/m ³]	[g/m ³]	[%]				
i_{SI}	0.026	S_I		11.9			16.9			20.8	
$i_{SS,COD,Bio}$	0.160	S_S		60.3			85.6			105.6	
		S_{COD}	31.2	72.2	232	102.0	102.5	100	169.8	126.4	74
A	0.250	X_I		68.8			97.6			120.4	
$i_{BH,COD,Bio}$	0.180	X_S		248.9			353.1			435.4	
$i_{COD,VSS}$	1.450	X_{COD}	426.6	385.6	90	547.5	547.0	100	631.2	674.6	107
		COD	457.8	457.8	100	649.5	649.5	100	801.0	801.0	100
B	0.272	TSS	154.6	341.4	221	370.0	484.4	131	944.4	597.3	63
$i_{XTSS,COD}$	0.570										
$i_{TSS,XI}$	0.750										
$i_{TSS,XS}$	0.750										
$i_{TSS,XB}$	0.900										
$i_{TSS,Inorg}$	1.000										
$i_{N,SS}$	0.030	S_{NH}	20.8	8.9	43	34.0	28.6	84	83.0	74.5	90
$i_{N,XS}$	0.030	N_{org}	0.0	18.0	0	20.17	25.6	127	40.9	31.6	77
$i_{N,SI}$	0.020										
$i_{N,XI}$	0.045										
$i_{N,XB}$	0.080										

Overall, modeling results show a good agreement for S_{COD} and X_{COD} concentrations at retention tanks and at the WWTP inlet over the whole range except for lower S_{COD} concentrations at the WWTP inlet. In contradiction, the standard parameterization is not able to capture the measured variability of TSS, ammonium and organic nitrogen both at the retention tanks and at the WWTP inlet. From the fractionation model description according to Equation 6-8 to Equation 6-22 and the chosen default parameterization shown in Table 6-19 it can be assumed that this is caused by the exceptionally high ratios for COD to TSS and COD to BOD_5 .

The correlation between measured and modeled fractions according to the used ASM1 fractionation model calibration is illustrated in Figure 6-27. The correlation analysis confirms the weakness of the fractionation model to model S_{COD} from total COD at the retention tanks and the overestimation of TSS modeled from COD according to the standard parameterization shown in Table 6-19. The decreasing correlation for TSS and COD between the fractionation results at the retention tanks and at the WWTP can be explained by the chosen constant mean ratio between S_{COD} and X_{COD} because of missing measurements in the WWTP self-supervision data. This assumption leads to a perfect correlation for S_{COD} and X_{COD} at the WWTP inlet. The correlation analysis results also confirms the bad agreement of measured and modeled NH_4-N and N_{org} concentrations during DWF due to the TSS overestimation. Thereby, NH_4-N shows both for the investigated retention tanks and the WWTP inlet an acceptable correlation. But model results for NH_4-N are generally underestimated.

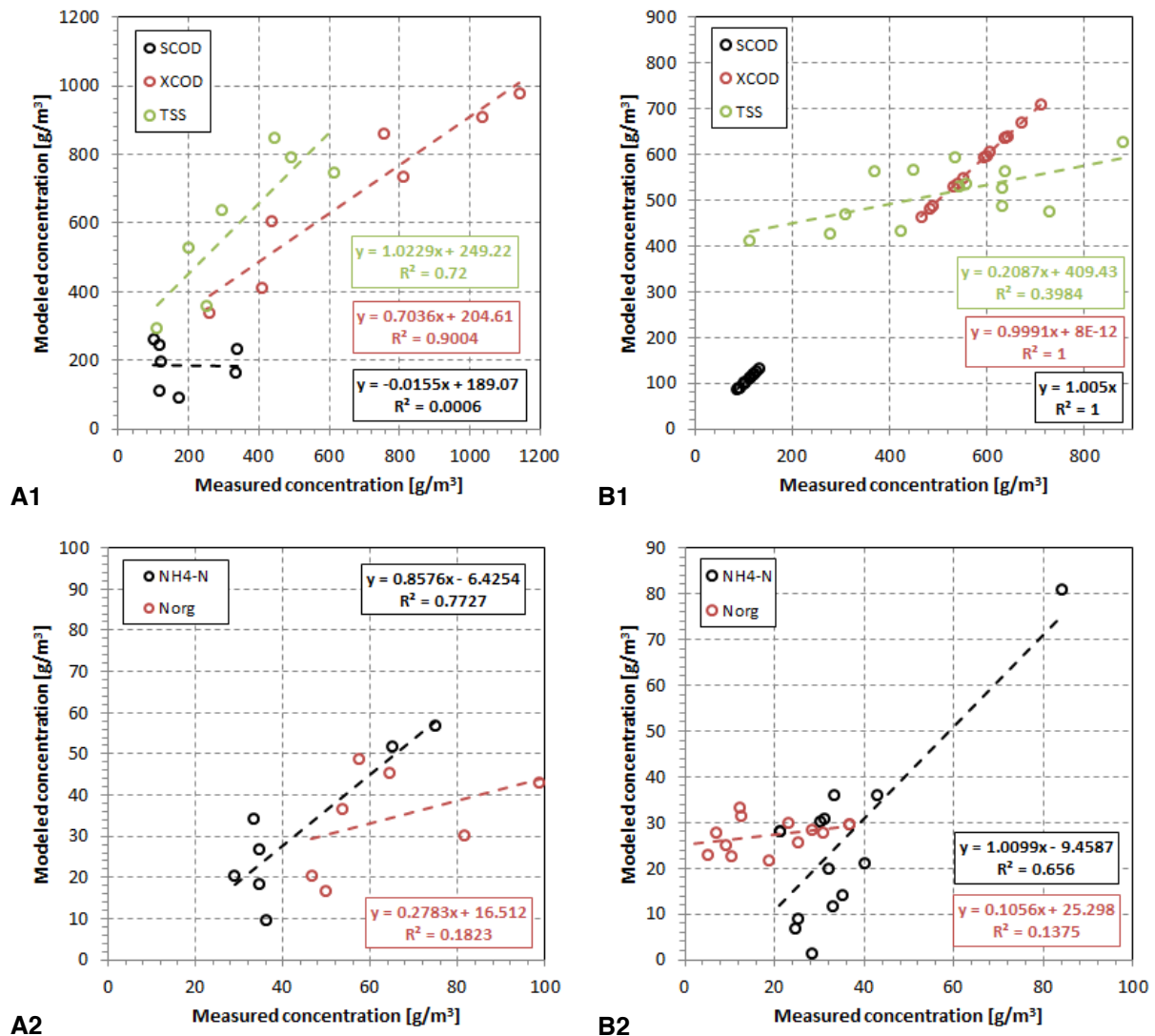


Figure 6-27: Comparison of wastewater fractionation results according to measurements from (A) the retention tank effluent and (B) the WWTP inlet

6.2.3.2. CWWF

Table 6-22 presents the results of the sum parameter fractionation according to ASM1 at retention tanks during CWWF similar to section 6.2.3.1. The COD balance shows a massive overestimation of X_{COD} for lower concentrations at the retention tanks while higher X_{COD} concentrations are only slightly underestimated. These results correspond to the modeling of TSS. Altogether, the modeling of TSS from COD at the retention tanks during CWWF shows better results than during DWF. On the contrary, higher S_{COD} concentrations are massively overestimated while lower S_{COD} concentrations are strongly underestimated. While $\text{NH}_4\text{-N}$ is strongly underestimated in lower concentration ranges the modeling of higher concentration ranges shows good results. In comparison to the fractionation results at the retention tanks during DWF, the modeling of $\text{NH}_4\text{-N}$ shows concentrations which are indeed generally underestimated but within a tolerable range. In contradiction, N_{org} is generally overestimated. Differences in the fractionation model performance during DWF and CWWF can be related to different COD to TSS and COD to BOD_5 relations which show in the present case during CWWF a better correspondence with the given standard parameterization to model TSS from COD and $\text{NH}_4\text{-N}$ from TKN.

Table 6-22: Results of the CWWF sum parameter fractionation at retention tanks according to ASM1

Parameter Name	Value	Fract.	Concentrations								
			Min			Mean			Max		
			Meas.	Model	[%]	Meas.	Model	[%]	Meas.	Model	[%]
			[g/m ³]	[g/m ³]	[%]	[g/m ³]	[g/m ³]	[%]	[g/m ³]	[g/m ³]	[%]
i_{SI}	0.039	S_I		1.0			16.9			182.7	
$i_{SS,COD,Bio}$	0.182	S_S		3.5			55.9			603.9	
		S_{COD}	7.8	4.5	57	73.0	72.8	100	280.0	786.5	281
A	0.250	X_I		6.8			109.5			1183.4	
$i_{BH,COD,Bio}$	0.180	X_S		12.1			195.8			2116.8	
$i_{COD,VSS}$	1.450	X_{COD}	6.0	22.3	372	379.9	360.6	95	4404.0	3897.5	88
		COD	26.8	26.8	100	433.3	433.3	100	4684.0	4684.0	100
B	0.272	TSS	6.0	24.2	404	436.3	391.5	90	4728.0	4232.4	90
$i_{XTSS,COD}$	0.957										
$i_{TSS,XI}$	0.750										
$i_{TSS,XS}$	0.750										
$i_{TSS,XB}$	0.900										
$i_{TSS,Inorg}$	1.000										
$i_{N,SS}$	0.030	S_{NH}	0.6	0.0	0	6.4	4.8	75	33.3	33.6	101
$i_{N,XS}$	0.030	N_{org}	0.6	1.1	190	12.9	17.2	134	130.4	186.3	143
$i_{N,SI}$	0.020										
$i_{N,XI}$	0.045										
$i_{N,XB}$	0.080										

Table 6-23 shows the corresponding results of the ASM1 fractionation model calibration during CWWF at the WWTP inlet. The results show a perfect match for S_{COD} and X_{COD} thanks to the assumption of a constant mean S_{COD} to X_{COD} ratio according to the

measurements in the catchment. Nevertheless, TSS is in average slightly overestimated showing strong overestimations for lower TSS concentrations. $\text{NH}_4\text{-N}$ is strongly underestimated while N_{org} is strongly overestimated. This again corresponds to the balance with particulate matter in the fractionation model.

Table 6-23: Results of CWWF sum parameter fractionation at the WWTP according to ASM1

Parameter Name	Value	Fract.	Concentrations								
			Min			Mean			Max		
			Meas.	Model		Meas.	Model		Meas.	Model	
			[g/m ³]	[g/m ³]	[%]	[g/m ³]	[g/m ³]	[%]	[g/m ³]	[g/m ³]	[%]
i_{SI}	0.025	S_I		2.0		16.8			84.8		
$i_{SS,COD,Bio}$	0.150	S_S		9.7		81.9			412.5		
		S_{COD}	11.8	11.7	100	99.0	98.8	100	498.7	497.3	100
A	0.250	X_I		13.2		110.8			558.0		
$i_{BH,COD,Bio}$	0.180	X_S		43.5		366.0			1842.6		
$i_{COD,VSS}$	1.450	X_{COD}	68.3	68.4	100	574.8	575.1	100	2894.3	2895.7	100
		COD	80.1	80.1	100	673.9	673.9	100	3393.0	3393.0	100
B	0.272	TSS	49.9	66.6	303	420.0	560.3	124	2114.6	2821.2	187
$i_{XTSS,COD}$	0.623										
$i_{TSS,XI}$	0.750										
$i_{TSS,XS}$	0.750										
$i_{TSS,XB}$	0.900										
$i_{TSS,Inorg}$	1.000										
$i_{N,SS}$	0.030	S_{NH}	1.7	0.00	0	19.9	5.99	30	60.3	52.72	87
$i_{N,XS}$	0.030	N_{org}	0.0	3.16	100	6.0	26.63	446	20.3	134.06	659
$i_{N,SI}$	0.020										
$i_{N,XI}$	0.045										
$i_{N,XB}$	0.080										

6.2.3.3. System-wide continuity

The calibration results of the COD fractionation model calibration for DWF and CWWF presented in the previous sections 6.2.3.1 and 6.2.3.2 show a good agreement of the measured and modeled S_{COD} and X_{COD} fractions at the retention tanks and at the WWTP both during DWF and CWWF. Table 6-24 shows the comparison of the corresponding ASM1 fractionation model parameter sets and the chosen parameter set for consistent system wide modeling during DWF and CWWF according to the average of all sets. The calibrated parameter sets show a very small fraction of soluble inert COD i_{SI} . While i_{SI} at the WWTP inlet is the same during DWF and CWWF the calibration results show a definitive difference between DWF and CWWF at the retention tanks. The fraction of S_S from biodegradable COD is generally smaller than the proposed default values. While $i_{SS,COD,Bio}$ shows no definitive differences during DWF and CWWF at the WWTP inlet $i_{SS,COD,Bio}$ decreases during CWWF at the retention tanks. A is kept constant for all calibration scenarios. The same is for $i_{BH,COD,Bio}$. Due to the limited data B is kept constant for all scenarios. Calibration results for $i_{XTSS,COD}$ show even larger values than the already large proposition of 250g TSS per 620 g

COD. This reflects the generally large ratio of COD to TSS investigated in the measurement data. Due to the balance of the total data, a distinctive ratio of the particulate COD is modeled as biodegradable. Overall, it was decided to choose the average of all calibration results for a system-wide fractionation model during DWF and CWWF.

Table 6-24: Comparison of the calibrated COD fractionation parameter sets according to ASM1

Parameter	Default	DWF		CWWF		Chosen
		Catchment	WWTP	Catchment	WWTP	
i_{SI}	0.050 – 0.100	0.019	0.026	0.039	0.025	0.026
$i_{SS,COD,Bio}$	0.250	0.220	0.160	0.182	0.150	0.155
A	0.200 – 0.350	0.250	0.250	0.250	0.250	0.250
$i_{BH,COD,Bio}$	0.180	0.180	0.180	0.180	0.180	0.180
$i_{COD,VSS}$	1.450	1.450	1.450	1.450	1.450	1.450
B	0.200	0.272	0.272	0.272	0.272	0.272
$i_{XTSS,COD}$	0.403	0.391	0.570	0.957	0.623	0.596

The results of TSS modeling from COD resp. NH_4-N and N_{org} modeling from COD and TKN according to the standard parameterization of the chosen fractionation model shows a general overestimation of TSS and N_{org} due to the unusual high ratio of COD to TSS investigated in the measurement campaigns. Due to the balance with particulate matter soluble NH_4-N is consequently underestimated using the presented standard parameterization. The results clearly show the need for additional fractionation analysis in the case of immission-based modeling approaches.

6.3. Deterministic - phenomenological reference model

The presented approach for system-wide FPC of integrated WCTSSs will be evaluated based on an integrated reference model. As described in section 6.2.1.1 four rain gauges provide data on precipitation for the rainfall-runoff simulation. Consequently, four to eight sub-catchments of between 18.8 ha (rain gauge Arsdorf) and 68.5 ha (rain gauge Esch/Sûre) aggregated impervious catchment area per rain gauge receive the same rainfall time-series. Studies on radar rainfall data reveal relevant spatial variability of rainfall already for small urban scales. Schellart et al. (2012) show significant modeling errors for CSO volume according to reduced information of spatial rainfall variability by using rain gauge data instead of radar rain data. Consequently, uncertainty in rainfall data also significantly influences modeled pollution loads (Kleidorfer *et al.* 2009). Areal correction coefficients for rain gauge data are alternatives to radar rainfall data. Focusing on small urban catchments areal correction coefficients have been investigated by Vaes et al. (2005) showing a significant spatial rainfall variability already for drainage area radii of one kilometer. In their case correction coefficients were based on data from the Flanders region in Belgium with lowland topography which is different to the mountainous topography in the present study. Rainfall tends to increase with rising elevation due to the orographic effect of mountainous terrain (Goovaerts 2000). Thereby, air is lifted vertically and condensation occurs due to adiabatic cooling. However, to take into account information on the spatial variability of rainfall in between the four rain gauges it is acceptable to derive this information indirectly

from the corresponding rainfall-runoff measured at each retention tank. Thereby, the system-wide evaluation of the rainfall-runoff coefficient (RRC) distribution is used:

- to consider uncertainties according to given impervious catchment data,
- to consider spatial rainfall variability in addition to the given four rain gauges and
- to consider rain derived infiltration.

Double mass analysis is an established graphical method to investigate homogeneity of rainfall time series (Buishand 1982). Double mass curves are obtained by plotting continuously accumulated rainfall records from rain gauges to be compared against each other (Equation 6-23 and Equation 6-24).

$$x_i = X_i + \sum_{j=1}^{i-1} X_j \quad \text{Equation 6-23}$$

and

$$y_i = Y_i + \sum_{j=1}^{i-1} Y_j \quad \text{Equation 6-24}$$

with: $X_i \dots$ a homogenous time series for a given variable at a reference station, $Y_i \dots$ a time series for the same period of the same variable at another station for which homogeneity resp. heterogeneity needs to be analyzed, $i = 1, \dots, n$ and $j = 1, \dots, i-1$

For homogenous data sets the resulting curve is a line. The coefficient of determination R^2 is used to express homogeneity resp. heterogeneity of the double mass curve (Equation 6-25 to Equation 6-29). RRCs describing the relation between measured rainfall at the corresponding rain gauge and the runoff volume at each retention tank are similarly evaluated and the resulting R^2 distribution representing the spatial variability of runoff will be compared to the rainfall variability.

$$R^2 = 1 - \frac{SS_{res}}{SS_{tot}} \quad \text{Equation 6-25}$$

$$SS_{res} = \sum_i (y_i - \hat{y}_i)^2 \quad \text{Equation 6-26}$$

$$\hat{y}_i = a_f + b_f x_i \quad \text{Equation 6-27}$$

$$SS_{tot} = \sum_i (y_i - \bar{y})^2 \quad \text{Equation 6-28}$$

$$\bar{y} = \sum_{i=1}^n y_i / n \quad \text{Equation 6-29}$$

with: $R^2 \dots$ the coefficient of determination, $SS_{res} \dots$ the residual sum of squares, $SS_{tot} \dots$ the total sum squares, $\hat{y}_i \dots$ the regression among the full set f and $\bar{y} \dots$ the mean of the data set Y_i .

6.3.1. Rainfall homogeneity evaluation

Figure 6-28 to Figure 6-30 show the spatial and temporal distribution of precipitation in the catchment according to annual double mass analysis in the observed period of three years. To this end, aggregated rainfall time series are plotted against each other for yearly periods.

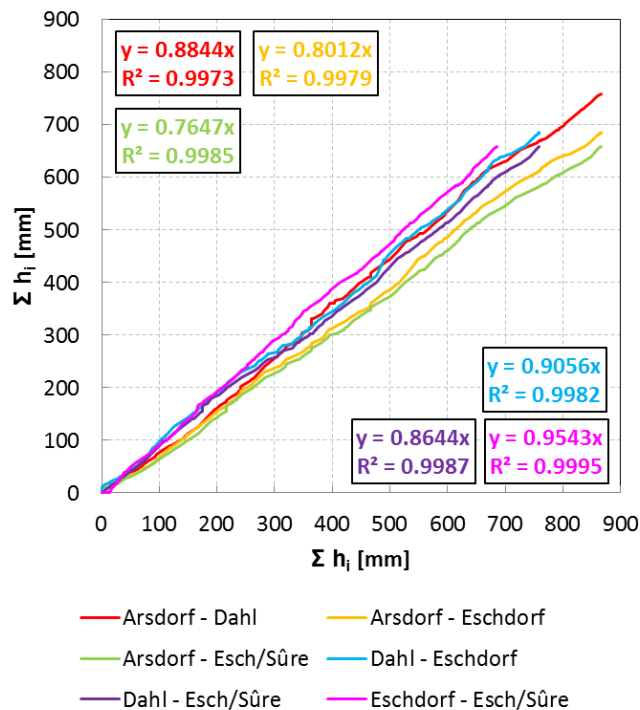


Figure 6-28: Double sum analysis for pairwise spatial rainfall distribution analysis from 4 rain gauges in 2010

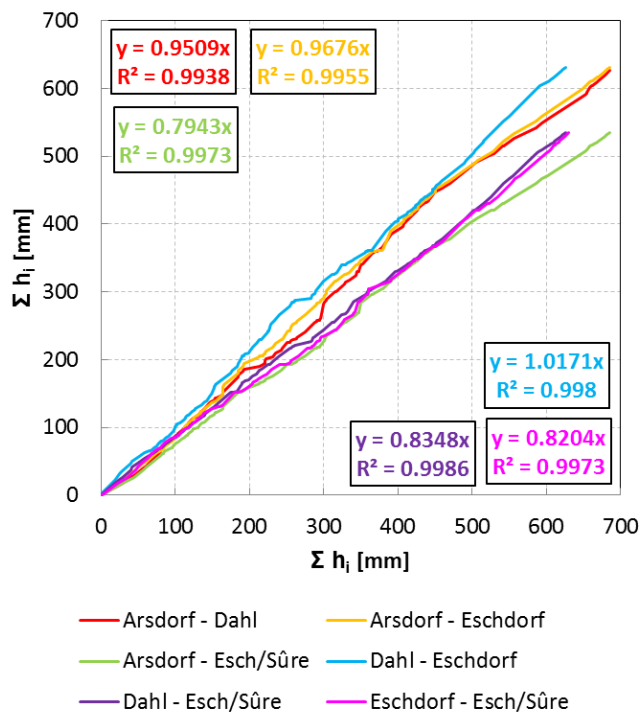


Figure 6-29: Double sum analysis for pairwise spatial rainfall distribution analysis from 4 rain gauges in 2011

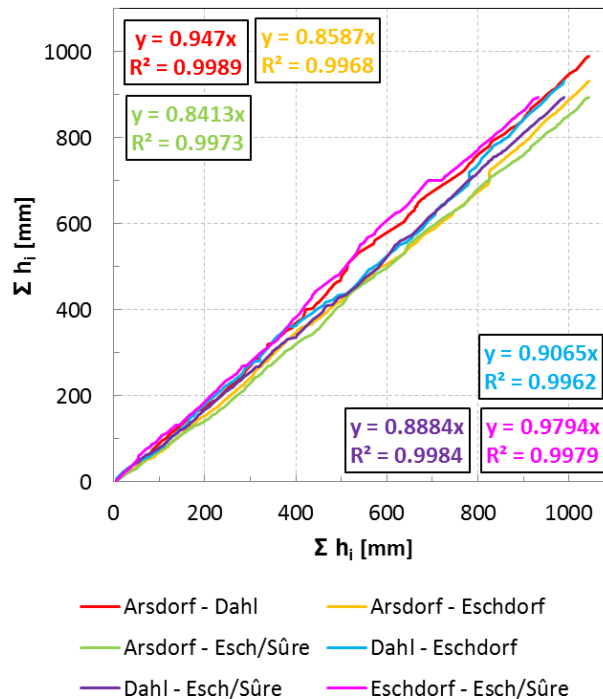


Figure 6-30: Double sum analysis for pairwise spatial rainfall distribution analysis from 4 rain gauges in 2012

Double mass analysis is an established method in hydrology and meteorology to investigate inhomogeneity in time series by investigating the linearity between these. Thereby, the slope of the linear correlation line describes the mean percentage difference in rainfall and the coefficient of determination R^2 is a relative indicator of the spatial rainfall distribution. The method is less suitable to quantify the absolute variability of the investigated time series but to provide an approach to compare the relative variability of the present rainfall time series with the relative variability of the corresponding rainfall runoff time-series.

The analysis of the annual rainfall time series show mean percentage differences in rainfall between two and 24 percent. The coefficient of determination R^2 varies in the range of 0.9938 to 0.9995. The rainfall time series of 2011 (Figure 6-29) show the largest divergence of the aggregated pluviographs with a mean R^2 of 0.9966 followed by 2012 (Figure 6-30) with a mean R^2 of 0.9976 and 2010 (Figure 6-28) with a mean R^2 of 0.9984. This divergence of rainfall time series is caused by their spatial variability. Thereby, summer storms, which usually show the largest variability of areal rainfall intensity distributions, are the predominant cause for divergence between rainfall time series from neighbored rain gauges. Due to this, such events usually provide the largest reserve capacity for sewer network real-time control based on the corresponding spatial variability of rainfall-runoff (Berndtsson and Niemczynowicz 1988).

6.3.2. Rainfall-runoff homogeneity evaluation

In combined sewer systems wastewater is retained in retention tanks during CWWF events for the delayed treatment at the WWTP. If the storage volume of retention tanks is exceeded

CSO is discharged to receiving waters. In the present case the system-wide equipment for hydraulic sewer network real-time control consisting of inductive discharge and pressure based water level measurement devices at each retention tank and at the WWTP inlet allowed to calculate the runoff from corresponding rainfall measurements. Rainfall runoff volume (Equation 6-32) is calculated according to the sum of retained CWWF discharged to the WWTP (Equation 6-30) and CSO volume discharged to receiving waters (Equation 6-31). RRCs are evaluated in a monthly resolution.

$$V_{RT} = \sum_{event} Q_{out} \cdot \Delta t \quad \text{Equation 6-30}$$

$$V_{CSO} = \sum_{event} Q_{over} \cdot \Delta t \quad \text{Equation 6-31}$$

$$V_{CWWF} = V_{RT} + V_{CSO} \quad \text{Equation 6-32}$$

with: V_{RT} ... the runoff volume of a rain event drained to the WWTP, V_{CSO} ... the runoff volume of a rain event discharged to the receiving water, V_{CWWF} ... the total runoff of a rain event, Q_{out} ... the outflow of a retention tank and Q_{over} ... the overflow of a retention tank to the receiving water

6.3.2.1. Combined sewer overflow estimation

Given the equipment for discharge measurement at retention tanks only the volume drained to the WWTP is available. Still CSO per retention tank can be calculated based on the water level that is measured continuously at each retention tank (Equation 6-33). If the critical water level at which CSO occurs is not available, it can be identified from the observations of continuous water level measurements. Indeed, CSO causes waves during CSO. I.e., the water level oscillates around the weir crest level significantly increasing the corresponding frequency (Brombach *et al.* 1999). Figure 6-31 illustrates the approach. (Brombach *et al.* 1999) propose to choose the bend below the peak as critical level for CSO. In the present case the peak itself gives more realistic values while lower levels according to (Brombach *et al.* 1999) create mean CSO volumes about two to three times the retained CWWF volume drained to the WWTP. The weir flow coefficient representing the hydraulic influence of the weir crest is chosen to be equal to 0.5.

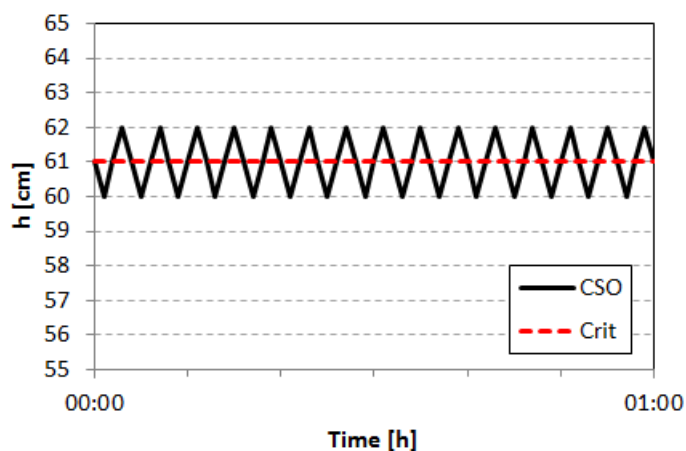


Figure 6-31: Principally retention tank water level oscillation during CSO ((Brombach *et al.* 1999), modified)

$$Q_{over} = \frac{2}{3} \mu \sqrt{2g} \cdot w \cdot h^{\frac{2}{3}} \cdot c \quad \text{Equation 6-33}$$

with: w ... the width of the overflow weir, h ... the depth of water flow above the weir, μ ... the weir flow coefficient and c ... the reduction coefficients for screens.

Screens installed on top of the weir crest are assumed to retain 50% of the overflow. Figure 6-32 illustrates the approach for identifying the critical water level for CSO at retention tank Dahl. Figure 6-32 A1 and B1 illustrate the water level frequency data for the year 2012 according to exceeded water levels (A) and levels equal to a specific one (B). For detailed identification Figure 6-32 A2 and B2 zoom into the critical range. According to this, the results of the frequency analysis for the investigated time series of retention tank Dahl in 2012 reveals a critical water level of 61 cm at the CSO structure at the inlet of the retention tank which represents the height of the CSO weir crest. Based on this, CSO can be calculated for retention tank water levels exceeding the critical water level according to Equation 6-33.

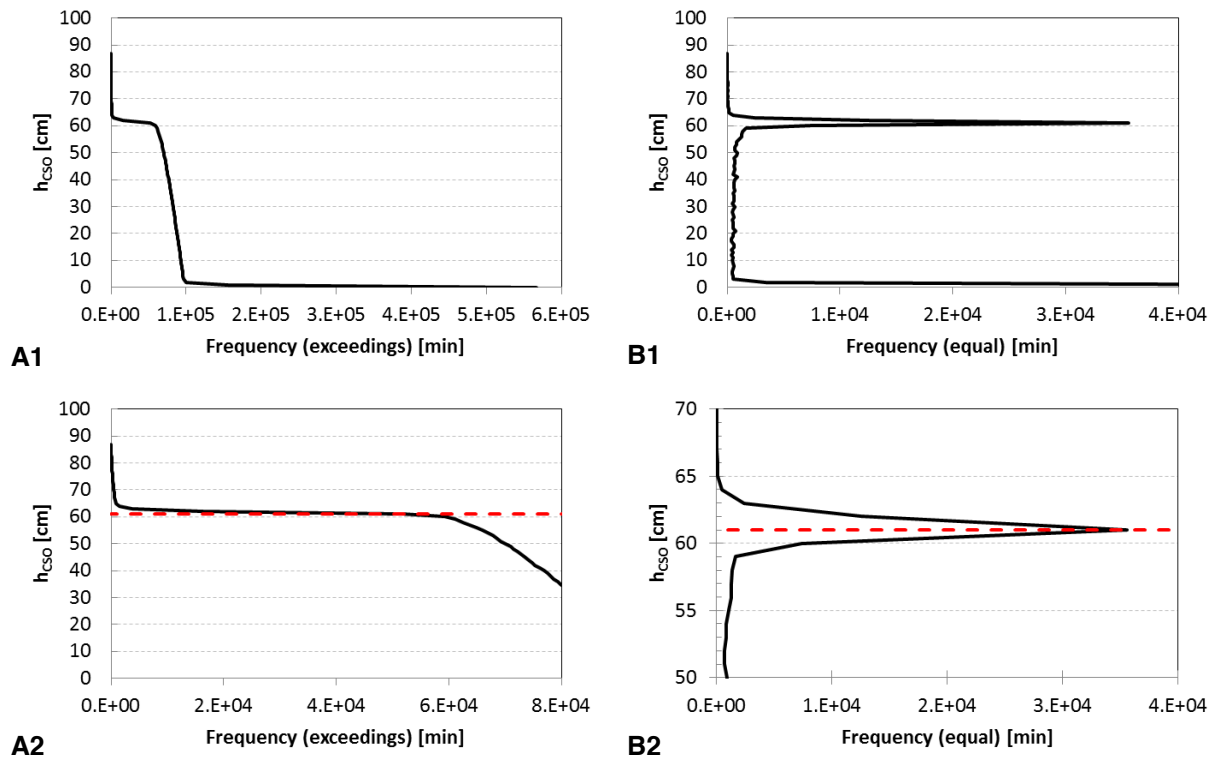


Figure 6-32: Water level frequency analysis at retention tank Dahl for the evaluation of the critical water level causing CSO (dashed red line) based on continuous water level measurements in 2012 (A: frequency of water levels exceeding the critical water level, B: frequency of water levels equal to the critical water level, 1: total value range, 2: zoom)

Figure 6-33 illustrates the corresponding critical water level for CSO in the time series of water levels at the retention tank Dahl in the second half of 2012. Due to the screen mounted on top of the CSO weir crest CSO water levels can be up to 20 cm. Due to missing information the hydraulic detention of the screens is assumed to be 50%. The CSO volume

during the investigated period was 25790 m³ while the volume of wastewater discharged to the WWTP was 30629 m³.

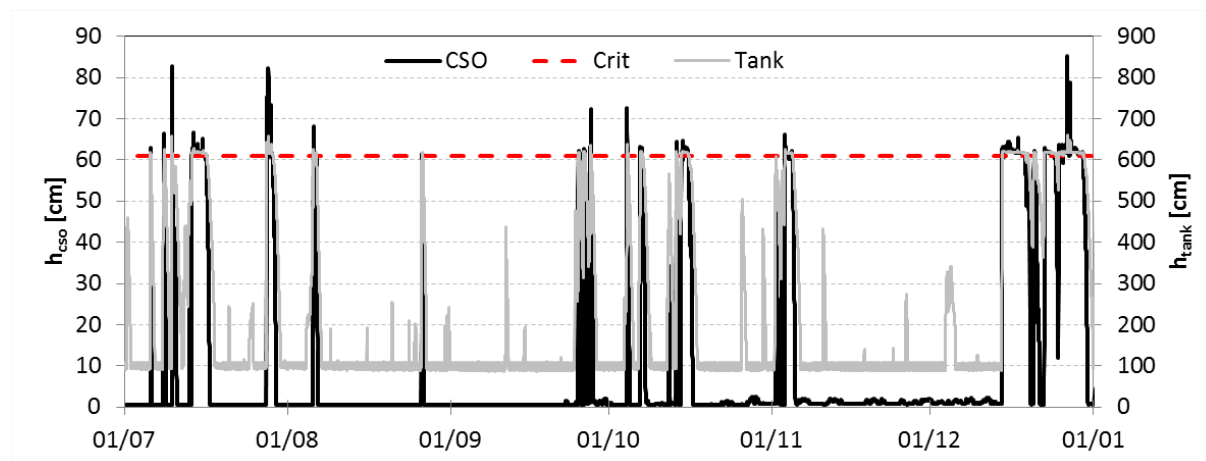


Figure 6-33: CSO illustration for the time series of measured water levels at the CSO weir (black line) and in the retention tank (grey line) at retention tank Dahl between July 2012 and January 2013 according to the critical water (dashed red line)

6.3.2.2. Rainfall-runoff coefficient distribution

In the following, monthly rainfall runoff coefficients (RRC) are calculated from the monitored rainfall and the runoff per retention tank according to Equation 6-34 and subsequently analyzed with respect to their spatial homogeneity. In the case of precise input data concerning rainfall and surfaces contributing to runoff, RRCs are in the range of zero and one. For RRCs equal to one runoff occurs without any losses according to depression or evaporation, etc. from runoff contributing catchment surfaces. Similar to the rainfall homogeneity analysis presented in section 6.3.1 the RRCs must be aggregated for each retention tank and correlated according to the approach of double mass analysis. Since double mass analysis is a relative approach the correlation lines for the aggregated rainfall time series can be compared to the correlation lines for the aggregated rainfall-runoff coefficients according to their variations.

$$RRC = \frac{V_{CWWF}}{h_I \cdot A_{imp}} \quad \text{Equation 6-34}$$

with: h_I ... the rainfall height, A_{imp} ... the impervious catchment surface, V_{CWWF} ... the monitored CWWF

Figure 6-34 shows the results from the system-wide evaluation of monthly RRCs. RRCs larger than five are excluded assuming measurement errors. Rain gauge data is allocated according to Figure 6-5. The boxplot analysis shows a wide range of rainfall-runoff coefficients due to the nonlinear rainfall-runoff process. The large proportion of RRCs greater than one (see Figure 6-35) indicates either runoff-contributions from other catchment surfaces connected to the sewer network or underestimated surfaces contributing to runoff. In the case of catchment Dahl where the mean RRC is about one it can be assumed that the given impervious catchment surface size is underestimated. Rainfall-runoff from pervious catchments could be modeled according to increased loss assumptions for runoff from rainfall.

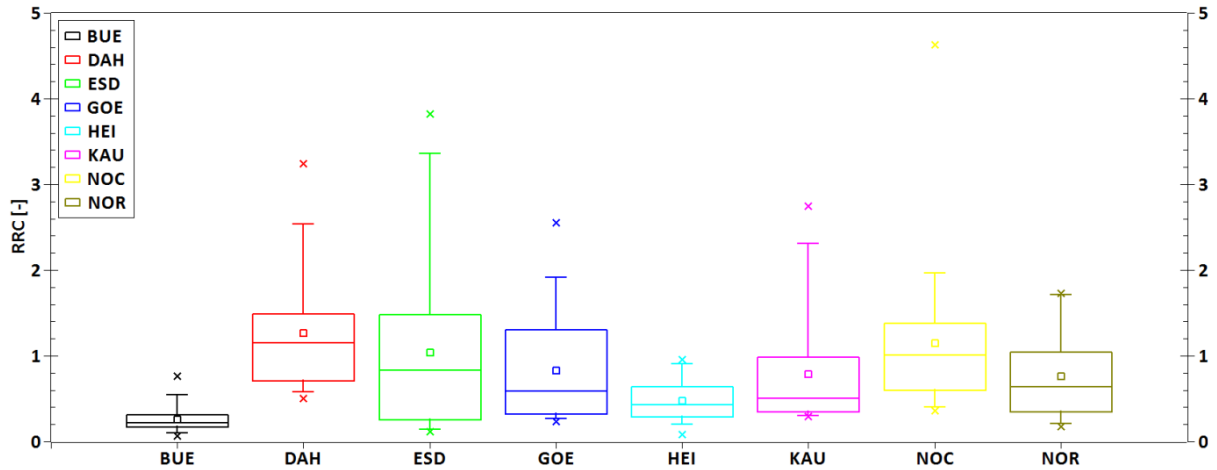


Figure 6-34: System-wide evaluation of RRCs according to measurement data in the period June 2010 to December 2012

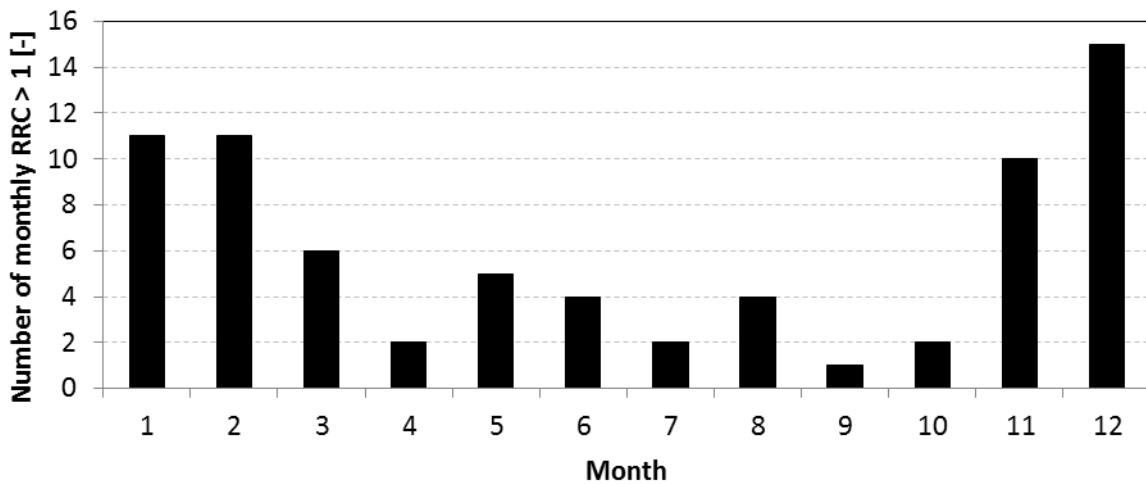


Figure 6-35: System-wide evaluation of monthly RRC larger than one in the period from June 2010 to December 2012 state 2010

According to Figure 6-35 increased frequencies of RRCs larger than one occur especially during the winter months (November to February). This indicates seasonal infiltration in the local sewer networks due to increased groundwater levels in winter (Weiß *et al.* 2002). However, besides the seasonal variability especially the simultaneous variation of RRCs is of interest since the latter is assumed to increase the capacity (Berndtsson and Niemczynowicz 1988). This assumption is coherent with the screening for real-time control potential of urban wastewater systems (see Zacharof *et al.* (2004)) which principally investigates the diversity of the system to be controlled.

Within the reference simulation model each sub-catchment connected to a retention tank is fed by rainfall time series from the closest rain gauge (see Figure 6-5). Figure 6-36 illustrates the variation of monthly RRCs for the five sub-catchments which are fed by the rain gauge

Dahl in the system state 2010. Rainfall time series from the rain gauges Eschdorf, Esch/Sauer and Arsdorf are only used for two, one resp. zero sub-catchments in the system state 2010. In the final system state seven sub-catchments will be fed with rainfall time series from rain gauge Dahl. Consequently, the RRC variation investigated according to Figure 6-36 is assumed to represent the variation of RRCs within the sub-catchments fed by rain gauge Dahl in the final reference simulation model state and to be transferable to the sub-catchments fed by the other rain gauges. The evaluation of simultaneous RRCs allocated to rain gauge Dahl according to Figure 6-36 shows that the behavior of rainfall-runoff principally can be grouped according to seasonal effects. While in summer and autumn the RRCs are below one, the RRCs in winter are except for Buderscheid larger than one showing groundwater infiltration in the local sewer-systems according to increased groundwater levels in winter. This corresponds to findings of Weiß *et al.* (2002) for rural catchments. The constantly small RRCs for Buderscheid indicate an error in the assumption of the runoff contributing surface. Deviations of the single graphs from parallelism indicate randomness within the system-wide rainfall-runoff behavior.

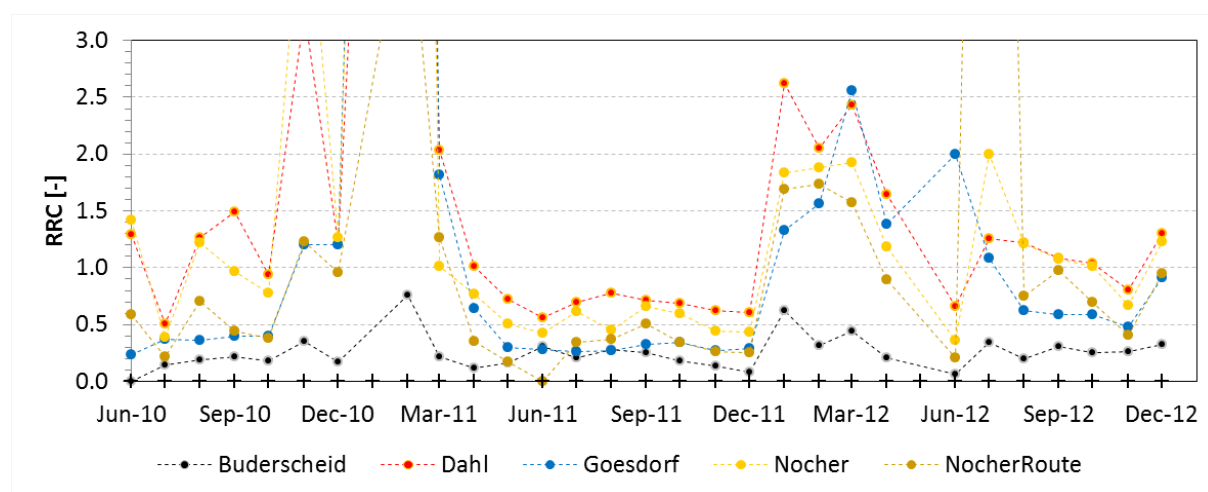


Figure 6-36: Time series of RRCs of the five catchments allocated to rainfall data from rain gauge Dahl

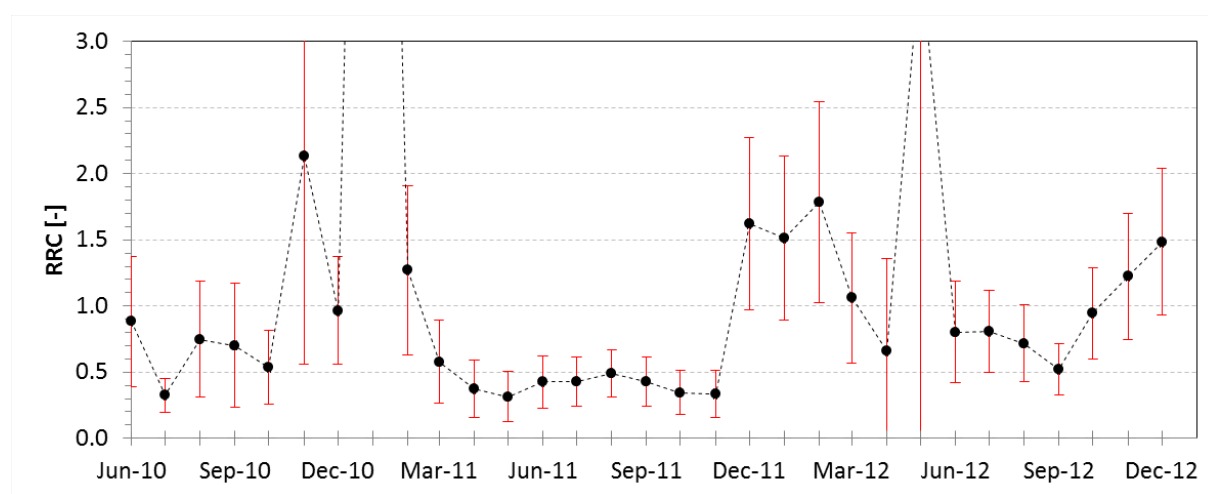


Figure 6-37: Time series of monthly mean RRCs related to rain gauge DAH (black dots) with standard deviation (red whiskers).

Figure 6-37 shows the resulting mean monthly RRCs to be used for the calibration of the hydraulic reference simulation model. The standard deviations show that the rainfall-runoff variability is also strongly influenced by seasonal effects.

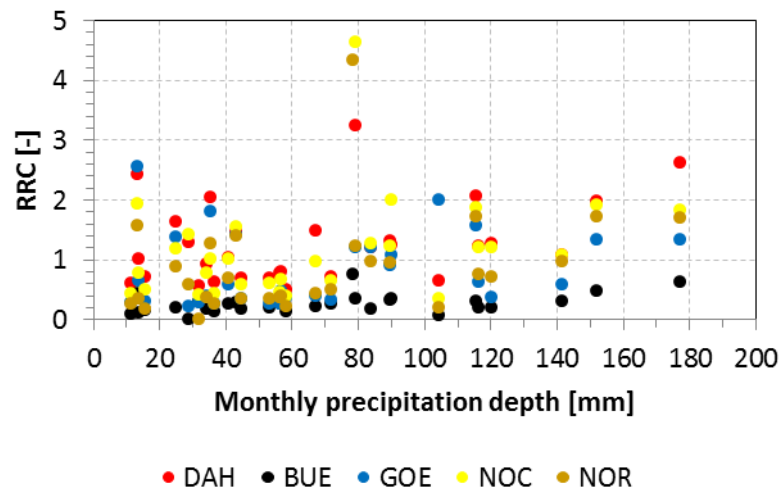


Figure 6-38: Mean monthly RRCs plotted against monthly precipitation depths for retention tanks allocated to rain gauge Dahl in the period June 2010 to December 2012

Figure 6-38 illustrates the distribution of mean monthly RRCs for sub-catchments allocated to rain gauge Dahl according to monthly precipitation depths. The analysis shows no correlation. Consequently, the process is assumed to be random.

Corresponding to the rainfall homogeneity analysis presented in section 6.3.1 the RRCs are aggregated and analyzed according to a double sum analysis. Figure 6-39 shows the resulting comparison of accumulated RRCs for rain gauge Dahl for the years 2010 to 2012. The results show a good linear correlation. The slopes of the correlation lines describe the constant differences in rainfall-runoff when assuming no spatial variability in the rainfall distribution. They indicate constant errors. The coefficients of determination describe the degree of random disturbances according to the assumption of no spatial variability in the rainfall distribution. Compared to Figure 6-28 to Figure 6-30 which show the system-wide variability of rainfall according to four rain gauges, the evaluation of RRCs per rain gauge according to the slopes of correlation lines and the coefficients of determination reveals for all investigated years reasonably higher degrees of variability concerning the rainfall-runoff within the investigated sub-catchments allocated to the rain gauge Dahl. Figure 6-40 shows the corresponding evaluation for rain gauge Eschdorf. The results are consistent with the results for rain gauge Dahl. Figure 6-41 shows the corresponding comparison of all rain gauges except for Arsdorf which is not used in the model representing the system state 2010. Again, the results are consistent with the others. Overall, the analysis of measured system-wide RRCs reveals additional variability which exceeds the variability of rainfall-runoff behavior to be assumed according to the use of four different rainfall time series.

As illustrated in Figure 6-38 the process can be assumed to be random. Hence, deterministic modeling of the process will be inadequate. Instead, it is proposed to consider the

investigated disturbances in the deterministic integrated reference simulation model by adding a phenomenological approach in order to investigate the influence of the investigated RRC variability on the proposed system-wide FPC approach. Consequently a random coefficient representing the seasonal variability according to the investigated monthly standard deviation of the investigated RRCs will be added to the runoff of each catchment allocated to the same rain gauge. Due to the seasonal impact on the standard deviation according to Figure 6-37 the proposed model will be described and parameterized according to the chosen periods for the simulation based evaluation of the proposed FPC approach according to the sections 7.3.1 and 7.3.3. The effects of considering representative RRC variability according to a deterministic – phenomenological reference simulation model on the performance of the system-wide FPC approach will be analyzed in section 7.3.3.

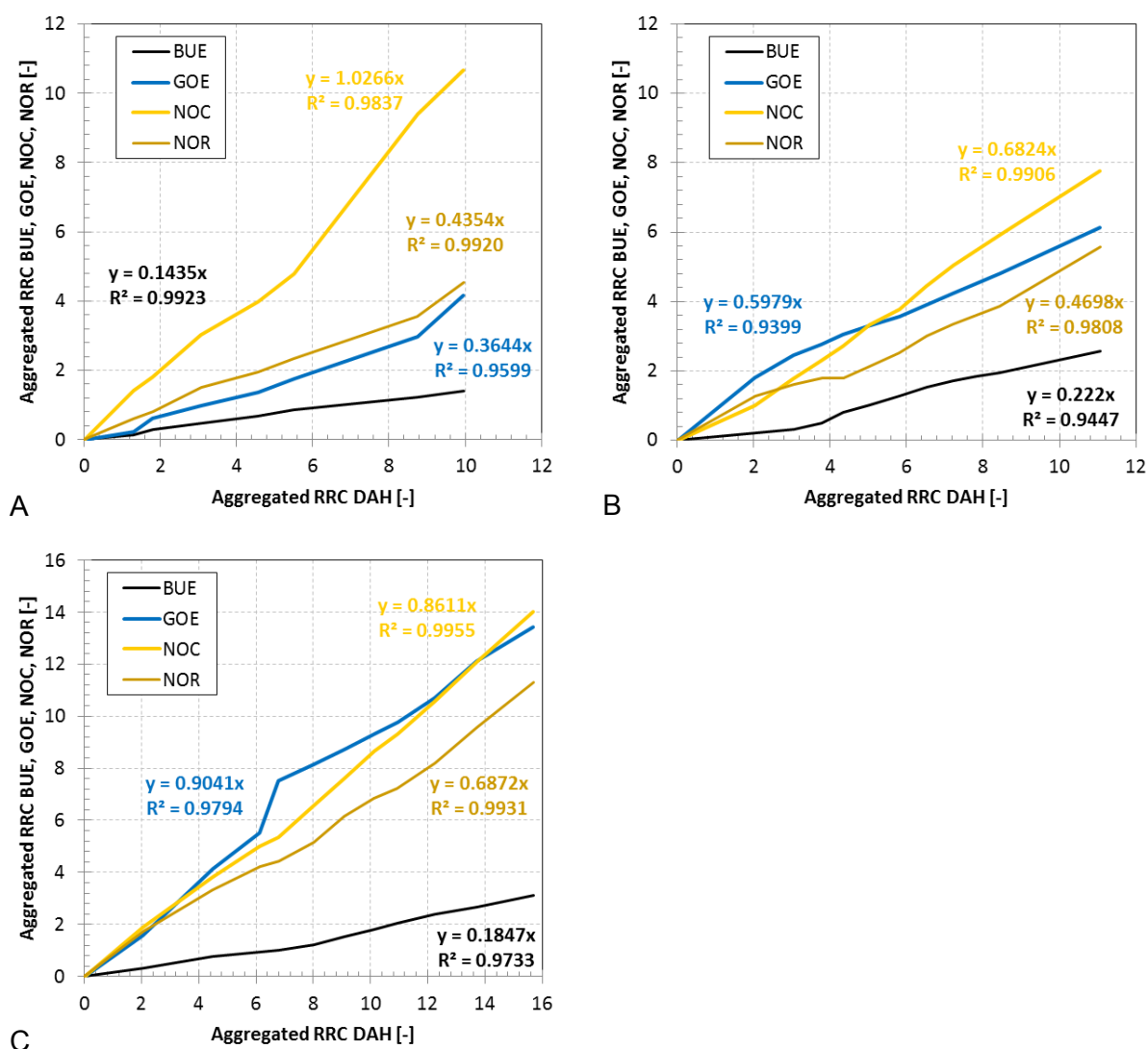


Figure 6-39: Comparison of aggregated monthly RRCs for sub-catchments allocated to rain gauge DAH for the period June to December considering the years (A) 2010, (B) 2011 and (C) 2012

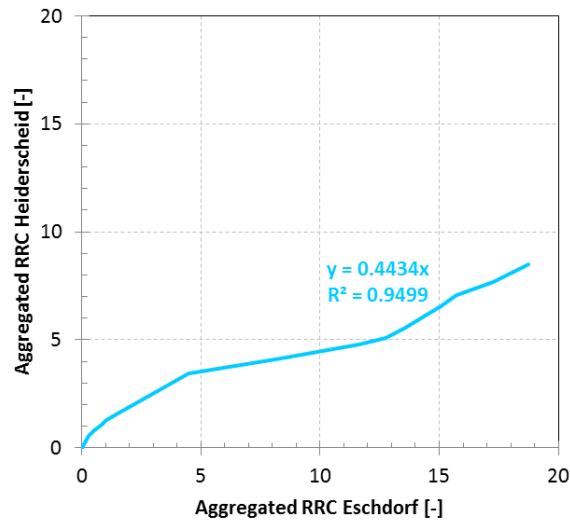


Figure 6-40: Comparison of aggregated RRCs for sub-catchments allocated to rain gauge ESD (June 2011 to December 2012)

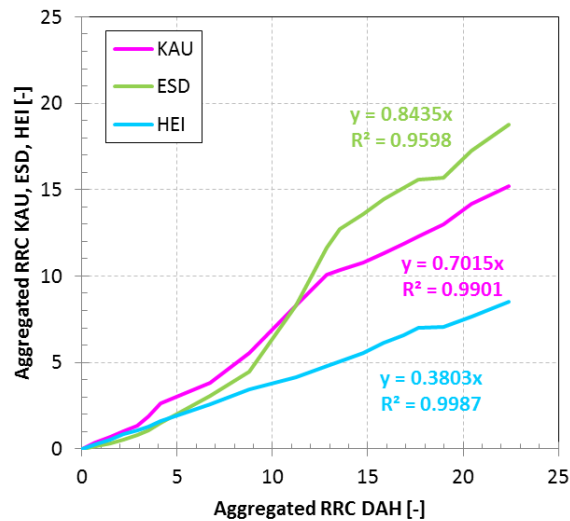


Figure 6-41: Comparison of aggregated RRCs for retention tanks DAH, KAU, ESD and HEI (June 2011 to December 2012)

6.3.3. Model description

After a detailed review of available software tools for IUWSs modeling SIMBA[®] was chosen for implementing the reference model predominantly because of its implementation in MATLAB[®] since this provides many possibilities to implement the presented approach for integrated FPC.

- **Sewer system**

In SIMBA[®] Sewer rainfall-runoff is modeled according to an approach of variable losses. Effective rainfall is calculated from the total rainfall and losses of various kinds distinguishing between initial and event-depending losses. Then surface runoff is modeled by Nash-cascades. The SIMBA[®] Sewer default approach with constant concentrations for COD and TKN for rainfall-runoff was replaced by a model for accumulation and wash-off.

Accumulation of pollutants during dry periods is calculated according to (Equation 6-35). The approach considers accumulation on the catchment surface and sewer depositions. Wash-off through rainfall is modeled by (Equation 6-36). Then, RWF is superposed with DWF. Flow in the sewer pipes is modeled by translation. Retention tanks are modeled as completely mixed tanks. Overflow is calculated from the maximum storage capacity of a retention tank. Details on the model are given in ifak system GmbH (2009).

$$M_a(t) = M_{max} - (M_{max} - M_{residual}) \cdot e^{-k_1 \cdot t} \quad \text{Equation 6-35}$$

with: $M_a(t)$... the pollution mass accumulated at time t , M_{max} ... the pollution mass accumulation limit, $M_{residual}$... the residual pollution mass after a rain event and k_1 ... the accumulation coefficient

$$\frac{\Delta M_e}{\Delta t} = M_a(t) \cdot (1 - e^{-k_2 \cdot q^w \cdot \Delta t}) \quad \text{Equation 6-36}$$

with: M_e ... the eroded pollution mass, k_2 ... the wash-off coefficient, $q(t)$... the runoff at time t and w ... a coefficient to adapt the form of the pollutograph

The sewer network sub-model describing the final state consists of 24 sub-catchments. For rainfall-runoff modeling each sub-catchment is described by one runoff contributing surface. Each sub-catchment drains into an on-line bypass retention tank. Table 6-3 summarizes the data describing the sewer network sub-model. Table 6-2 summarizes the corresponding data describing the model in the system state 2010. Table 6-4 summarizes the data describing the ISN.

- **Wastewater treatment plant**

ASM1 (Henze *et al.* 1987) was used to model the oxidation ditch and the double-exponential settling velocity approach within a 10-layer 1D clarifier model according to Takács *et al.* (1991) is used to model the SST. For detailed model descriptions the interested reader is referred to the specific publications. At low loaded oxidation ditches with SASS primary treatment only consists of coarse and fine screens followed by an aerated sand trap. Mechanical treatment is modeled according to the results of the measurement campaign constantly reducing particulate COD by 10%. Effects on TKN were insignificant (two percent) resp. could not be found in the case of TP.

6.3.4. Model calibration

The aim of the reference simulation model is to test the developed system-wide FPC approach for integrated rural WCTSS. Hence, this model must represent the dynamic variations observed by the measured data for DWF and CWWF. To this end, the reference model is limited to capture the diversity of monitored events. Additionally, seasonal DWF load variability due to tourism and the change of temperature are significant factors represented by the reference model.

6.3.4.1. Sewer network

Dry weather flow

DWF hydrographs were derived from inflow measurements during the DWF monitoring campaigns. Results are shown in Figure 6-42. A comparison to a typical hydrograph for residential catchments according to ATV-A 134E (DWA 2000) shows a good agreement. DWF pollutographs for the sum parameters COD and TKN are derived from the system-wide load balance presented in section 6.2.2.1. Therefore, a constant infiltration $0.030 \text{ m}^3/(\text{d}\cdot\text{PE})$ of clean water in the ISN during DWF is added to match the mean DWF concentrations measured in the retention tanks (see Figure 6-17). The resulting mean DWF pollutographs injected in each catchment are shown in Figure 6-43.

Table 6-25 shows the adapted system-wide balance for DWF including the effluent of the aerated sand trap. The mechanical primary treatment is modeled according to a constant reduction of particulate COD of 10%. The effect of two percent reduction of TKN is not taken into account. The resulting concentration balance corresponds to the design assumptions according to ATV-A 131 (DWA 1992b).

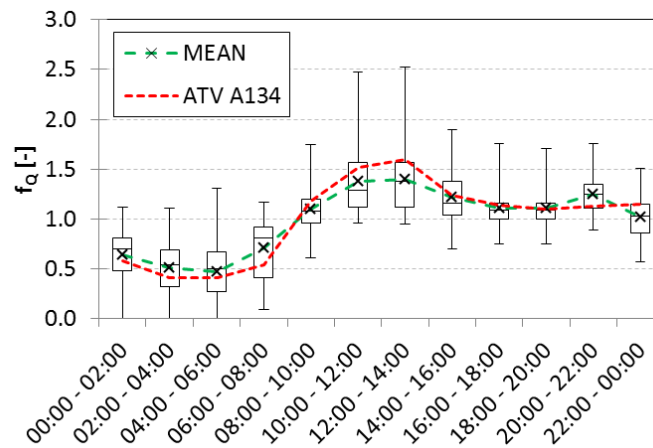


Figure 6-42: Mean DWF hydrograph in the catchments

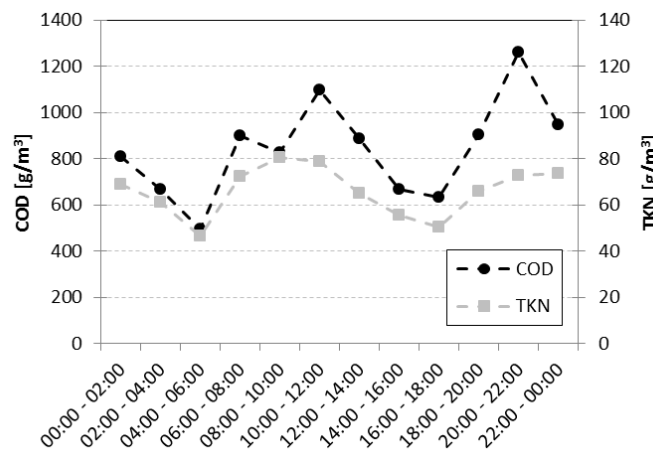


Figure 6-43: DWF pollutographs for COD and TKN

Table 6-25: Adapted system-wide concentration balance

	Catchment	WWTP		ATV-A131 (DWA 1992b)		
		Inlet	Sand trap			
COD [g/m ³]	877	725	650	90%	647	100%
TKN [g/m ³]	67.1	55.5	54.2	98%	59.3	91%

Combined wet weather flow**Hydraulic model**

Based on the results of the hydraulic balance according to section 6.2.2.2 a linear RDII of 15% is added to the CWWF in the ISN. Due to the seasonal impact on RRCs the hydraulic model calibration is presented along with the chosen reference months for the integrated FPC evaluation presented in section 7.3.1.

Pollution load model

During CWWF results from the DWF pollution load model are superposed with results from the pollution load model for wet weather flow. Assuming constant concentrations for DWF during CWWF rainfall-runoff driven pollution loads based on accumulation and wash-off can be balanced according to the measured pollutographs. Table 6-26 summarizes the results of the reference model calibration using the measured hydrographs for pollution load modeling. The table summarizes accumulated and eroded COD and TKN pollution loads for specific CWWF events. Accumulation is modeled according to the preceding DWF period. The modeled wash-off load is compared to the measured wash-off load considering the corresponding DWF loads. The presented results provide an overview on the performance variability of the pollution load model. The results reflect the difficulty to represent the diversity of the observed events ranging between good agreement and strong overestimation. Thereby, the performance for COD and TKN modeling are different per event. Figure 6-44 A to E show the corresponding agreement of the resulting pollutographs with the measured grab samples. The observed large dynamics of short initial concentration peaks followed by dilution phases are reflected by the model. Table 6-27 provides the corresponding overall parameterization. In the present case rain events predominantly erode the total accumulated load ($L_{\text{residual}} = 0$). Consequently, the maximum accumulated loads L_{max} are limited to the antecedent DWF period. The corresponding observed mean values for L_{max} are quite small, compared to other studies. But, in the case of COD results from Paulsen (1987) confirm the present observation. Literature data for TKN is very limited. The present results for net accumulated TKN loads correspond to the findings of Van Wensen (2001). Accumulation according to k_1 corresponds to the range of values presented in literature. The present wash-off according to k_2 is much slower in the present case in order to model the dynamics of the monitored pollutographs. A main difficulty in the present case is the reflection of strong first-flush peaks followed by a delayed load contribution during the subsequent dilution phase. This behavior can be observed by each fraction which is illustrated by the results of the first flush analysis in section 6.2.2.2. Figure 6-20 and Figure 6-21 predominantly show a superior behavior along the whole event. This corresponds to MFF-values larger than one along most parts of the event as shown in Figure 6-22 and Figure 6-23. These initial peak flows are modeled according to the parameter w . Overall, the

results confirm the well-known uncertainties in pollution load modeling during CWWF (Willems 2008).

Table 6-26: Calibration results of the accumulation and wash-off model according to calculated wash-off loads from measured CWWF loads and mean DWF loads for specific CWWF events

Event	Vol [m ³]	P _{DWF} [d]	Accumulation		Wash-off					
			COD [kg/ha]	TKN [kg/ha]	Measured		Modeled			
					COD [kg/ha]	TKN [kg/ha]	COD [kg/ha]	TKN [kg/ha]	COD [%]	TKN [%]
12/07/10	89	1.5	1.58	0.028	2.59	0.05	3.84	148	0.08	152
19/05/11	135	4.2	3.72	0.075	4.10	0.19	3.76	92	0.08	41
31/05/11	418	8.9	5.89	0.143	6.89	0.23	10.64	154	0.25	108
07/06/11	151	1.2	1.35	0.024	0.23	0.00	4.91	2130	0.11	3712
22/06/11	324	0.2	0.19	0.003	0.00	0.00	0.19	0	0.00	100

Table 6-27: Results of the parameter estimation for the accumulation and wash-off model and comparison to results from literature review

Study		L _{max}	L _{residual}	k ₁	k ₂	W
		[kg/ha]	[kg/ha]	[1/d]	[1/mm]	[-]
Haute-Sûre	COD	8	0	0.15	0.01	4.5
	TKN	0.4	0	0.05	0.01	5.5
Paulsen (1987)	COD	4.4 – 12	-	0.0627 – 0.0786	0.84 – 0.95* ¹	-
Van Wensen (2001)	COD	22.5	32	0.18	1	0.8
	TKN	1.4	0.7	0.16	0.5	0
Schmitt-Heidereich (1995)	COD	0 – 200	-	0.01 – 0.2	0.05 – 1.0	-

Additionally, the variability of the background DWF load that is typical for small rural catchments contributes to the difficulties to calibrate the RWF pollution load model. Assuming a mean background load according to section 6.2.2.1 the differences in measured and modeled load reflect these dynamics as well as uncertainties concerning accumulation and wash-off in rural catchments. Overall, the calibrated model reflects the characteristics and dynamics of the observed CWWF events.

Wastewater pollutant flows and modeling in rural WCTs

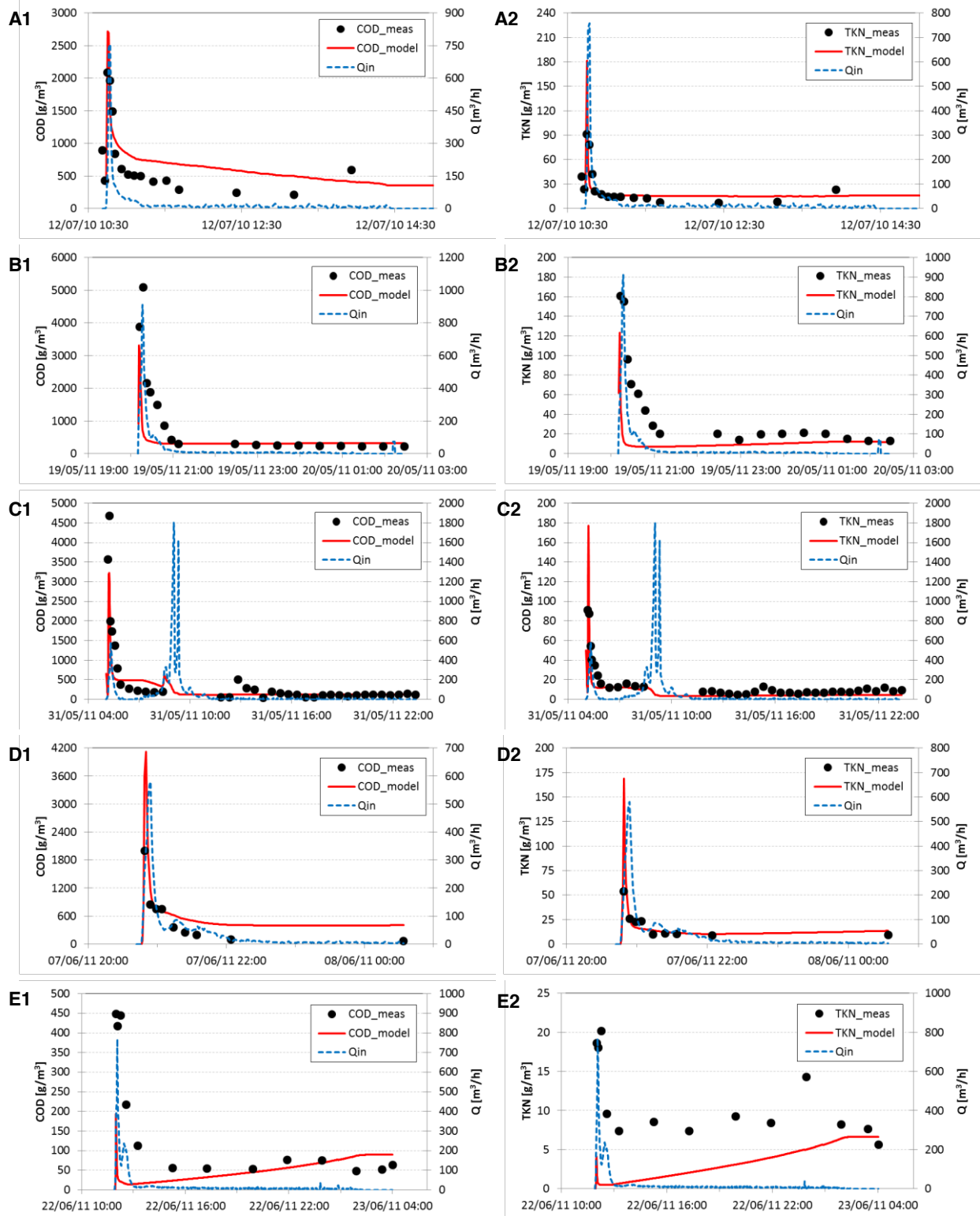


Figure 6-44: Results of the model calibration for accumulation and wash-off (A = KAU 12/07/2010, B = GOE 19/05/2011, C = GOE 31/05/2011, D = GOE 07/06/2011, E = GOE 22/06/2011; x.1 (left) showing COD, x.2 (right) showing TKN)

6.3.4.2. Wastewater treatment plant

According to the recommendations of the IWA task group for Good Modeling Practice (Rieger *et al.* 2013) it was decided to stick to the standard BSM1 parameterization of ASM1 (Copp 2001). Consequently, the calibration of the WWTP reference model remained limited:

- to the layout necessary to reflect the measured dynamics of the oxidation ditch and
- to the aeration system in order to reflect the oxygen input.

Oxidation ditches are space-saving concepts to implement nitrification and denitrification in a single reactor. Tank geometry and aeration are designed to have both processes either simultaneously or intermittently. In order to avoid sedimentation during aeration pauses for denitrification oxidation ditches are equipped with propellers to create circulation flows larger than 30 cm/s. Usually, these small plants can be assumed to be completely mixed, except for DO that exhibits spatial variability (Insel *et al.* 2005). Since oxygen injection is limited to discrete aeration fields within the tank, the DO concentration decreases along the flow path due to the bacterial respiration activity (Abusam *et al.* 2001). Vice versa, the kinematics depend on the DO-profile along the flow path in the ditch. This can be modeled by a series of completely mixed tanks with an internal recirculation flow corresponding to the mixing behavior (Abusam and Keesman 1999). Therefore, a DO concentration profile in the oxidation ditch was measured during DWF. Figure 6-45 shows the setup of the test. "SIDEN" marks the stationary DO probe for the control of the aeration according to a constant DO set-point of 1.5 g/m^3 for continuous aeration during the test. Points "1" to "6" mark the additional monitoring stations during the test. They are chosen according to local bridges that provided accessibility. A YSI 6920 DO probe was used for the test. During the test aeration was continuous. Overall, the probe remained at least two hours at each measurement point. The DO profile is illustrated in Figure 6-46. The investigated standard deviations show the systems dynamics according to the dynamic loading. According to the results a linear course was assumed.

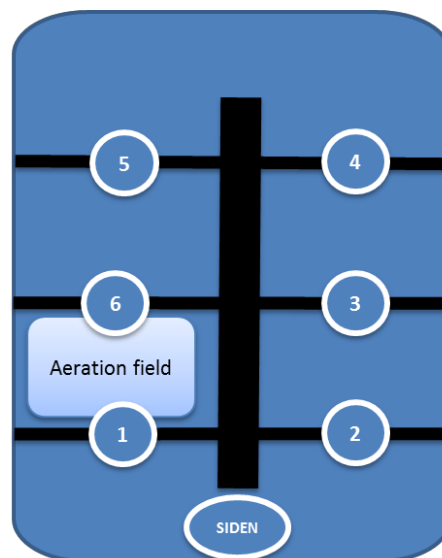


Figure 6-45: DO-profile measurement setup

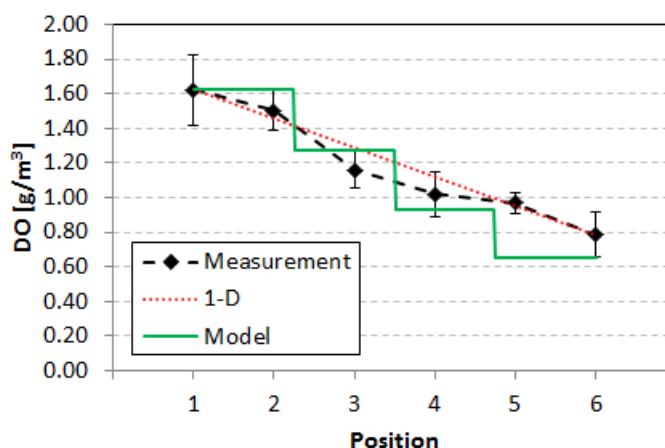


Figure 6-46: AST DO profile at WWTP Heiderscheidergrund 04/2011

As explained in section 5.2.2 the layout of the prediction model and the reference model will be the same in this study. Consequently, the model layout must be chosen to find a good balance of accuracy and computational effort. Since in the present case the aeration field size is about $\frac{1}{4}$ of the total tank surface four tanks-in-series were found to be a practicable compromise. Model calibration was done according to the DO-profile along the tank during continuous aeration (see Figure 6-46) supported by results from an aeration test conducted with clean water before the startup of the WWTP. Aim of this test was to measure the real oxygen input into the system provided by the installed blowers. Table 6-28 provides the results of the measured oxygen input R_{air} for clear water at 6.4°C giving a mean value of 19.55 g/(m³_Nm).

Table 6-28: Results of a clean water test to measure the real oxygen input and bottom flow rates

Pos.	Tank 1				Pos.	Tank 2			
	R_{air} [g/(m ³ _N m)]	OC [kg/h]	OP [kg/kWh]	v_{bottom} [cm/s]		R_{air} [g/(m ³ _N m)]	OC [kg/h]	OP [kg/kWh]	v_{bottom} [cm/s]
1	19.8	48.8	3.5	31.2	1	20.2	49.8	3.5	32.8
2	19.8	48.6	3.5	45.4	2	20.0	49.3	3.5	32.0
3	19.1	46.9	3.4	44.9	3	19.9	48.9	3.5	47.3
4	18.9	46.5	3.3	47.6	4	18.7	46.1	3.3	46.5

Oxygen input in ASM1 is described according to Equation 6-38. With an immersion depth of 5.86 m and $S_{\text{O}_2, \text{sat}} = 8.63736 \text{ g/m}^3$ in the present case two unknown variables are left in Equation 6-38. As described before the aeration field in the present case is about $\frac{1}{4}$ of the total tank surface. Hence, the aerated volume is assumed to be $\frac{1}{4}$ of the total volume. According to recommendations for sub-surface aerators with small bubbles the oxygen transfer rate α is assumed to be 0.6. The internal cycling flow in the oxidation ditch is calculated from bottom flow rate measurements performed during the clean water aeration test. The results showed a mean bottom flow rate of $v_{\text{bottom}} = 41.0 \text{ cm/s}$. Additionally, surface flow rates were measured at position 3 (Figure 6-45) showing $v_{\text{surface}} = 16.6 \text{ cm/s}$. Assuming

a linear vertical velocity profile the mean internal cycling flow can be calculated according to Equation 6-40. For an average water level of 6.165 m and a channel width of 3.925 m the mean internal circulation flow Q_{circ} is about 600000 m³/d. During model calibration Q_{circ} is used to adapt the monitored DO profile to the measured one. Thereby, Q_{circ} is reduced to 300000 m³/d. The resulting profile is shown in Figure 6-46. The reduction in flow can be explained by hydraulic swirls caused by the aeration field. Zhang et al. (2009) generally confirm the hydraulic impact of aeration fields on the flow in oxidation ditches based on computational fluid dynamics studies.

Aerobic wastewater treatment processes need large amounts of dissolved oxygen in the wastewater. Oxygen is injected into the aerobic reactor either using surface aerators or pressurized aeration systems. The oxygen transfer rate (OTR) is modeled according to Equation 6-37. The temperature depending saturation point of dissolved oxygen concentrations is calculated according to Equation 6-39.

$$OTR = k_{La} \cdot (S_{O,sat} - S_O) \tag{Equation 6-37}$$

with: OTR ... the oxygen transfer rate, k_{La} ... the oxygen transfer coefficient, $S_{O,sat}$... the oxygen saturation concentration and S_O ... the current oxygen concentration.

$$k_{La} = \frac{\alpha \cdot Q_{air} \cdot R_{air} \cdot h}{S_{O,sat} \cdot V} \tag{Equation 6-38}$$

with: k_{La} ... the oxygen transfer coefficient, α ... the mass transfer rate, Q_{air} ... the air flow rate, R_{air} ... the specific oxygen input, h ... the immersion depth of the oxygen input, $S_{O,sat}$... the oxygen saturation concentration and V ... the aerated volume.

$$S_{O,sat} = 13.89 - 0.3825 \cdot T + 0.007311 \cdot T^2 - 0.00006588 \cdot T^3 \tag{Equation 6-39}$$

with: $S_{O,sat}$... the oxygen saturation concentration and T ... the temperature.

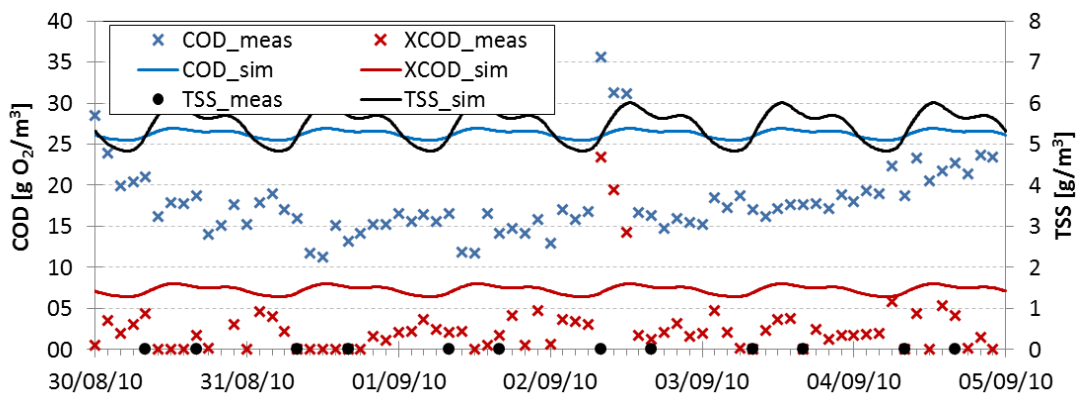


Figure 6-47: WWTP effluent COD and TSS concentrations during DWF with continuous nitrification according to the average DWF pattern

Wastewater pollutant flows and modeling in rural WCTSS

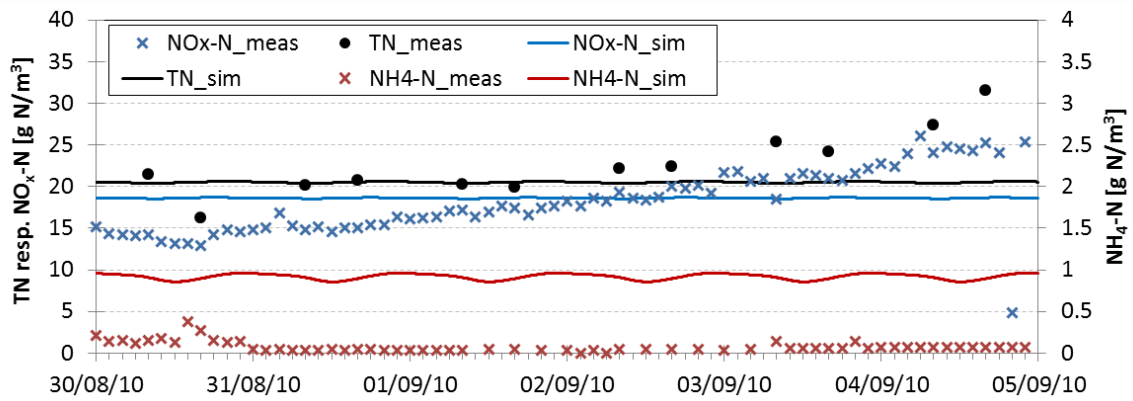


Figure 6-48: WWTP effluent nitrogen concentrations during DWF with continuous nitrification according to the average DWF pattern

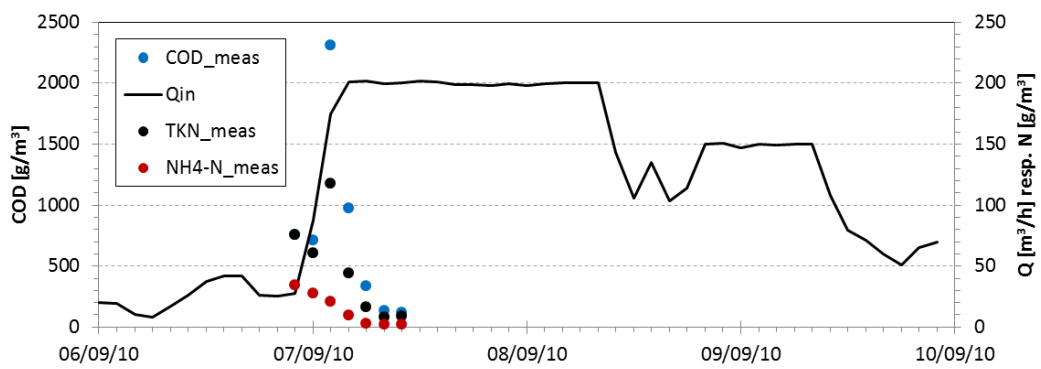


Figure 6-49: Hydraulic and pollutant peak loading during the CWWF campaign in 2010

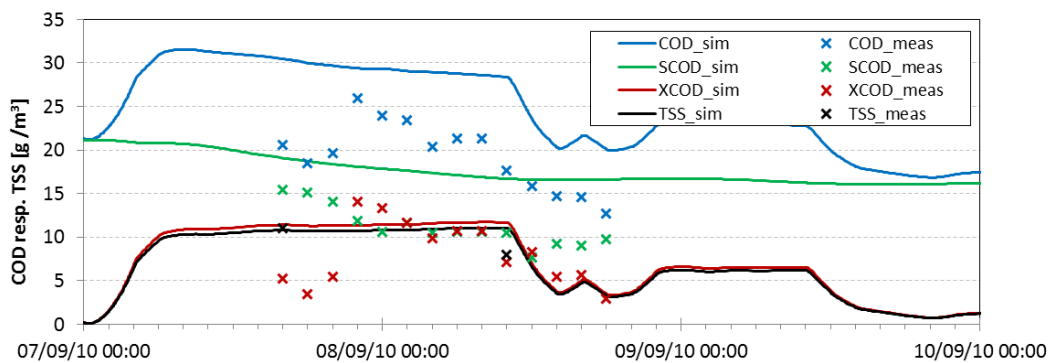


Figure 6-50: Effluent COD and TSS concentration calibration results during the CWWF campaign in 2010

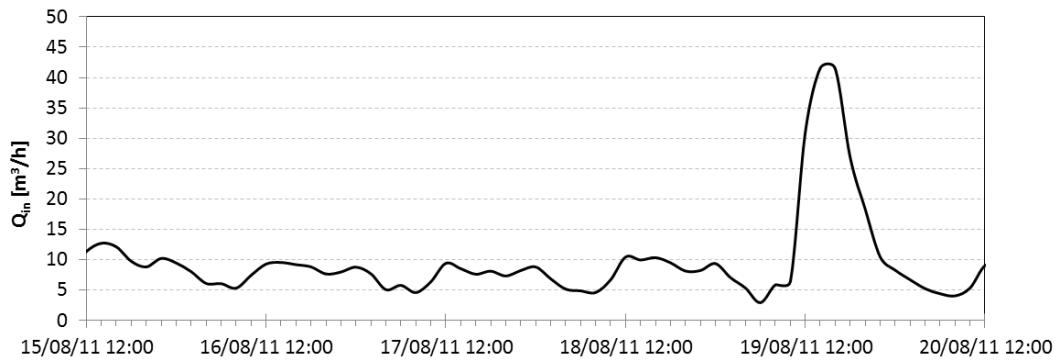


Figure 6-51: Hydraulic loading during the DWF campaign in 2011

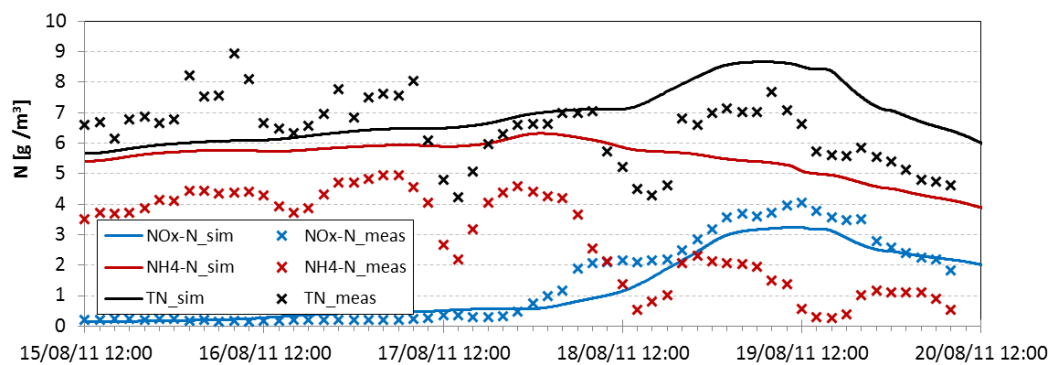


Figure 6-52: Effluent calibration results for the denitrification DWF campaign 2011

Figure 6-47 and Figure 6-48 show the calibration results for nitrification during the DWF measurement campaign in 2010. Despite the aforementioned uncertainties due to the underloaded situation the four tanks-in-series model based on the mean DWF inflow reflects the effluent concentrations in an appropriate range. Figure 6-49 and Figure 6-50 show the results of the model calibration during CWWF. COD and TSS effluent concentrations and dynamics are reflected by the model sufficiently to investigate hydraulic peak loading. Figure 6-51 and Figure 6-52 show the calibration results for denitrification. Although the 4 tanks-in-series model does not reflect the hourly dynamics of denitrification, even small dynamics according to hydraulic disturbances created by CWWF are modeled quite well. Therefore, it can be assumed that the chosen model setup is appropriate for further investigations of integrated control approaches during CWWF.

6.3.4.3. Model interfaces

Sewer network – Receiving water

From the immission-based point of view receiving water models need information regarding TSS, COD, BOD₅ and NH₄-N. Given the results of the fractionation analysis in section 6.2.3, fractionation results according to ATV-DVWK-A131E (DWA 1992b) and BSM1 (Copp 2001) is compared by linear regression of the simulation and the results of the monitoring campaign. Figure 6-53 and Figure 6-54 show the results for COD and TSS. The linear correlation performs better than the complex ASM1 fractionation model which confirms the large organic fraction in TSS during CWWF. Figure 6-55 and Figure 6-56 illustrate the

comparison of modeling BOD₅ from COD, the first based on the complex ASM1 fractionation model the latter based on linear modeling. Both approaches show comparably good results. Figure 6-57 and Figure 6-58 show the results for modeling NH₄-N from TKN respectively COD. For CWWF, modeling of NH₄-N according to the ASM1 fractionation model outperforms linear modeling from TKN only because of the balance with particular organic nitrogen. Nevertheless, uncertainties concerning the modeling of NH₄-N are quite high. Consequently, modeling of TSS and BOD₅ from CSO is chosen according to Equation 6-40 and Equation 6-41.

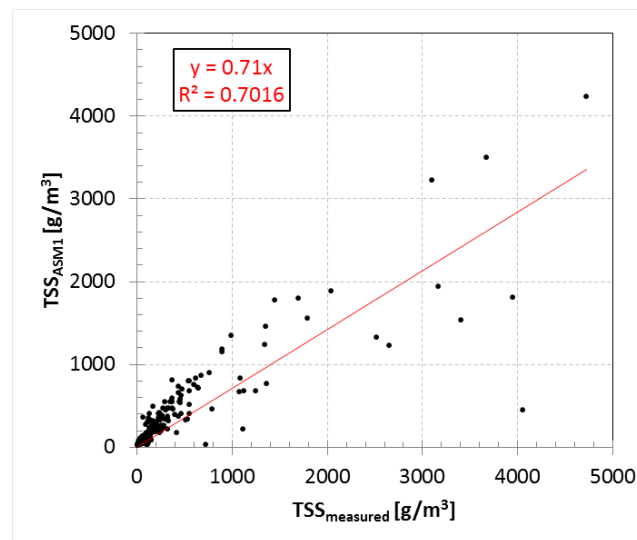


Figure 6-53: Correlation of TSS_{measured} – TSS_{ASM1}

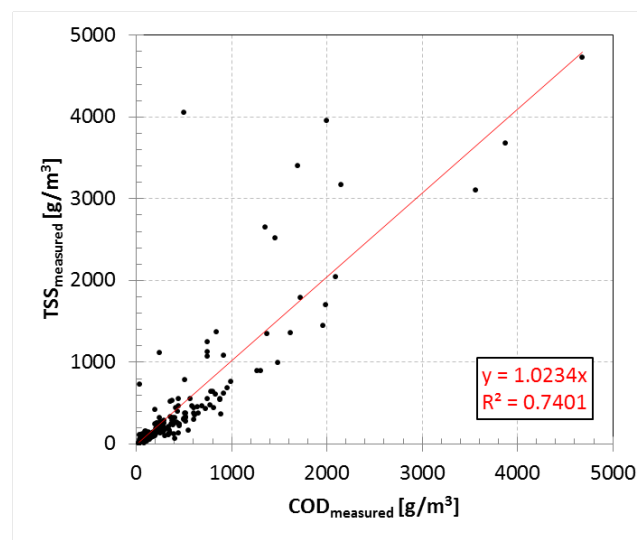


Figure 6-54: Correlation of COD_{measured} – TSS_{measured}

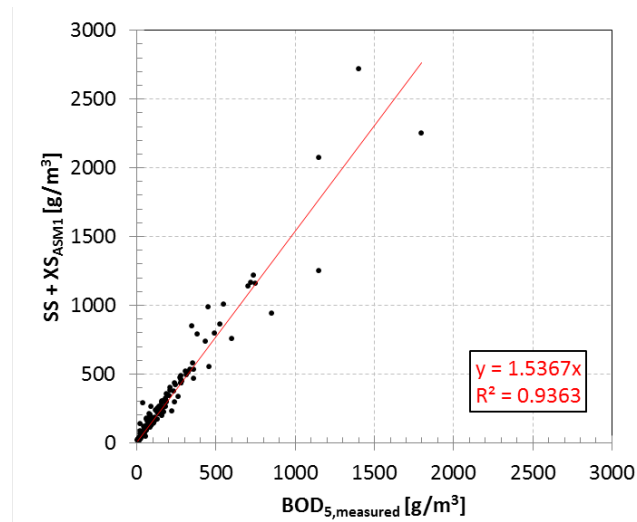


Figure 6-55: Correlation of $BOD_{5,measured} - S_S + X_{S,ASM1}$

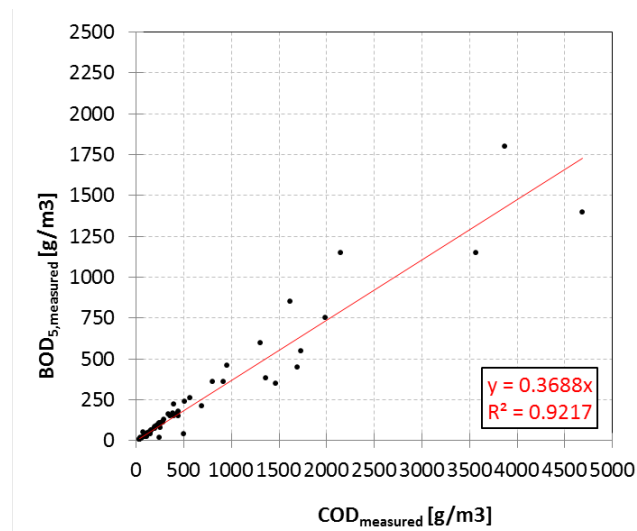


Figure 6-56: Correlation of $COD_{measured} - BOD_{5,measured}$

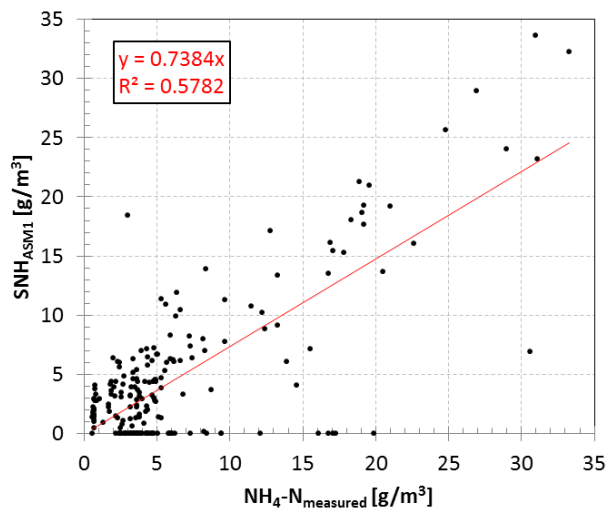


Figure 6-57: Correlation $NH_4-N_{measured} - SNH_{ASM1}$

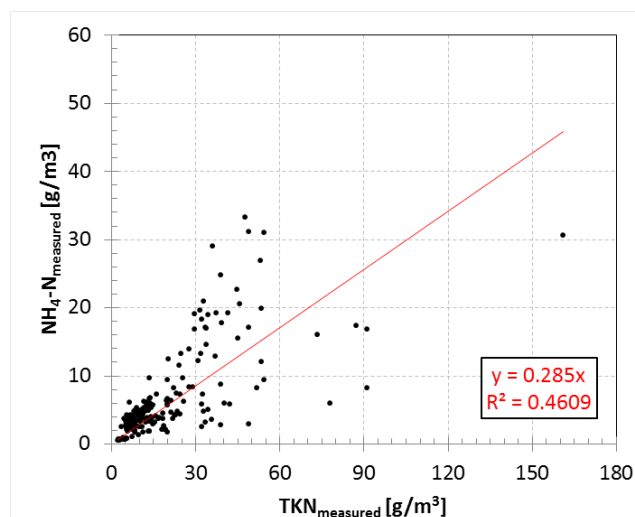


Figure 6-58: Correlation of $TKN_{measured} - NH_4-N_{measured}$

$$TSS_{CSO} = 1.0234 \cdot COD_{CSO}$$

Equation 6-40

$$BOD_{5,CSO} = 0.3688 \cdot COD_{CSO}$$

Equation 6-41

6.3.5. Disturbance modeling

6.3.5.1. Population equivalents

Tourism plays an important role in the Haute-Sûre catchment. In summer the number of PEs connected to the WWTP Heiderscheidergrund increase from 6687 to 12042. Hence the WWTP is designed with two lanes, one for winter operation, two for summer operation. This is linked to summer holidays but what is the development like? This is an interesting approach especially regarding taking the second lane into operation. Camping site Bissen pumps its wastewater to the WWTP. Hence, the information of the monthly wastewater volume can help visualizing the development of tourism in summer. Figure 6-59 shows the results of the evaluation of the data from 2011. Maximum wastewater production occurs in July and August followed by May and June with about 50 percent of the maximum. According to these results summer operation of WWTP Heiderscheidergrund is necessary in July and August with a transition phase in May and June where approximately 50 percent of tourism can be assumed. Camping site Bissen represents 394 PE. In August 2011 a volume of 583.7 m³ was discharged to the WWTP. This equals only 47.8 l of wastewater per PE and day. This is about 1/3 of the average DWF per PE and day. Figure 6-59 illustrates the evolution of tourism according to the monthly wastewater volume of camping site Bissen discharged to the WWTP in 2011.

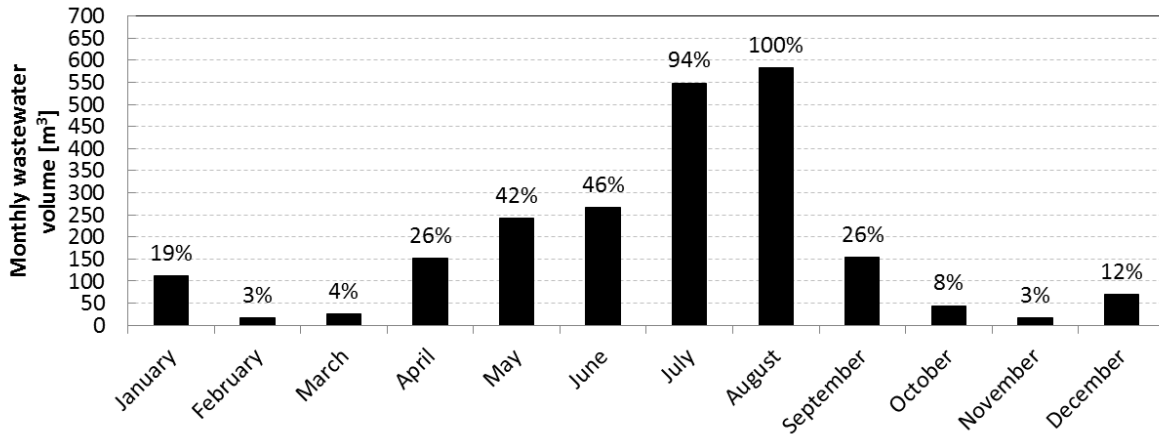


Figure 6-59: Evolution of tourism according to the monthly wastewater volume of camping site Bissen discharged to the WWTP in 2011

6.3.5.2. Temperature

Treatment processes are temperature sensitive. Additionally, constraints for WWTP operation with SASS are also linked to temperature. WWTP Heiderscheidergrund is equipped with temperature sensors in the effluent of the aerated sand trap and the effluent of the SST. The evaluation of the monitoring data of the period 2010 to 2012 is shown in Figure 6-60. The temperature of the wastewater varies between 5.8 °C in February and 16.4 °C in August which is quite high. The corresponding standard deviation varies between 0.5 °C in February and 1.2 °C in May. The mean annual wastewater temperature of 11.2 °C with a standard deviation of 0.9 °C which is close to the design temperature of 12 °C chosen for the WWTP.

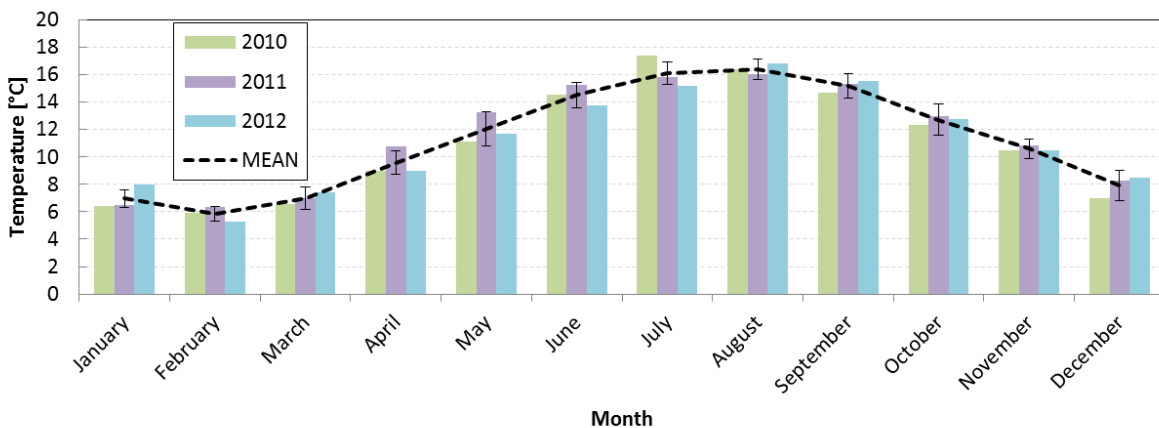


Figure 6-60 Wastewater temperature profile WWTP Heiderscheidergrund in the period 2010 to 2012

7. Simulation-based evaluation of the integrated fuzzy predictive control approach

This chapter describes the implementation of the integrated FPC approach for simulation-based evaluation based on the theoretical background presented in chapters 2 to 5 according to the chosen case study, describes in chapter 6. The case study defines the objectives of the system-wide FPC approach consisting of goals and constraints. Fuzzy objectives are first linguistically formulated and then translated into MFs. After the choice of a fuzzy norm for decision-making the chosen approach for nonlinear optimization and the choice of horizons for prediction, evaluation and control are described. The approach is tested according to two rainfall time series representing mean and extended monthly CWWF. The chapter finishes with the performance evaluation according to the comparison to different static reference scenarios. The presented model is implemented on an Intel Pentium Dual Core PC clocked at 2.53 GHz with 3 GB RAM. This choice was made to make it practicable for small and medium-size consulting engineering companies. The chosen software bundle for the simulation-based testing consists of the following components according to Table 7-1.

Table 7-1: Software components

Component	Software
Shell	MATLAB [®] & Simulink [®]
Integrated reference model	SIMBA [®] and Simulink [®]
Sewer network prediction model	MATLAB [®] & Simulink [®] (M programming language)
WWTP prediction model	Simulink [®] (C programming language)
Fuzzy Decision-Making	Fuzzy Logic Toolbox (MATLAB [®] & Simulink [®])
Pattern Search	Global Optimization Toolbox (MATLAB [®] & Simulink [®])

MATLAB[®]/Simulink[®] is used to interface the single software components. The software provides the Fuzzy Logic Toolbox[®] used to implement the proposed FPC approach based on FDM. Additionally, the MATLAB[®] Global Optimization Toolbox[®] is used for derivative-free optimization in nonlinear FPC. Because of its implementation in MATLAB[®]/Simulink[®], SIMBA[®] could be chosen as simulation tool to implement the integrated reference model according to section 6.3. The WWTP process model of the integrated approach, as described in section 5.2, which is used to predict future states within the FPC approach, is implemented in Simulink[®] based on the C programming language. The process model components considering the sewer network are directly implemented in MATLAB[®]/Simulink[®] based on the M programming language.

Due to the computational load induced by nonlinear integrated MPC approaches the performance evaluation had to be limited to monthly periods. The effect of different monthly rainfall depths and intensities is analyzed according to two different monthly precipitation time series representing mean and heavy loading of the WCTSs. Additionally, the seasonal evaluation of rainfall-runoff coefficients contributes to the analysis of seasonal impacts on the calibration of rainfall-runoff models for hydraulic sewer network modeling.

Linear correlation analysis and principal least squares (PLS) analysis are used to analyze the results of FPC for two months of local rainfall runoff series representing mean and intensive monthly rainfall.

7.1. Objectives of the integrated control

As described in section 5.2.4 control objectives of sewer networks and WWTPs are case-specific. In the present case, SASS has a significant impact on the objectives of the integrated control. Objectives consist of goals and constraints. Constraints in MPC can be linear or nonlinear. Linear constraints are predominantly based on physical limitations of actuators or legal effluent concentrations. Nonlinear constraints occur according to nonlinear objective functions such as in the present case. As described before, one feature of FDM is the equal treatment of goals and constraints. Consequently, the term objectives will be used instead in the following. In order to simplify the complexity of the aggregated objective function linear constraints are handled conventionally in the present case. For clarity reasons objectives are categorized according to sewer network and WWTP objectives.

In sewer network MPC retention tank discharges are controlled according to a threshold given by the WWTP (Fiorelli *et al.* 2013). In order to investigate the integrated optimization of system-wide control of WCTs according to the FDM of conflicting objectives this threshold for sewer network MPC should correspond to the current WWTP capacity. As explained before, WWTPs are highly nonlinear systems. Due to this, there is no explicit equation to calculate the current treatment capacity under dynamic conditions, especially during CWWF. Reported capacity limiting processes during CWWF are predominantly sedimentation in the SST (see e.g. Rauch and Harremoës (1996)) and nitrification in the AST (see e.g. Tränckner *et al.* (2007a)). Therefore, it was decided to derive the current WWTP capacity according to the simulation-based evaluation of a WWTP process model for FPC equal to the WWTP reference simulation model based on ASM1 (Henze *et al.* 1987) for the AST and the double-exponential settling velocity approach within a 10-layer 1D SST model according to Takács *et al.* (1991). Thereby, the challenge in integrated multi-criteria optimization of sewer network FPC and WWTP FPC is to continuously find hydro- and pollutographs at the WWTP inlet that simultaneously represent the current WWTP capacity and the trajectory for sewer network FPC. Due to compromises of conflicting objectives in system-wide FPC of WCTs it can be assumed that hydro- and pollutographs describing the WWTP capacity are not necessarily equal to the hydro- and pollutographs resulting from sewer network FPC according to this trajectory. In order to analyze this integrated conflict a hybrid optimization approach is chosen. For each integrated control step first the current WWTP capacity is derived from the integrated process model according to FPC only considering the objectives to optimize the loading and performance of the WWTP according to section 7.1.2 resp. 7.2.1.2. By not considering the FDM in the sewer network within this step, a hydro- and pollutograph is derived according to the chosen evaluation horizon which reflects the current WWTP capacity. During the following control steps for sewer network FPC within the integrated control step the so derived WWTP capacity is used as a trajectory for sewer network FPC only considering the objectives to optimize the sewer network control according to section 7.1.1 resp. 7.2.1.1. Thereby, the Lagrangian ISN observer model presented in section 5.2.3 is used as a link between the local retention tanks and the central WWTP to track the hydro- and pollutograph for continuous integrated control and optimization. Hydro- and pollutographs, used to estimate the current WWTP capacity, are

predicted according to discrete retention tank discharges, which are controlled in 10 minutes intervals, assuming the wastewater pollution concentrations measured at each retention tank to be constant during each interval. Coalescing wastewater discharges in the ISN are mixed completely within this 10-minutes-pattern.

7.1.1. Sewer network

As described in section 5.3.1 the main objective of sewer network MPC approaches is to minimize CSO volume and pollutant load to receiving waters (rules 1 to 3 in Table 7-2). To this end, the retention tanks shall empty as fast as possible in order to maximize the capacity for follow-up CWWF events (rule 4). CSO at the WWTP inlet is restricted to emergency (rule 5). Due to the reduced balancing retention tank volume for CWWF treatment at the WWTP inlet, in rural WCTs with decentralized retention tank volume and widespread ISNs, a second major objective is the homogeneous loading of the WWTP according to its current treatment capacity. Thereby, the WWTP must be loaded evenly (rules 6 and 7). These rules reflect the small buffer capacity of the retention tank at the WWTP inlet with an emergency CSO structure. This requires evenly distributed hydro- and pollutographs in the ISN (rules 8 and 9) according to the current capacity of the WWTP (rules 10 to 12). Table 7-2 summarizes the linguistic description of the sewer network objective functions in system-wide analysis and hydraulic control of rural WCTs chosen from the literature review in section 3.4.2.1.

Table 7-2: Linguistic description of sewer network objective functions for system-wide analysis and control of rural WCTs

No.	Description
1*	Minimize the total CSO volume at retention tanks in the sewer network
2	Minimize the total CSO COD load at retention tanks in the sewer network
3	Minimize the total CSO TKN load at retention tanks in the sewer network
4*	Minimize the total CWWF volume in all retention tanks for fast emptying
5	Homogenize the use of all retention tanks
6*	Minimize the emergency CSO volume at the WWTP
7*	Harmonize the inflow to the WWTP
8*	Maximize the flow to the WWTP along the ISN according to the reference value
9*	Harmonize the flow to the WWTP along the ISN according to the reference value
10*	Maximize the hydraulic load to the WWTP according to the current treatment capacity
11	Maximize the COD load to the WWTP according to the current treatment capacity
12	Maximize the TKN load to the WWTP according to the current treatment capacity

* used for FPC

Only objectives marked with an asterisk are used for FPC. The present limitation of sewer network control to hydraulic objectives results from computational limitations due to the chosen hard- and software setup and the complexity of the case study consisting of 24 retention tanks which, however, is typical for rural WCTs. Since the objectives concerning pollution loads are evaluated according to their MFs (see Table 7-6), the corresponding impact on the FDM between hydraulic and pollution load objectives can still be evaluated according to their MF results resembling the satisfaction of each objective according to

corresponding conflicts. In that case the decision-making corresponds to the absolute prioritization of hydraulic objectives.

In the sewer network the controlled variables consist of the 24 retention tank throttled discharges $Q_{thr,i}$. The corresponding actuators consist of retention effluent throttles and pumps. The observed variables consist of the hydraulic CSO loads at each retention tank and the ISN hydrograph. Figure 7-1 illustrates the system. The hydraulic capacity of the final conduit of the ISN upstream of the WWTP is calculated according to complete filling and gravity flow. In order to respect the maximum capacity of the ISN, the hydraulic capacity of the WWTP is expressed as a percentage of the ISN capacity.

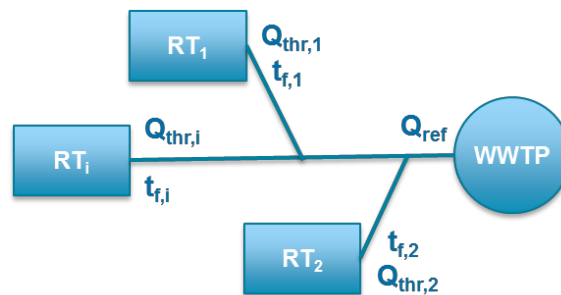


Figure 7-1: Control of discharges at retention tanks according to the WWTP reference load

Linear inequality constraints for FPC within the sewer network arise from physical limits of the installed equipment. Due to simplicity, linear constraints are implemented conventionally. The hydraulic capacities of the throttles and pumps at each retention tank are considered as linear inequality constraints according to Table 7-3.

Table 7-3: Maximum throttle flows per retention tank

Retention tank	$Q_{thr,max}$ [m ³ /d]	Retention tank	$Q_{thr,max}$ [m ³ /d]	Retention tank	$Q_{thr,max}$ [m ³ /d]
BAS	10800	ESE	2771	KUB	5530
BAU	1382	FLE	10800	LIE	10800
BAV	10800	GOE	12022	MEC	8467
BOE	8035	HEI	2771	NOC	1037
BUE	10786	HEG	2771	NOR	1296
BUU	2592	HIE	2771	NOT	9072
DAH	864	INB	2564	RIN	4662
ESC	28685	KAU	10786	TAD	9256

7.1.2. WWTP

Legal effluent concentrations for WWTPs in Luxembourg are given by the EC urban wastewater directive (EC 1991). Table 7-4 shows the corresponding valid operational range for WWTP Heiderscheidergrund. In the case of BOD₅, COD and TN the evaluation distinguishes between concentration limits for 2h composite samples and 24h composite

samples. Their consideration forms the core of the presented FPC approach. Since BOD₅ and pH are not explicitly considered in ASM1 (Henze *et al.* 1987) they will not be taken into account in the present approach. While from an ecological point of view SST effluent concentrations should be minimized, from an economical point of view wastewater treatment close to these legal effluent limits can be cost-effective due to reduced aeration effort. Especially from the integrated point of view the capacity of the WWTP plays an important role in order to reduce CSO to receiving waters (Tränckner *et al.* 2007a).

Table 7-4: Legal effluent concentration limits for WWTP Heiderscheidergrund

Parameter	Limit	Sample
TSS	< 30 g/m ³	24 h composite sample
	< 30 g/m ³	2 h composite sample
BOD ₅	< 15 g/m ³ O ₂	24 h composite sample
	< 20 g/m ³ O ₂	2 h composite sample
TCOD	< 75 g/m ³ O ₂	24 h composite sample
	< 90 g/m ³ O ₂	2 h composite sample
NH ₄ -N	< 3 g/m ³	24 h composite sample
	< 3 g/m ³	2 h composite sample
TN	< 15 g/m ³	24 h composite sample
	< 15 g/m ³	2 h composite sample
TP	< 1 g/m ³	24 h composite sample
	< 1 g/m ³	2 h composite sample
pH	7 – 8.5	

Consequently, the design of MFs for WWTP FPC during CWWF must distinguish between compromises and preferences in the case of conflicting objectives. Well-known is the conflict between hydraulic loading and SST effluent TSS concentrations during CWWF due to activated sludge washout (Rauch and Harremoës 1996). Assuming good sludge settleability in the SST, increased concentrations of TSS in the SST effluent can be solely linked to hydraulic loading. Consequently, in order to maximize the hydraulic load to the WWTP the SST effluent TSS concentration must also be maximized according to the corresponding valid operational range. MFs for simultaneous minimization of absolute effluent TSS concentrations and hydraulic load maximization during CWWF would cause a compromise inevitably leading to WWTP loadings below its capacity. This example illustrates the complexity of MF design for FDM of conflicting objectives and hence the importance of expert knowledge concerning the processes to be controlled. Table 7-5 summarizes the objectives of the integrated FPC based WWTP capacity estimation and control. Rule 1 illustrates the maximization of the effluent TSS concentration to support the corresponding WWTP hydraulic loading maximization during CWWF (rule 6). Rules 2 to 4 reflect the minimization of COD, SNH and TN in order to optimize the wastewater treatment with respect to legal effluent limits according to Table 7-4. Rule 5 reflects the objective for SASS according to a desired NH₄-N concentration in the AST. Rule 7 illustrates the corresponding predictive optimization of the aeration. Hence, the aggregation of rules 2, 3, 4, 5 and 7 must describe the compromise between ecology and economy. Figure 7-2 and Figure 7-3 illustrate the recommendations of the German design guideline DWA-A 226 (DWA 2009) to

increase the process stability of WWTP with SASS. Major control requirements are related to the minimum aerated volume in the oxidation ditch and operational TS concentrations which are implemented in the global control of the WWTP. In order to keep the number of variables in a practicable range linear inequality constraints are implemented conventionally. In the case of the WWTP this is the hydraulic capacity of the return sludge pump. For a constant SRT of 25 days and a minimum DO concentration in aerated phases during CWWF of 0.7 g/m^3 , relations between temperature, aerated and non-aerated volumes resp. aeration periods and TS-concentrations are derived from Figure 7-2 and Figure 7-3 and taken into account, especially during DWF periods between single rain events. Due to these objectives the chosen controlled variables for system-wide FPC at the WWTP are the SST effluent TSS, COD, $\text{NH}_4\text{-N}$ and TN concentrations and the $\text{NH}_4\text{-N}$ concentration in the oxidation ditch. Corresponding manipulated variables are the WWTP inflow Q_{in} and the DO set-point in the oxidation ditch.

Table 7-5: Linguistic description of WWTP objective functions for capacity estimation, system-wide control and analysis of rural WCTs during CWWF

No.	Description
1*	Maximize the effluent TSS concentration according to legal effluent limits
2*	Minimize the effluent COD concentration with respect to legal effluent limits
3*	Minimize the effluent SNH concentration with respect to legal effluent limits
4*	Minimize the effluent TN concentration with respect to legal effluent limits
5*	Balance the $\text{NH}_4\text{-N}$ concentration in the oxidation ditch to 1.5 g/m^3
6	Maximize the hydraulic loading
7*	Optimize the DO reference concentration in the oxidation ditch for optimized treatment

* used for FPC

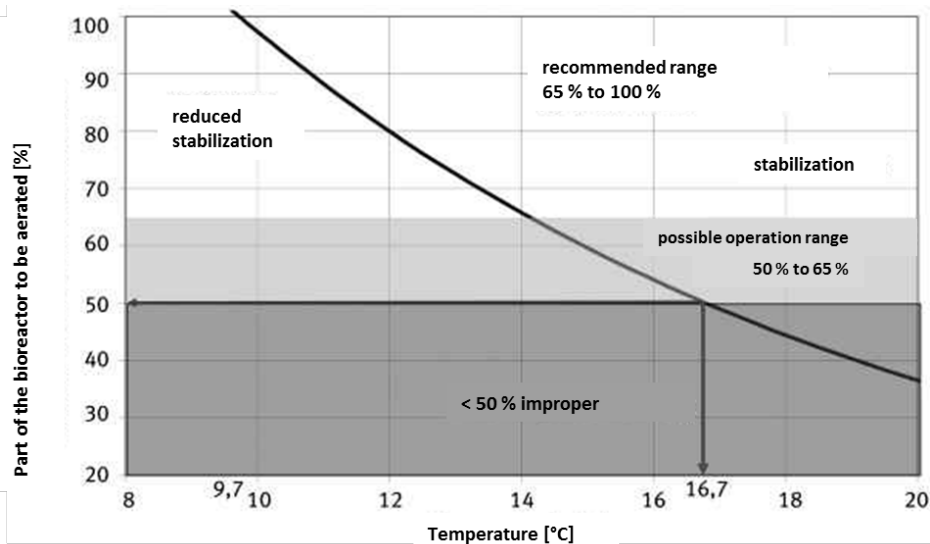


Figure 7-2: Recommended aerated fraction of the activated sludge tank depending on the temperature (taken from DWA-A226 (DWA 2009), modified)

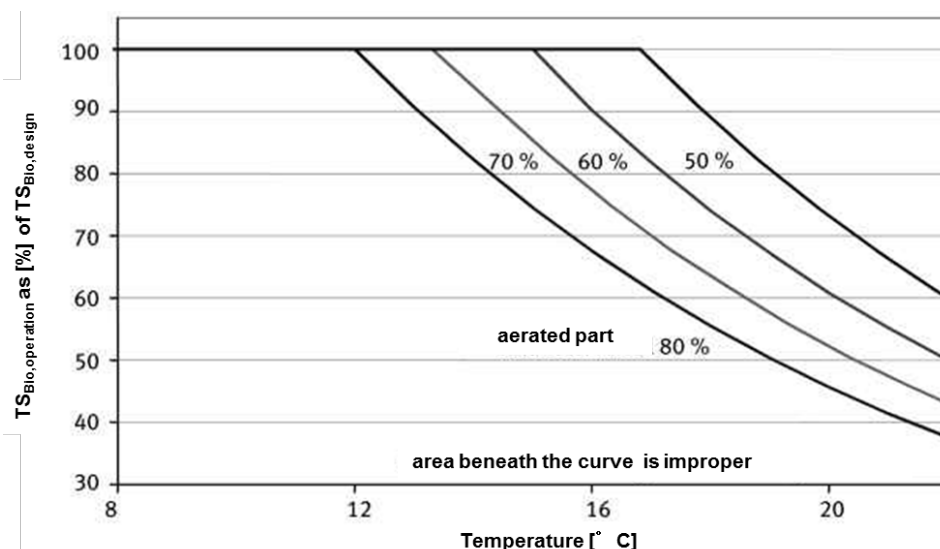


Figure 7-3: Recommended activated sludge tank TS concentration depending on the temperature and the aerated part of the activated sludge tank (taken from ATV-A226 (DWA 2009), modified)

7.2. Controller

7.2.1. Membership functions

The MFs used in the present case are triangular, described by three points, namely a , m and b with a and b defining the support of the MF and m defining the core where MF values are equal to one. In triangular MFs the core is reduced to a single number (for details see section 4.3.1). Specific parameterizations are used to transform the chosen objectives presented in section 7.1 into fuzzy objectives. In FPC results of the process model for prediction are fed into MFs in order to calculate their degree of membership, representing their preference in the decision-making process. Based on the receding horizon approach the evaluation by the controller is done each control step resulting in a set of actuator settings. The integrated process model for performance prediction is described in section 5.2.

7.2.1.1. Sewer network

As described in section 7.1.1 sewer network control within the system-wide FPC approach must be limited to hydraulic objectives due to the computational effort. Nevertheless, MFs taking pollution loads into account will be used to evaluate the hydraulic based sewer network FPC from a pollution point of view. In terms of decision-making this corresponds to an absolute preference for hydraulic objectives. The analysis then reveals the conflicts between hydraulic and pollution based objectives in sewer network control. Table 7-6 shows the chosen parameterization of triangular MFs corresponding to the linguistic objectives presented in Table 7-2. MFs with asterisk are used for FPC in the present case. A significant difference between FPC and conventional MPC is the normalization of objectives using MFs. Thereby, the support of each MF must be defined in advance. This can either be done using static support ranges based on expert knowledge or using dynamic support ranges based on fuzzy dynamic programming. The latter is preferably used to decrease the support range leading to differentiated MF curves and decreased computational effort during numerical

optimization (Kacprzyk and Esogbue 1996). Fuzzy dynamic programming was chosen to evaluate CSO volume (MF1) and CSO loads (MF2 and MF3). The emptying degree of all retention tanks (MF4) can be described according to their relative filling degrees where zero equals an empty tank and one equals a completely filled retention tank. Consequently, the upper limit of the corresponding MF support range is equal to 24 resp. the number of retention tanks in the system.

Table 7-6: Specific triangular MFs used for sewer network control and analysis in system-wide FPC of integrated rural WCTs

MF	Parameters	Input x	Explanation
1*	a = 0 m = 0 b = $\sum V_{in,RT,i}$	$\sum V_{over,RT,i}$	x is the sum of CSO volumes at all retention tanks. b is the inflow to all retention tanks.
2	a = 0 m = 0 b = $\sum L_{COD,in,RT,i}$	$\sum L_{COD,over,RT,i}$	x is the sum of CSO COD load at all retention tanks. b is the inflow COD load to all retention tanks.
3	a = 0 m = 0 b = $\sum L_{TKN,in,RT,i}$	$\sum L_{TKN,over,RT,i}$	x is the sum of CSO TKN load at all retention tanks. b is the inflow TKN load to all retention tanks.
4*	a = 0 m = 0 b = 24	$\sum f_{Vol,i}$	Filling degrees of retention tanks range between 0 and 1. b = 24 represents the total filling of all retention tanks. x is the sum of all filling degrees.
5	a = 0 m = 0 b = 0.5	STD($f_{Vol,i}$)	Filling degrees of retention tanks range between 0 and 1. b = 0.5 represents the maximum standard deviation. x is the sum of all filling degrees.
6*	a = 0 m = 0 b = 0	$V_{over,WWTP}$	The WWTP inlet has an emergency CSO structure. In order to avoid emergency CSO b is set to 0. x is the CSO volume at the WWTP.
7*	a = 0 m = 0 b = MEAN($Q_{in,WWTP}$)	STD($Q_{in,WWTP}$)	b is the mean of the WWTP inflow hydrograph. x is the standard deviation of the WWTP inflow hydrograph.
8*	a = 0 m = 0 b = $Q_{ref,WWTP}$	MAX(Q_{ISN})	b is the reference inflow to the WWTP describing its current treatment capacity. x is the peak discharge in the ISN.
9*	a = 0 m = 0 b = $Q_{ref,WWTP}$	MEAN(Q_{ISN})	b is the reference inflow to the WWTP describing its current treatment capacity. x is the mean discharge in the ISN.
10*	a = 0 m = $V_{in,ref,WWTP}$ b = $V_{in,ref,WWTP}$	$V_{in,WWTP}$	b and m are equal to the treatable reference volume. x is the volume to be treated.
11	a = 0 m = $L_{COD,in,ref,WWTP}$ b = $L_{COD,in,ref,WWTP}$	$L_{COD,in,WWTP}$	b and m are equal to the treatable reference COD load. x is the COD load to be treated.
12	a = 0 m = $L_{TKN,in,ref,WWTP}$ b = $L_{TKN,in,ref,WWTP}$	$L_{TKN,in,WWTP}$	b and m are equal to the treatable reference COD load. x is the COD load to be treated.

* used for FPC

In order to avoid emergency CSO at the WWTP MF5 is parameterized with zeroes. Consequently no CSO at the WWTP gives MF values equal to one and a CSO gives MF values equal to zero with no further differentiation. MF6 to MF8 use dynamic support ranges to evaluate the dynamics in the ISN during CWWF. MF9 to MF11 use dynamic support ranges to evaluate the dynamic WWTP loading during CWWF. For details on fuzzy dynamic programming the interested reader is referred to Esogbue and Kacprzyk (1998). Inputs and parameters of each MF are predictions resulting from the process model (see section 5.2) according to the chosen prediction-, evaluation- and control horizons (see section 7.2.3) and the rainfall time series to be simulated.

7.2.1.2. WWTP

Table 7-7 shows the MFs used for WWTP capacity estimation, control and analysis in system-wide FPC of integrated rural WCTSSs. The chosen parameterization translates the linguistic objectives according to Table 7-5 into MFs for computational evaluation. In the case of the WWTP solely static parameterization is used to define the MFs. MF1 to MF4 describe the constraints concerning legal effluent concentration limits.

Table 7-7: Specific triangular MFs used for WWTP capacity estimation, control and analysis in system-wide FPC of integrated rural WCTSSs

MF	Parameters	Input x	Explanation
1*	a = 0 m = 30 b = 30	MEAN($C_{TSS,eff,WWTP}$)	b and m are chosen equal to the legal effluent concentration limit to maximize the TSS effluent concentrations according to legal limits. x is the mean effluent TSS concentration.
2*	a = 0 m = 0 b = 75	MEAN($C_{COD,eff,WWTP}$)	b equals the legal effluent COD limit. x is the mean effluent COD concentration.
3*	a = 0 m = 0 b = 3	MEAN($C_{NH4-N,eff,WWTP}$)	b equals the legal effluent ammonium limit. x is the mean effluent ammonium concentration.
4*	a = 0 m = 0 b = 15	MEAN($C_{TN,eff,WWTP}$)	b equals the legal effluent total nitrogen limit. x is the mean effluent total nitrogen concentration.
5*	a = 0 m = 1 b = 3	MEAN($C_{NH4-N,bio,WWTP}$)	b and m describe the desired range of ammonium in the oxidation ditch ideally about 1 g/m ³ during CWWF operation. x is the mean ammonium concentration in the oxidation ditch.
6	a = 0 m = 1 b = 1	$V_{in,WWTP}/V_{max,ISN}$	b and m describe the desired maximum loading according to the hydraulic capacity of the ISN. $V_{in,WWTP}$ is the hydraulic load and $V_{max,ISN}$ is calculated from $Q_{max,ISN} = 21313 \text{ m}^3/\text{d}$ during the evaluation horizon.
7*	a = 0 m = 0.7 b = 5	MEAN(DO_{bio})	b and m describe the desired DO concentration in the oxidation ditch for SASS during CWWF. x is the mean DO concentration in the oxidation ditch.

* used for FPC

As described in section 7.1.2, TSS effluent concentrations are maximized in order to maximize the hydraulic load to the WWTP according to the current SST capacity. The remaining pollutants (MF2 to MF4) are minimized in order to maximize the WWTP removal performance. The Lagrangian ISN observer model enables a continuous prediction of WWTP inflow hydro- and pollutographs for 120 minutes. Corresponding to this evaluation horizon of 120 minutes, a continuous legal effluent limit of 75 g/m³ for COD is chosen according to Table 7-4. This also guarantees effluent COD concentrations below 90 g/m³ for 24h composite samples. MF5 is used to consider sufficient aeration according to the objectives of SASS guaranteeing a mean NH₄-N concentration in the oxidation ditch of about 1 g/m³. The upper limit of 3 g/m³ enables effluent NH₄-N concentration according legal effluent concentration limits. MF6 is used to maximize the hydraulic load to the WWTP with reference to the fixed hydraulic capacity of the ISN. MF7 is used to achieve a mean DO concentration of about 0.7 g/m³ during CWWF operation.

7.2.2. Fuzzy aggregation

In the present case, FPC is chosen to investigate the impact of system-wide control on the integrated performance of WCTSS. In FPC, MFs represent both goals and constraints. Within the decision-making process goals and constraints are treated equally. The support of the MF defines the set of the domain where function values are larger than zero. By assigning zero to values outside the support domain, values outside the range are penalized comparable to penalty functions used in classic MPC. In the present case, the number of respected objectives should be as high as possible. Consequently, compensation effects are suppressed using the fuzzy min t-norm for the aggregation of the single objectives (see Table 4-1). Equation 7-1 shows the chosen aggregated MF as objective functions for sewer network FPC in integrated rural WCTSS. Equation 7-2 shows the corresponding aggregated MF for WWTP FPC resp. capacity estimation in integrated rural WCTSS.

$$MF_{tot} = (1 - MF_1) + (1 - MF_4) + (1 - MF_6) + (1 - MF_7) + (1 - MF_8) + (1 - MF_9) + (1 - MF_{10}) \quad \text{Equation 7-1}$$

$$MF_{tot} = (1 - MF_1) + (1 - MF_2) + (1 - MF_3) + (1 - MF_4) + (1 - MF_5) + (1 - MF_7) \quad \text{Equation 7-2}$$

Finally, decision-making is done according to the minimization of Equation 7-1 and Equation 7-2 (see section 4.3). Pattern search and Latin hypercube sampling are chosen for optimization in the presented approach according to the descriptions in section 5.5.2.

7.2.3. Horizons

Time limitations play an important role in MPC of continuous systems (da Costa Sousa and Kaymak 2001). Figure 3-4 describes the different time levels necessary for MPC. In the case of nonlinear MPC one major difficulty is to solve the numerical optimization problem within the control horizon (Heusch 2011). Due to the lack of rainfall radar data Fiorelli et al. (2013) assume constant inflow to retention tanks within a prediction horizon of 10 minutes for a sewer network MPC approach in a rural system. In combination with a control step size of 10 minutes they achieve good performances. According to this experience the approach is adapted to the present integrated case. Smaller time resolutions are assumed to be

inappropriate since the resolution of available rainfall data used for simulation is mm per 10 minutes, too. Due to computational limitations the WWTP performance and hence the reference load for sewer network FPC is predicted every 30 minutes. The DO set-point in the oxidation ditch is adapted in a corresponding control step size of 30 minutes.

The problem of different horizons and control step sizes within the integrated approach is solved by using a hybrid process model. The integrated process model consisting of sub-models for retention tanks, the ISN and the WWTP is looped according to its control step size of 30 minutes. Within this control loop a sewer process model solely consisting of sub-models for retention tanks and the ISN is looped twice with a control step size of 10 minutes. While the sewer process model is implemented within a Simulink S-function block to run in parallel with the integrated simulation model, the integrated process model is implemented in a separate hybrid Simulink model Matlab code approach to run sequentially with the integrated simulation model. Consequently, process states must be saved and reloaded when switching between the integrated simulation model and the process models for FPC. Ideal hardware and software sensors are modeled by adapting the simulation model states at retention tanks and at the WWTP in the process models when switching. Figure 7-4 illustrates the implementation of the hybrid process model for system-wide FPC in the simulation model.

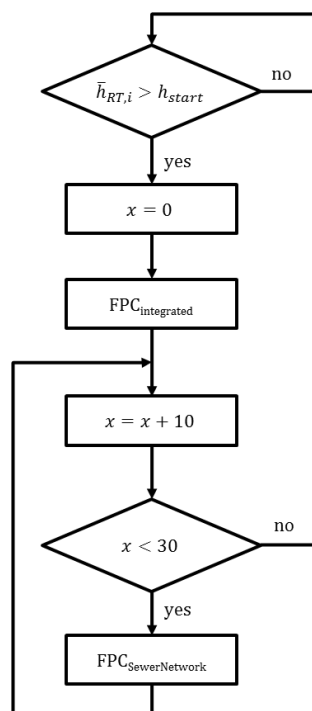


Figure 7-4: Hybrid process model implementation

Table 7-8 explains the different horizons chosen for the present approach.

Table 7-8: Horizons chosen in the present FPC approach and their explanation

Sub-system	Horizon	Step size [min]	Explanation
Sewer	Prediction	120 / 10*	Due to the evaluation of the WWTP process model wastewater flows are monitored within the ISN according to the Lagrangian ISN process model for 120 min. Predicted inflow to each retention tank is assumed to be constant during the next 10 minutes.
	Evaluation	120 / 10*	Flow and concentrations in the ISN are compared to the predicted WWTP capacity according to the evaluation of the WWTP process model of 120 minutes. CSO minimization is evaluated according to one control step of 10 minutes.
	Control	20	The chosen control step size is 10 minutes. In order to consider sufficient hydraulic capacity within the ISN in the next control step the control horizon is chosen twice the control step size by assuming the same throttle flows at the retention tanks in the next control step.
WWTP	Prediction	120	The prediction horizon is chosen according to the evaluation horizon. Inflow hydro- and pollutographs are predicted according to the Lagrangian ISN process model.
	Evaluation	120	The evaluation horizon is chosen according to the minimum requirements of performance evaluation due to legal effluent limits (see Table 7-4).
	Control	120	The WWTP control step size is chosen according to the balance of robustness and simulation speed of 30 minutes. The control horizon is assumed to be constant during the prediction resp. evaluation horizon.

* ISN / retention tank

7.3. Performance analysis and discussion

7.3.1. Choice of simulation periods

While model evaluation in urban wastewater management is usually based on long-term simulation, control models are predominantly evaluated using single events. In the case of WWTPs, reactions on different control decisions take place at different time levels (Brdys *et al.* 2008). While the manipulation of DO set-points or recirculation flow rates affects the treatment process in a range of hours, manipulation of e.g. the SRT affects the treatment process over a range of days. Consequently, effects on the sludge household and hence the current treatment capacity are noticeable only in the range days. In the sewer network the spatial distribution of rain events has a major impact on the efficiency of the chosen control approach (Fiorelli and Schutz 2009). Consequently, a longer period with a variety of events provides more insights regarding the variability of the performance of the approach than one single event. Due to the required computational effort an evaluation period of one month was chosen in the present case. The simulation of sequential events shall provide insights into the consequences of the integrated control on follow-up events concerning the WWTP capacity. The choice of specific months for the evaluation of the presented approach is based on the evaluation of measurement data with focus on CWWF volume, rainfall, runoff and antecedent DWF periods according to Figure 7-5 to Figure 7-7. The monthly rainfall heights are the mean values of the rain gauges DAH, ESC, ESD and ARS from 2010 to

2012. Mean antecedent DWF periods are included to consider the influence of the DWF – CWWF ratio on the monthly WWTP performance. Figure 7-5 shows no correlation between monthly rainfall depths and mean antecedent DWF periods. The 75-percentile is chosen to represent increased monthly rainfall resp. increased mean antecedent DWF periods. The mean and 75-percentile of the antecedent DWF period are very close to each other. Figure 7-6 shows the correlation of mean monthly rainfall heights and corresponding standard deviations of daily rainfall measured at the chosen rain gauges. The data shows a good correlation. Consequently, one can say that the spatial distribution of rainfall increases with rainfall depths. Figure 7-7 shows the nonlinear relation between monthly mean rainfall depths and corresponding aggregated monthly CWWF volume calculated from discharge measurements and water level measurements for the estimation of the CSO volume. Due to the statistical impact of extreme events the mean monthly CWWF volume is about the same volume as the 75-percentile. Based on this evaluation, June 2012 is close to the 75-percentile of the considered criteria and August 2011 is close to the mean of the considered criteria. Figure 7-5 to Figure 7-7 illustrate the placing of the chosen months within the overall measured data.

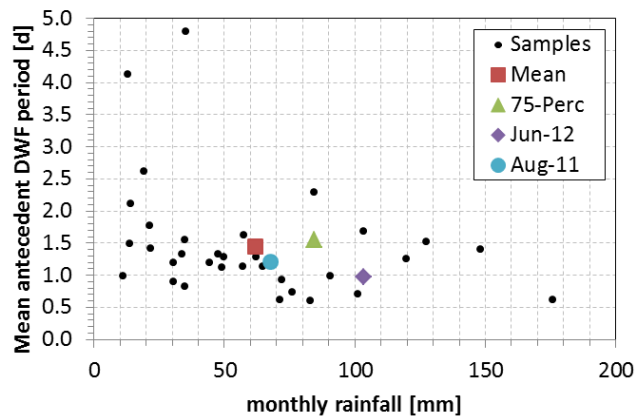


Figure 7-5: Correlation of monthly rainfall depth and corresponding mean antecedent DWF periods

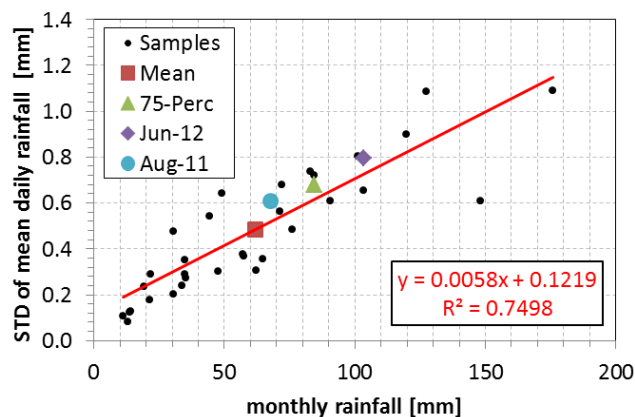


Figure 7-6: Correlation of the monthly rainfall depth and the corresponding standard deviations (STD) of mean daily rainfall heights of rainfall data from rain gauges DAH,ESC, ESD and ARS

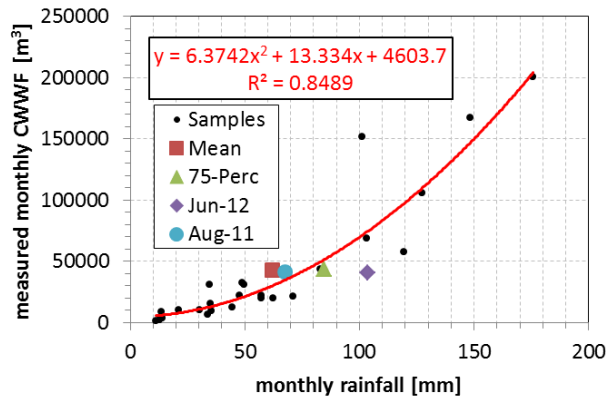


Figure 7-7: Correlation of monthly rainfall and monthly measured CWWF volume

7.3.1.1. Rainfall time series August 2011

The rainfall time series of August 2011 was chosen to represent the mean monthly rainfall height. Figure 7-8 shows the corresponding time series of the available rain gauges ARS, DAH, ESC and ESD. Figure 7-9 shows the double sum analysis of the accumulated rainfall time series illustrating the spatial variability of the rainfall according to the available rain gauges.

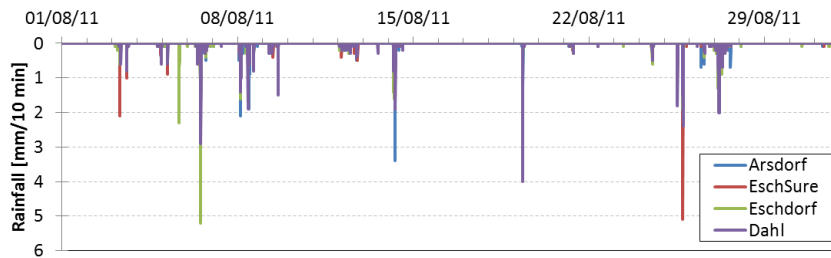


Figure 7-8: Rainfall time series August 2011

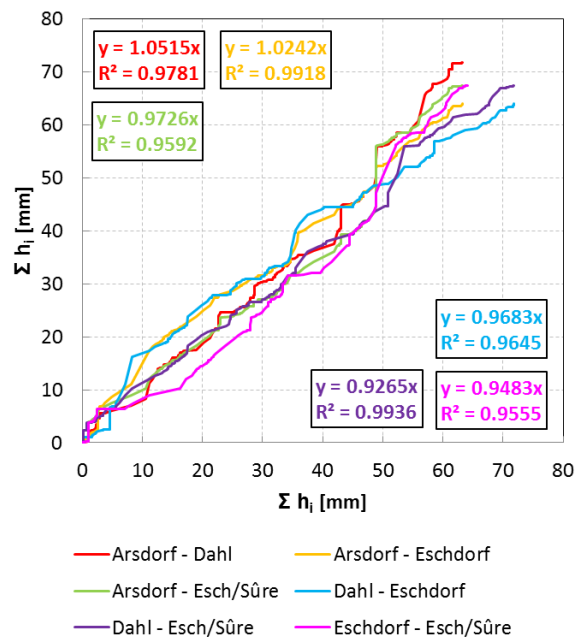


Figure 7-9: Spatial variability of the rainfall time series August 2011 according to the double sum analysis

According to decreased coefficients of determination compared to the results shown in section 6.3.1, the analysis of the spatial rainfall variability in a monthly resolution shows increased variability in comparison to the annual evaluation. According to the smaller range of regression line slopes the quantitative rainfall variability in August 2011 is below the annual mean.

7.3.1.2. Rainfall time series June 2012

The rainfall time series of June 2012 was chosen to represent an increased monthly rainfall height according to the 75-percentile. Figure 7-10 shows the corresponding time series of the available rain gauges ARS, DAH, ESC and ESD. The mean rainfall depth is about 60% larger than the mean rainfall depth of August 2011. Figure 7-11 shows the double sum analysis of the accumulated rainfall time series illustrating the spatial variability of the rainfall according to the available rain gauges. According to decreased coefficients of determination compared to the results shown in section 6.3.1, the analysis of spatial rainfall variability of a monthly resolution shows increased variability in comparison to the annual evaluation. According to the similar range of regression line slopes the quantitative rainfall variability in June 2012 is comparable to the annual mean.

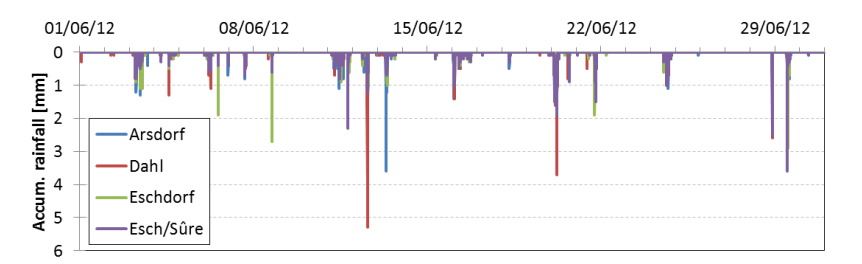


Figure 7-10: Rainfall time series June 2012

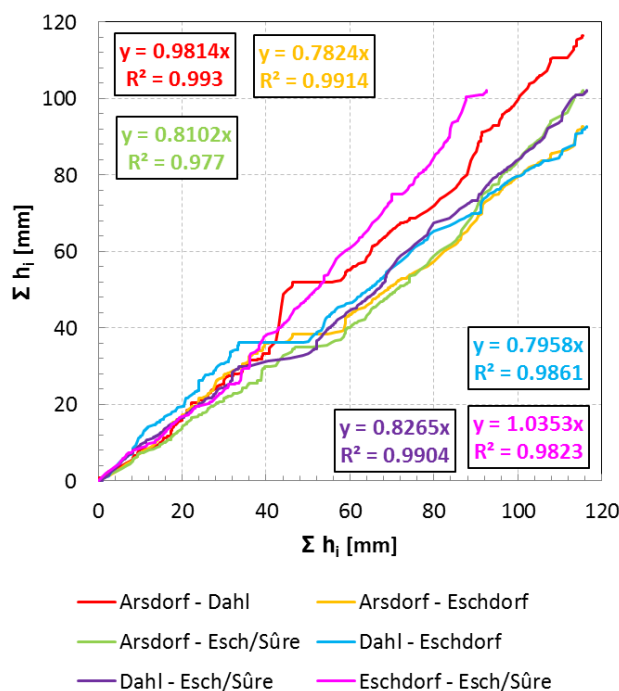


Figure 7-11: Spatial variability of the rainfall time series June 2012 according to the double sum analysis

7.3.2. Hydraulic calibration of the sewer network reference model

Besides the spatial variability, the rainfall-runoff homogeneity evaluation according to section 6.3.2 also indicates temporal variability. This additionally increases the difficulty to calibrate the hydrologic reference simulation model for simulation-based evaluation of the presented approach for system-wide FPC of integrated WCTs. Due to the spatial variability the hydraulic calibration of the rainfall-runoff model is done according to:

- simple volumetric balances for wastewater treated at the WWTP and wastewater discharged to receiving waters by CSO and
- hydrographs measured at the WWTP inlet and at the outlet of each retention tank.

The temporal variability is taken into account by adapting the reference simulation model calibration to the two months chosen in section 7.3.1. The reference simulation model structure is described in section 6.3.3. Rainfall-runoff modeling is based on the loss rates approach. Thereby, the fraction of surface contributing to rainfall-runoff increases exponentially from A_0 to A along the event. A_0 is the percentage of the surface contributing to runoff at the beginning of the event, after the subtraction of the wetting losses. This percentage of the surface has no depression losses. A describes the percentage of surface contributing to the runoff from rainfall at the end of the rainfall event which corresponds to the percentage of the effective surface (ifak 2009). Table 7-9 shows the resulting parameterization after model calibration based on trial-and-error. The default parameterization gives a good volumetric agreement of measured and modeled rainfall-runoff for the mean of all monthly rainfall time series and in detail for the rainfall time series of August 2011. In the present case the lack of the hydrologic reference model to model backwater effects is compensated by using virtual storage tanks upstream of retention tanks. After the calibration of the monthly total rainfall runoff volume, the virtual volume necessary to balance the measured ratio of runoff discharged to the WWTP and CSO volume is calibrated according to the measurements of the rainfall time series of June 2012 due to the uncertainties concerning the estimation of smaller CSO discharges according to the rainfall time series of August 2011. A mean virtual retention tank volume of 25% gives the best agreement to balance the monthly sum of CSO volume V_{CSO} and the volume discharged to the WWTP V_{WWTP} . Table 7-10 shows the corresponding results. Especially the standard deviation of monthly volumetric deviations illustrates the need of month-specific calibrations according to temporal variations of runoff from rainfall. The corresponding agreement of measured and modeled WWTP inflow hydrographs is illustrated in Figure 7-12 for the rainfall time series of August 2011 and Figure 7-13 for the rainfall time series of June 2012. While Figure 7-12 shows a very good agreement for the rainfall time series of August 2011 Figure 7-13 shows significant differences between the measured and the modeled hydrograph due to the lacking ability of the latter to model sloping ramps in the wake of larger events (for instance on 22/06/2012). This can be explained by:

- non-representative local rainfall data,
- infiltration in local sewer networks on catchment level and in the ISN and
- the lacking ability to model retention effects in the ISN due to the chosen translative approach.

Table 7-9: Parameterization of the rainfall run-off model for impervious catchment surfaces

Parameter		Value		
		Present	ifak system GmbH (2009)	ATV-DVWK (2006)
A ₀	Runoff contributing surface at the beginning of the rain event [%]	25	25	-
A	Runoff contributing surface at the end of the rain event [%]	85	85	-
L _{wet}	Wetting loss [mm]	0.7	0.7	0.3 – 0.7
L _{dep}	Depression loss [mm]	1.8	1.8	0.5 – 2.0

Table 7-10: Mean rainfall runoff model calibration results

Month	Measurement			Model					
	V _{WWTP} [m ³]	V _{CSO} [m ³]	V _{total} [m ³]	V _{WWTP} [m ³]	[%]	V _{CSO} [m ³]	[%]	V _{total} [m ³]	[%]
2010-07	19274	818	31130	20652	116	2066	253	37781	121
2010-08	41595	17178	57628	58033	104	19162	112	70154	122
2010-09	25605	4050	19790	23553	95	7057	174	23553	119
2010-10	12168	0	9859	7618	78	743	0	9273	94
2010-11	48728	40824	43593	41437	125	12819	31	41437	95
2010-12	52325	4234	21485	38258	145	10394	245	39061	182
2011-01	80448	511415	591863	41126	51	12969	3	54095	9
2011-02	38080	0	38080	11318	30	288	0	11605	30
2011-03	12712	0	12712	1751	14	0	0	1751	14
2011-04	4346	0	4346	3794	87	0	0	3794	87
2011-05	9752	2933	12685	14677	150	5879	200	20556	162
2011-06	28988	105	29093	14877	51	2047	1946	16924	58
2011-07	11250	7275	18525	21574	192	9965	137	31538	170
2011-08	27145	2425	29570	24786	91	6279	259	31065	105
2011-09	13377	1974	15352	17439	130	8559	434	25998	169
2011-10	10939	167	11106	6348	58	1173	702	7521	68
2011-11	2830	0	2830	1747	62	0	0	1747	62
2011-12	105397	123748	229145	104019	99	38337	31	142355	62
2012-01	80530	102754	183284	54963	68	15370	15	70333	38
2012-02	28366	150	28516	4212	15	0	0	4212	15
2012-03	23917	2504	26421	7630	32	2402	96	10032	38
2012-04	46203	34618	80821	36990	80	12634	36	49624	61
2012-05	60372	228486	288858	32446	54	17835	8	50282	17
2012-06	55600	10140	65741	37934	68	10134	100	48068	73
2012-07	65297	35821	101118	61388	94	30389	85	91777	91
2012-08	16966	1272	18238	11756	69	1588	125	13344	73
2012-09	20085	6151	26235	24634	123	9996	163	34630	132
2012-10	48022	18192	66214	192503	401	138620	762	331124	500
2012-11	37175	10075	47250	19009	51	7041	70	26050	55
2012-12	90317	95840	186158	86332	96	31526	33	117858	63
MEAN					94		201		96
STD					70		375		89

Although the calibrated rainfall runoff model simulates only 73% of the measured runoff for the rainfall time series of June 2012 the corresponding modeled runoff volume is still about 155% compared to the modeled runoff from the rainfall time series of August 2011 and hence can still be seen as increased runoff compared to the mean represented by the rainfall time series of August 2011. Especially the good agreement of modeled and measured hydrographs at the WWTP inlet (Figure 7-12) confirms the usability of the hydrologic reference models in ISNs with discharge control at retention tanks. This is additionally confirmed by a flow time test based on discrete discharges using pounded DWF done in the present catchment. Details on the test and results are given by Regneri *et al.* (2012). The modeled hydrograph indicates an overestimation of wetting losses for small events creating no runoff. The effect of such events on the WWTP performance is assumed to be negligible and hence insignificant for the evaluation of the present system-wide FPC approach.

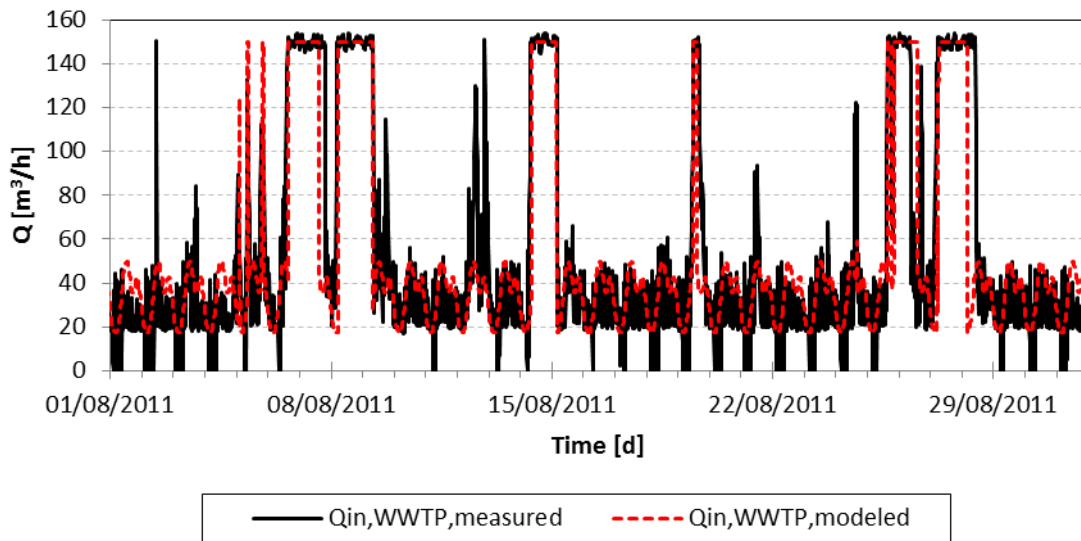


Figure 7-12: Rainfall runoff model calibration results for the WWTP inlet hydrograph according to the rainfall time series of August 2011

The Janus coefficient according to Equation 7-3 is used to evaluate the model adequacy by comparing fits for the calibration step and the validation step (Rieger *et al.* 2013). A Janus coefficient equal to one resembles equal predictive performance for model calibration and model validation. The Janus coefficient itself does not indicate a good predictive performance per se. A Janus coefficient J^2 of 28 in the present case confirms the change in model structure for model validation (Rieger *et al.* 2013) indicated by the calibration results shown in Table 7-10.

$$J^2 = \frac{\frac{1}{n} \sum_{i=1}^n (P_{validation,i} - O_i)^2}{\frac{1}{n} \sum_{i=1}^n (P_{calibration,i} - O_i)^2} \quad \text{Equation 7-3}$$

with: J ... Janus coefficient, n ... number of samples, P ... predicted values and O ... observed values

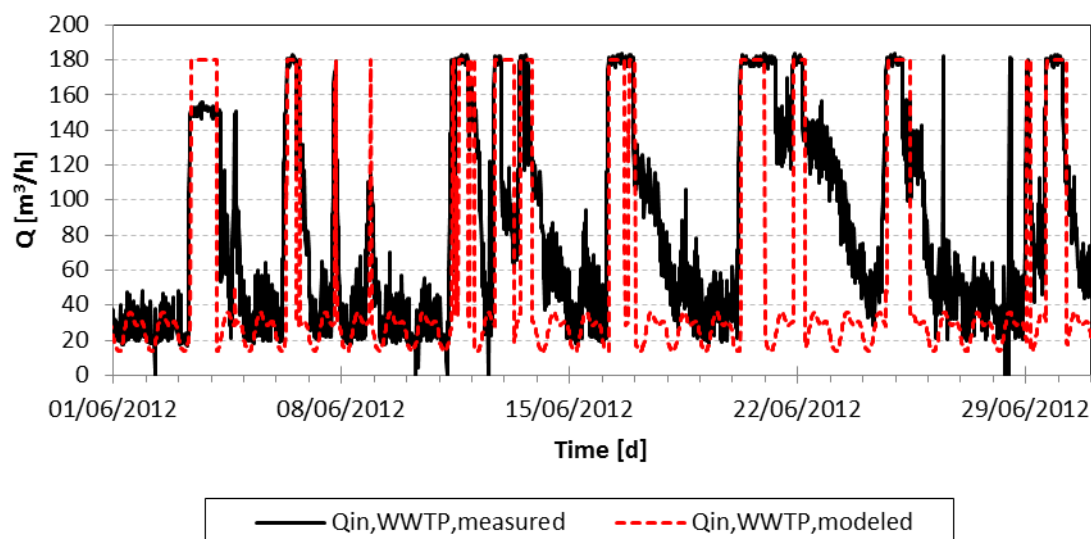


Figure 7-13: Rainfall runoff model calibration results for the WWTP inlet hydrograph according to the rainfall time series of June 2012

7.3.3. Phenomenological rainfall runoff distribution model

The system-wide analysis of RRCs according to section 6.3.2 reveals a differentiated runoff behavior from rainfall across the year but also for neighbored sub-catchments related to the same rainfall data. Assuming comparable rainfall runoff behavior, this reveals on the one hand uncertainties linked to the given catchment characteristics such as impervious and pervious surface sizes but also shows additional hydrological dynamics which cannot be captured by using 4 rain gauges in a total catchment of about 60 km². In order to take these uncertainties into account, results from the RRC evaluation of sub-catchments related to rain gauge DAH are transferred to the final model state according to section 6.3.5.

The standard deviation of monthly RRCs associated to rain gauge DAH is considered by adding a random multiplicative coefficient to the deterministic rainfall-runoff model according to Equation 7-4 in each sub-catchment of a rain gauge group.

$$Q_{rand,i,j} = Q_{0,i} \cdot (1 \pm X) \quad X \in \{0, \sigma_{RRC_{DAH}}\} \quad \text{Equation 7-4}$$

with: Q_{rand} ... randomly modified runoff from rainfall, Q_0 ... initial runoff from rainfall, X ... uniformly distributed pseudo random number, RRC_{DAH} ... rainfall-runoff coefficients associated to rain gauge DAH, σ ... standard deviation, i ... rain gauge and j ... sub-catchment

For the final catchment state the distribution of RRCs must be considered as random since they cannot be evaluated from the currently available measurement data. In the final model the standard deviation of RRCs can be expected to be even larger since sub-catchments RIN and TAD additionally are linked to the DAH rainfall data. RRC distributions for the other rain gauge groups are assumed to be equal although the number of sub-catchments per rain gauge group is different from rain gauge group DAH. The mean RRC at rain gauge group DAH in June 2012 was 0.8 with a standard deviation of 0.4. Table 7-11 shows the impact of the deterministic – phenomenological model on the performance of the nonlinear FPC

approach. Figure 7-14 shows the results of the corresponding correlation analysis. From the results of one month of simulation with increased rainfall it can be stated that the impact on the CSO volume is very small. The evaluation shows an average increase of CSO volume of six percent using the deterministic – phenomenological simulation model. This principally constant performance according to comparable rainfall time series with different spatial rainfall distributions shows the robustness of the present nonlinear hydraulic FPC approach. In literature rainfall heterogeneity is reported to be beneficial for sewer network control (Schütze *et al.* 2008).

In the present case, the additional loading variability of the retention tanks does not provide further potential for CSO minimization. Consequently, the present results must be Pareto optimal according to the chosen objective function based on FDM. Conversely of, the evaluation of the CSO loads according to Figure 7-14 shows a clear benefit using a deterministic – phenomenological simulation model. While the correlation analysis shows a reduction of TSS, COD and BOD₅ CSO loads in average by 18 percent when considering the additional RRC dynamics, on the contrary, these additional dynamics show no impact on the NH₄-N CSO load. This can be explained by the process of CSO reduction in sewer network MPC. Thereby, the use of a retention tank volume according to the differentiated loading of all retention tanks is maximized with the objective to fill all retention tanks completely before CSO occurs. Consequently, unavoidable CSO, due to capacity exceeded once, occurs with delay compared to the uncontrolled situation. Thereby, the effect of CSO load minimization increases with increasing first flush characteristics of the specific pollutant.

Table 7-11: Comparison of CSO volumes and loads from system-wide FPC according to static and phenomenological rainfall runoff distribution June 2012

Event	V [m ³]		L _{TSS} [kg]		L _{COD} [kg]		L _{BOD5} [kg]		L _{NH4-N} [kg]	
	RR _{const}	RR _{phen}	RR _{const}	RR _{phen}	RR _{const}	RR _{phen}	RR _{const}	RR _{phen}	RR _{const}	RR _{phen}
1	4438	4800	283	209	276	204	102	75	5.97	5.96
2	0	4	0.00	0.08	0.00	0.08	0.00	0.03	0.00	0.00
3	91	119	5	3	5	3	2	1	0.14	0.07
4	3784	3929	17	19	16	19	6	7	0.65	0.74
5	1517	1546	25	66	25	65	9	24	0.88	2.25
6	158	185	17	36	16	35	6	13	0.59	0.64
7	17052	18162	1338	994	1308	971	482	358	9.94	9.18
8	125	71	5	3	4	3	2	1	0.08	0.05
9	1441	1447	465	659	455	644	168	238	0.46	0.26
10	0	0	0	0	0	0	0	0	0	0
11	2224	2166	317	308	310	301	114	111	4.22	4.21
Total	30829	32428	2472	2298	2415	2245	891	828	22.93	23.35

Due to the smaller first flush characteristics in the case of NH₄-N, the dynamics in the pollutograph are smaller and hence the time of CSO and consequently the effect on CSO loads is less important. Overall, the additional RRC variability according to the presented deterministic – phenomenological reference simulation model has a significant impact on the performance evaluation of the presented FPC approach and should therefore be taken into account.

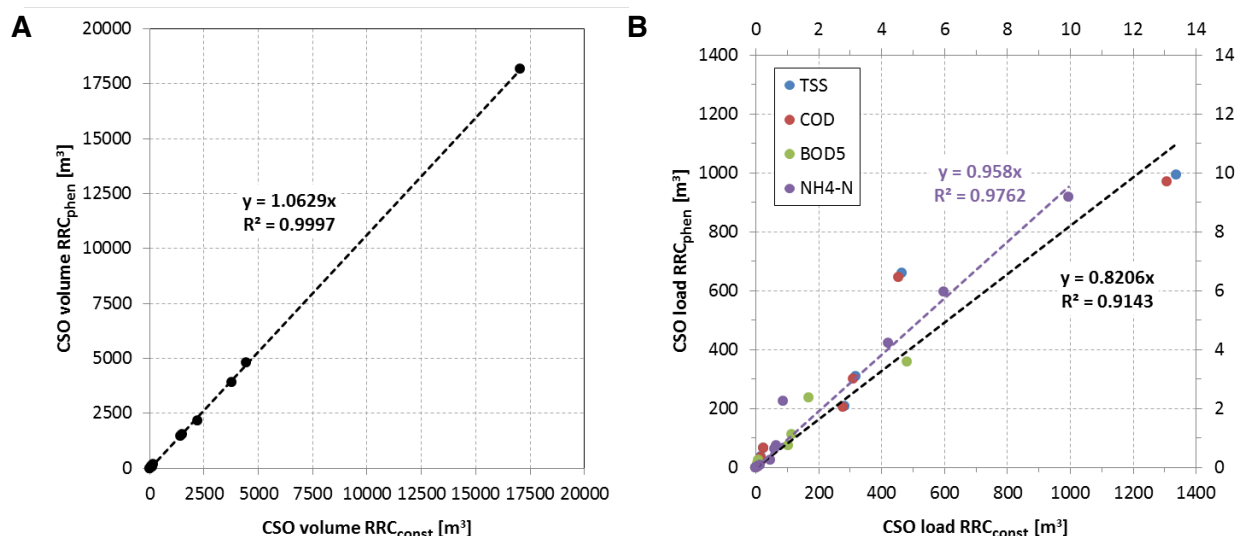


Figure 7-14: Correlation analysis of CSO volumes (A) and loads (B) from system-wide FPC according to constant (RRC_{const}) and phenomenological (RRC_{phen}) rainfall runoff distributions in June 2012

7.3.4. Exemplary analysis of event #1 of the rainfall time series of June 2012

In the following, the first CWWF event of the rainfall time series of June 2012 is used to illustrate the results of the presented FPC approach for system-wide control of integrated WCTs. Subsequently, results are summarized according to this methodology for the rainfall time series of August 2011 and June 2012. Due to the computational effort of controlling the overall system, simulation of small events according to the chosen rainfall time series should be avoided. Consequently, the present FPC approach for system-wide control of integrated WCTs is triggered according to a mean normalized water level in the retention tanks of 0.1 providing a balance of good control performance to reduce CSO and small rain events irrelevant for system-wide control. During DWF the oxidation ditch is aerated according to recommendations of the German guideline DWA-A 226 for WWTPs with SASS (DWA 2009). Due to a mean temperature of 14 °C in June according to Figure 6-60 an aeration cycle ratio of 65% is chosen (see Figure 7-2 and Figure 7-3). A cycle length of two hours for intermittent aeration and a set-point of 1.5 g/m³ for DO PID control are found to be best for DWF operation. Further, a constant SRT of 25 days is chosen according to these recommendations. Constant SRT control is achieved via PID control. During CWWF operation, continuous aeration with simultaneous denitrification is selected.

7.3.4.1. Evaluation of the FDM

Figure 7-10 shows the applied rainfall time series. Figure 7-15 shows the results of FDM for continuous integrated WWTP capacity estimation. For the explanation of specific MFs see Table 7-5 and Table 7-7. While for specific MFs the satisfaction increases with increasing values, the total performance (MF_{tot}) worsens with increasing values. The total satisfaction according to the selected control objectives varies along CWWF event #1. In the beginning the total CWWF performance is predominantly determined by extended aeration (MF7) according to NH₄-N concentrations in the AST differing from the objective for SASS (MF5). With decreasing NH₄-N concentrations in the AST total performance increases due to reduced aeration effort. Towards the end of the event the total CWWF performance

decreases predominantly due to the decreasing loading of the WWTP (MF6) accompanied by decreasing TSS effluent concentrations (MF1) which must be maximized during CWWF in order to simultaneously maximize hydraulic loading. Additionally, the aeration effort increases and COD effluent concentrations (MF2) decrease. The total nitrogen treatment performance (MF4) is very good and almost constant during the whole event.

The evaluation of mean MF values and corresponding standard deviations illustrates the conflict of increasing TSS effluent concentrations and decreasing COD effluent concentrations. The chosen objective for aeration according to SASS corresponds to the aspired $\text{NH}_4\text{-N}$ concentrations in the AST. Consequently, there is a conflict with increased $\text{NH}_4\text{-N}$ concentrations in the SST effluent. MF₃ provides additional treatment performance which is not necessary during this event thanks to sufficient aeration. In order to decrease treatment costs objectives for SASS could be adapted to reduce conflicts. The mean hydraulic loading is about 40 percent of the capacity of the ISN.

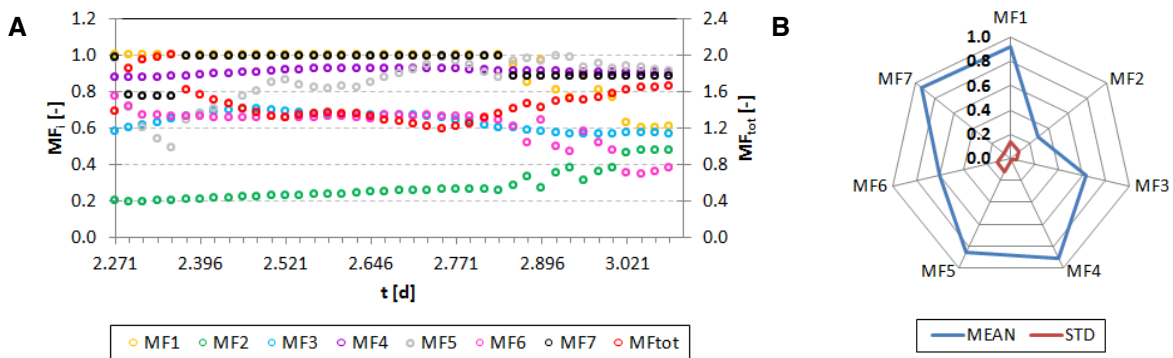


Figure 7-15: FDM results for the integrated WWTP capacity estimation and FPC during event #1 June 2012 (A) and statistical evaluation (B)

Figure 7-16 illustrates the results of FDM in the sewer network for system-wide FPC. For the explanations of specific MFs, see Table 7-2 and Table 7-6.

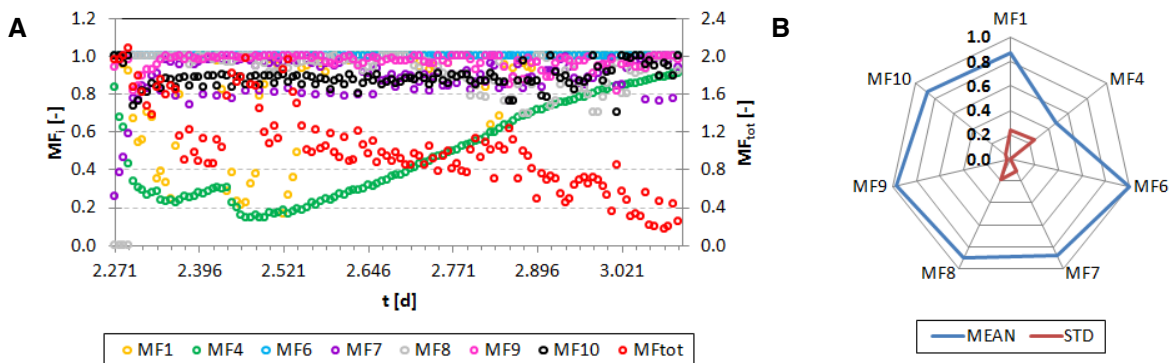


Figure 7-16: FDM results in the sewer network of CWWF event #1 of the rainfall time series of June 2012 (A) and statistical evaluation (B)

The total performance (MFtot) almost continuously increases along the event and is predominantly determined by CSO (MF1), the homogeneous loading of the WWTP (MF7,

MF8, MF9 and MF10) which varies in a range of about 20 percent along the event and the emptying of all retention tanks (MF4). Conflicts between CSO minimization and homogeneous WWTP loading can be seen in the beginning of the CWWF event. Toward the end of the CWWF the satisfaction of homogeneous WWTP loading fluctuates corresponding to the decreasing WWTP loading investigated in Figure 7-15. For this CWWF event emergency CSO at the WWTP (MF1) could be avoided. The evaluation of event mean MF values and standard deviations corresponds to the described investigations.

Figure 7-17 visualizes the corresponding continuous prediction of hydrographs and corresponding COD and TKN pollutographs according to discrete retention tank discharge observations in the ISN during CWWF event #1.

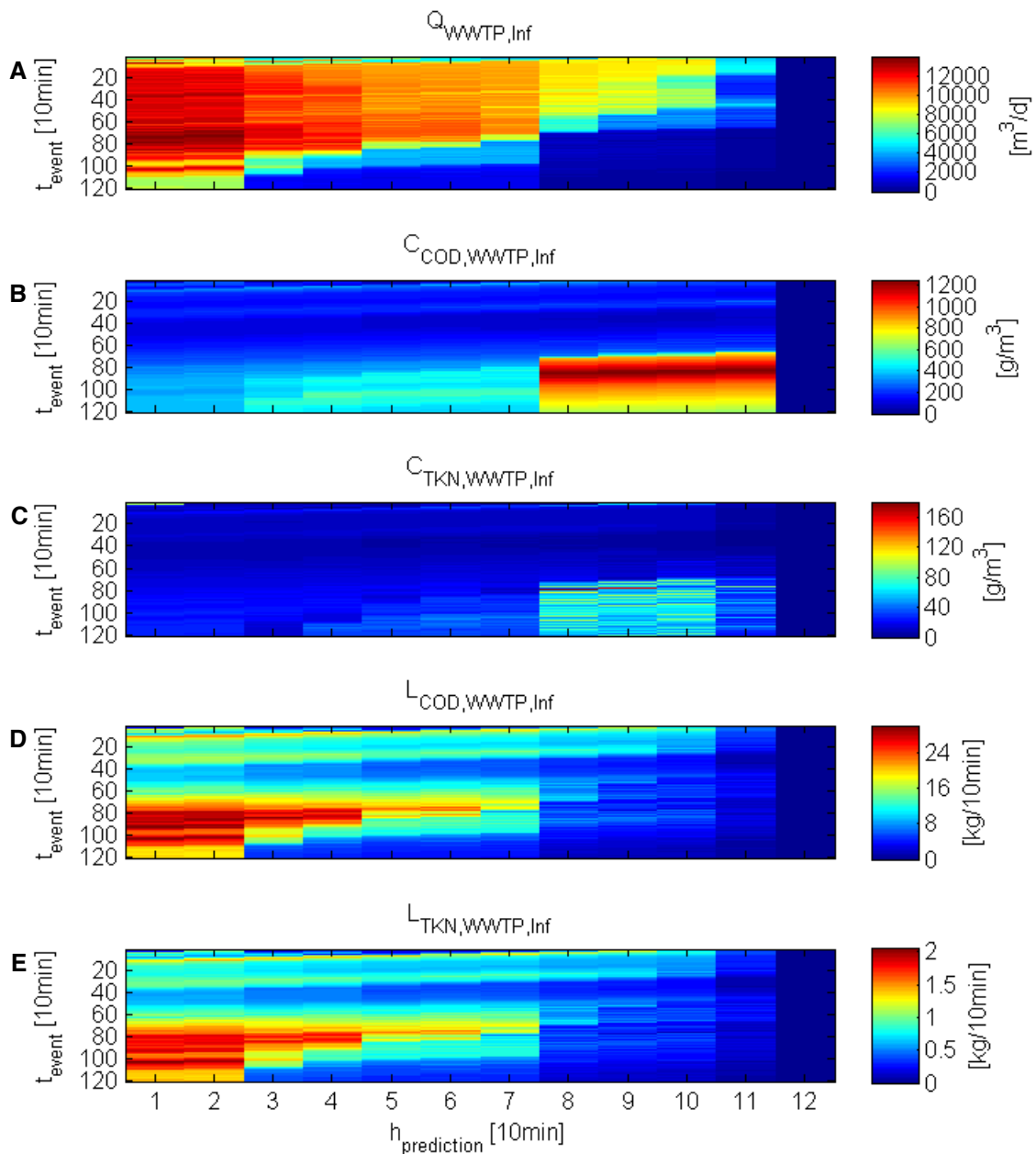


Figure 7-17: Lagrangian ISN observer model based hydrographs (A) and pollutographs (B through E) for CWWF event #1 of rainfall time series June 2012.

The axis describe a two-dimensional time frame where vertical axes illustrate from top to bottom the event time and horizontal axes illustrate from left to right the corresponding prediction horizon each in discrete steps of 10 minutes according to the chosen control step size for sewer network FPC. Numerical values are illustrated according to a color scale.

Figure 7-17 illustrates the continuous build-up of the hydrograph with decreasing residual flow times in the ISN according to the dynamic capacity of the WWTP. The resulting hydrograph resembles the results of the integrated FDM for maximized WWTP loading and CSO minimization according to a homogeneous flow in the ISN. Thereby, the hydraulic capacity is constant during most of the event and then constantly decreases towards the end of the event according to the emptying of retention tanks. The corresponding pollutographs for COD and TKN show a homogenous distribution of concentrations. Due to a control step size of 10 minutes the sewer network FPC causes a constant mixing of retention tank discharges with various concentrations. This decreases the characteristics of the first flush at the WWTP inlet. Towards the end of the event the impact of DWF increases but concentrations are reduced along the flow through the ISN due to mixing with other retention tank discharges. The beginning impact of DWF concentrations after the emptying of retention tanks is particularly noticeable due to the discrete character of the observer model and the hydrologic character of the reference simulation model. For the simulation-based WWTP capacity estimation the approach observes COD and TKN pollutographs discharged to the WWTP. The model itself can be applied to any pollutant.

7.3.4.2. Performance evaluation of the process model for FPC

In the following, the mean absolute percentage difference (MAPD) (Equation 7-5) is used to evaluate the prediction performance of the Lagrangian ISN observer model by comparing predicted hydro- and pollutographs with corresponding results from the integrated reference simulation model. A major feature of the MAPD is to highlight the existence of systematic under- or over-predictive models.

$$MAPD = \frac{1}{n} \sum_{i=1}^n \frac{|P_i - O_i|}{O_i} \quad \text{Equation 7-5}$$

with: *MAPD* ... mean absolute percentage difference, *P_i* ... predicted values and *O_i* ... observed values from the integrated reference simulation model

Figure 7-18 compares predicted treatable hydro- and pollutographs for COD and TKN at the WWTP inlet representing the current WWTP capacity with corresponding discharges from sewer network FPC according to reference simulation model results. Noticeable is the strong deviation between the predicted hydraulic WWTP capacity and loading during most of the CWWF event followed by a good coherence towards the end of the event. The coherence of COD and TKN concentrations according to the WWTP capacity prediction and corresponding reference simulation results is comparably better. This corresponds to the before mentioned homogenization of pollutant concentrations according to the mixing of wastewater discharges from various retention tanks. Table 7-12 summarizes the resulting MAPD between WWTP capacity estimation and WWTP loading for event #1 of the rainfall time series of June 2011 ranging between 63 percent for the hydraulic WWTP loading and

31 percent for corresponding COD and TKN concentrations. These deviations represent the impact of sewer network objectives in the hybrid FPC approach for integrated system-wide control.

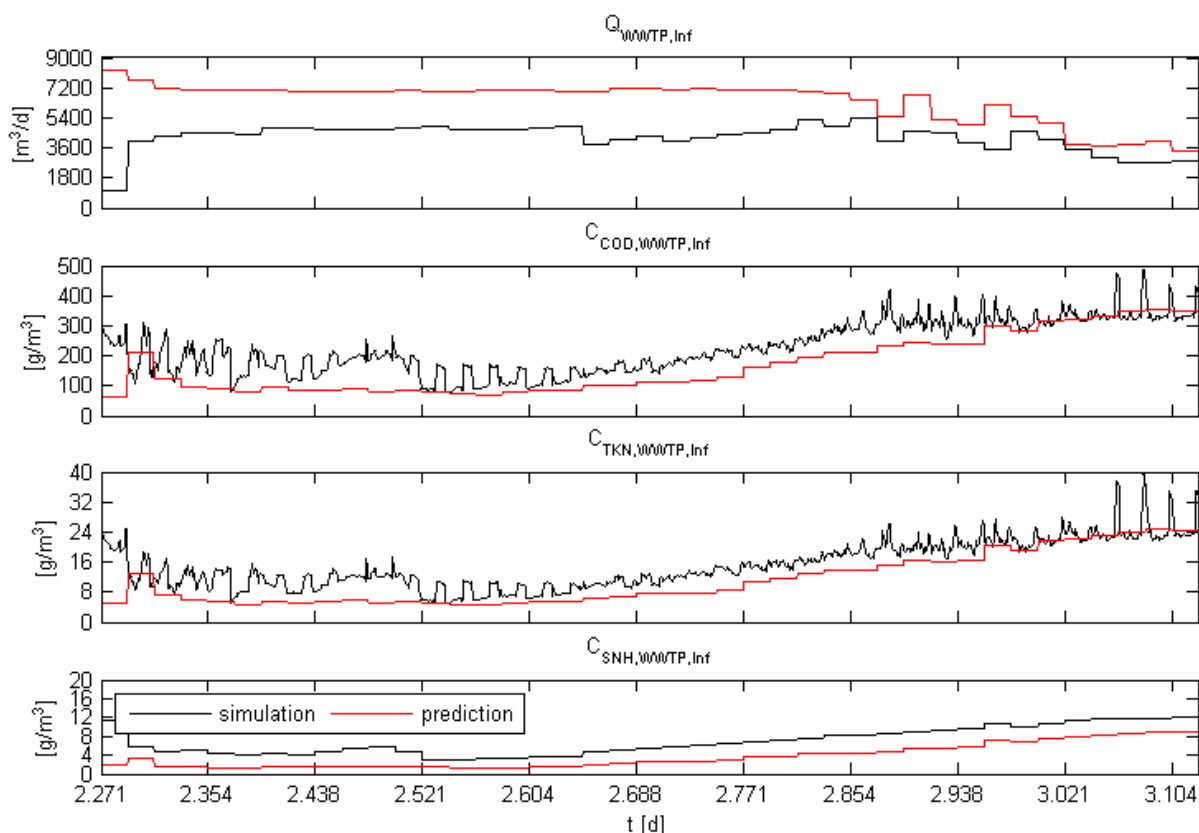


Figure 7-18: Comparison of WWTP influent prediction according to the WWTP capacity and WWTP loading according to sewer network FPC from reference model simulation for event #1 of the rainfall time series of June 2012.

Table 7-12: MAPDs of hydro- and pollutographs for WWTP loading based on the Lagrangian ISN observer model for event #1 of the rainfall time series of June 2012

	WWTP _{in}		
	Q	C _{COD}	C _{TKN}
	[%]	[%]	[%]
MAPD	63	31	31

Figure 7-19 illustrates the comparison of WWTP capacity prediction and simulation results according to the loading from the sewer network fuzzy predictive controller for selected states in the AST during CWWF event #1. When both treatment lanes of the WWTP are in operation, equal loading, operation and treatment is assumed for both lanes. Hence, only results of one treatment lane are illustrated. To be highlighted are the small deviations between prediction and simulation. Discrete steps in the graphs, which illustrate the predicted WWTP behavior, show the adjustment of the process model for FPC to the reference simulation model during each WWTP performance prediction and control step.

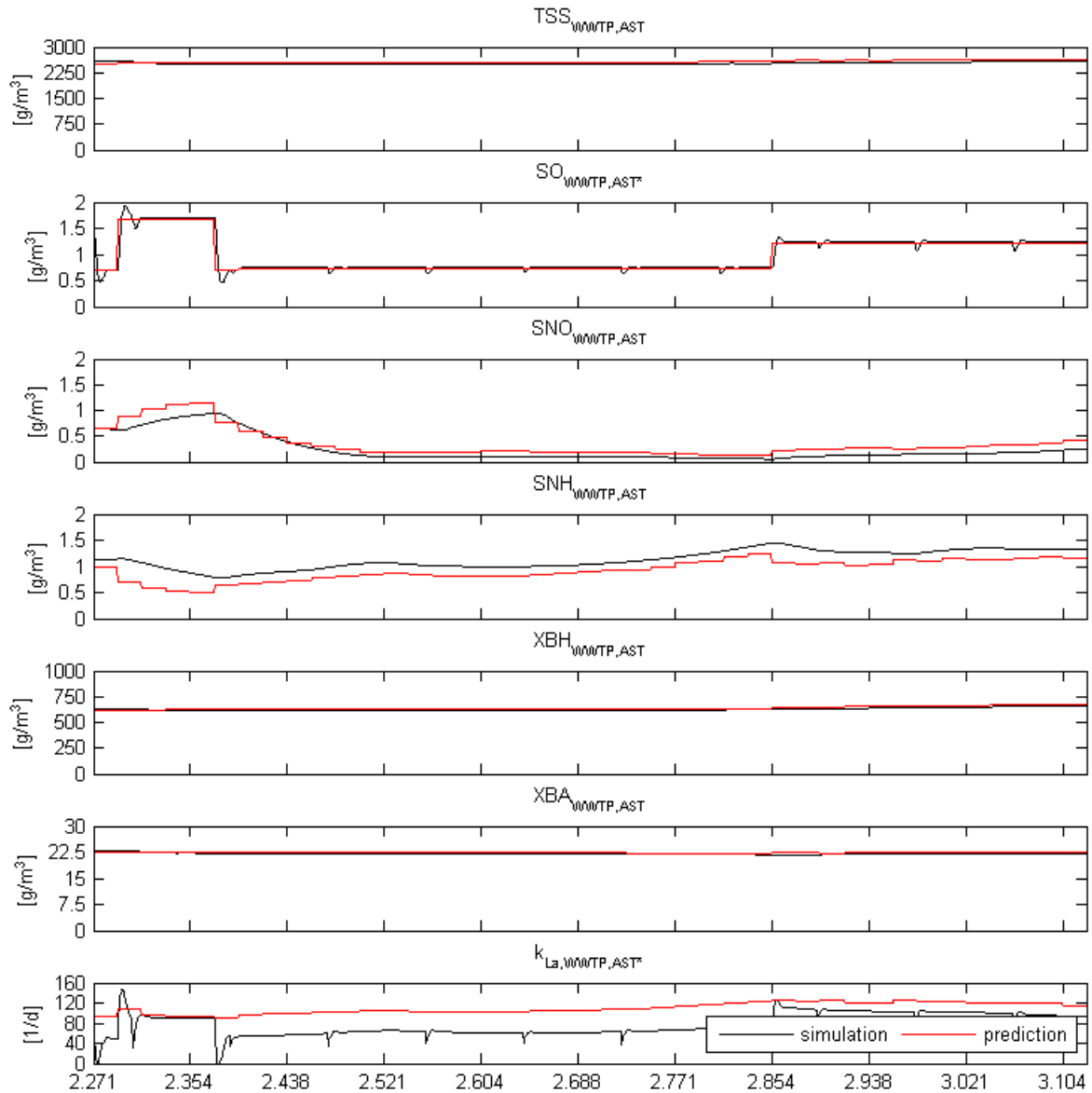


Figure 7-19: Comparison of specific predicted WWTP AST parameters and corresponding reference simulation model parameters for event #1 of the rainfall time series of June 2012

Table 7-13: MAPDs of the WWTP capacity estimation and loading according to the reference simulation model for selected AST parameters during CWWF event #1 of the rainfall time series of June 2012

	WWTP _{AST}						
	TS	SO	SNO	SNH	XBH	XBA	k _{La}
	[%]	[%]	[%]	[%]	[%]	[%]	[%]
MAPD	2	4	74	19	2	2	93

Table 7-13 presents the MAPDs between the WWTP capacity estimation and the corresponding WWTP loading for specific wastewater parameters in the AST during event #1 of the rainfall time series of June 2012. Due to the good agreement of both the heterotrophic (two percent) and autotrophic biomass (two percent) between the WWTP capacity estimation and the corresponding WWTP loading and the feedback control of DO,

nitrogen loading differences directly lead to deviations of ammonium and nitrate concentrations in the AST. Consequently, the predicted aeration effort according to k_{La} differs in average about 93 percent. Due to the increased aeration nitrogen loading differences lead to comparably higher deviations for nitrate (74 percent) and smaller deviations for ammonium (19 percent).

Figure 7-20 illustrates the comparisons of predicted SST effluent concentrations for WWTP capacity estimation and reference model simulation results according to sewer network FPC for CWWF event #1 of the rainfall time series of June 2012. Except for the flow, predictions for capacity estimation and reference model simulations show a good agreement. Table 7-14 shows the corresponding MAPDs illustrating the WWTP performance for selected effluent parameters according to integrated loading during CWWF event #1. Due to continuous operation of the WWTP the MAPD of the SST outflow is similar to the MAPD of the WWTP inflow. Despite the increased loading effluent concentrations show only small dynamics. This can be explained by:

- the increased specific treatment volume according to the design of low loaded WWTPs,
- the implemented PID control for an increased sludge age of 25 days and
- the homogenized pollutant loading according to sewer network FPC.

All effluent concentrations are always below their legal limit. Thanks to the predictive aeration control nitrification according to SASS within the AST is optimized during this event showing a mean reserve capacity of only four percent. Reserve capacities concerning TSS, COD and TN are 42, 41 respectively 25 percent. Consequently, it can be stated that sewer network control has a significant impact on WWTP capacity utilization.

Table 7-14: MAPDs of the WWTP capacity estimation and loading according to the reference simulation model for selected SST effluent parameters during CWWF event #1 of the rainfall time series of June 2012

	WWTP _{Eff}				
	Q	TSS	COD	SNH	TN
	[%]	[%]	[%]	[%]	[%]
MAPD	63	42	41	4	25

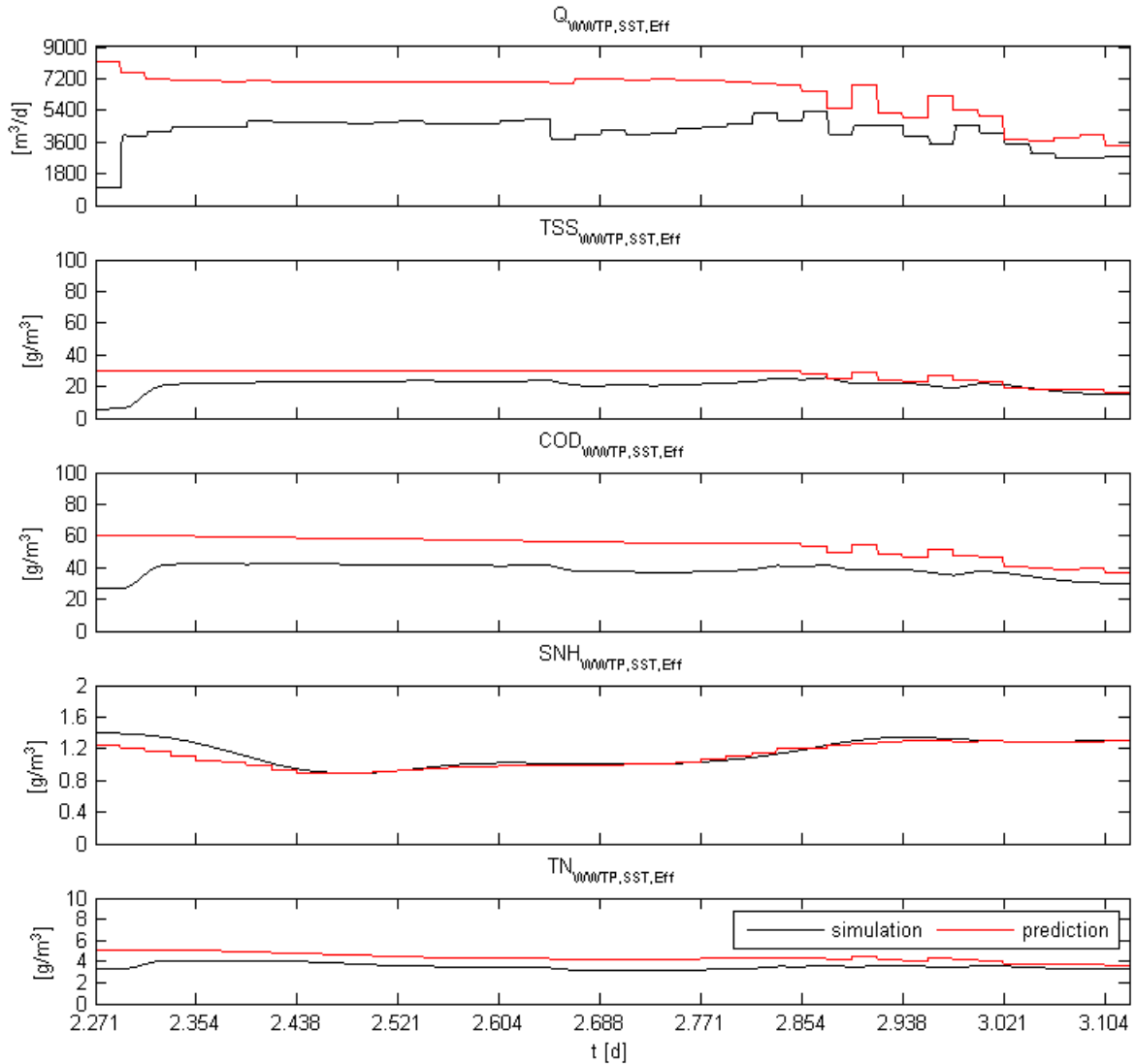


Figure 7-20: Comparison of SST effluent predictions for WWTP capacity estimation and reference model simulation results for CWWF event #1 of the rainfall time series of June 2012

Figure 7-21 illustrates the reactions in the SST on the hydraulic shock load according the 1-dimensional model of Takács et al. (1991). In this model the SST is vertically divided into 10 equally distributed layers. The 10 subplots describe the TS concentrations in each of the 10 horizontal layers which are equally distributed along the height of the SST. Layer 1 is the top layer, layer 10 is the bottom layer. Hydraulic shock loading at the beginning of the event is continuously reduced to meet the legal effluent concentration limits. Figure 7-21 illustrates the TS concentration in each layer. Mean predicted TS concentrations and TS concentrations according to reference model simulation are comparable to each other. The impact of the increased hydraulic loading is small thanks to the small hydraulic increments. In the present case the hydraulic performance of the SST is additionally increased thanks to:

- rather small TS concentrations due to the low loaded treatment approach and
- the oversized SST for increased safety during CWWF according to a reduced sludge volume surface loading of 297 l/(m² h) instead of 500 l/(m² h).

Consequently, the compressed sludge layer only occurs in the bottom layer 10.

Simulation-based evaluation of the integrated fuzzy predictive control approach

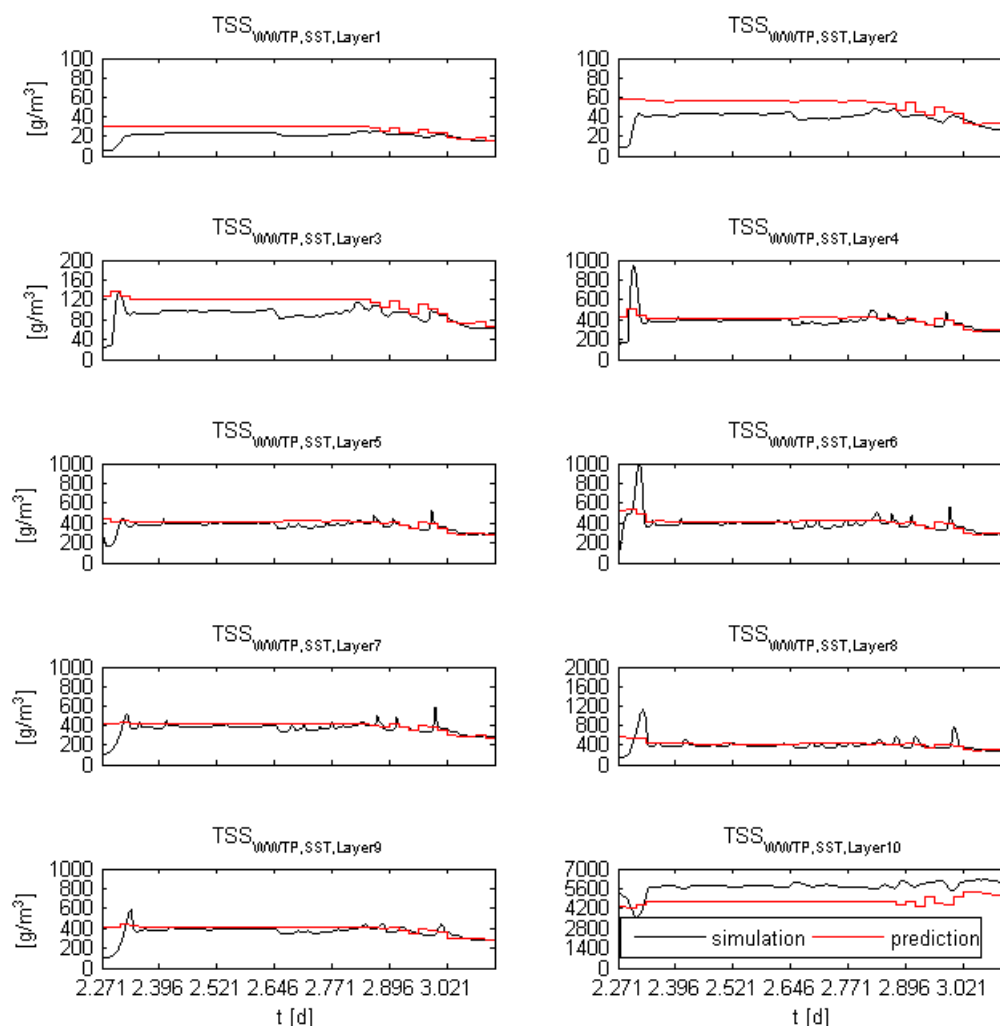


Figure 7-21: Comparison of the predicted hydraulic impact of CWWF event #1 of the rainfall time series of June 2012 on TSS concentrations in the SST and reference simulation model results from integrated FPC according the 1-dimensional model of Takács et al. (1991) (Layer 1 = top layer, layer 10 = bottom layer).

For the whole event the correlation of MFs for hydraulic loading of the WWTP and SST TSS effluent concentrations shows a linear relation (see Figure 7-22).

Due to the significantly different loadings for WWTP capacity prediction and reference model simulation during CWWF event #1 feedback control of return and waste activated sludge flows and concentrations show significant differences (see Figure 7-23).

Figure 7-24 illustrates the results of the multi-criteria predictive control of nitrification according to the objectives of SASS. The figure indicates the control of hydraulic loading according to the current NH₄-N concentration in the AST, the corresponding nitrogen influent load and the DO set-point optimization.

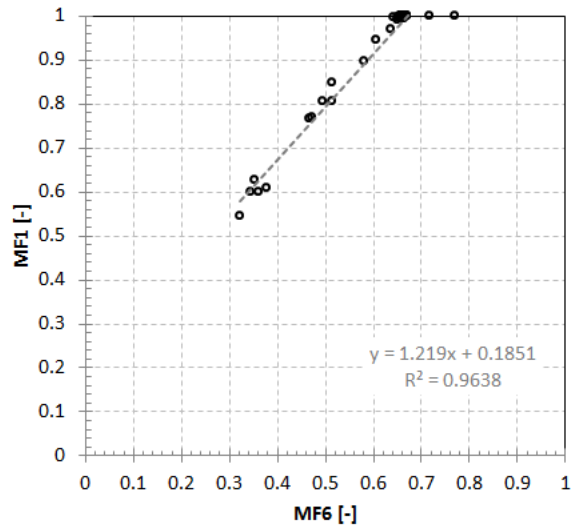


Figure 7-22: Linear correlation between MFs for hydraulic loading of the WWTP (MF6) and the SST effluent TSS concentration (MF1) for CWWF event #1 of the rainfall time series of June 2012.

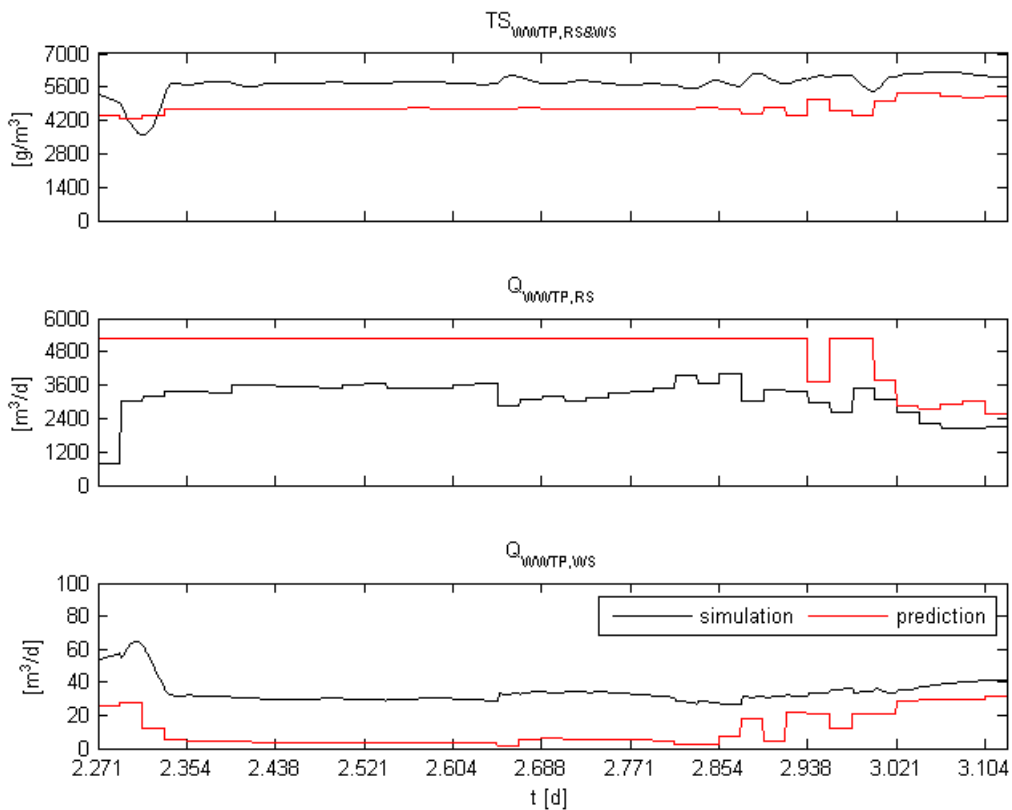


Figure 7-23: Comparison of predicted and simulated SST effluent concentrations for CWWF event #1 of the rainfall time series of June 2012

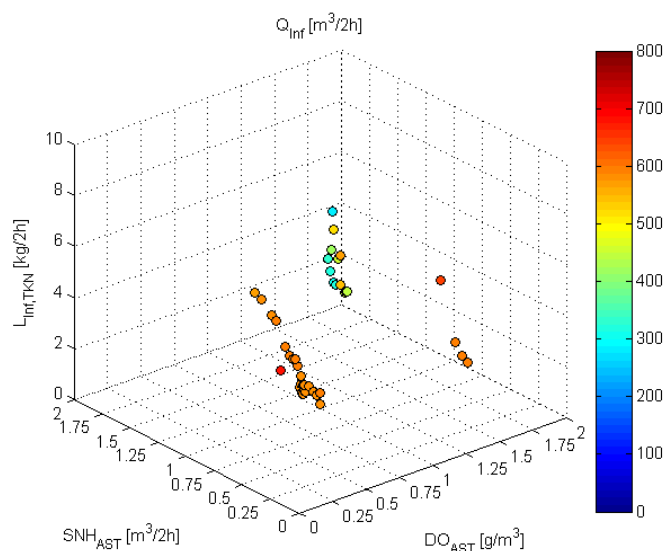


Figure 7-24: WWTP multi-objective predictive hydraulic loading according to TKN influent load and SNH_{AST} concentrations and corresponding DO_{AST} set-point optimization for CWWF event #1 of the rainfall time series of June 2012

7.3.4.3. Discriminant analysis

In contradiction to conventional MPC, FPC uses objective functions based on FDM to describe the compromises of conflicting objectives. Due to the absence of weighting coefficients for specific objectives in the present case, MF values resulting from FPC can be used to analyze the behavior of the presented approach for each CWWF event. The global satisfaction of objectives is evaluated according to the mean values of MF values and their standard deviations. Figure 7-15 illustrates the results for event #1 of the rainfall time series of June 2012.

In order to compare event-specific dynamics of FDM in system-wide FPC of integrated rural WCTs the correlation of each two MF values was decomposed according to principal least squares (PLS) discriminant analysis (DA). Similar to principal component analysis correlated data sets are decomposed through clustering and geometrically interpreted as density constant contours – ellipsoids (Tomita *et al.* 2002). This group structuring approach makes PLS appropriate for statistical classification and discrimination comparable to canonical correlation analysis (Barker and Rayens 2003). Elliptical scatterers F (Equation 7-6) for two correlated MFs are characterized by their center of gravity (Equation 7-9 and Equation 7-10), correlation coefficient (Equation 7-11) considering one standard deviation (Equation 7-7 and Equation 7-8) in the present case and axis transformation angle β between the x-axis of the scattering ellipse and the main coordinate system derived from the eigenvector (Phatak and De Jong 1997).

$$F = s_x \cdot s_y \cdot \sqrt{1 - r^2}$$

Equation 7-6

$$s_x = \sqrt{\frac{\sum_{i=1}^N (x_i - \bar{x})^2}{N - 1}} \quad \text{Equation 7-7}$$

$$s_y = \sqrt{\frac{\sum_{i=1}^N (y_i - \bar{y})^2}{N - 1}} \quad \text{Equation 7-8}$$

$$\bar{x} = \frac{\sum_{i=1}^N x_i}{N} \quad \text{Equation 7-9}$$

$$\bar{y} = \frac{\sum_{i=1}^N y_i}{N} \quad \text{Equation 7-10}$$

$$r = \frac{\sum_{i=1}^N (x_i - \bar{x}) \cdot (y_i - \bar{y})}{(N - 1) \cdot s_x \cdot s_y} \quad \text{Equation 7-11}$$

with: N ... the number of samples

The approach can be transferred to the n-dimensional space according to the concept of the Mahalanobis distance (Tomita *et al.* 2002). Comprehensive details on the use of PLS as a tool for statistical discrimination are given e.g. by Barker and Rayens (2003).

Figure 7-25 illustrates the corresponding clustering of MF results for DO_{AST} set-point optimization (MF7), effluent NH₄-N minimization (MF3), effluent TN minimization (MF4) and NH₄-N optimization for SASS (MF5) according to PLS-DA.

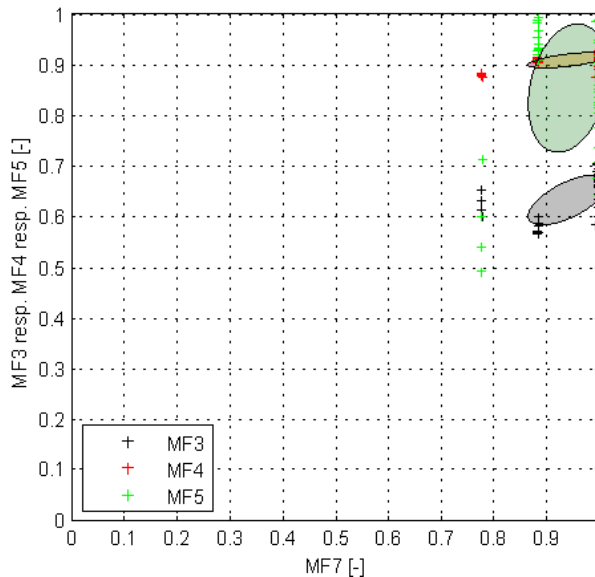


Figure 7-25: PLS-DA of MF results for DO_{AST} set-point optimization (MF7) and effluent NH₄-N minimization (MF3), effluent TN minimization (MF4) and AST NH₄-N optimization (MF5) for CWWF event #1 of the rainfall time series of June 2012

Simulation-based evaluation of the integrated fuzzy predictive control approach

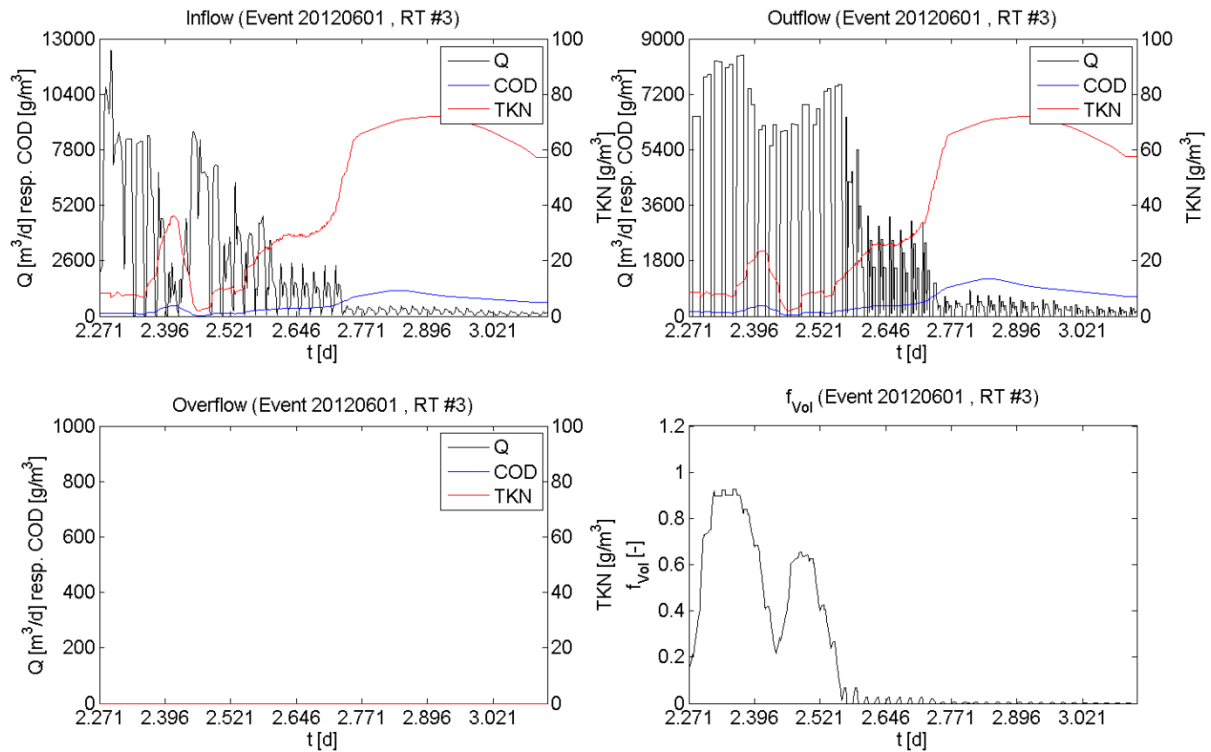


Figure 7-26: FPC of retention tank #3 to minimize CSO during CWWF event #1 of the rainfall time series of June 2012

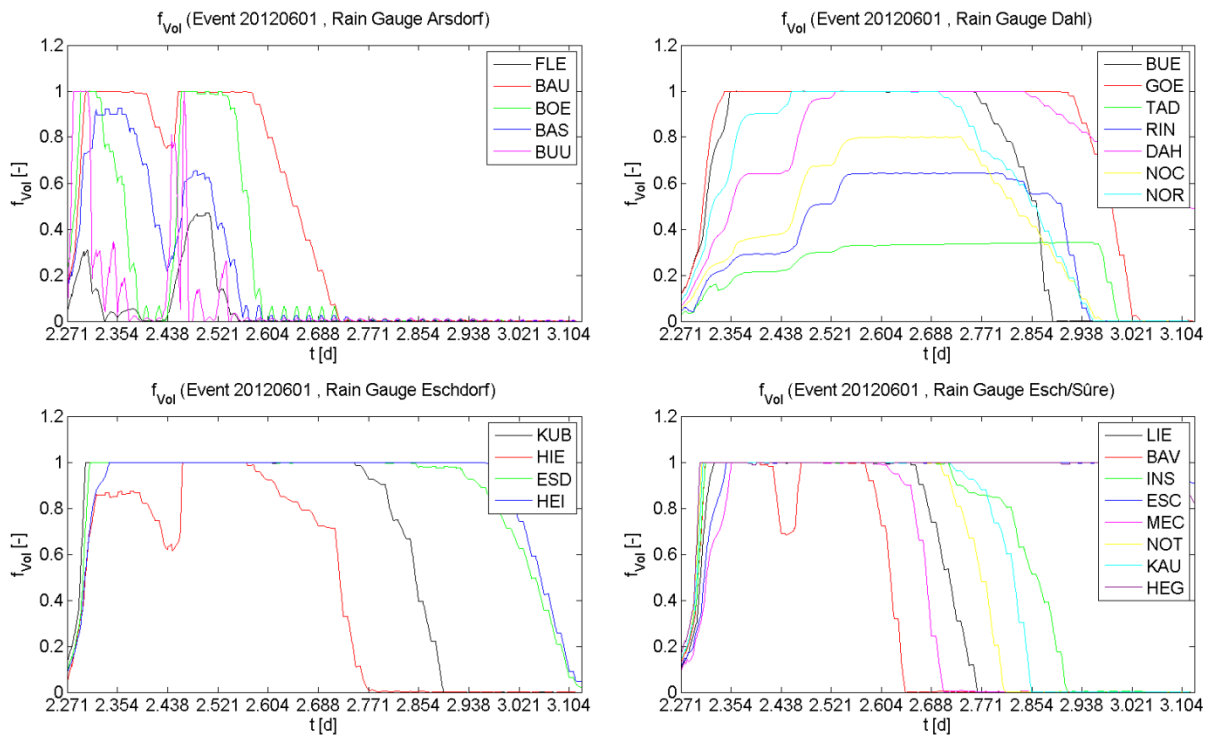


Figure 7-27: Comparison of the specific retention tank utilization of all retention tanks for different rainfall inputs according to the sewer network FPC approach for CWWF event #1 of the rainfall time series of June 2012

While the center of gravity of each ellipsoid shows the mean MF satisfaction of the corresponding conflict, the radius of each ellipsoid shows the event-specific variability of the

specific MF satisfaction. According to the size of the ellipsoids, MF7 shows the largest dynamics in the process of the DO set-point optimization followed by MF3 and MF4. Due to the buffering effect of the SST volume effluent $\text{NH}_4\text{-N}$ concentrations are less sensitive. Due to the balance between $\text{NH}_4\text{-N}$ and $\text{NO}_x\text{-N}$ concentration TN effluent concentrations are even less sensitive in the FDM process for WWTP capacity estimation.

Due to the number of retention tanks Figure 7-26 exemplary illustrates only the results of FPC for retention tank #3 with the conflicting objectives to minimize CSO and simultaneously contribute to the homogeneous loading of the WWTP. Assuming constant inflows during prediction steps of ten minutes the retention discharge is optimized to minimize CSO.

Figure 7-27 illustrates the comparison of the utilization of all retention tanks during the CWWF event. Despite the phenomenological extension of the reference model the FPC is not able to homogenize the retention tank utilization completely so as to avoid CSO. This is mainly caused by the nonlinear controller that optimizes the flow in the ISN according to the WWTP reference loading.

Figure 7-28 illustrates the regression between MF results for hydraulic CSO minimization and corresponding COD resp. TKN CSO load minimization. In contradiction to Figure 7-25 the regression shows an excellent correlation that indicates that for CWWF event #1 the present hydraulic based FPC approach simultaneously satisfies decision-making objectives for CSO minimization regarding COD and TKN loads in the case of online bypass retention tanks. For this kind of retention tanks CSO pollutant concentrations are equal to the retention tank influent pollutant concentrations from the upstream sewer network. The corresponding MFs compare for each control step the system-wide CWWF retention tank influent volume and pollution load to the corresponding CSO volume and pollution load.

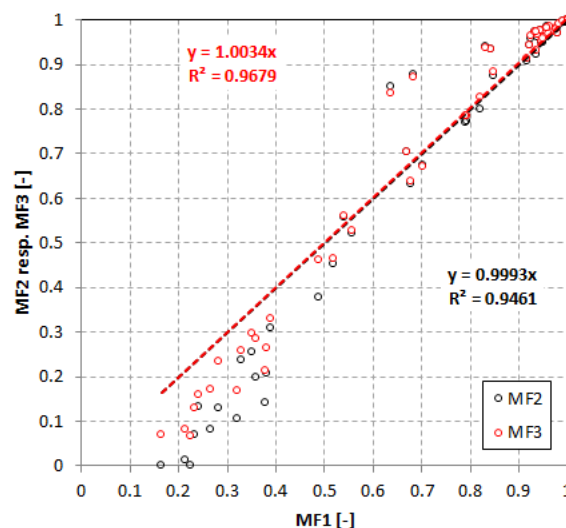


Figure 7-28: Correlation of MF results for total CSO volumes (MF1) and total COD CSO loads (MF2) and TKN CSO loads (MF3) for CWWF event #1 of the rainfall time series of June 2012

Due to the functional principle of sewer network MPC, unavoidable CSO is constantly delayed as much as possible by maximizing the total use of retention tank volume. Thereby,

pollutant concentrations in the inflow decrease thanks to the decreasing impact of wash-off (see section 6.2.2.2). Consequently, the objective of minimizing CSO pollutant loads is satisfied simultaneously.

Figure 7-29 illustrates the analysis of conflicting MF results between the homogenization of hydraulic states in the ISN (according to the minimum of MF8 and MF9) and the homogeneous use of the retention tank volume (MF5) resp. the homogeneous WWTP loading (MF10) according to PLS-DA for CWWF event #1.

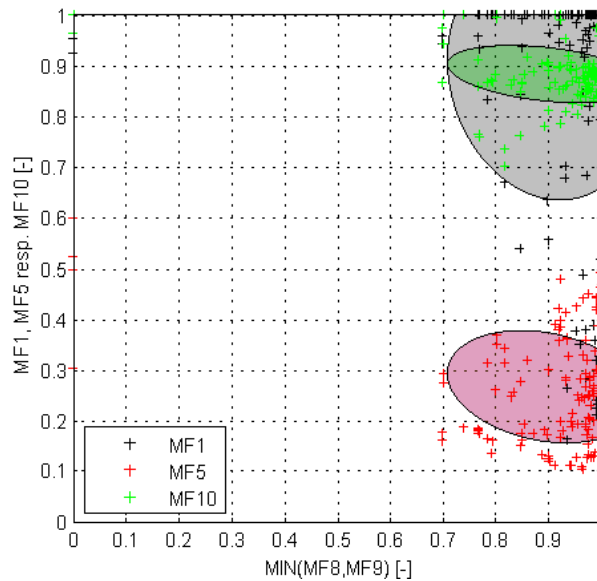


Figure 7-29: PLS-DA of MF results for ISN hydraulic homogenization (MF8 and MF9) and CSO volume minimization (MF1), retention tank use homogenization (MF5) resp. WWTP hydraulic loading homogenization (MF10) for CWWF event #1 of the rainfall time series of June 2012

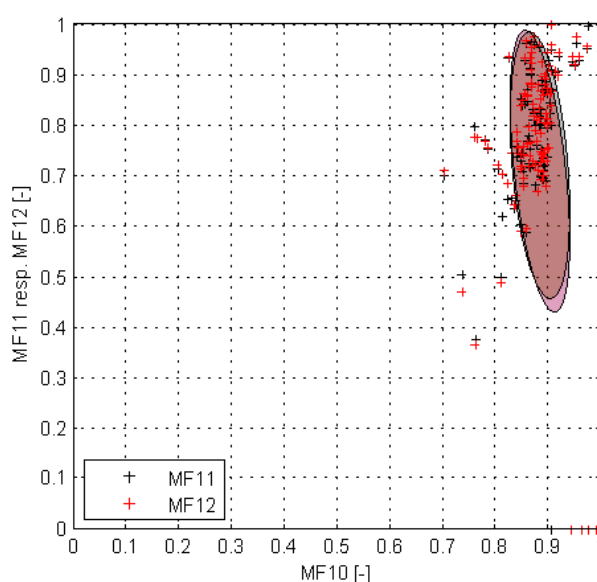


Figure 7-30: PLS-DA of MF results for WWTP hydraulic loading (MF10) and WWTP COD loading (MF11) resp. WWTP TKN loading (MF12) for CWWF event #1 of rainfall time series June 2012

The correlating good satisfaction of MF8, MF9 and MF10 clearly shows the need of the controller to homogeneously load the WWTP. The large ellipse for the correlation of the minimum of MF8 and MF9 and MF1 shows no conflicts when there is no risk of CSO but strong conflicts when avoiding CSO. The generally bad satisfaction of MF5 illustrates the strong conflict concerning the simultaneous homogenization of the total retention tank volume use. Overall, the event-specific results show, that there is a strong conflict between the homogeneous WWTP loading and CSO minimization if there is no retention tank at the WWTP to buffer the hydraulic loading during CWWF.

Figure 7-30 illustrates the analysis of conflicting MF results between the homogenized hydraulic loading of the WWTP (MF10) and corresponding pollutant loads for COD (MF11) and TKN (MF12) according to PLS-DA for CWWF event #1 of rainfall time series June 2012. According to the center of gravity of each ellipse the objective to maximize the pollutant load to the WWTP is satisfied for about 75 percent when maximizing the hydraulic load to the WWTP. Consequently, a control approach concerning the maximization of pollutant loads during CWWF towards the WWTP would disturb the hydraulic homogeneity accordingly.

7.3.5. Summary of results August 2011

This section presents the summary of the analysis of five CWWF events according to the rainfall time series of August 2011 analogous to the exemplary analysis of CWWF event #1 of the rainfall time series of June 2012. Table 7-15 and Table 7-16 summarize the mean results of MF values and corresponding standard deviations of all events for sewer network control and WWTP capacity estimation concerning FPC. Figure 7-31 illustrates the evaluation of MF results chosen for system-wide control according to their mean values and mean STDs. Although the observed mean satisfaction of each MF and STDs corresponds to the event mean results according to CWWF event #1 of rainfall time series of June 2012 presented in Figure 7-15 and Figure 7-16, Table 7-15 and Table 7-16 show significant differences for mean MF results for each event. This supports the need for variable weighting coefficients when aggregating objectives for multi-criteria optimization in control of dynamic systems such as WCTs instead of using constant weighting coefficients as usually done (e.g. Fiorelli et al. (2013)).

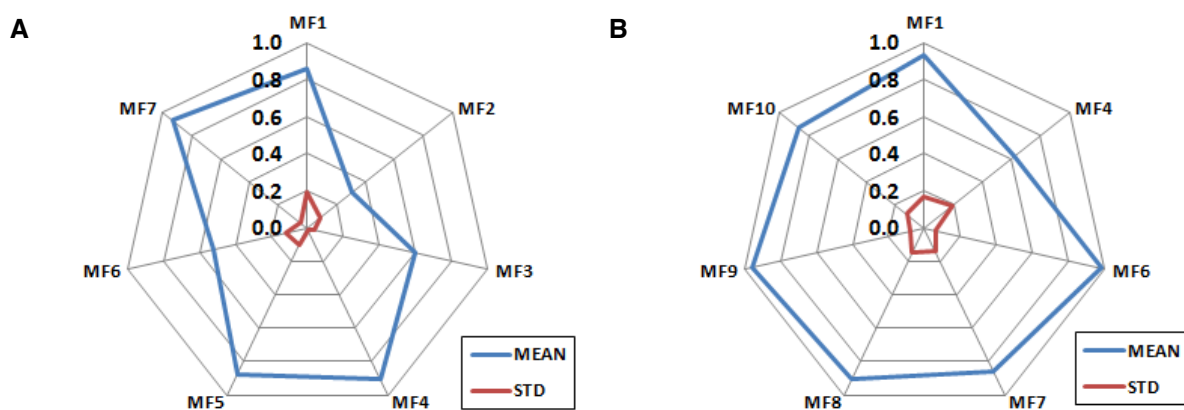


Figure 7-31: FDM mean results and STDs of 5 CWWF events according to the rainfall time series of August 2011 for WWTP capacity estimation and control (A) and sewer network control (B)

Table 7-15: Summary of WWTP mean MF values and standard deviations for CWWF events of August 2011

Event	MF1 [-]		MF2 [-]		MF3 [-]		MF4 [-]		MF5		MF6		MF7 [-]		MFtot [-]	
	Mean	Std	Mean	Std	Mean	Std	Mean	Std	Mean	Std	Mean	Std	Mean	Std	Mean	Std
1	0.75	0.33	0.28	0.14	0.70	0.05	0.92	0.03	0.75	0.18	0.51	0.18	0.98	0.01	1.61	0.38
2	0.76	0.29	0.46	0.16	0.57	0.03	0.90	0.01	0.96	0.03	0.44	0.21	0.94	0.03	1.41	0.17
3	0.90	0.13	0.31	0.08	0.55	0.01	0.89	0.01	0.96	0.04	0.54	0.09	0.93	0.04	1.47	0.07
4	0.96	0.07	0.23	0.03	0.54	0.01	0.89	0.01	0.91	0.07	0.59	0.06	0.86	0.09	1.62	0.09
5	0.92	0.12	0.25	0.05	0.61	0.07	0.91	0.02	0.82	0.17	0.54	0.08	0.96	0.05	1.53	0.15
Mean	0.86	0.19	0.31	0.09	0.59	0.04	0.90	0.01	0.88	0.10	0.52	0.12	0.93	0.04	1.53	0.17

Table 7-16: Summary of sewer network mean MF values and standard deviations for CWWF events of August 2011

Event	MF1 [-]		MF2 [-]		MF3 [-]		MF4 [-]		MF5		MF6		MF7 [-]		MF8 [-]		MF9 [-]		MF10 [-]		MF11 [-]		MF12 [-]		MFtot [-]	
	Mean	Std	Mean	Std	Mean	Std	Mean	Std	Mean	Std	Mean	Std	Mean	Std	Mean	Std	Mean	Std	Mean	Std	Mean	Std	Mean	Std	Mean	Std
1	1.34	1.17	0.93	0.16	0.93	0.18	0.57	0.20	0.27	0.09	0.89	0.32	0.79	0.22	0.76	0.35	0.91	0.23	0.83	0.20	0.53	0.40	0.48	0.40	1.34	1.17
2	0.74	0.38	0.99	0.04	0.99	0.04	0.70	0.17	0.35	0.10	1.00	0.00	0.81	0.22	0.95	0.12	0.97	0.04	0.87	0.15	0.53	0.41	0.52	0.42	0.74	0.38
3	0.72	0.32	0.93	0.20	0.94	0.16	0.62	0.23	0.35	0.11	1.00	0.00	0.91	0.11	0.93	0.13	0.98	0.04	0.90	0.05	0.54	0.41	0.53	0.40	0.72	0.32
4	0.71	0.40	0.98	0.07	0.98	0.06	0.71	0.14	0.33	0.16	1.00	0.00	0.89	0.06	0.97	0.05	0.95	0.04	0.85	0.05	0.77	0.22	0.73	0.28	0.71	0.40
5	0.92	0.38	0.88	0.26	0.89	0.25	0.51	0.23	0.27	0.15	1.00	0.00	0.90	0.10	0.92	0.12	0.98	0.04	0.87	0.16	0.76	0.27	0.73	0.32	0.92	0.38
Mean	0.88	0.53	0.94	0.15	0.95	0.14	0.62	0.19	0.31	0.12	0.98	0.06	0.86	0.14	0.91	0.15	0.96	0.08	0.86	0.12	0.63	0.34	0.60	0.36	0.88	0.53

Simulation-based evaluation of the integrated fuzzy predictive control approach

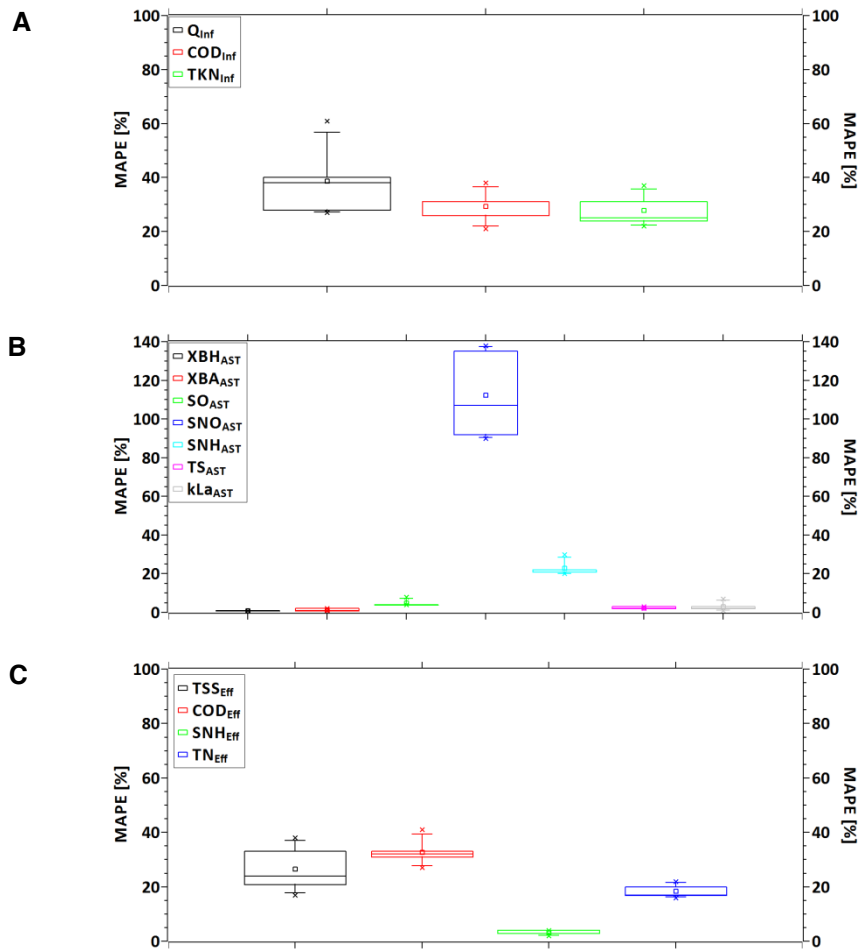


Figure 7-32: Evaluation of MAPDs between model based WWTP capacity estimations and results from reference simulation based loading for the rainfall time series of August 2011 (A = WWTP loading, B = AST, C = SST effluent)

Figure 7-32 summarizes the MAPDs between the WWTP capacity estimation according to FPC and the simulated loading according to the FPC of the sewer network for five CWWF events according to the rainfall time series of August 2011. The presented MAPDs hence illustrate the reserve capacity of the WWTP during CWWF due to compromises of conflicting objectives according to sewer network FPC. Since studies about the integrated control of WCTs predominantly investigate control strategies there is no equivalent information available about reserve capacities of WWTPs in integrated WCTs according to multi-criteria optimization. Mean hydraulic reserve capacities of 40 percent illustrate the impact of sewer network FPC in the integrated control approach. Effluent MAPDs for COD and TN correspond to the influent MAPDs, showing reserve capacities of about 25 percent due to the objectives for SASS. A MAPD of 4 percent for NH_4-N effluent concentrations is a proof of sufficient aeration for nitrification during most of the time. MAPDs of about 100 percent and about 25 percent for NO_3-N resp. NH_4-N AST concentrations show the sensitivity of MPC of nitrification during CWWF. Simulation results of MPC for aeration during DWF investigated by Holanda et al. (2008) show better results due to smaller pollution load uncertainties.

Figure 7-33 confirms the linear correlation between hydraulic loading and SST TSS effluent concentrations according to the results of their linear MFs. Thereby, all 5 CWWF events in August 2011 show the same hydraulic limit of about 60% of the ISN capacity in the present case. Overall, this static behavior of the SST is in contradiction to other studies of integrated control of WCTSSs which propose online sludge level measurements to deal with these dynamics (e.g. Seggelke et al. (2013)). In the present case, this behavior can be explained by the small compressed activated sludge layer in the SST due to the comparably smaller activated sludge content of low loaded WWTPs for SASS.

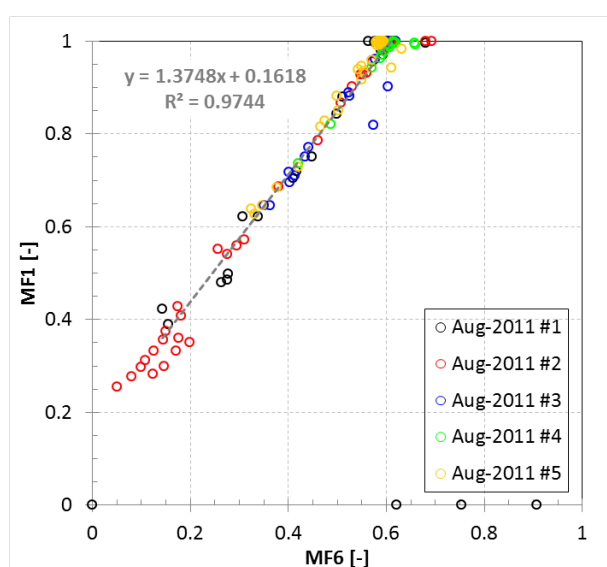


Figure 7-33: Correlation of MF values for WWTP inflow and SST effluent TSS concentrations of 5 CWWF events according to the rainfall time series of August 2011

Figure 7-34 shows the results of the multi-criteria predictive control of nitrification according to the objectives of SASS. The figure demonstrates the control of hydraulic loading according to the current $\text{NH}_4\text{-N}$ concentration in the AST, the corresponding nitrogen influent load and the DO set-point optimization. Proposed hydraulic loadings increase with decreasing $\text{NH}_4\text{-N}$ concentrations in the AST, decreasing TKN influent loads and increasing DO set-points in the AST. In contrast to other studies (e.g. Tränckner et al. (2007a)) limitations of WWTP loading due to limited nitrification capacities have not been observed. This can be explained by:

- the increased specific AST volume according to the design of low loaded WWTPs and
- the extended aeration for SASS.

Predominantly, aeration according to the preferred DO set-point of 0.7 g/m^3 for SASS is sufficient to treat pollutant loads during CWWF. Optimization results are in the range of 0.5 to 2.0 g/m^3 . This extended aeration leads to the desired low $\text{NH}_4\text{-N}$ concentrations about 1 g/m^3 in the AST according to the objectives of SASS. The objective to simultaneously consider the legal effluent $\text{NH}_4\text{-N}$ concentration limit of 3 g/m^3 adds additional treatment capacities and degrees of freedom in FDM. Nevertheless, $\text{NH}_4\text{-N}$ concentrations do not exceed 2 g/m^3 due to the objectives for SASS.

The outlier, proposing the largest hydraulic load for the largest TKN influent load illustrates the risk of derivative free numerical optimization approaches to get stuck in local minima. This has also been investigated in studies about nonlinear sewer network MPC (Heusch 2011). For the investigated month only one such failure was observed. Hydraulic failure of the SST leading to activated sludge wash-out is prevented by the emergency CSO structure at the inlet of the WWTP.

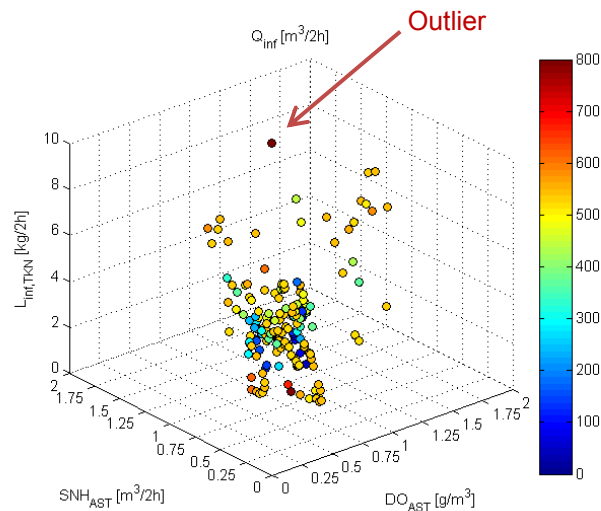


Figure 7-34: WWTP multi-objective predictive hydraulic loading according to TKN influent load and SNH_{AST} concentrations and corresponding DO_{AST} set-point optimization for 5 CWWF events according to the rainfall time series of August 2011

Figure 7-35 illustrates the corresponding evaluation of MF results from FDM of multiple objectives for the investigated five CWWF events. PLS-DA reveals event-specific degrees of satisfaction concerning compromises for the DO set-point optimization according to SASS and conflicting objectives such as the SST effluent NH_4-N concentration minimization (A), the SST effluent TN concentration minimization (B) and the AST NH_4-N concentration optimization according to SASS (C). Similar to the results illustrated in Figure 7-25 the satisfaction of AST NH_4-N concentrations show the largest dynamics in the FDM process while optimizing the aeration both within each event and for all events compared to each other. Due to the buffering effect of the SST volume satisfaction results concerning SST effluent NH_4-N concentration show less dynamics. In the case of SST effluent TN concentrations the balance with NO_x-N concentrations and the process of simultaneous nitrification – denitrification contributes to the general excellent satisfaction of MF4 showing no conflicts with the DO set-point optimization. Overall, the mean satisfaction of MFs is satisfying for MF3, excellent for MF4 and good for MF5 while the satisfaction of MF7 is predominantly excellent. The results clearly show the conflict of the optimization of AST NH_4-N concentrations according to SASS and the maximization of SST effluent NH_4-N concentrations according to legal effluent limits. Comparable studies about multi-objective optimal control of integrated WCTs by Fu et al. (2008) investigated Pareto optimal solutions for the parameterization and comparison of control strategies regarding their impact on the receiving water. Thereby, the investigation of the Pareto front contributes to the offline decision-making process for operators of WCTs.

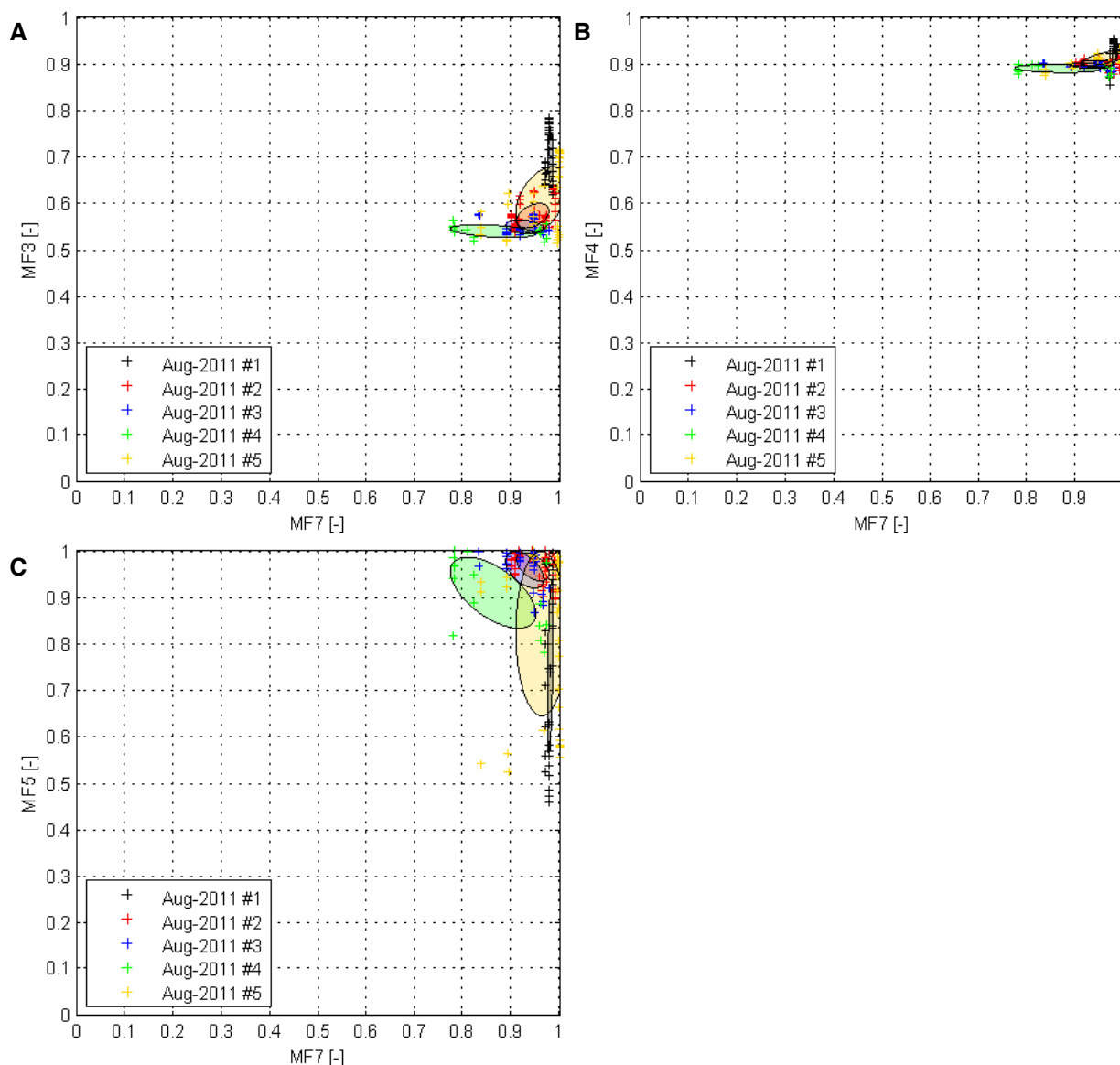


Figure 7-35: PLS-DA of MF results for DO_{AST} set-point optimization (MF7) and effluent (A) NH_4 -N minimization (MF3), (B) effluent TN minimization (MF4) and (C) AST NH_4 -N optimization (MF5) for 5 CWWF events according to the rainfall time series of August 2011

Figure 7-36 illustrates the event-specific correlation of MF results for the system-wide hydraulic CSO minimization and the system-wide COD resp. TKN CSO load minimization. Compared to the results of CWWF event #1 according to the rainfall time series of June 2012 (see Figure 7-28) the results for five CWWF events according to the rainfall time series of August 2011 show poorer correlations. Nevertheless, coefficients of determination R^2 of 0.75 for COD resp. 0.70 for TKN still show a significant correlation. Thinking of the coefficient of determination as a percent this means that by applying hydraulic-based sewer network FPC the objective of CSO COD minimization is about 75% resp. 70% concerning TKN. Or vice versa, pollution-based sewer network FPC should have a reserve capacity of 25% for COD CSO load reduction resp. 30% for TKN CSO reduction. This principally corresponds to the findings of Lacour and Schütze (2011) who demonstrated based on

simulations the benefit of turbidity-based real-time control approaches to reduce pollutant loads from CSO compared to hydraulic rule-based real-time control approaches. While their rule-based real-time control analysis only showed reserve capacities for CSO pollution load reduction of about 10% the present analysis based on FDM indicates significantly larger reserve capacities when using FPC. The observed correlation between CSO volume minimization and CSO pollution load minimization can be explained according the behavior of the sewer network FPC approach. As explained in section 7.3.3 the approach tries to minimize unavoidable CSO by delaying CSO through the maximization of the total retention tank volume in the system. By doing this continuously from the beginning of each CWWF event retention tank influent and hence CSO overflow pollution concentrations predominantly decrease along the CWWF event due to dilution. Most of the investigated CWWF pollutographs observed in the measurement campaign (see Figure 6-44) confirm this behavior. The present observations are limited to online bypass retention tanks where CSO pollution concentrations correspond to the retention tank influent concentrations. Additionally, these results emphasize the importance of modeling the accumulation and wash-off of pollutants for the simulation-based evaluation of sewer network control approaches.

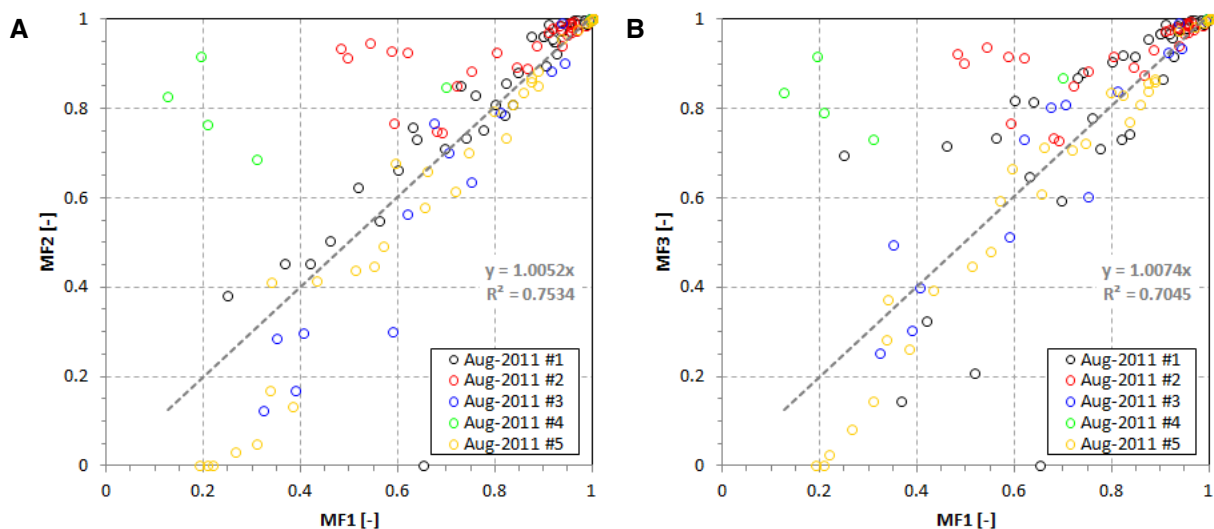


Figure 7-36: Correlation of MF results for (A) total CSO volumes (MF1) and total COD CSO loads (MF2) and (B) TKN CSO loads (MF3) for 5 CWWF events according to the rainfall time series of August 2011

Figure 7-37 illustrates the evaluation of MF results from FDM of multiple objectives for the investigated five CWWF events according to the rainfall time series of August 2011. PLS-DA reveals event-specific degrees of satisfaction concerning compromises for the hydraulic homogenization in the ISN and conflicting objectives such as CSO volume minimization (A), homogeneous retention tank use (B) and hydraulic WWTP loading (C). While Figure 7-37 (B) clearly shows a similar general conflict between the homogenized hydraulic loading of the WWTP and the homogenized retention tank utilization due to the centered arrangement of the ellipsis, Figure 7-37 (C) shows the general agreement of the homogenized flows in the ISN and the homogenized loading of the WWTP. This indicates that the homogenized retention tank utilization according to sewer network FPC is a structural problem while the

latter emphasizes the need of observer models in the case of complex ISNs. From Figure 7-37 (A) it can be seen that CSO volume minimization shows less conflicts concerning ISN flow homogenization than the homogenization of retention tank use due to the rainfall independent impact of the specific retention tank storage volume (see Figure 6-3). Thereby, the variability is event-specific due to the variability of rainfall and corresponding runoff.

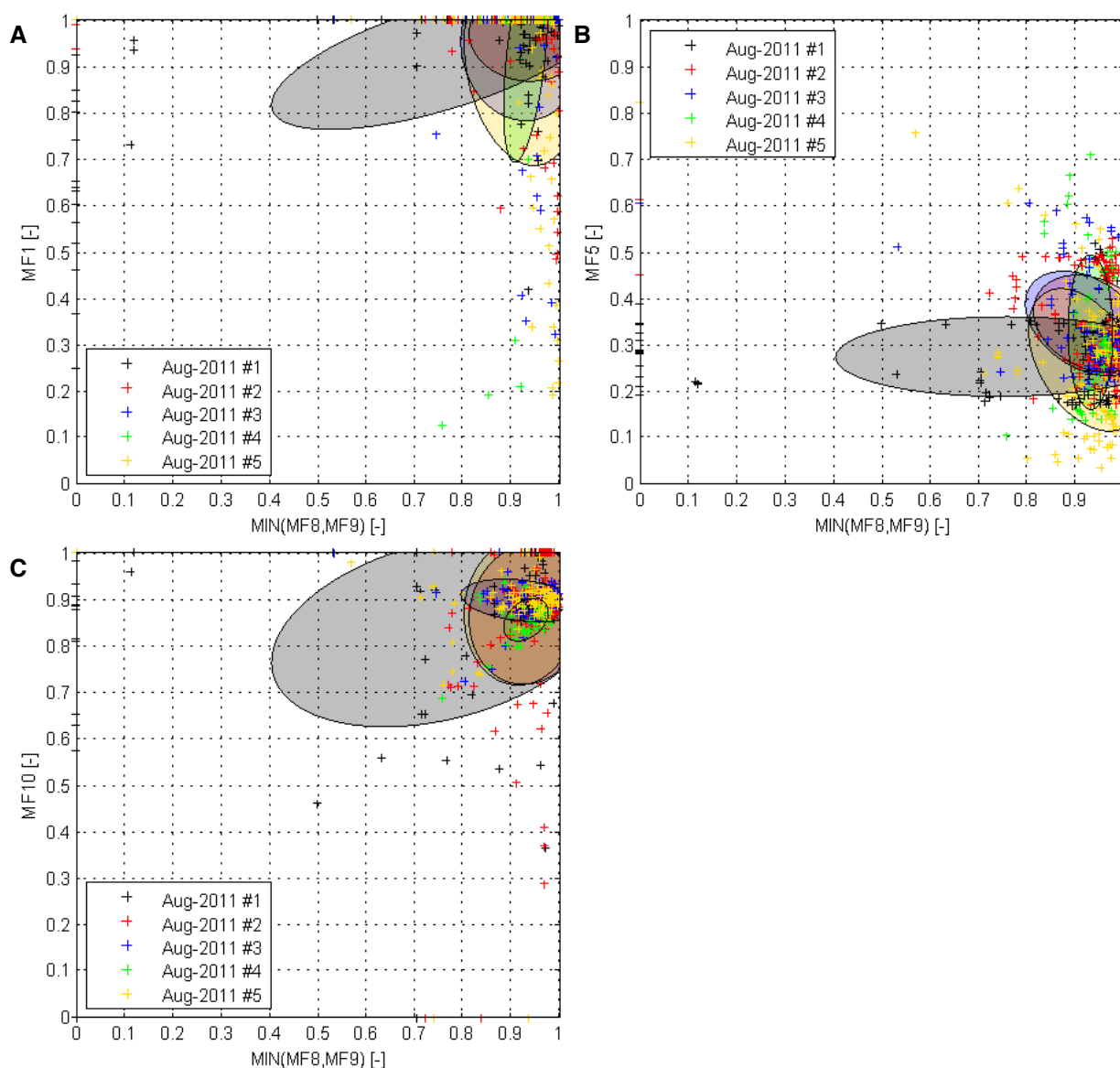


Figure 7-37: PLS-DA of MF results for ISN hydraulic homogenization (MF8 and MF9) and (A) CSO volume minimization (MF1), (B) retention tank use homogenization (MF5) and (C) WWTP hydraulic loading homogenization (MF10) for 5 CWWF events according to the rainfall time series of August 2011

Figure 7-38 illustrates the evaluation of MF results from FDM of multiple objectives for the investigated five CWWF events according to the rainfall time series of August 2011. PLS-DA reveals event-specific degrees of MF satisfactions concerning compromises for the hydraulic WWTP and the corresponding COD loading (A) resp. TKN loading (B). Thereby, the degree

of variability differs according to the event-specific pollution load. Vice versa, pollution-based WWTP loading during CWWF would disturb the hydraulic loading.

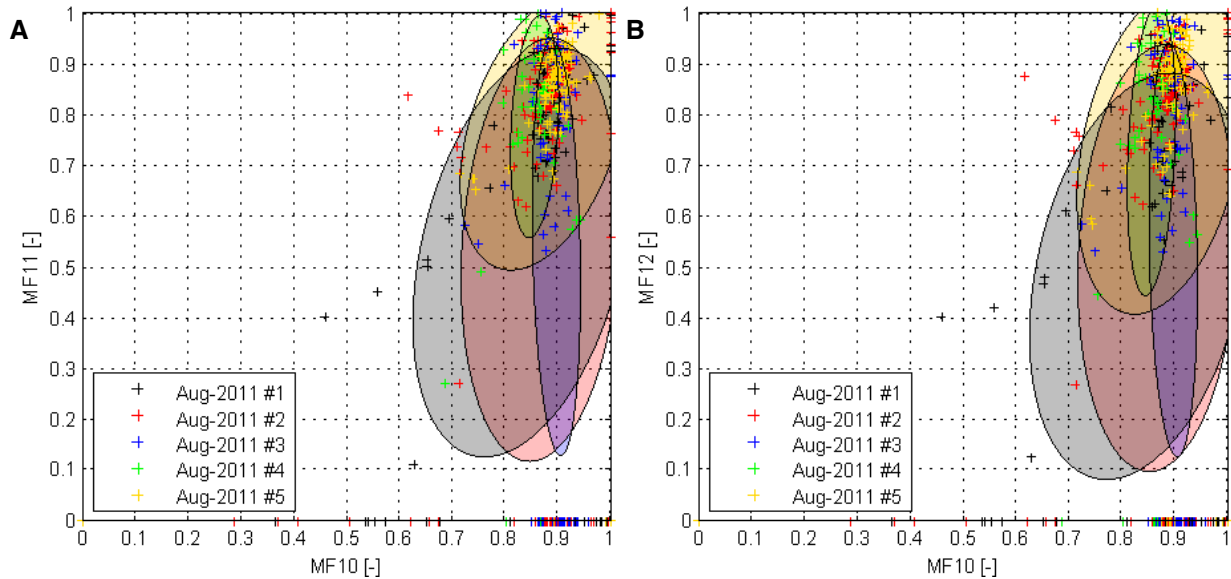


Figure 7-38: PLS-DA of MF results for WWTP hydraulic loading (MF10) and (A) WWTP COD loading (MF11) and (B) WWTP TKN loading (MF12) for 5 CWWF events according to the rainfall time series of August 2011

7.3.6. Summary of results June 2012

In the following the impact of increased CWWF on the proposed FPC approach for system-wide control of integrated rural WCTs is investigated according to the rainfall time series of June 2012 providing 11 CWWF events. Table 7-17 and Table 7-18 summarize the mean results of MF values and corresponding standard deviations of all events for sewer network control and WWTP capacity estimation based on FPC. Figure 7-39 illustrates the evaluation of MF results chosen for system-wide control according to their mean values and mean standard deviations. The observed mean satisfaction for each MF and standard deviations corresponds to the event mean results according to the rainfall time series of August 2011 presented in Figure 7-31, indicating similar conflicting objectives.

Figure 7-40 summarizes the MAPDs between the FPC WWTP capacity estimation and simulated loading according to FPC for 11 CWWF events. Showing principally comparable results to Figure 7-32, Figure 7-40 additionally reveals large uncertainties concerning k_{La} for the predictive aeration for nitrification.

Figure 7-41 shows linear correlation results concerning the SST performance, comparable to what was observed for August 2011 (see Figure 7-33).

Figure 7-42 to Figure 7-46 show results comparable to the findings for August 2011. Despite the increased variability in FPC of conflicting objectives, especially the results according to PLS-DA, indicate a behavior comparable to the results for August 2011. Figure 7-44 confirms the reserve capacity of pollution-based FPC of 20%. Consequently, a significant influence on the system-wide control behavior of integrated rural WCTs cannot be found.

Table 7-17: Summary of WWTP mean MF values and standard deviations for CWWF events of June 2012

Event	MF1 [-]	MF2 [-]	MF3 [-]	MF4 [-]	MF5	MF6	MF7 [-]	MFtot [-]								
	Mean	Std	Mean	Std	Mean	Std	Mean	Std								
1	0.92	0.14	0.28	0.09	0.63	0.05	0.91	0.02	0.85	0.12	0.60	0.11	0.94	0.07	1.47	0.20
2	0.97	0.05	0.31	0.03	0.63	0.03	0.89	0.01	0.89	0.06	0.63	0.05	0.98	0.00	1.33	0.07
3	0.89	0.16	0.35	0.09	0.59	0.02	0.90	0.01	0.95	0.04	0.57	0.13	0.96	0.04	1.37	0.11
4	0.91	0.15	0.40	0.08	0.64	0.05	0.89	0.02	0.87	0.10	0.59	0.13	0.95	0.04	1.34	0.11
5	0.81	0.23	0.47	0.12	0.66	0.03	0.91	0.00	0.87	0.10	0.52	0.17	0.96	0.02	1.31	0.13
6	0.89	0.20	0.38	0.11	0.61	0.06	0.90	0.02	0.86	0.07	0.57	0.17	0.95	0.05	1.40	0.16
7	0.93	0.10	0.32	0.05	0.63	0.06	0.91	0.02	0.85	0.14	0.60	0.09	0.93	0.04	1.42	0.13
8	0.95	0.08	0.35	0.05	0.57	0.04	0.87	0.02	0.96	0.03	0.59	0.07	0.95	0.01	1.35	0.07
9	0.96	0.08	0.21	0.06	0.79	0.15	0.94	0.05	0.27	0.33	0.60	0.07	0.99	0.01	1.83	0.21
10	0.97	0.04	0.27	0.02	0.52	0.00	0.85	0.01	0.89	0.03	0.63	0.07	0.94	0.02	1.58	0.05
11	0.83	0.22	0.37	0.13	0.52	0.03	0.89	0.01	0.86	0.08	0.48	0.17	0.93	0.02	1.59	0.13
Mean	0.91	0.13	0.34	0.07	0.62	0.05	0.90	0.02	0.83	0.10	0.58	0.11	0.95	0.03	1.45	0.12

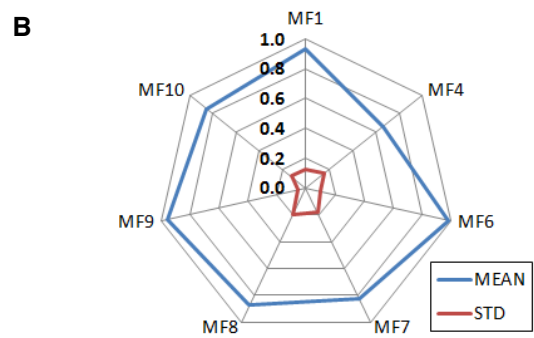
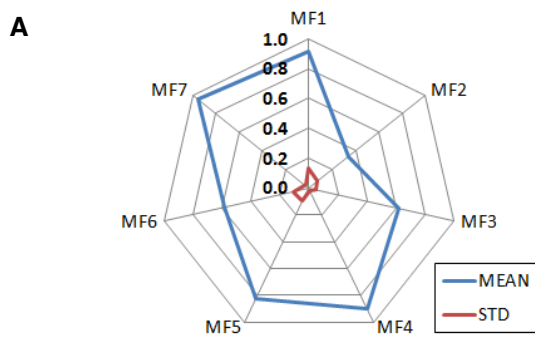


Figure 7-39: FDM mean results and STDs of 11 CWWF events according to rainfall time series June 2012 for WWTP capacity estimation and control (A) and sewer network control (B)

Table 7-18 Summary of sewer network mean MF values and standard deviations for CWWF events of June 2012

Event	MF1 [-]	MF2 [-]	MF3 [-]	MF4 [-]	MF5	MF6	MF7 [-]	MF8 [-]	MF9 [-]	MF10 [-]	MF11 [-]	MF12 [-]	MFtot [-]														
	Mean	Std	Mean	Std	Mean	Std	Mean	Std	Mean	Std	Mean	Std	Mean	Std													
1	0.87	0.24	0.86	0.29	0.87	0.27	0.48	0.25	0.27	0.11	1.00	0.00	0.88	0.11	0.90	0.18	0.97	0.04	0.88	0.06	0.72	0.26	0.71	0.28	1.02	0.45	
2	1.00	0.01	1.00	0.00	1.00	0.81	0.07	0.58	0.13	0.97	0.17	0.83	0.17	0.83	0.17	0.79	0.30	0.94	0.06	0.88	0.08	0.60	0.36	0.61	0.37	0.78	0.51
3	0.99	0.04	1.00	0.01	1.00	0.81	0.07	0.47	0.14	1.00	0.00	0.84	0.15	0.84	0.15	0.92	0.16	0.96	0.05	0.87	0.11	0.68	0.32	0.66	0.35	0.61	0.33
4	0.93	0.19	0.98	0.07	0.98	0.61	0.06	0.61	0.22	0.29	0.13	0.99	0.12	0.81	0.22	0.92	0.17	0.94	0.06	0.80	0.16	0.62	0.29	0.62	0.30	1.00	0.62
5	0.88	0.18	0.98	0.03	0.98	0.65	0.03	0.65	0.18	0.25	0.12	0.96	0.19	0.78	0.21	0.84	0.18	0.96	0.05	0.87	0.10	0.54	0.37	0.57	0.37	1.07	0.66
6	0.99	0.02	1.00	0.01	1.00	0.73	0.36	0.45	0.11	0.40	0.09	0.96	0.19	0.78	0.26	0.93	0.15	0.95	0.06	0.80	0.17	0.67	0.34	0.65	0.36	0.85	0.54
7	0.74	0.32	0.74	0.35	0.74	0.36	0.45	0.28	0.28	0.20	0.99	0.10	0.85	0.13	0.82	0.21	0.96	0.05	0.86	0.14	0.63	0.31	0.62	0.31	1.32	0.80	
8	0.99	0.04	0.99	0.02	0.99	0.70	0.12	0.36	0.16	1.00	0.00	0.92	0.10	0.92	0.10	0.93	0.16	0.96	0.07	0.88	0.07	0.59	0.41	0.55	0.42	0.62	0.25
9	0.93	0.15	0.92	0.18	0.92	0.56	0.17	0.56	0.20	0.27	0.16	1.00	0.00	0.89	0.13	0.92	0.13	0.96	0.07	0.87	0.06	0.82	0.13	0.81	0.16	0.87	0.30
10	1.00	0.00	1.00	0.00	1.00	0.86	0.05	0.62	0.03	1.00	0.00	0.79	0.22	0.74	0.38	0.94	0.38	0.94	0.05	0.84	0.24	0.60	0.37	0.62	0.39	0.83	0.73
11	0.90	0.17	0.94	0.13	0.94	0.60	0.21	0.25	0.10	0.89	0.31	0.74	0.27	0.88	0.19	0.97	0.19	0.97	0.05	0.83	0.22	0.52	0.43	0.52	0.43	1.21	0.72
12	0.93	0.12	0.95	0.10	0.95	0.66	0.16	0.37	0.13	0.98	0.10	0.83	0.18	0.87	0.20	0.96	0.20	0.96	0.06	0.85	0.13	0.63	0.33	0.63	0.34	0.93	0.54
Mean	0.87	0.24	0.86	0.29	0.87	0.27	0.48	0.25	0.27	0.11	1.00	0.00	0.88	0.11	0.90	0.18	0.97	0.04	0.88	0.06	0.72	0.26	0.71	0.28	1.02	0.45	

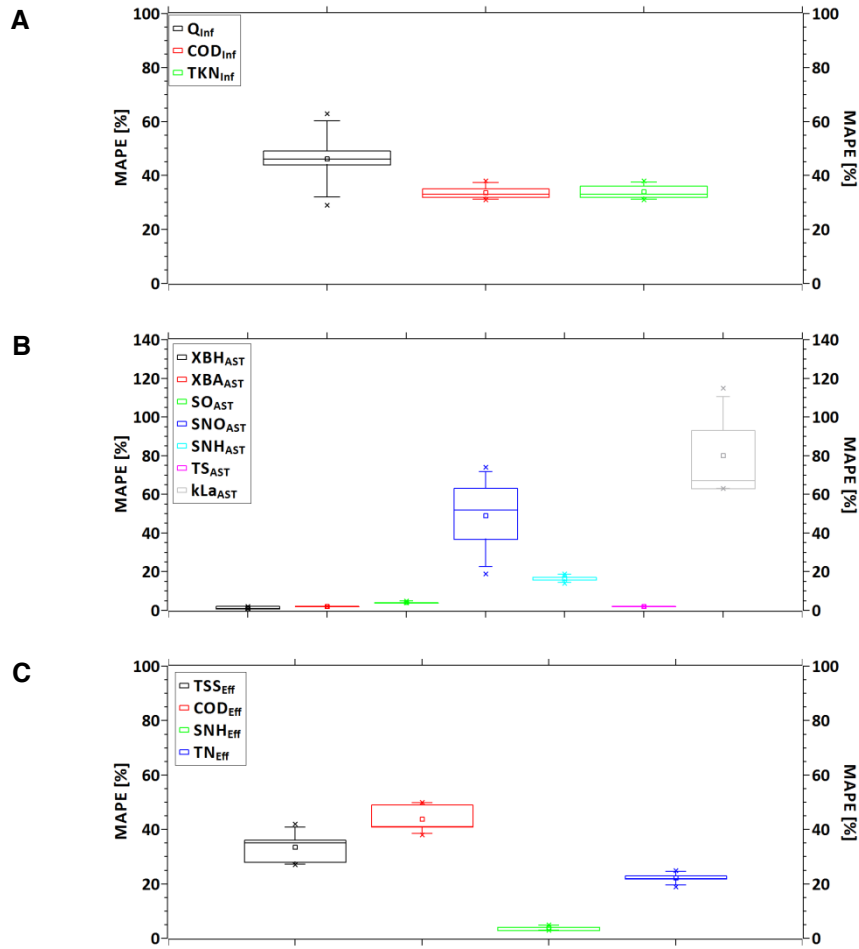


Figure 7-40: Evaluation of MAPDs between model based WWTP capacity estimations and results from reference simulation based loading for the rainfall time series of June 2012 (A = WWTP loading, B = AST, C = SST effluent)

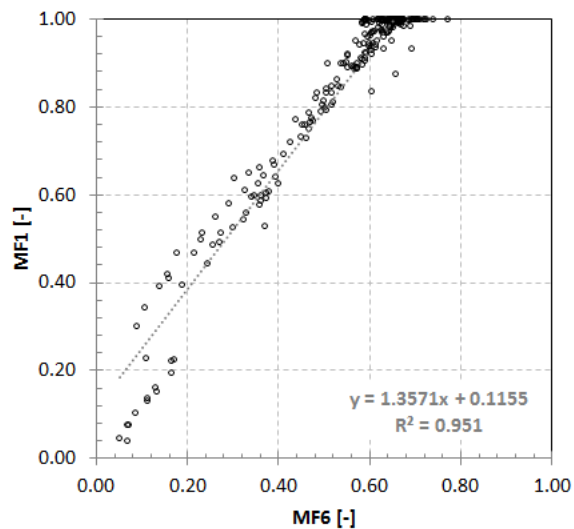


Figure 7-41: Correlation of MF values for WWTP inflow and SST effluent TSS concentrations of 11 CWWF events according to the rainfall time series of June 2012

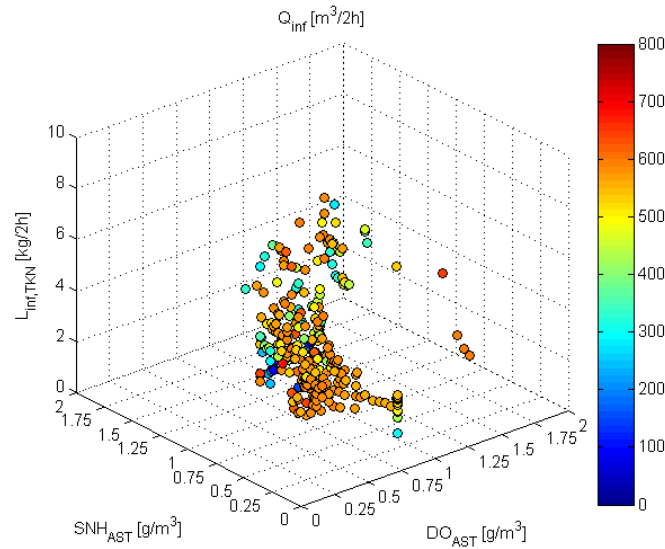


Figure 7-42: WWTP multi-objective predictive hydraulic loading according to TKN influent load and SNH_{AST} concentrations and corresponding DO_{AST} set-point optimization for 11 CWWF events according to the rainfall time series of June 2012

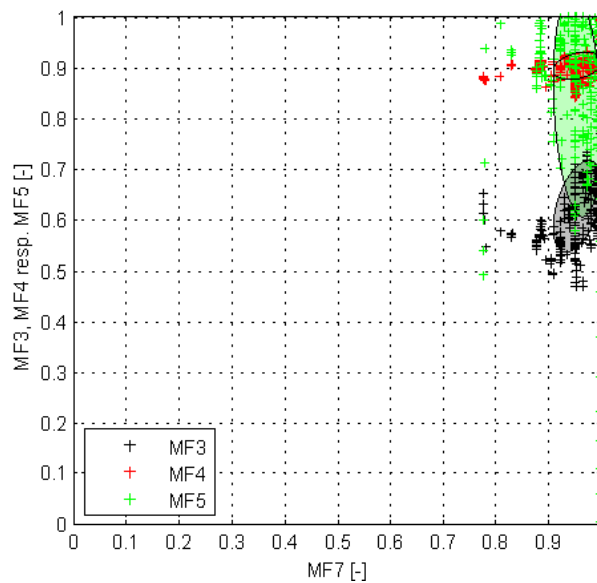


Figure 7-43: PLS-DA of MF results for DO_{AST} set-point optimization (MF7) and effluent NH₄-N minimization (MF3), effluent TN minimization (MF4) and AST NH₄-N optimization (MF5) for 11 CWWF events according to the rainfall time series of June 2012

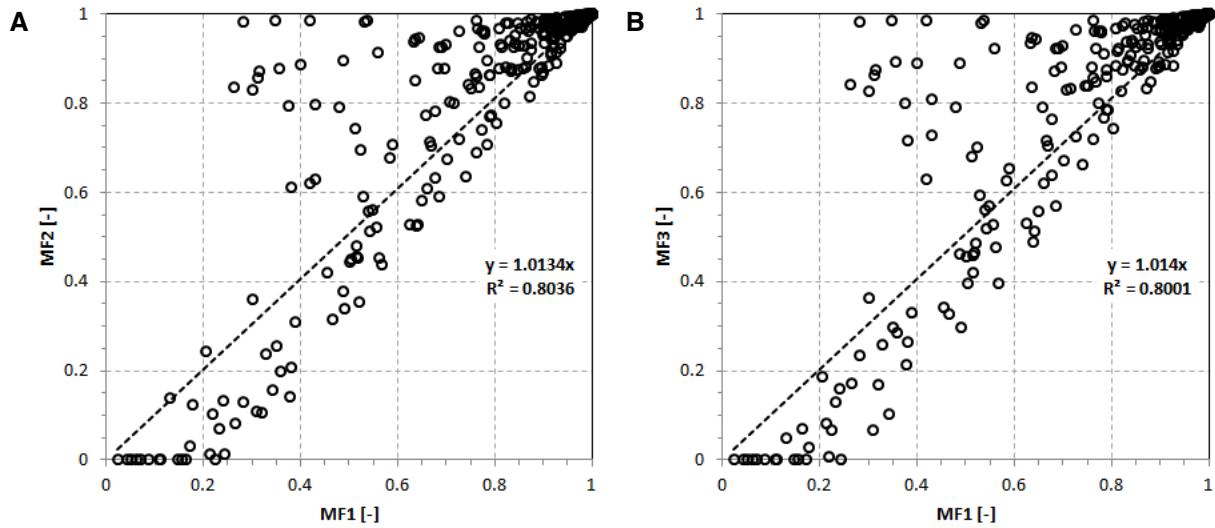


Figure 7-44: Correlation of MF results for (A) total CSO volumes (MF1) and total COD CSO loads (MF2) and (B) TKN CSO loads (MF3) for 11 CWWF events according to the rainfall time series of June 2012

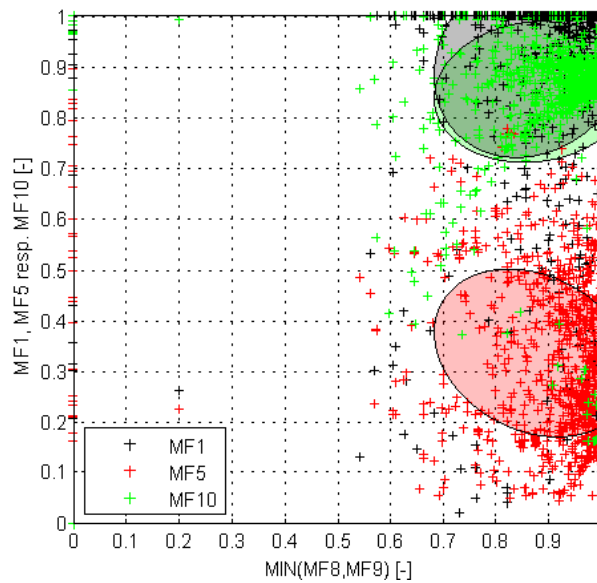


Figure 7-45: PLS-DA of MF results for ISN hydraulic homogenization (MF8 and MF9) and CSO volume minimization (MF1), retention tank use homogenization (MF5) and WWTP hydraulic loading homogenization (MF10) for 11 CWWF events according to the rainfall time series of June 2012

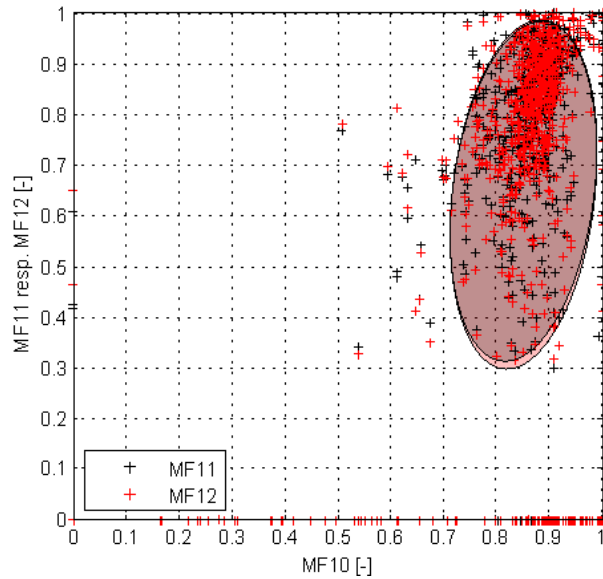


Figure 7-46: PLS-DA of MF results for WWTP hydraulic loading (MF10) and (A) WWTP COD loading (MF11) and (B) WWTP TKN loading (MF12) for 11 CWWF events according to the rainfall time series of June 2012

From these confirmations of the results from August 2011 it can be concluded that FPC is an appropriate tool for the integrated capacity estimation of WWTP with SASS in rural catchments. These systems seem to be robust in integrated FPC due to high SRTs and extended aeration. Additionally, smaller TS concentrations contribute to a linear behavior of the SST during CWWF loading due to comparably small activated sludge compression layers. Increased nitrification for SASS contributes to the process stability in the AST. The regression of objectives to minimize CSO volumes and CSO loads illustrate correlation between CSO volume reduction and CSO pollution load reduction and additionally quantify the reserve capacity for pollution-based real-time control approaches to additionally reduce CSO pollution loads. Nevertheless, nonlinear reserve capacities even exceed the findings from other studies. Increased CWWF does not affect the control manner of the presented controller based on FDM.

8. Comparison to static control scenarios and discussion of results

In the following, the results of the proposed integrated FPC approach for system-wide control of rural WCTs will be discussed in comparison with the results from reference scenarios based on isolated feedback control approaches. These basic controllers consist of PID controllers with static set-points. Table 8-1 summarizes variables and set-points of the controllers applied in the chosen reference scenarios. Major differences between the proposed integrated FPC approach and the reference control scenarios can be summarized as follows:

- Instead of a predefined static WWTP reference inflow $Q_{Ref,WWTP}$ the integrated FPC approach estimates a dynamic $Q_{Ref,WWTP}$ according to the actual WWTP capacity along the receding horizon.
- Instead of controlled throttle flows according to identical and constant set-points at all retention tanks, the integrated FPC approach calculates a set of controlled throttle flows for the sum of all retention tanks optimized according to the minimization of CSO volumes and the dynamic WWTP reference inflow along the receding horizon.

Table 8-1: Variables and set-points of feedback controllers used in the reference scenarios

Location	Variable	Set-point
Retention tanks	Q_{Eff}	$Q_{Ref,WWTP}/24$
WWTP	Q_{Inf}	$Q_{Ref,WWTP}$ according to the specific reference scenario
WWTP	Q_{WAS}	SRT equal to 25 days
WWTP	DO_{AST}	1.5 g/m ³ during DWF 0.7 g/m ³ during CWWF
WWTP	S_{NH}	1.0 g/m ³

The present simulation results are compared to results from a literature review. Additionally, membership function (MF) values resulting from the integrated optimization according to FPC are used:

- to investigate and illustrate conflicting objectives and
- to describe the capacity of the integrated system

in comparison to static control

In the present case, as discussed in section 7.3.1, performance analysis is limited to CWWF events of two months of rainfall. From a hydrological point of view, where long-term analysis is the common method, this small period can only indicate the potentials and limitations of the presented approach. Nevertheless, from a control engineering point of view the diversity of the investigated events is sufficient to show the performance range of the presented approach. The performance is discussed according to:

- volumes and pollution loads of CWWF treated at the WWTP and their treatment,
- the applied aeration at the WWTP and
- CSO volume and pollution loads discharged to receiving waters.

8.1. Reference scenarios

According to Table 8-1 reference scenarios can be described according to the WWTP reference discharge $Q_{\text{Ref,WWTP}}$, the trajectory for sewer network control. For static, isolated sewer network control, the WWTP reference discharge is equally distributed to all retention tanks taking RDII within the ISN into account according to section 6.2.2.2. The following reference scenarios were considered:

- **Scenario ATV-A 198 (Ref1)**

The German design standard ATV-A 198 (DWA 2003) proposes an optimum CWWF to the WWTP depending on the treatment plant size. In the present case (12000 PE) the proposed range is about 4.5 to 7.5 times the annual mean DWF and infiltration flow. In an integrated sense, this is already an improvement over previous recommendations of only two times the DWF plus RDII. In order to investigate a broad range of reference scenarios the proposed lower limit is chosen as the smallest reference scenario. Due to the seasonal impact of tourism on PE a reference WWTP inflow during CWWF of $Q_{\text{Ref,WWTP}} = 7200 \text{ m}^3/\text{d}$ is chosen for the summer months with two lined operation.

- **Scenario $Q_{\text{Design,WWTP}}$ (Ref2)**

The design hydraulic WWTP loading during CWWF is equal to $10680 \text{ m}^3/\text{d}$ for two treatment lanes resp. $5340 \text{ m}^3/\text{d}$ for one treatment lane.

- **Scenario $Q_{\text{Max,WWTP}}$ (Ref3)**

The maximum CWWF to the WWTP is derived from the evaluation of the integrated FPC approach. Figure 7-33 for August 2011 and Figure 7-41 for June 2012 show both a linear correlation between MF values for the WWTP inflow normalized according to the maximum ISN hydraulic capacity and SST effluent TSS concentrations, indicating a hydraulic capacity of the SST of about 60% of the ISN hydraulic capacity. This corresponds to a reference hydraulic loading of $Q_{\text{Ref,WWTP}} = 12500 \text{ m}^3/\text{d}$ for both treatment lanes. Consequently, the WWTP is continuously loaded during CWWF according to this maximum set-point.

- **Scenario $Q_{\text{Mean,FPC}}$ (Ref4)**

For this scenario the WWTP is continuously loaded according to the mean WWTP inflow proposed by the integrated FPC approach. This scenario is used to investigate the performance of the integrated FPC approach in terms of sewer network control. According to the results presented in section 7.3.5 $Q_{\text{Ref,WWTP}}$ is equal to $8490 \text{ m}^3/\text{d}$ in August 2011 resp. equal to $9170 \text{ m}^3/\text{d}$ in June 2012 according to the results presented in section 7.3.6.

In order to evaluate the AST DO set-point optimization of the presented FPC approach regarding the choice between DO set-point control according to recommendations for SASS during CWWF and ammonia set-point control according to recommendations for SASS during CWWF, each reference scenario additionally considers two variants:

- $DO_{\text{AST,CWWF}}$: Aeration control based on a constant DO set-point of 0.7 g/m^3 in the oxidation ditch according to recommendations for SASS during CWWF (DWA 2009).

- $SNH_{AST,CWWF}$: Aeration control based on a constant S_{NH} concentration of about 1.0 g/m^3 in the oxidation ditch according to recommendations for SASS during CWWF (DWA 2009).

For all scenarios, the control of the return activated sludge flow rate is equal to the WWTP inlet flow rate during DWF and equal to 75% of the WWTP inlet flow rate during CWWF.

8.2. Performance analysis

In the following the performance of the integrated FPC approach for system-wide control of WCTSSs will be compared to the results of the chosen reference scenarios presented before. Performance is calculated according to Equation 8-1. In the results, reference scenario performance results excelling the present FPC approach get a positive sign, performances worse than the presented FPC approach get a negative sign.

$$\frac{(y_{Ref,i} - y_{FPC})}{y_{FPC}} \quad \text{Equation 8-1}$$

The event-specific evaluation period to calculate the WWTP performance during CWWF is chosen according to the longest hydrograph of all reference scenarios. For CWWF event-specific evaluations, corresponding to the CSO evaluation, the WWTP CWWF influenced period is chosen to be similar to the CWWF influent period.

The WWTP reference inflow has a significant impact on the emptying time of retention tanks. Consequently, smaller WWTP reference inflows can cause overlaps in the WWTP inflow hydrograph while larger WWTP reference inflows do not. In order to analyze and compare isolated CWWF events, some CWWF events according to the rainfall time series of June 2012 must be aggregated. Table 8-2 describes the aggregation.

Table 8-2: Aggregation of CWWF events for the rainfall time series of June 2012

Aggregated events	Single events
1	1
2	2
3	3, 4, 5
4	6
5	7
6	8
7	9
8	10, 11

8.2.1. Integrated combined wastewater balance

In order to evaluate the performance of the presented FPC approach for the system-wide control of rural WCTSSs from an integrated point of view, the ratio of combined wastewater treated at the WWTP and spilled into receiving waters according to CSO is investigated in the following. Table 8-3 summarizes event-specific combined wastewater volumes and pollution loads for the rainfall time series of August 2011. Figure 8-1 shows the

corresponding relative results of sewer network control according to the comparison of CSO volumes and CWWF loads discharged to the WWTP. The product of the event-specific distribution between CSO loads and WWTP influent loads according to Figure 8-1 and the total event-specific CWWF load according to Table 8-3 gives event specific absolute CSO load resp. CWWF load discharged to the WWTP. Table 8-4 and Figure 8-2 show the corresponding results for the rainfall time series of June 2012.

Table 8-3: Event-specific CWWF volumes and pollution loads according to the rainfall time series of August 2011

Event [-]	CWWF			
	Volume [m ³]	L _{COD} [kg]	L _{TKN} [kg]	L _{NH4-N} [kg]
20110801 (#1)	6301	822	43	17
20110802 (#2)	4860	703	53	28
20110803 (#3)	4651	526	38	19
20110804 (#4)	4939	911	50	17
20110805 (#5)	6863	1614	76	23
TOTAL	27613	4575	261	103

For all CWWF events in August 2011 the results show a similar performance ranking with respect to volumetric WWTP loading resp. CSO discharge. The event-specific WWTP loading equivalently increases as the CSO decreases. In average, the presented FPC approach outperforms reference scenarios Ref1, Ref2 and Ref4. Despite the conflicting objectives concerning homogeneous WWTP loading presented in section 7.3, the results show that the presented FPC approach competes with reference scenario Ref3 for continuous maximized WWTP loading according to the maximum SST hydraulic capacity of 5340 m³/d per treatment lane. Despite similar mean reference WWTP inflows, the FPC approach shows in average ten percent less CSO volume compared to reference scenario Ref4 indicating the potential of the presented integrated FPC approach regarding sewer network FPC. Neither the presented FPC approach nor the reference scenario is able to avoid CSO in any of the CWWF events for the rainfall time series of August 2011. With respect to the simulation results of scenario Ref1 the model confirms relative CSO volumes of 30 to 85% of the total CWWF volumes resp. pollution loads between 10 and 60% of the total CWWF loads observed during the monitoring campaign. The results with respect to CSO pollution loads show a similar scenario performance ranking, except for event 20110805. This principally confirms the findings according to sewer network FPC (see section 7.3) that volumetric CSO minimization linearly correlates with CSO pollution load minimization.

Event-specific CSO volumes from the CWWF events according to the rainfall time series of June 2012 (see Figure 8-2) principally confirm the hydraulic performance observed for the events of August 2011 giving a similar performance ranking concerning hydraulic CSO load reduction. Due to the comparatively poor performance of the FPC approach during the heaviest storm event #5 the total CSO volume reduction performance for June 2012 compared to the reference scenarios shows a poorer performance for the total month as

Comparison to static control scenarios and discussion of results

compared to the total performance in August 2012. Consequently, for the total month the FPC approach shows an only slightly increased performance compared to scenarios Ref1 and Ref4. Thanks to this, it can be assumed that during such heavy storm events constant retention tank discharges perform better as the proposed FPC approach.

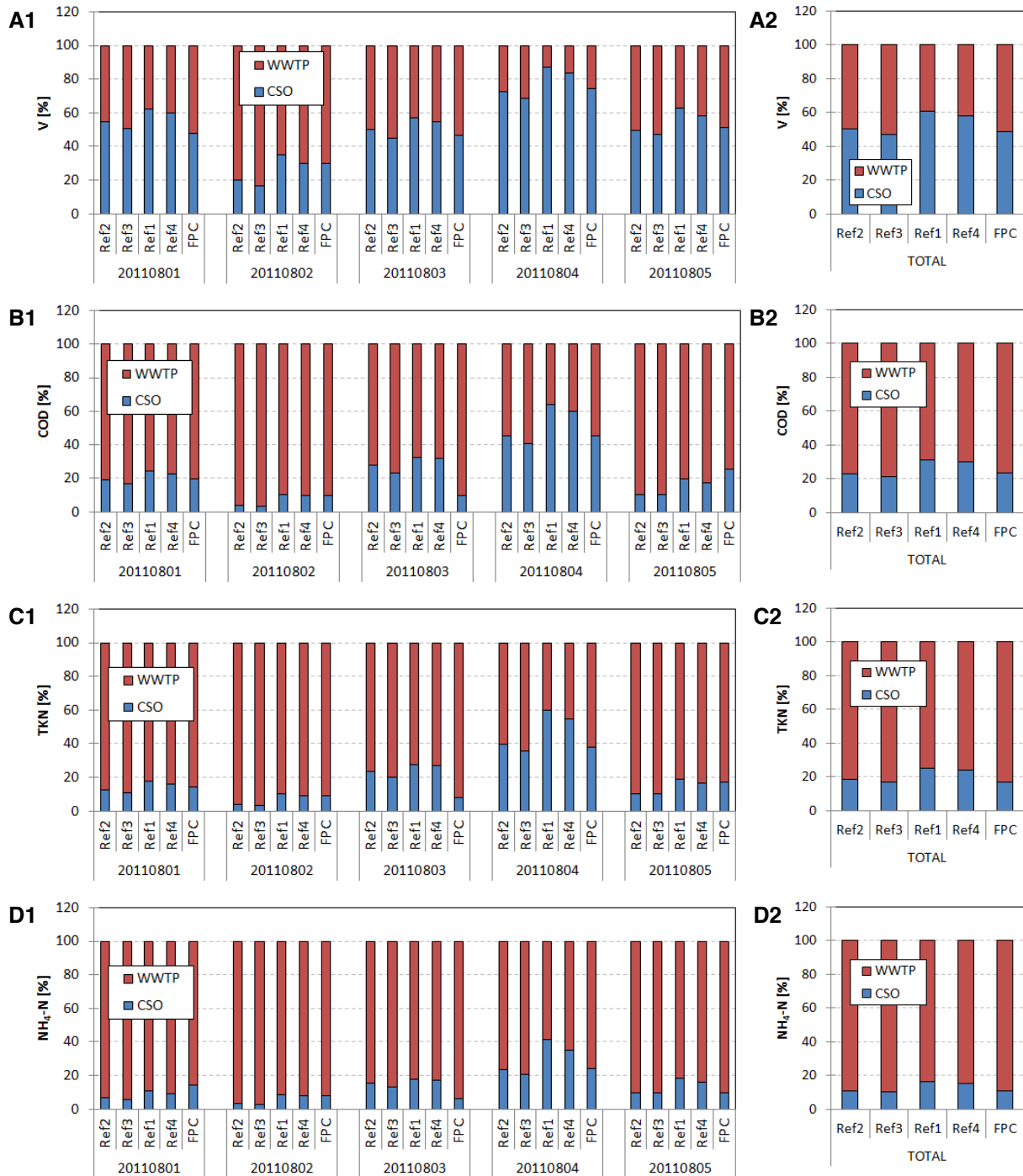


Figure 8-1: Event-specific (1) and total (2) ratios of CWWF treated at the WWTP and CSO for each scenario according to rainfall time series August 2011 (A: Volume, B: COD, C: TKN, D: NH_4-N)

Table 8-4: Event-specific CWWF volumes and pollution loads according to the rainfall time series of June 2012

Event [-]	CWWF			
	Volume [m ³]	L _{COD} [kg]	L _{TKN} [kg]	L _{NH4-N} [kg]
20120601 (#1)	8413	998	66	30
20120602 (#2)	1228	91	8	4
20120603 (#3)	12480	1125	82	40
20120604 (#4)	4079	688	48	24
20120605 (#5)	21353	1745	90	29
20120606 (#6)	1500	161	11	5
20120607 (#7)	3981	1556	40	1
20120608 (#8)	5136	985	59	22
TOTAL	58168	7349	403	156

Despite these hydraulic performance results showing at least small hydraulic CSO reduction improvements compared to scenarios Ref1 and Ref4, the corresponding total CSO pollution loads show even poorer performances under the FPC approach in June 2012. This is predominantly due to the results of the FPC approach for the CWWF events #7 and #8 which show very large CSO pollution loads compared to all reference scenarios. Since the hydraulic performance of the FPC approach shows good results, competing with scenario Ref3, this performance is contradictory to the findings of correlating MF objectives regarding CSO volume minimization and CSO load minimization presented in section 7.3.6 during CWWF. Possible underlying causes are investigated in the following section.

Comparison to static control scenarios and discussion of results

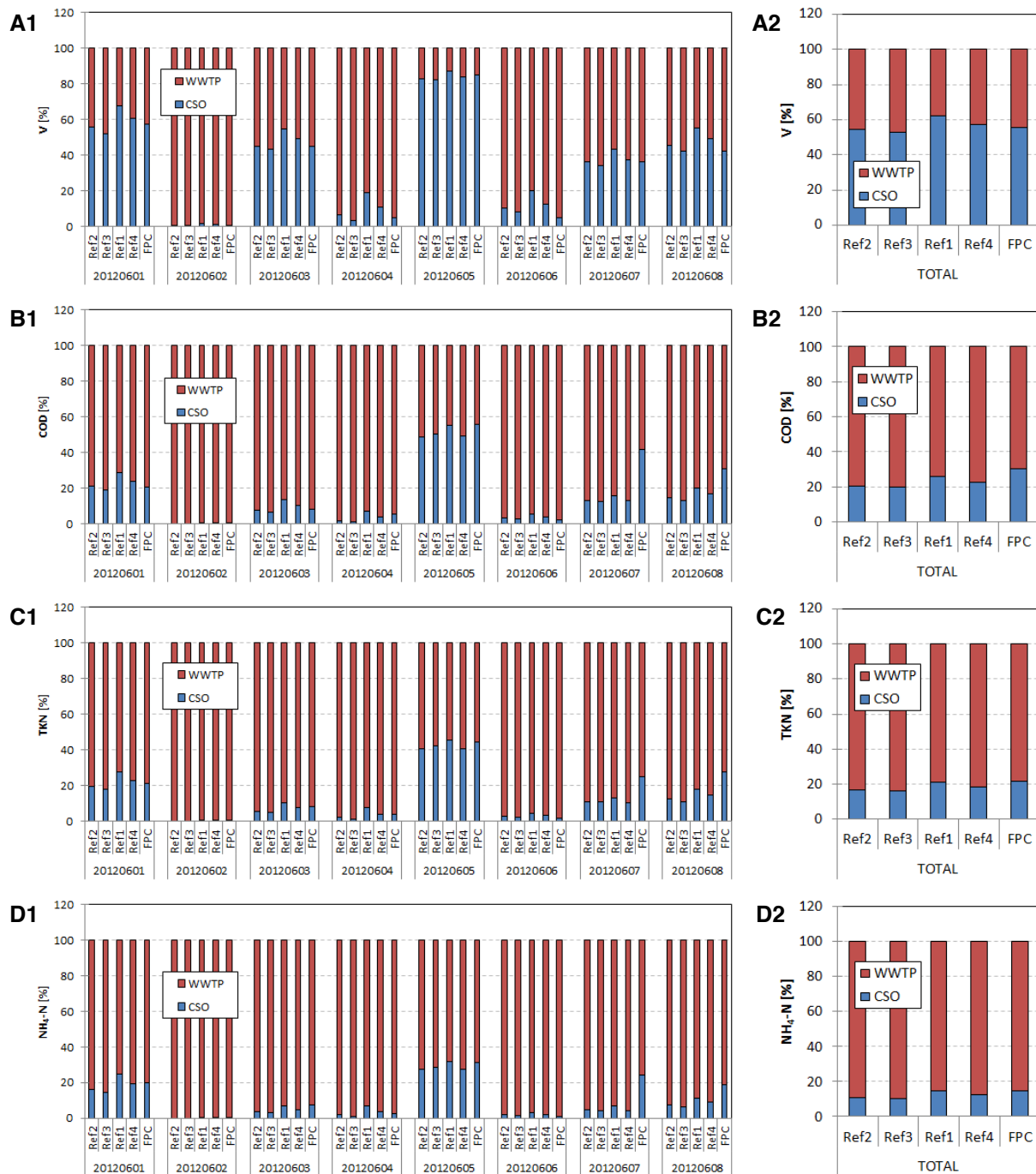


Figure 8-2: Event-specific (1) and total (2) ratios of CWWF treated at the WWTP and CSO for each scenario according to the rainfall time series of June 2012 (A: Volume, B: COD, C: TKN, D: $\text{NH}_4\text{-N}$)

8.2.2. Combined sewer network

Since COD and TSS resp. COD and BOD_5 concentrations are highly correlated during CWWF (see section 6.2.3.2), the presented results of CSO pollution concentrations could be limited to COD, TKN and $\text{NH}_4\text{-N}$.

The analysis of CWWF event-mean CSO concentrations according to Figure 8-3 for the rainfall time series of August 2011 and Figure 8-4 for the rainfall time series of June 2012 reveal strongly increased COD, TKN and $\text{NH}_4\text{-N}$ concentrations for the events #5 of August

2011 and #4, #7 and #8 of June 2012. In the case of June 2012 CWWF event #7 CSO concentrations are even close to DWF concentrations. These high CSO pollution concentrations explain the increased CSO pollution loads for these events leading to a relatively poorer performance compared to the corresponding hydraulic performance.

As described in section 6.3.3 retention tanks are modeled as online bypass tanks in the hydrologic sewer network reference model. Hydrologic sewer network models sometimes inadequately model backwater effects. Due to the computational effort of the integrated simulation reference model and the integrated FPC approach, sewer pipes in the reference simulation model are simply modeled according to the translation of wastewater. In the case of ponded retention tanks the upstream local sewer network should also be ponded according to the corresponding water level. Translative sewer network models do not model the storage available within the pipe. Consequently, CSO occurs immediately if retention tanks are filled completely. In order to still model back water effects, this lack is compensated by using virtual retention tanks upstream of the real retention tanks with complete mixing of DWF and RWF. The virtual retention tank volume is calibrated according to the estimated monthly CSO volume (see section 7.3.2).

In the case of bypass retention tanks, CSO pollution concentrations are similar to the influent concentrations coming from the upstream local sewer network. Due to the manner of functioning of sewer network FPC, CSO is minimized according to the optimized use of retention tank volume. In the case of unavoidable CSO, this is delayed according to the use of the present total retention tank capacity. Thanks to dilution, pollution concentrations thereby decrease along CWWF events before dilution decreases at the end of the event and DWF starts again.

For the presented events showing increased event-mean CSO pollution concentrations, some retention tanks are still completely filled towards the end of the CWWF events (due to the conflicting objective of homogenizing the hydraulic WWTP loading) and thus cause CSO with important fractions of DWF. Due to the fact that even for bypass retention tanks the upstream local sewer network must be filled according to the corresponding weir crest level of the CSO structure to cause CSO, the chosen virtual retention tank volume can be assumed to be insufficient in these specific cases.

The results from the hydraulic calibration of the necessary virtual retention tank volume according to estimated CSO volumes from measured water levels emphasize the need for event-specific virtual retention tank volumes. The unrealistic reference simulation model behavior discussed above could be avoided by either choosing a different approach for the reference simulation model such as hydrodynamic approaches or alternatives as proposed by Solvi et al. (2005) or by using larger virtual retention tank volumes. Since the virtual retention tank volume is calibrated according to hydraulic observation (see section 7.3.2) this inevitably affects CSO volumes and loads.

In the case of sufficient virtual retention tank volume resp. smaller CWWF events the results principally correspond to the investigated correlation between the objectives of CSO volume minimization and CSO pollution load minimization.

Comparison to static control scenarios and discussion of results

Figure 8-5 and Figure 8-6 illustrate the nonlinear regression between CWWF event-specific CSO volumes and CSO pollution loads according to FPC resp. the reference scenarios Ref1 to Ref4 considering the CWWF events of August 2011 and June 2012.

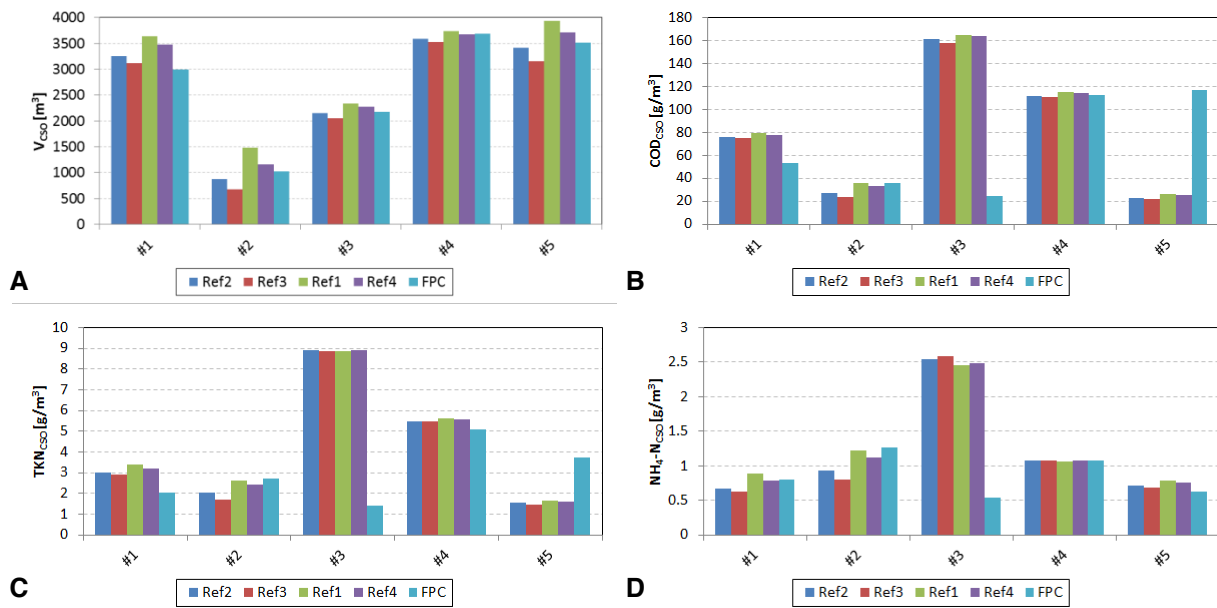


Figure 8-3: Event-specific comparison of aggregated CSO volumes and event mean CSO concentrations for the rainfall time series of August 2011 (A: Vol, B: COD, D: TKN, E: NH₄-N)

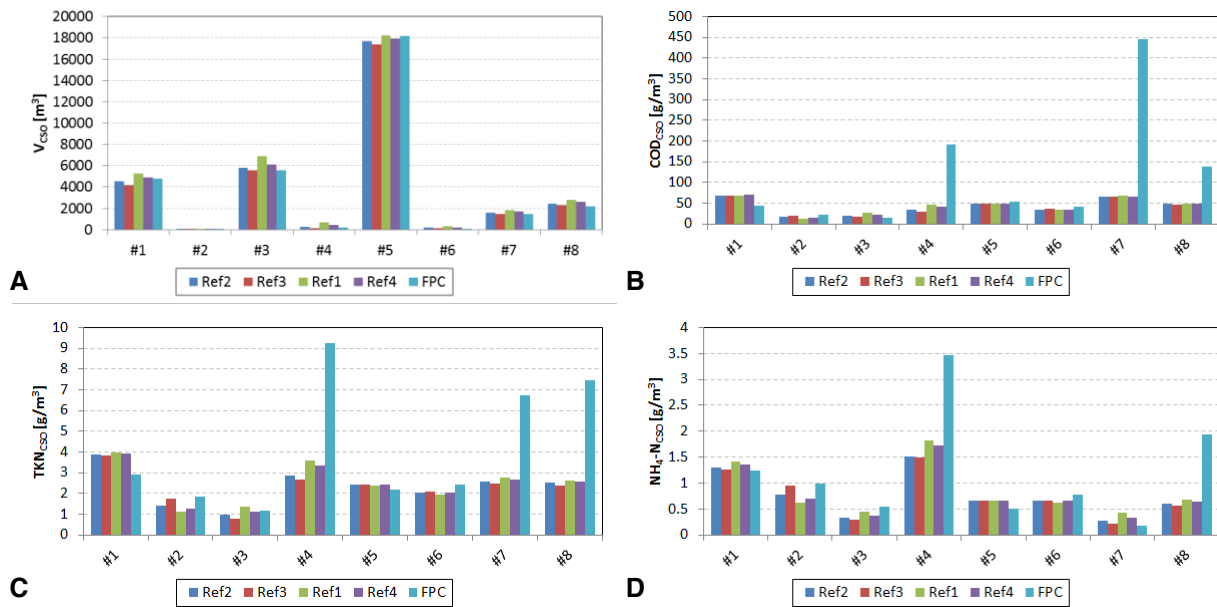


Figure 8-4: Event-specific comparison of aggregated CSO volumes and event mean CSO concentrations for the rainfall time series of June 2012 (A: Vol, B: COD, D: TKN, E: NH₄-N)

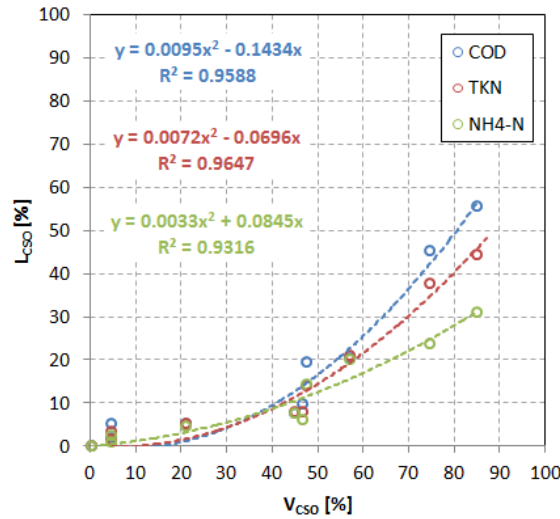


Figure 8-5: Nonlinear regression between event-specific CSO volumes and CSO loads according to FPC

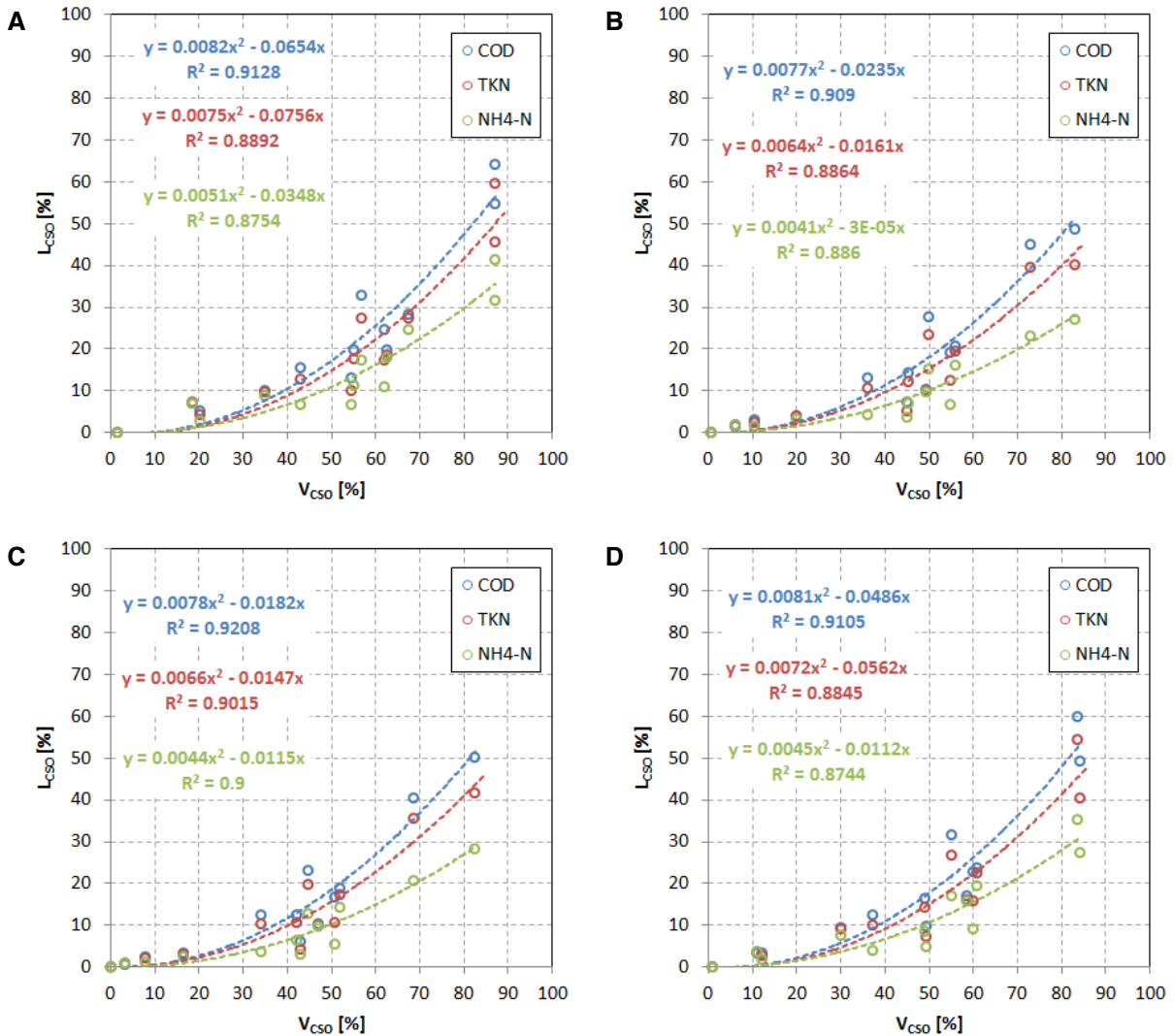


Figure 8-6: Nonlinear regression between event-specific CSO volumes and CSO loads according to reference scenarios (A) Ref1, (B) Ref2, (C) Ref3 and (D) Ref4

Comparison to static control scenarios and discussion of results

In the case of FPC the CWWF events #5 of August 2011 and #7 and #8 of June 2012 are not considered due to the described atypical behavior concerning CSO pollution loads which is explained to be caused by the reference simulation model. CSO volumes and loads are described as a percentage of the corresponding event-specific total CWWF load. All results show a similar nonlinear regression between event-specific CSO volumes and CSO loads which is described by a second order equation.

Due the observed scenario independent relation between CSO volumes and CSO pollution loads it can be reasoned that the online bypass retention tank predominantly retain the first flush of CWWF events. For example, CSO volumes equal to 40% of the total CWWF volume correspond to COD CSO loads of only 10% of the total COD load during the specific CWWF event. This corresponds to the short first-flush peaks observed during the measurement campaign (see Figure 6-44). Since for online bypass tanks CSO pollution concentrations are equal to the retention tank influent concentrations CSO concentrations are predominantly low due to the diluted CWWF after the first flush peak. While the results according to Ref1 to Ref4 (Figure 8-6) show a similar coefficient of determination of $R^2 \sim 0.9$ for COD, TKN resp. $\text{NH}_4\text{-N}$, the corresponding results according to sewer network FPC show coefficients of determination of $R^2 = 0.96$ for COD, $R^2 = 0.96$ for TKN resp. $R^2 = 0.93$ for $\text{NH}_4\text{-N}$ (Figure 8-5). This confirms the findings for FDM that the objectives of CSO volume minimization and CSO pollution load minimization convergent within each control step especially when the CWWF retention tank influents are diluted (see Figure 7-14, Figure 7-28 and Figure 7-36). Consequently, in the dilution phase where CSO pollution load reduction can be assumed to be predominantly correlated to CSO volume reduction, an additional CSO pollution load reduction according to the global nonlinear regression is only possible through the delaying of CSO in the case of unavoidable CSO. Thereby, the reserve capacity within the dilution phase is limited according to the event-specific convergent dilution concentration of the retention tank influent. In order to make use of the correlation between CSO volumes and loads CSO volume reduction must be continuous. Thanks to this correlation, the presented hydraulic based FPC approach shows increased CSO pollution load reductions based on the reduction of CSO volumes, even in the case of unavoidable CSO, by delaying CSO according to the optimized use of retention tank capacities. Consequently, the negative impact of the presented FPC approach shown before can be corrected considering similar additional benefits according to the demonstrated hydraulic performance.

Comparable studies principally confirm the nonlinear behavior between CSO volumes and CSO loads (Lau *et al.* 2002). Consequently, the authors question the common approach to use CSO spill volume and frequency as indicator of the receiving water quality impact. Modeling studies on rule-based real-time control approaches considering wastewater quality show that minimizing the CSO volume not necessarily minimizes the CSO pollution load (e.g. Lacour and Schütze (2011), Weinreich et al. (1997)). The results of the FDM between objectives to minimize CSO volumes and COD pollution loads and the comparison to reference scenarios illustrate the limitations of hydraulic-based real-time control approaches to minimize CSO pollution loads.

The present CSO volume reduction results correspond to the investigations of Fiorelli et al. (2013) for heavy rainfall using a convex sewer network MPC approach. Both studies use the

same sewer network case study. This confirms the performance of the present nonlinear FPC approach for sewer network real-time control. In the present case, the chosen now-cast approach, based on the assumption of 10 minutes continuous inflow to retention tanks, could be optimized using rainfall runoff predictions based on rainfall radar forecasting (Petrucek *et al.* 2003) and stochastic approaches taking prediction uncertainties into account (Löwe *et al.* 2012). For the present case study, detailed rainfall forecast approaches would additionally provide 5 to 12% of CSO volume reduction (Fiorelli *et al.* 2013).

Performance data reported in literature on MPC-based CSO reduction is rare. Available data ranges between 26% for CSO reduction on a yearly basis (Gelormino and Ricker 1994) and up to total CSO prevention reported for single events (Pleau *et al.* 2005). Besides the applied prediction model and control approach (Heusch 2011), the CSO reduction potential additionally depends on design assumptions for retention tank volumes. Altogether, the case study principally shows large CSO volumes. Consequently, the total efficiency obtained here with the presented FPC is rather small compared to reported results from literature. This can be explained by the reduced retention tank volumes for rural catchments according to the applied German design guideline (DWA 1992a) and the chosen rainfall time series representing average and increased monthly rainfall. This is confirmed by the reference control scenarios Ref1 to Ref4 which also were not able to totally prevent CSO for the investigated time series. Currently, the Luxembourg water administration gets aware of the reflectively high CSO according to reduced retention tank volumes in rural catchments. The discussion on the future application of reduced retention tank volumes in rural catchments in Luxembourg is ongoing.

Reported CSO reductions according to MPC and the results of the reference scenarios Ref2 and Ref3 emphasize the findings that in the case of system-wide control of WCTs, especially in rural catchments, with reduced retention tank volumes and absence of retention tank volume at the WWTP affects CSO minimization due to the inhomogeneous distribution of flow times from each retention tank to the WWTP and conflicting objectives for CSO volume minimization.

Additionally, the present findings emphasize the importance of pollution load models considering first flush effects in the performance evaluation of system-wide control approaches for integrated WCTs. Uncertainties from model simplifications that are necessary especially in the case of complex integrated WCTs, can lead to wrong performance evaluations of control approaches. The importance of representative model simplifications was investigated in detail by (Meirlaen *et al.* 2002).

8.2.3. Wastewater treatment plant

While in the present case the aeration of the WWTP during DWF is operated intermittently for the optimized control of nitrification and denitrification (Chachuat *et al.* 2005), during CWWF aeration control is switched to continuous operation at a lower DO set-point for simultaneous nitrification and denitrification. General details on simultaneous nitrification-denitrification are provided for instance by Trivedi (2009). This operational modification is predominantly done to simplify the MPC approach for optimized aeration during CWWF. By switching to continuous aeration with simultaneous nitrification and denitrification the

optimization problem is reduced from four variables (the set-point for DO and the cycle time with corresponding nitrification and denitrification periods) to one variable (the set-point for DO). As shown in Figure 6-46 the DO concentration in oxidation ditches decreases along the flow path during continuous aeration. By adapting the DO set point of the aeration system aerobic and anoxic zones occur in parallel in the AST according to the respective DO-profile along the oxidation ditch. It is the objective of the present FPC approach to optimize the DO set-point in a feed-back control loop for the predicted hydro- and pollutograph according to the Lagrangian ISN observer model. Studies on simultaneous nitrification-denitrification for WWTPs with extended aeration for instance by Bertanza (1997) and Collivignarelli and Bertanza (1999) to increase the nitrogen treatment performance show good results comparable to conventional treatment. The obtained results confirm the feasibility of simultaneous nitrification-denitrification for the control of oxidation ditches with SASS during CWWF.

8.2.3.1. Pollution removal

Mean monthly CWWF loads – August 2011

In the presented FPC approach, the current WWTP capacity is determined according to nonlinear MPC and an objective function based on FDM for system-wide control of the integrated WCTS. Besides the objective to maximize the WWTP reference inflow during CWWF with respect to the present legal effluent concentration limits according to Table 7-4, additional recommendations concerning SASS are taken into account in the FDM process. Table 8-3 summarizes the monthly CWWF loads for the rainfall time series of August 2011. Differences in wastewater volumes and pollution loads result from different CSO volumes due to scenario specific WWTP reference inflows. Figure 8-1 illustrates the scenario-based differences in wastewater volumes and pollutant loads discharged to the WWTP per CWWF event according to the rainfall time-series of August 2011.

Besides the adaptive hydraulic loading, the main difference between the presented FPC approach and the chosen reference scenarios based on control according to constant set-points is the FPC of the DO set-point optimization at the WWTP. Consequently, the decision-making is translated into two variants of reference scenarios (see section 8.1). Table 8-5 summarizes the results of monthly pollution loads treated at the WWTP during CWWF and corresponding mean effluent concentrations concerning COD, S_{NH} and TN for the presented FPC approach and both variants of all reference scenarios according to the rainfall time series of August 2011.

Table 8-5: Monthly pollutant loads treated at the WWTP during CWWF and corresponding mean effluent concentrations according to rainfall time series August 2011

Variant	Scenario	TSS _{Eff}		COD _{Eff}		BOD _{5,Eff}		TN _{Eff}		NH ₄ -N _{Eff}	
		[kg]	[g/m ³]	[kg]	[g/m ³]	[kg]	[g/m ³]	[kg]	[g/m ³]	[kg]	[g/m ³]
	FPC	344	22.6	577	39.7	213	14.6	53	3.7	17	1.3
DO _{AST}	Ref1	181	18.8	361	38.2	133	14.1	40	4.2	20	2.1
	Ref2	313	23.0	567	43.6	209	16.1	59	4.6	27	2.2
	Ref3	376	25.2	663	46.6	245	17.2	67	4.8	30	2.2
	Ref4	214	20.7	407	40.3	150	14.9	44	4.4	21	2.1
SNH _{AST}	Ref1	181	18.8	332	35.2	122	13.0	35	3.6	9	0.9
	Ref2	314	23.0	519	39.5	191	14.6	51	3.9	13	1.1
	Ref3	377	25.2	604	41.9	223	15.5	57	4.0	15	1.1
	Ref4	214	20.7	375	37.2	138	13.7	38	3.8	10	1.0

Figure 8-7 and Figure 8-8 illustrate the corresponding event-specific results for five CWWF events. Due to the large SRT of 25 days and the extended aeration for SASS, all scenarios principally show good pollution treatment results, with performances comparable to each other. All scenarios and variants respect the legal effluent concentration limits according to Table 7-4. The analyzed wastewater treatment performance expressed in removal percent according to Figure 8-7 and Figure 8-8 is in the range of 60 to 90%.

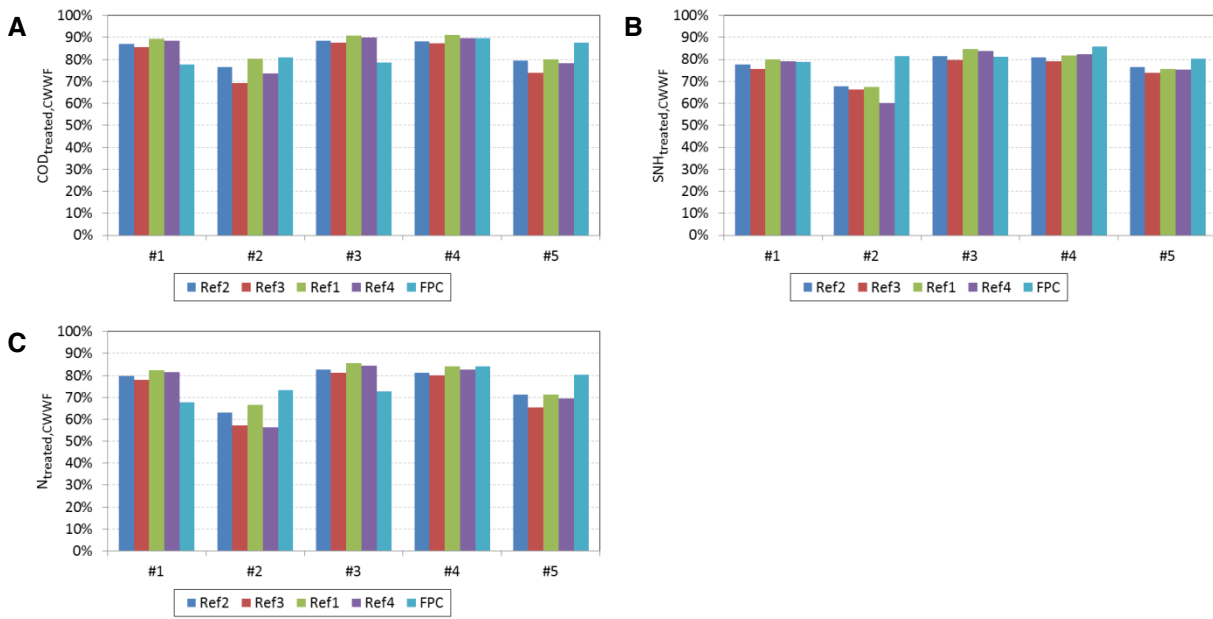


Figure 8-7: Event-specific scenario comparison of the WWTP CWWF performance according to the rainfall time series of August 2011 variant DO_{set,CWWF} = 0.7 g/m³ (A = COD, B = NH₄-N, C = TN)

Comparison to static control scenarios and discussion of results

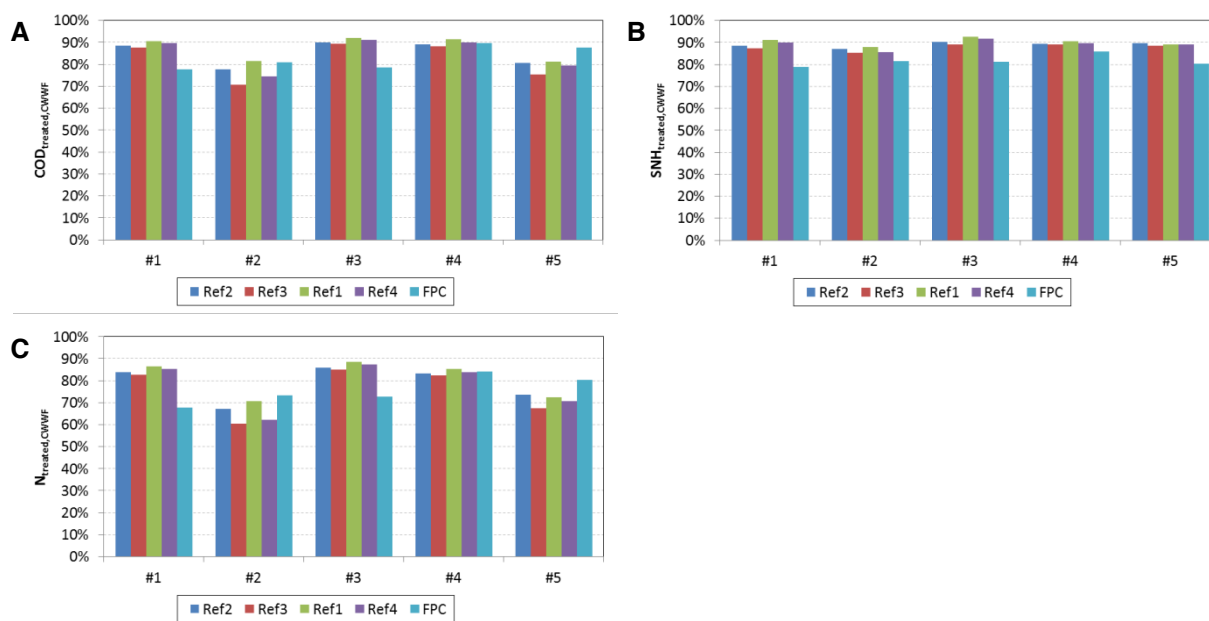


Figure 8-8: Event-specific scenario comparison of the WWTP CWWF performance according to the rainfall time series of August 2011 variant $SNH_{AST,CWWF} = 1.0 \text{ g/m}^3$ (A = COD, B = $NH_4\text{-N}$, C = TN)

This is comparable to the long-term performance of WWTPs investigated e.g. by Giokas et al. (2002) and Makinia et al. (2005). Thanks to extended aeration, low-loaded WWTPs with SASS perform quite robust during CWWF by providing sufficient oxygen for constant nitrification, even during long hydraulic peak loading as evidenced by the results of reference scenario Ref3.

Comparing the S_{NH} removal results with respect to both reference variants the presented FPC approach shows a good balance between the recommended aeration for SASS during CWWF according to variant $DO_{AST,CWWF}$ and the recommended nitrification for SASS according to variant $SNH_{AST,CWWF}$. Concerning the S_{NH} treatment variant $SNH_{AST,CWWF}$ increases the nitrification in the reference scenarios in average by 48 percent. Given the already good nitrogen removal during CWWF according to variant $DO_{AST,CWWF}$, variant $SNH_{AST,CWWF}$ increases the TN treatment about five percent. Thanks to sufficient aeration according to variant $DO_{AST,CWWF}$, variant $SNH_{AST,CWWF}$ has no impact on COD removal. Further comparison of the aeration effort in section 8.2.3.3 will help to better understand the benefits of the developed FPC approach in comparison to the conventional control approaches.

While other studies on integrated control of WCTs report sporadic WWTP treatment failures due to limited nitrification capacities (e.g. Meirlaen (2002)), nitrification limits are no problem in the present case thanks to extended aeration for SASS during CWWF.

Increased monthly CWWF loads – June 2012

The simulation results of the rainfall time series of June 2012 according to Table 8-6 and Table 8-7 resp. Figure 8-9 to Figure 8-10 principally confirm the findings from the simulation results of the rainfall time series of August 2011. The results show a good and robust wastewater treatment even during increased CWWF loading. Again, main treatment

differences can be made out concerning ammonium effluent concentrations according to the investigated variants $DO_{AST,CWWF}$ and $SNH_{AST,CWWF}$. Due to feedback control of the aeration process, effluent concentrations for all pollutants again show good results, in a comparable range for all investigated scenarios. Again all legal effluent concentration limits (Table 7-4) are respected. Due to the general good performance of all scenarios, impacts of increased CWWF treatment will be investigated according to respective aeration efforts.

Table 8-6: Monthly CWWF WWTP effluent loads and mean concentrations according to rainfall time series June 2012

Variant	Scenario	TSS _{Eff}		COD _{Eff}		BOD _{5,Eff}		TN _{Eff}		NH ₄ -N _{Eff}	
		[kg]	[g/m ³]	[kg]	[g/m ³]	[kg]	[g/m ³]	[kg]	[g/m ³]	[kg]	[g/m ³]
	FPC	592	22.2	937	35.7	346	13.2	93	3.6	29	1.2
DO _{set}	Ref1	377	17.2	692	31.8	255	11.7	76	3.5	32	1.5
	Ref2	591	21.0	995	36.0	367	13.3	103	3.8	41	1.6
	Ref3	690	23.3	1115	38.5	411	14.2	111	3.9	43	1.6
	Ref4	496	19.4	863	34.2	318	12.6	92	3.7	38	1.5
SNH _{set}	Ref1	364	16.6	642	29.4	237	10.9	82	3.8	16	0.8
	Ref2	571	20.2	911	32.8	336	12.1	106	3.8	21	0.8
	Ref3	666	22.5	1019	35.0	376	12.9	112	3.9	22	0.8
	Ref4	480	18.8	795	31.4	293	11.6	95	3.8	19	0.8

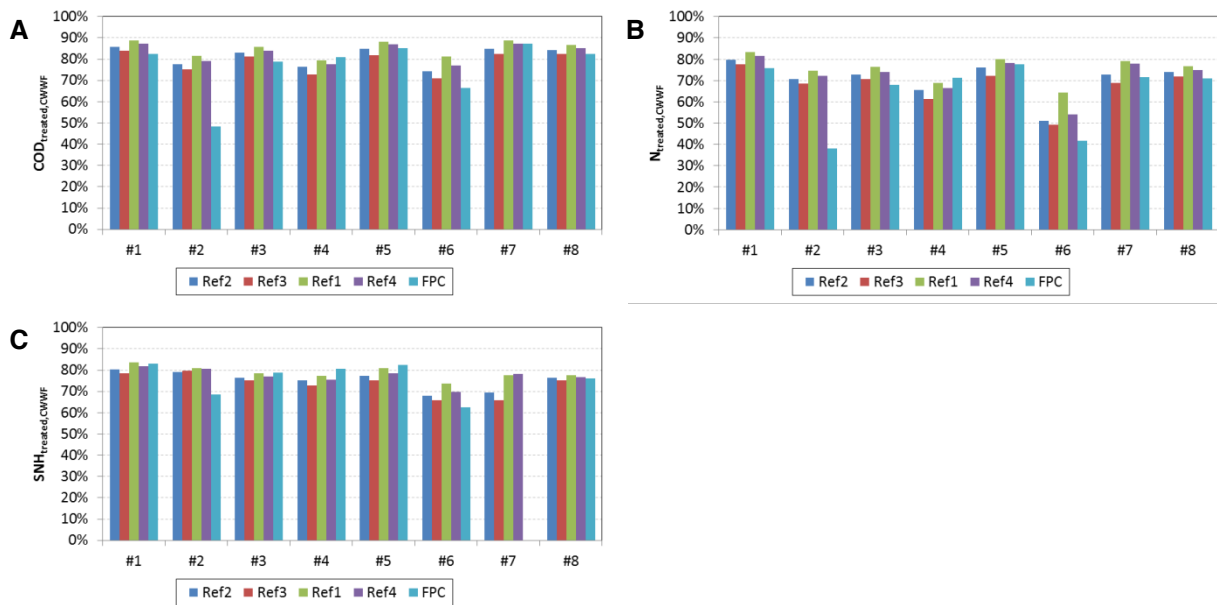


Figure 8-9: Event-specific scenario comparison of the WWTP CWWF performance according to the rainfall time series of June 2012 variant $DO_{set,CWWF} = 0.7 \text{ g/m}^3$ (A = COD, B = NH₄-N, C = TN)

Comparison to static control scenarios and discussion of results

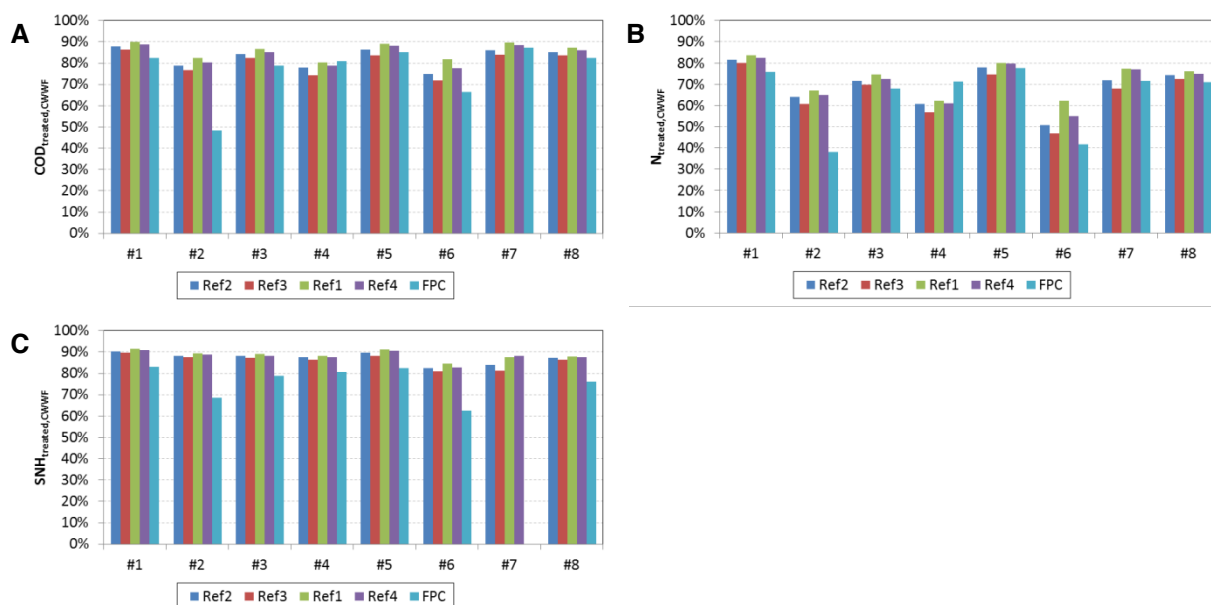


Figure 8-10: Event-specific scenario comparison of the WWTP CWWF performance according to the rainfall time series of June 2012 variant $SNH_{AST,CWWF} = 1.0 \text{ g/m}^3$ (A = COD, B = TN, C = $NH_4\text{-N}$)

8.2.3.2. Hydraulic loading

Modeling studies of SST based on one-dimensional dynamic models such as the one by Takács *et al.* (1991) show increased hydraulic capacities compared to static design standards based on steady state assumptions (Joannis *et al.* 1999). Simplified, SSTs can be vertically separated into four zones. From top to bottom these are: (1) the clarification zone with effluent pollutant concentrations X_e , (2) the dilution zone with diluted pollutant concentrations X_f , (3) the thickening zone with sludge blanket concentrations X_{sb} and the compression zone with return sludge concentrations X_r (Stamou *et al.* 2008). The sludge blanket level separates the thickening zone from the dilution zone. The feed point, where wastewater from the AST enters the SST, is usually located between the clarification zone and the dilution zone. Disturbances of the sludge blanket level occur as a result of the entrance of mixed liquid from the AST diluting sludge in the compression and thickening zones. Thereby, settled sludge is displaced into the upper zones of the SST. Especially in the context of integrated control these dynamics define the current hydraulic capacity of the WWTP and consequently the WWTP reference inflow for sewer network control in system-wide approaches for WCTSS.

Compared to modeling results from Stamou *et al.* (2008), for instance, Figure 7-21 shows only thin compression and thickening zones in the SST. The hydraulic capacity of the SST is analyzed according to the regression between MF values for the hydraulic loading and MF values for TSS effluent concentrations. Thereby, TSS MF values equal to one represent the maximum legal effluent concentration. Correlation analysis according to Figure 7-22, Figure 7-33 and Figure 7-41 reveal a linear relation between the hydraulic WWTP loading and corresponding SST TSS effluent concentrations convergent at 60% of the maximum ISN hydraulic capacity. In comparison to WWTPs with anaerobic sludge digestion, low loaded

WWTPs with SASS show less sludge production. Consequently, sludge blanket level height dynamics predominantly result from hydraulic shock loadings.

In the present case the oversized SST tank additionally might contribute to the observed correlation between the hydraulic loading and effluent TSS concentrations.

Figure 8-11 shows the analysis of the WWTP hydraulic capacity estimation during CWWF according to rainfall time series (A) August 2011 and (B) June 2012. The four-dimensional regression analysis shows the corresponding DO set-point and nitrification optimization according to the objectives of SASS to simultaneously optimize the hydraulic loading. The results of both rainfall time series predominantly show hydraulic capacities according to the maximum capacity from the correlation with TSS effluent concentrations. The DO set-point optimization adapts the aeration to TKN influent loads to be expected and AST S_{NH} concentrations optimized concerning SASS. Reduced hydraulic capacities predominantly result from emptying retention tanks due to the ISN states for the integrated WWTP capacity estimation. The corresponding histograms demonstrate the TSS effluent concentrations as the dominating criteria within the integrated capacity estimation for hydraulic loading.

Overall, especially the results from the reference scenario Ref3 confirm the hydraulic capacity proposed by the FPC approach. Due to the FDM of conflicting objectives regarding sewer network FPC reduces the hydraulic load discharged to the WWTP.

Comparison to static control scenarios and discussion of results

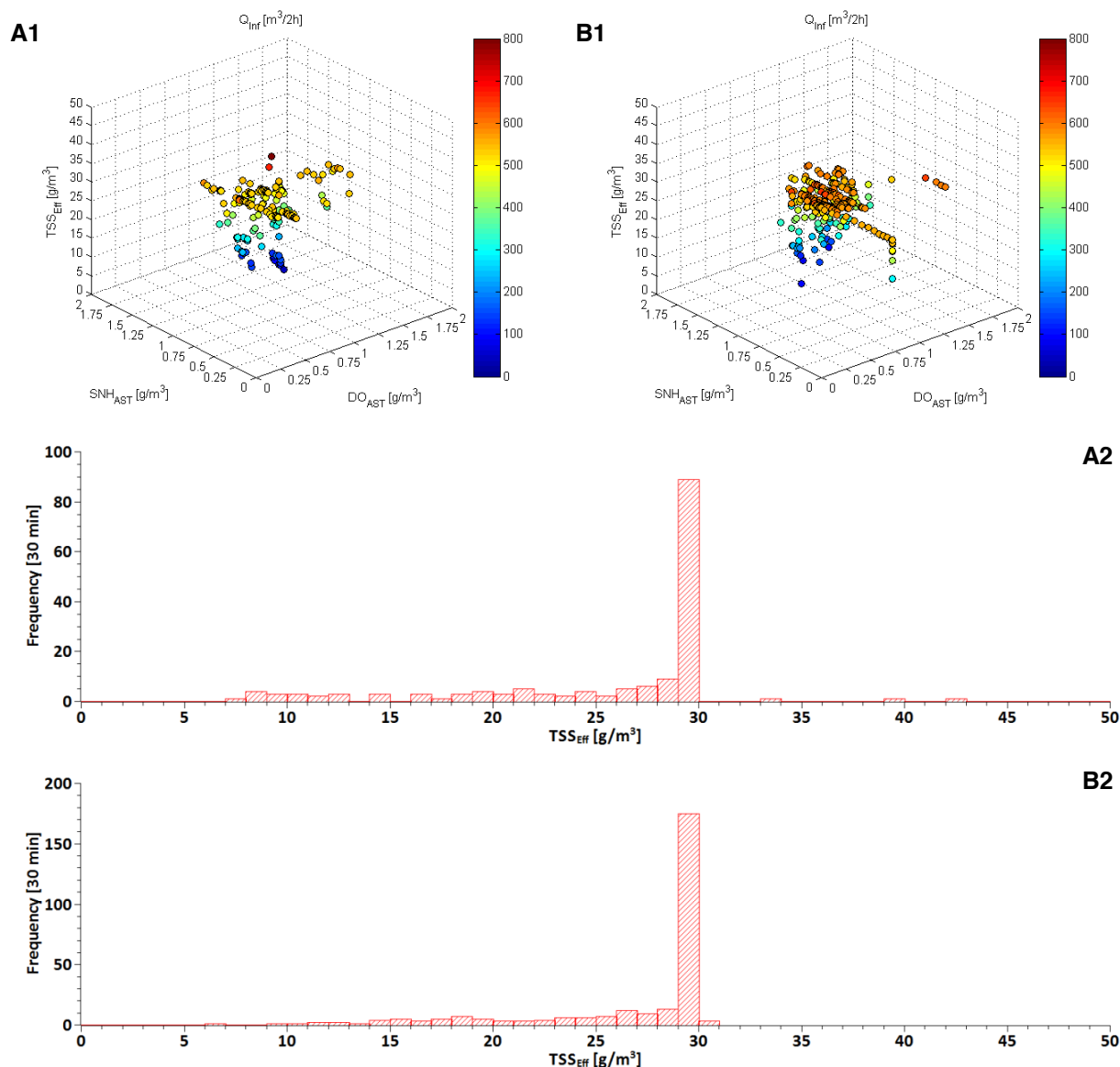


Figure 8-11: WWTP hydraulic capacity estimation according to rainfall time series (A) August 2011 and (B) June 2012 (1: correlation of SNH_{AST} , DO_{AST} and TSS_{Eff} , 2: frequency analysis)

8.2.3.3. Aeration effort

The evaluation of all scenarios and variants shows that the target DO concentration of 0.7 g/m³ recommended for CWWF treatment is sufficient to provide nitrogen treatment assigned by legal WWTP effluent demands. Additionally taking a NH₄-N-reference value of 1 g/m³ in the AST into account to enhance SASS, the FPC approach suggests mean DO set-points up to +75% in comparison to the reference DO set-point, depending on the nitrogen loading during CWWF and the FDM for nitrification. Table 8-7 summarizes the results.

Due to the large SRT of 25 days and extended aeration, the treatment of COD and N is good for all scenarios. All results are below the legal effluent concentration limits. Consequently, the evaluation of treatment costs, especially according to aeration and WAS production, get increased importance. The advantage of the FPC approach is to balance the objectives of SASS according to $DO_{set} = 0.7$ g/m³ and $S_{NH} = 1.0$ g/m³ in the oxidation ditch. Table 8-8

summarizes the comparison of the monthly aeration effort for each scenario and variant according to the rainfall time series of August 2011.

Table 8-7: Results DO set-point optimization

Month	Event	DOset [g/m^3]	
		MEAN	STD
August 2011	#1	0.79	0.02
	#2	0.93	0.16
	#3	0.99	0.20
	#4	1.23	0.45
	#5	0.85	0.23
June 2012	#1	0.79	0.02
	#2	0.93	0.16
	#3	0.99	0.20
	#4	1.23	0.45
	#5	0.85	0.23
	#6	0.79	0.02
	#7	0.93	0.16
	#8	0.99	0.20
	#9	1.23	0.45
	#10	0.85	0.23
	#11	0.79	0.02
	#12	0.93	0.16

Table 8-8: Comparison of the aeration effort during CWWF events according to rainfall time series August 2011

Variant	Scenario	V_{Air} [Nm^3]	$V_{\text{Air}}/V_{\text{Inf}}$ [Nm^3/m^3]	$V_{\text{Air}}/\text{TKN}_{\text{Inf}}$ [Nm^3/kg]	f_{COD} [%]	f_{SNH} [%]	f_{N} [%]
DO _{set}	FPC	28344	2.0	130	84	81	76
	Ref1	22029	2.3	116	87	78	79
	Ref2	24849	1.9	100	85	77	76
	Ref3	24894	1.8	96	83	76	74
	Ref4	20637	2.0	108	85	77	77
SNH _{set}	Ref1	28203	2.9	148	88	91	82
	Ref2	32224	2.4	130	86	89	80
	Ref3	32129	2.3	124	84	88	78
	Ref4	26749	2.6	140	87	90	80

Figure 8-12 illustrates the corresponding evaluation per event for both variants (A) $\text{DO}_{\text{AST,CWWF}} = 0.7 \text{ g}/\text{m}^3$ and (B) $\text{SNH}_{\text{AST,CWWF}} = 1.0 \text{ g}/\text{m}^3$. Figure 8-13 shows the corresponding linear correlations for both variants (A) $\text{DO}_{\text{AST,CWWF}} = 0.7 \text{ g}/\text{m}^3$ and (B) $\text{SNH}_{\text{AST,CWWF}} = 1.0 \text{ g}/\text{m}^3$. The analysis shows a reduced aeration effort per TKN influent load for the developed FPC control approach due to the predictive balancing of SASS objectives for $\text{DO}_{\text{AST,CWWF}} = 0.7 \text{ g}/\text{m}^3$ and $\text{SNH}_{\text{AST,CWWF}} = 1.0 \text{ g}/\text{m}^3$. Figure 8-12 shows the change of aeration effort for the reference scenarios Ref1 to Ref4 due to both variants and the comparison of the aeration effort according to FPC. Additionally to the illustration of the absolute aeration per CWWF event, the aeration effort is illustrated with respect to the CWWF influent volume and CWWF

Comparison to static control scenarios and discussion of results

influent TKN load. The results especially show the balance of the aeration effort according to FPC balancing the aeration effort for both aeration reference variants. Although the results show no absolute reduction of the aeration effort, especially the results of the correlation analysis between the event-specific aeration efforts and the corresponding TKN influent loads according to Figure 8-13 demonstrate the benefits of the FPC approach for efficient event specific aeration. While the regression analysis for both variants and each reference scenario Ref1 to Ref4 do not show any relations between the influent TKN load and the applied aeration V_{air} , the results of the FPC with respect to predictive aeration show an obvious correlation according to a coefficient of determination $R^2 = 0.748$. The results show that by the help of the Lagrangian ISN observer model treatment efficient aeration with respect to SASS is possible.

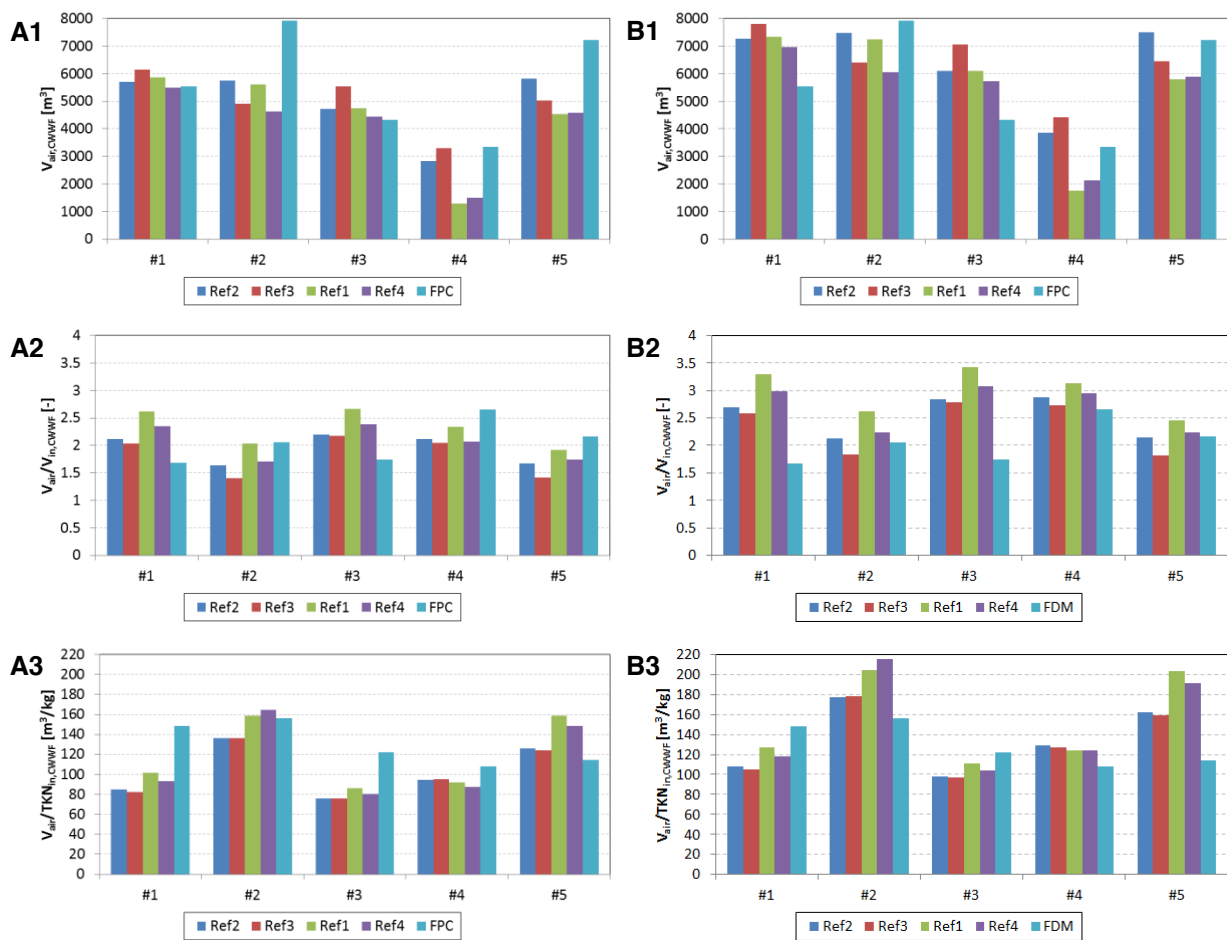


Figure 8-12: Comparison of WWTP aeration effort per wastewater load during CWWF events according to the rainfall time series of August 2011 (A: variant $DO_{set,CWWF} = 0.7 \text{ g/m}^3$, B: variant $SNH_{AST,CWWF} = 1.0 \text{ g/m}^3$; 1: V_{Air} , 2: V_{air}/V_{Inf} , 3: V_{Air}/TKN_{Inf})

Comparison to static control scenarios and discussion of results

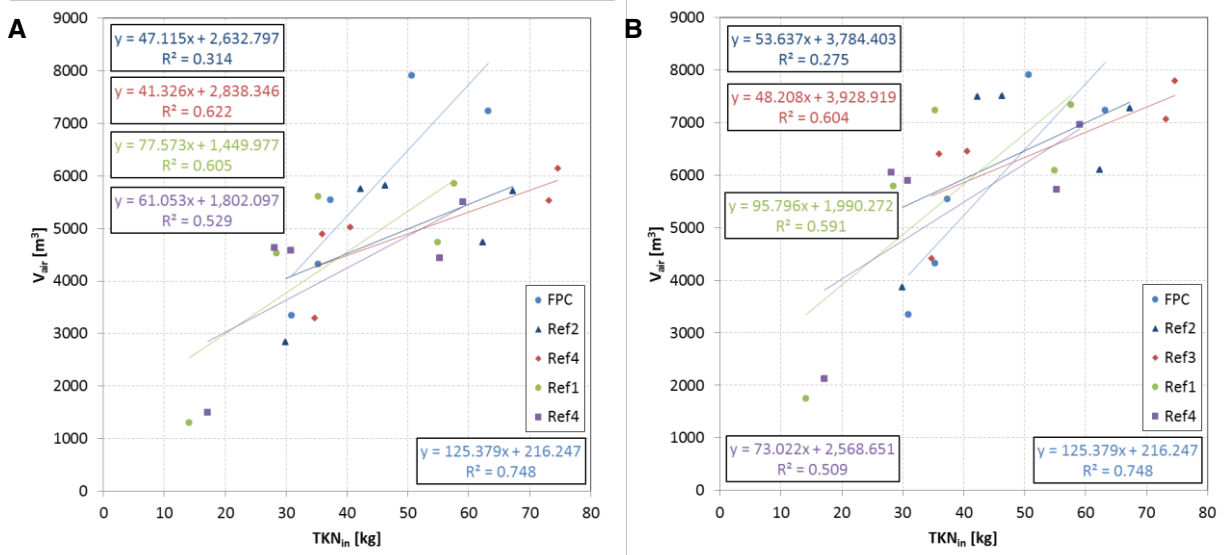


Figure 8-13: Correlations of aeration effort and TKN load during CWWF events according to rainfall time series August 2011 (A: variant $DO_{set,CWWF} = 0.7 \text{ g/m}^3$, B: variant $SNH_{AST,CWWF} = 1.0 \text{ g/m}^3$)

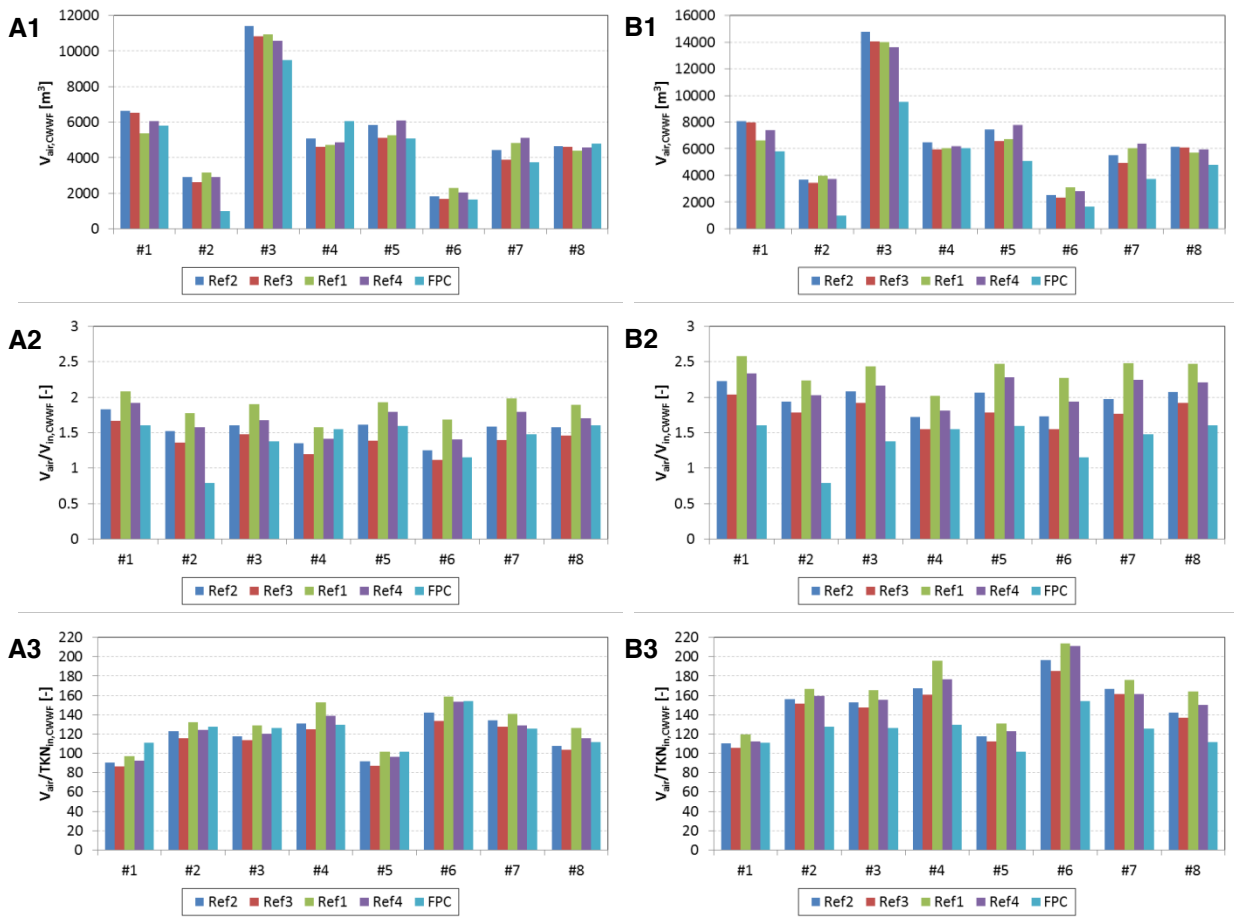


Figure 8-14: Comparison of WWTP aeration effort per wastewater load during CWWF events according to rainfall time series June 2012 (A: variant $DO_{set,CWWF} = 0.7 \text{ g/m}^3$, B: variant $SNH_{AST,CWWF} = 1.0 \text{ g/m}^3$; 1: V_{Air} , 2: V_{Air}/V_{Inf} , 3: V_{Air}/TKN_{in})

Table 8-9: Comparison of the aeration effort during CWWF events according to rainfall time series June 2012

Variant	Scenario	V_{Air} [Nm ³]	V_{Air}/V_{Inf} [Nm ³ /m ³]	V_{Air}/TKN_{Inf} [Nm ³ /kg]	f_{COD} [%]	f_{SNH} [%]	f_N [%]
DO _{set}	FPC	37552	1.5	119	82	78	70
	Ref1	40952	1.9	124	86	79	77
	Ref2	42721	1.6	111	83	77	73
	Ref3	39867	1.4	106	81	75	71
	Ref4	42229	1.7	115	85	78	75
SNH _{set}	Ref1	52232	2.4	158	87	89	75
	Ref2	54638	2.0	142	84	88	73
	Ref3	51334	1.8	136	82	87	70
	Ref4	53897	2.1	147	86	89	74

Table 8-9, Figure 8-14 and Figure 8-15 show the corresponding results of the aeration effort analysis for the rainfall time series of June 2012, representing increased monthly rainfall. The results principally confirm the findings for the rainfall time series of August 2011 representing mean monthly rainfall. For the rainfall time series of June 2012, the reference scenarios in Figure 8-15 now also show excellent correlations between the aeration effort and the corresponding TKN influent load comparable to the results for the FPC approach because of the increased CWWF loading in June 2012. Additionally, the FPC approach now shows an evident absolute or relative aeration effort reduction for most of the investigated CWWF events.

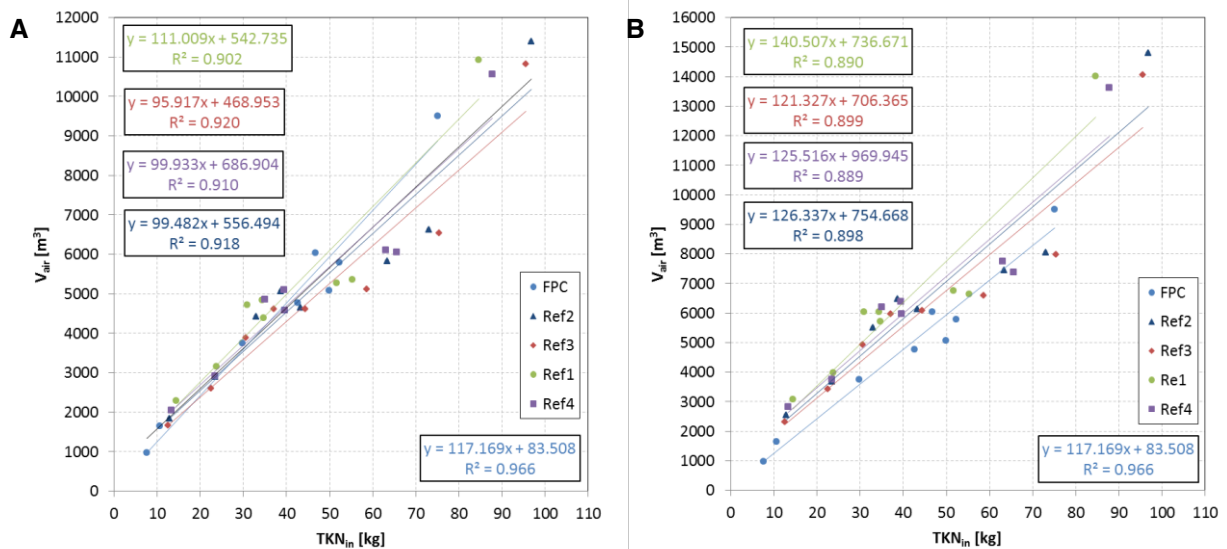


Figure 8-15: Correlations of aeration effort and TKN load during CWWF events according to rainfall time series June 2012 (A: variant $DO_{set,CWWF} = 0.7 \text{ g/m}^3$, B: variant $SNH_{AST,CWWF} = 1.0 \text{ g/m}^3$)

Impacts on the WWTP performance according to wastewater flow variations as investigated by Giokas et al. (2002) cannot be confirmed by the present results. This is mainly because of the different periods used to analyze. While the present work is based on two single month, the study of Giokas et al. (2002) is based on long-term data of three years. In the present

case increasing CWWF loads even seem to be beneficial, since the modeling results show lower aeration efforts and increased correlations between the aeration effort for SASS and the wastewater load to be treated.

8.2.4. Integrated system

Due to the large SRT of 25 days, the removal of COD and BOD₅ is generally very good and similar for all scenarios and variants. Thanks to the total removal of biodegradable COD at the WWTP for all scenarios the remaining inert COD discharged in the WWTP effluent to the receiving water can be balanced with the corresponding COD CSO loads. Figure 8-16 shows the corresponding results for TSS, COD and BOD₅ loads discharged to receiving waters during CWWF events by CSO structures and the WWTP. The results show that the total pollution load discharged to receiving waters is similar to each other for all scenarios. This should be caused by the good treatment at the WWTP thanks to the large SRT of 25 days.

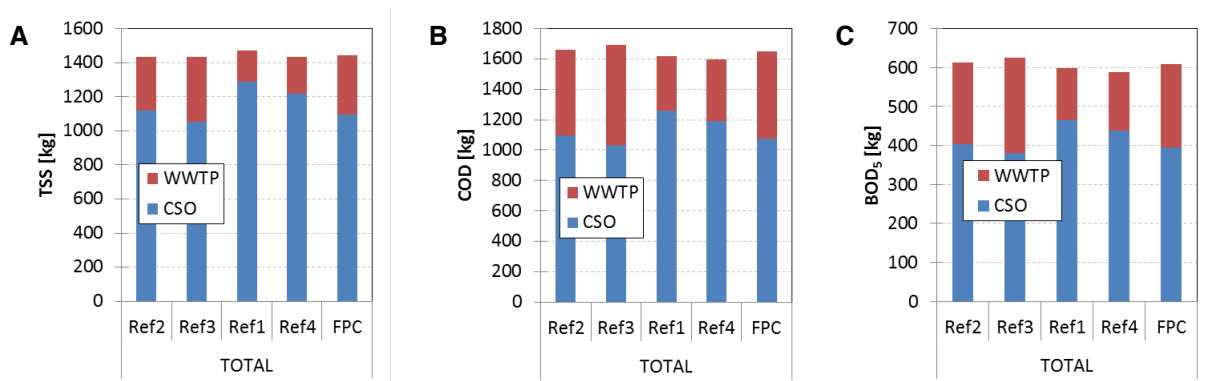


Figure 8-16: System-wide performance comparison of TSS (A), COD (B) and BOD₅ (C) pollution loads from CSO and WWTP discharged to receiving waters according to rainfall time series August 2011

Figure 8-17 and Figure 8-18 show the corresponding integrated global performance concerning the results for nitrogen loads discharged to the receiving waters by CSO and the WWTP according to the rainfall time series of August 2011 and June 2012. Especially Figure 8-17 shows the benefit of the presented approach to system-wide reduce ammonium emissions and to simultaneously increase the objectives according to SASS at the WWTP. Figure 8-18 illustrates that the approach even works during increased hydraulic loads based on the characteristics of the integrated approach discussed before. Figure 8-17 compares the aggregated monthly nitrogen loads discharged to the receiving water by the WWTP and CSOs in August 2011 for all scenarios and aeration variants. The results demonstrate that the FPC approach outperforms all reference scenarios for the variant $DO_{AST} = 0.7 \text{ g/m}^3$. The relative performance decreases when the FPC approach is compared to the aeration variant $SNH_{AST} = 1.0 \text{ g/m}^3$. Nevertheless, the FPC approach still shows the smallest TN effluent load. Monthly $NH_4\text{-N}$ loads are still similar to each other for this variant. Figure 8-18 demonstrates the limits of the integrated approach in the case of increased monthly rainfall according to the rainfall time series of June 2012. Nevertheless, monthly effluent loads are still similar to each other for both aeration variants. Thereby, the extreme storm event #5 extremely affects the monthly performance of the FPC for June 2012. Additionally, when

Comparison to static control scenarios and discussion of results

evaluating the still good results concerning nitrogen effluent loads in June 2012 one must consider the corresponding aeration effort reduction (see Figure 8-14).

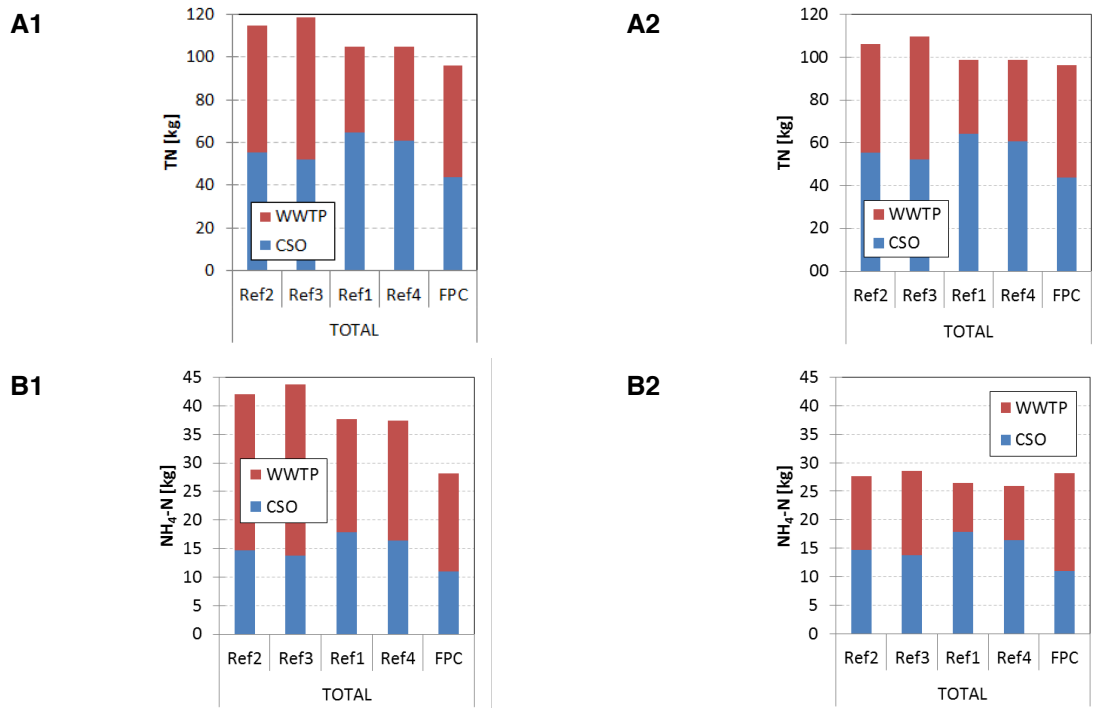


Figure 8-17: System-wide performance comparison of nitrogen pollution loads from CSO and WWTP discharged to receiving waters according to rainfall time series August 2011 (A = TN, B = NH₄-N; 1: DO_{AST} = 0.7 g/m³, 2: SNH_{AST} = 1.0 g/m³)

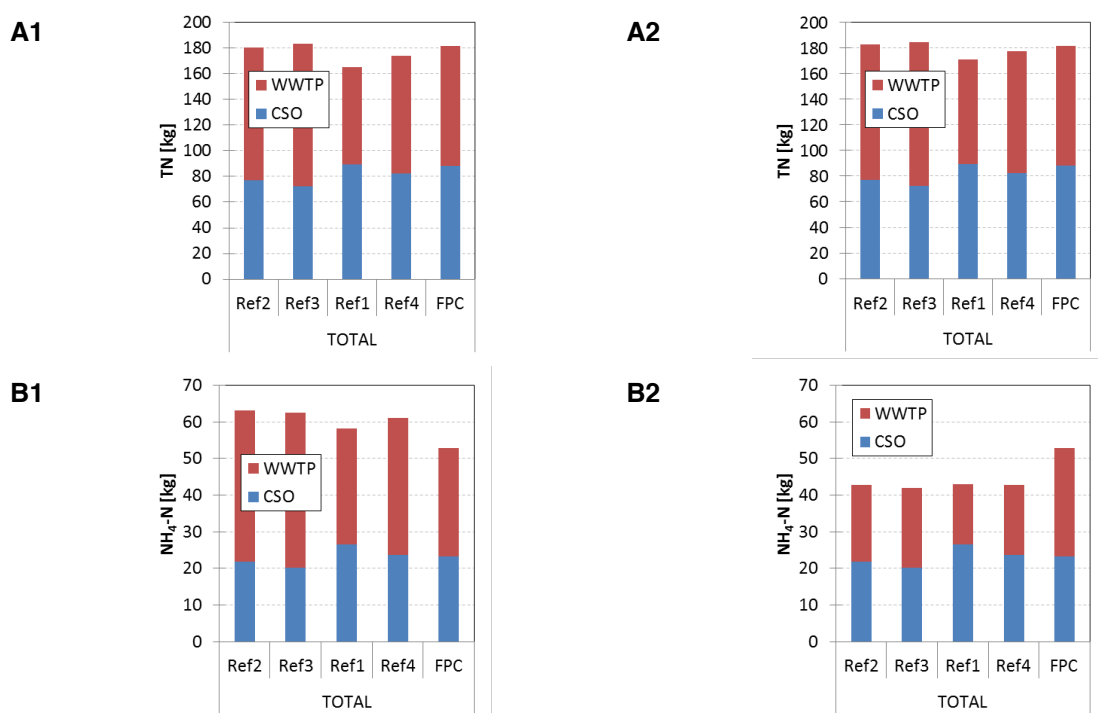


Figure 8-18: System-wide performance comparison of nitrogen pollution loads from CSO and WWTP discharged to receiving waters according to rainfall time series June 2012 (A = TN, B = NH₄-N; 1: variant DO_{AST} = 0.7 g/m³, 2: variant SNH_{AST} = 1.0 g/m³)

9. Conclusions and outlook

9.1. Conclusions

In this PhD study, a novel approach based on fuzzy predictive control was developed to investigate the influence of multi-criteria decision-making in system-wide control of integrated rural wastewater collection and treatment systems with wastewater treatment plants according to simultaneous aerobic sludge stabilization. Fuzzy predictive control is a model predictive control approach using an objective function based on fuzzy decision-making compromising conflicting objectives according to the preferences of the decision-maker for the control of complex nonlinear systems. Thereby, objectives consisting of goals and constraints are principally treated equally.

In order to implement fuzzy predictive control in integrated rural wastewater collection and treatment systems for system-wide control a Lagrangian pollution load observer model of interceptor sewer networks for wastewater collection and treatment systems with decentralized retention tanks was developed. The model tracks discrete wastewater discharges from retention tanks according to their volume and pollution load within the interceptor sewer network in order to simultaneously provide hydro- and pollutographs for the model-based determination of the current wastewater treatment plant capacity and trajectories for sewer network fuzzy predictive control according to the receding horizon optimal control approach. The observer model was calibrated based on discrete wastewater discharges from retention tanks in the interceptor sewer network according to a flow time test.

The integrated reference model for simulation-based evaluation of the presented integrated fuzzy predictive control approach was calibrated based on a system-wide measurement campaign to gain additional insights in the modeling of wastewater pollutants in integrated rural wastewater collection and treatment systems. Based on a proposed approach of chemical mass balances to consider loads under dry weather flow and rain weather flow in combined wet weather flow the contribution of rainfall-runoff on pollution load modeling in integrated wastewater collection and treatment systems was investigated. The analysis of system-wide results from pollution monitoring revealed linear correlations between COD, TSS and BOD₅. In contrast, the modeling of NH₄-N from TKN during CWWF exhibited large uncertainties. A system-wide analysis of rainfall-runoff coefficients, according to four local rain gauges, additionally provided insights into uncertainties in the hydraulic modeling of rural wastewater collection and treatment systems. Based on these results, a novel phenomenological-deterministic approach was proposed to consider these uncertainties in the integrated reference model. The approach considers the investigated random component of rainfall-runoff by adding a stochastic coefficient within the deterministic model. The approach shows a noticeable impact on the evaluation of CSO loads in case of the proposed FPC approach. This illustrates the importance of adequate reference models for the simulation-based evaluation of control approaches.

Based on the developed FPC approach for system-wide control of integrated rural WCTSS and the calibrated deterministic-phenomenological reference model, two months of local

Conclusions and outlook

rainfall time series were used for integrated simulation. These time series were chosen from a three years period of local rainfall data representing the mean monthly rainfall height and increased monthly rainfall according to the 75-percentile of the monthly rainfall height of the analyzed rainfall time series. In the present integrated FPC approach, the WWTP capacity along the receding horizon was determined according to simulation results based on ASM1 (Henze *et al.* 1987) and the one-dimensional SST model according to Takács *et al.* (1991). On the basis of fuzzy decision-making results, taking objectives for simultaneous aerobic sludge stabilization at low loaded wastewater treatment plants in rural catchments into account, the wastewater treatment plant capacity during CWWF is predominantly defined by the hydraulic capacity of the secondary settlement tank according to a linear correlation with effluent TSS concentrations. Thereby, the objectives of simultaneous aerobic sludge stabilization prevent the wastewater treatment plant from nitrification failures. Based on the Lagrangian interceptor observer model the fuzzy predictive aeration control of the activated sludge tank provides a load-specific aeration with respect to the objectives of simultaneous aerobic sludge stabilization.

The integrated FPC approach shows an average combined sewer overflow reduction potential of 12 percent according to mean monthly precipitation heights. Fuzzy decision-making illustrates the correlation between hydraulic and pollution load objectives indicating reserve capacities about 20 percent for water quality based control approaches.

Due to compromises between integrated conflicting objectives, predominantly consisting of homogenizing the hydraulic wastewater treatment plant loading and combined sewer overflow minimization, the mean wastewater treatment plant reserve capacity is about 40 percent for hydraulic loads and 25 percent for wastewater pollution loads.

Finally, the developed tool can be used to derive given weighting scenarios for conventional aggregated multi-criteria model predictive and rule-based real-time control approaches according to the preferences of a decision-maker.

The results emphasize the need of retention tank volume at the WWTP for influent buffering in order to decrease the conflict of hydraulic decision-making in order to exploit the investigated wastewater treatment plant reserve-capacities. Additionally, increased computational performance would be helpful to reduce the control step size. Increased prediction horizons based on e.g. radar rainfall forecasting should increase the performance of the approach.

9.2. Outlook

Long-term simulations should be beneficial in order to fully investigate the potential of the integrated approach.

Due to the ability to illustrate conflicting objectives of operators in the system-wide control of integrated rural wastewater collection and treatment systems, the developed integrated fuzzy predictive control approach can be used to investigate given weighting scenarios for conventional model predictive and rule-based real-time control approaches.

Based on the present findings, especially concerning the quite stable behavior of low-loaded wastewater treatment plants during combined wet weather flow, results from the fuzzy predictive control approach could be easily translated into fuzzy or conventional rule-based control approaches.

In the present case, measurement campaigns for the reference model calibration were done in the unfinished state of the integrated wastewater collection and treatment system. Because of this, conclusions regarding the behavior of the secondary settlement tank are done only model-based. Consequently, the reference model should be calibrated in the long-term for the real secondary settlement tank capacities under full loading conditions, determined by additional monitoring campaigns. Especially, in the case of real-world implementation this step is of crucial importance.

Studies on immission-based control approaches indicate reserve capacities according to the situation in the receiving waters (Meirlaen 2002). In order to consider this, the approach should be extended to work with immission-based objectives. This additionally could show impacts on the energy efficiency of the wastewater treatment plant performance.

Concerning the feed-forward loop for wastewater treatment plant model predictive control and capacity estimation, the robustness of the integrated approach can be increased by reducing control step sizes and increasing prediction horizons both for the sewer network and the wastewater treatment plant. This will have to be achieved by increasing computational resources and parallelization efforts of the integrated model. Additionally, robustness could be increased by considering different kinds of uncertainty in the integrated control and prediction. Especially the integrated modeling of ammonium needs further investigations as shown by the model calibration from measurement data.

Finally, in order to benefit from energy recovery according to anaerobic waste activated sludge digestion, the approach should be adapted to large urban wastewater collection and treatment systems with wastewater treatment plants for anaerobic waste activated sludge digestion. Thereby, future studies could benefit from the ability of the present approach then also including energy recovery.

Overall, this PhD study provided detailed insights into the modeling and system-wide control of integrated rural wastewater collection and treatment systems. In contradiction to comparable research work, the present study additionally provided the opportunity to investigate wastewater monitoring both in the sewer network and at the wastewater treatment plant, providing insights which are helpful to interpret corresponding models. Furthermore, detailed coding was necessary to develop the presented integrated fuzzy predictive control approach, another skill developed during the study.

10. References

- Abusam, A., Keesman, K.J. (1999) 'Effect of number of CSTR's on the modelling of oxidation ditches: steady state and dynamic analysis', in *Mededelingen - Faculteit Landbouwkundige En Toegepaste Biologische Wetenschappen Universiteit Gent*, Presented at the 13. Forum for Applied Biotechnology, Gent (Belgium), 91–94.
- Abusam, A., Keesman, K.J., Meinema, K., van Straten, G. (2001) 'Oxygen transfer rate estimation in oxidation ditches from clean water measurements', *Water Research*, 35(8), 2058–2064.
- Abusam, A., Keesman, K.J., Spanjers, H., van Straten, G., Meinema, K. (2002) 'Evaluation of control strategies using an oxidation ditch benchmark', *Water Science & Technology*, 45(4-5), 151–158.
- Achleitner, S., Fach, S., Einfalt, T., Rauch, W. (2009) 'Nowcasting of rainfall and of combined sewage flow in urban drainage systems', *Water Science & Technology*, 59(6), 1145.
- Achleitner, S., Möderl, M., Rauch, W. (2007) 'CITY DRAIN © – An open source approach for simulation of integrated urban drainage systems', *Environmental Modelling & Software*, Bayesian networks in water resource modelling and management, 22(8), 1184–1195.
- Ahnert, M., Tränckner, J., Günther, N., Hoefft, S., Krebs, P. (2009) 'Model-based comparison of two ways to enhance WWTP capacity under stormwater conditions', *Water Science & Technology*, 60(7), 1875.
- Audet, C., Béchar, V., Le Digabel, S. (2008) 'Nonsmooth optimization through mesh adaptive direct search and variable neighborhood search', *Journal of Global Optimization*, 41(2), 299–318.
- Audet, C., Dennis Jr, J.E., Le Digabel, S. (2010) 'Globalization strategies for mesh adaptive direct search', *Computational Optimization and Applications*, 46(2), 193–215.
- Baban, A., Talinli, I. (2009) 'Modeling of organic matter removal and nitrification in sewer systems — an approach to wastewater treatment', *Desalination*, 246(1–3), 640–647.
- Babuška, R., Verbruggen, H.B. (1996) 'An overview of fuzzy modeling for control', *Control Engineering Practice*, 4(11), 1593–1606.
- Bach, P.M., McCarthy, D.T., Deletic, A. (2010) 'Redefining the stormwater first flush phenomenon', *Water Research*, 44(8), 2487–2498.
- Bach, P.M., Rauch, W., Mikkelsen, P.S., McCarthy, D.T., Deletic, A. (2014) 'A critical review of integrated urban water modelling – Urban drainage and beyond', *Environmental Modelling & Software*, 54, 88–107.
- Bahakim, S.S., Ricardez-Sandoval, L.A. (2014) 'Simultaneous design and MPC-based control for dynamic systems under uncertainty: A stochastic approach', *Computers & Chemical Engineering*, 63, 66–81.
- Barco, J., Papiri, S., Stenstrom, M.K. (2008) 'First flush in a combined sewer system', *Chemosphere*, 71(5), 827–833.
- Barker, M., Rayens, W. (2003) 'Partial least squares for discrimination', *Journal of chemometrics*, 17(3), 166–173.
- Bauwens, W., Vanrolleghem, P., Smeets, M. (1996) 'An evaluation of the efficiency of the combined sewer-wastewater treatment system under transient conditions', *Water Science & Technology*, 33(2), 199–208.
- Beeneken, T., Erbe, V., Messmer, A., Reder, C., Rohlfing, R., Scheer, M., Schuetze, M., Schumacher, B., Weilandt, M., Weyand, M. (2013) 'Real time control (RTC) of urban drainage systems – A discussion of the additional efforts compared to conventionally operated systems', *Urban Water Journal*, 10(5), 293–299.
- Belarbi, K., Megri, F. (2007) 'A Stable Model-Based Fuzzy Predictive Control Based on Fuzzy Dynamic Programming', *IEEE Transactions on Fuzzy Systems*, 15(4), 746–754.

- Belchior, C.A.C., Araújo, R.A.M., Landeck, J.A.C. (2012) 'Dissolved oxygen control of the activated sludge wastewater treatment process using stable adaptive fuzzy control', *Computers & Chemical Engineering*, 37, 152–162.
- Bellman, R.E., Zadeh, L.A. (1970) 'Decision-Making in a Fuzzy Environment', *Management Science*, 17(4), B-141–B-164.
- Benedetti, L., Dirckx, G., Bixio, D., Thoeye, C., Vanrolleghem, P.A. (2006) 'Substance flow analysis of the wastewater collection and treatment system', *Urban Water Journal*, 3(1), 33–42.
- Benedetti, L., Meirlaen, J., Vanrolleghem, P.A. (2004) 'Model connectors for integrated simulations of urban wastewater systems', *Sewer Networks and Processes within Urban Water Systems. J.-L. Bertrand-Krajewski, M. Almeida, J. Matos and S. Abdul-Talib (eds.), Water and Environment Management Series (WEMS), IWA Publishing*, 13–21.
- De Bénédittis, J., Bertrand-Krajewski, J. (2005) 'Infiltration in sewer systems: comparison of measurement methods', *Water Science & Technology*, 52(3), 219–227.
- Berndtsson, R., Niemczynowicz, J. (1988) 'Spatial and temporal scales in rainfall analysis — Some aspects and future perspectives', *Journal of Hydrology*, 100(1–3), 293–313.
- Bertanza, G. (1997) 'Simultaneous nitrification-denitrification process in extended aeration plants: pilot and real scale experiences', *Water Science & Technology*, 35(6), 53–61.
- Bertrand-Krajewski, J., Bardin, J., Mourad, M., Branger, Y. (2003) 'Accounting for sensor calibration, concentration heterogeneity, measurement and sampling uncertainties in monitoring urban drainage systems', *Water Science & Technology*, 47(2), 95–102.
- Bertrand-Krajewski, J.-L., Chebbo, G., Saget, A. (1998) 'Distribution of pollutant mass vs volume in stormwater discharges and the first flush phenomenon', *Water Research*, 32(8), 2341–2356.
- Beven, K.J. (2011) *Rainfall-Runoff Modelling: The Primer*, John Wiley & Sons.
- Blumensaat, F., Staufer, P., Heusch, S., Reußner, F., Schütze, M., Seiffert, S., Gruber, G., Zawilski, M., Rieckermann, J. (2012) 'Water quality-based assessment of urban drainage impacts in Europe – where do we stand today?', *Water Science & Technology*, 66(2), 304.
- Boller, M. (1997) 'Small wastewater treatment plants - a challenge to wastewater engineers', *Water Science & Technology*, 35(6), 1–12.
- Borsanyi, P., Benedetti, L., Dirckx, G., De Keyser, W., Muschalla, D., Solvi, A.-M., Vandenberghe, V., Weyand, M., Vanrolleghem, P.A. (2008) 'Modelling real-time control options on virtual sewer systems', *Journal of Environmental Engineering and Science*, 7(4), 395–410.
- Brdys, M.A., Grochowski, M., Gminski, T., Konarczak, K., Drewa, M. (2008) 'Hierarchical predictive control of integrated wastewater treatment systems', *Control Engineering Practice*, 16(6), 751–767.
- Brombach, H., Steinriede, D., Weib, G., Wohrle, C. (1999) 'Measured overflow activity of combined sewer overflow (CSO) tanks', in *Proc. Eighth International Conference on Urban Storm Drainage*, Sydney, Australia.
- Brombach, H., Weiss, G., Fuchs, S. (2005) 'A new database on urban runoff pollution: comparison of separate and combined sewer systems', *Water Science & Technology*, 51(2), 119–128.
- Buishand, T.A. (1982) 'Some methods for testing the homogeneity of rainfall records', *Journal of Hydrology*, 58(1), 11–27.
- Bürger, R., Karlsen, K.H., Towers, J.D. (2005) 'A Model of Continuous Sedimentation of Flocculated Suspensions in Clarifier-Thickener Units', *SIAM Journal on Applied Mathematics*, 65(3), 882–940.
- Burlando, P., Montanari, A., Ranzi, R. (1996) 'Forecasting of storm rainfall by combined use of radar, rain gages and linear models', *Atmospheric Research*, 42(1–4), 199–216.
- Butler, D., Schütze, M. (2005) 'Integrating simulation models with a view to optimal control of urban wastewater systems', *Environmental Modelling & Software*, 20(4), 415–426.

References

- BWK (2001) *BWK Merkblatt 3: Ableitung von immissionsorientierten Anforderungen an Misch- und Niederschlagswassereinleitungen unter Berücksichtigung örtlicher Verhältnisse (Derivation of requirements for wet weather discharges with regard to local circumstances)*, Bund der Ingenieure für Wasserwirtschaft, Abfallwirtschaft und Kulturbau (BWK): Düsseldorf, Germany.
- BWK (2008) *BWK Merkblatt 7: Detaillierte Nachweisführung immissionsorientierter Anforderungen an Misch- und Niederschlagswassereinleitungen gemäß BWK-Merkblatt 3*, Bund der Ingenieure für Wasserwirtschaft, Abfallwirtschaft und Kulturbau (BWK): Düsseldorf, Germany.
- Camacho, E.F., Bordons, C. (2007) 'Nonlinear Model Predictive Control: An Introductory Review', in Findeisen, D.-I.R., Allgöwer, P.D.F. and Biegler, P.D.L.T., eds., *Assessment and Future Directions of Nonlinear Model Predictive Control*, Lecture Notes in Control and Information Sciences, Springer Berlin Heidelberg, 1–16.
- Campisano, A., Cabot Ple, J., Muschalla, D., Pleau, M., Vanrolleghem, P.A. (2013) 'Potential and limitations of modern equipment for real time control of urban wastewater systems', *Urban Water Journal*, 10(5), 300–311.
- Capodaglio, A.G. (1994) 'Transfer Function Modelling of Urban Drainage Systems, and Potential Uses in Real-Time Control Applications', *Water Science & Technology*, 29(1-2), 409–417.
- Caprara, A., Monaci, M., Toth, P., Guida, P.L. (2006) 'A Lagrangian heuristic algorithm for a real-world train timetabling problem', *Discrete Applied Mathematics*, 154(5), 738–753.
- Carstensen, J., Nielsen, M., Strandbk, H. (1998) Prediction of Hydraulic Load for Urban Storm Control of a Municipal WWT Plant [online], available: <http://www.iwaponline.com/wst/03712/wst037120363.htm> [accessed 13 Mar 2013].
- Cembrano, G., Quevedo, J., Salamero, M., Puig, V., Figueras, J., Martí, J. (2004) 'Optimal control of urban drainage systems. A case study', *Control Engineering Practice*, 12(1), 1–9.
- Chachuat, B., Roche, N., Latifi, M.A. (2005) 'Long-term optimal aeration strategies for small-size alternating activated sludge treatment plants', *Chemical Engineering and Processing: Process Intensification*, 44(5), 591–604.
- Chebbo, G., Bachoc, A., Laplace, D., Le Guennec, B. (1995) 'The transfer of solids in combined sewer networks', *Water Science & Technology*, 31(7), 95–105.
- Chen, C.-L., Chang, C.-Y., Sun, D.-Y. (2003) 'Solving multi-objective dynamic optimization problems with fuzzy satisfying method', *Optimal Control Applications and Methods*, 24(5), 279–296.
- Choe, J., Bang, K., Lee, J. (2002) 'Characterization of surface runoff in urban areas', *Water Science & Technology*, 45(9), 249–254.
- Chotkowski, W., Brdys *, M.A., Konarczak, K. (2005) 'Dissolved oxygen control for activated sludge processes', *International Journal of Systems Science*, 36(12), 727–736.
- Clarke, D.W., Mohtadi, C., Tuffs, P.S. (1987) 'Generalized predictive control—Part I. The basic algorithm', *Automatica*, 23(2), 137–148.
- De Clercq, B., Coen, F., Vanderhaegen, B., Vanrolleghem, P.A. (1999) 'Calibrating simple models for mixing and flow propagation in waste water treatment plants', *Water science & technology*, 39(4), 61–69.
- De Clercq, J., Nopens, I., Defrancq, J., Vanrolleghem, P.A. (2008) 'Extending and calibrating a mechanistic hindered and compression settling model for activated sludge using in-depth batch experiments', *Water Research*, 42(3), 781–791.
- Colas, H., Pleau, M., Lamarre, J., Pelletier, G., Lavallée, P. (2004) 'Practical perspective on real-time control', *Water quality research journal of Canada*, 39(4), 466–478.
- Collivignarelli, C., Bertanza, G. (1999) 'Simultaneous nitrification-denitrification processes in activated sludge plants: Performance and applicability', *Water Science and Technology*, 40(4–5), 187–194.
- Copp, J. (2001) *The COST Simulation Benchmark: Description and Simulator Manual.*, Office for Official Publications of the European Community: Luxembourg.

- Da Costa Sousa, J.M., Kaymak, U. (2001) 'Model predictive control using fuzzy decision functions', *IEEE Transactions on Systems, Man, and Cybernetics, Part B: Cybernetics*, 31(1), 54–65.
- Couillard, D., Zhu, S. (1992) 'Control strategy for the activated sludge process under shock loading', *Water Research*, 26(5), 649–655.
- Cruz Bournazou, M.N., Arellano-Garcia, H., Wozny, G., Lyberatos, G., Kravaris, C. (2012) 'ASM3 extended for two-step nitrification–denitrification: a model reduction for sequencing batch reactors', *Journal of Chemical Technology & Biotechnology*, 87(7), 887–896.
- Darsono, S., Labadie, J.W. (2007) 'Neural-optimal control algorithm for real-time regulation of in-line storage in combined sewer systems', *Environmental Modelling & Software*, 22(9), 1349–1361.
- Davey, K.R. (2008) 'Latin Hypercube Sampling and Pattern Search in Magnetic Field Optimization Problems', *IEEE Transactions on Magnetics*, 44(6), 974–977.
- Devisscher, M., Ciacci, G., Fé, L., Benedetti, L., Bixio, D., Thoeye, C., Gueldre, G.D., Marsili-Libelli, S., Vanrolleghem, P.A. (2006) 'Estimating costs and benefits of advanced control for wastewater treatment plants – the MAGIC methodology', *Water Science & Technology*, 53(4-5), 215.
- DHI (2009) *MIKE URBAN - Model Manager*, DHI: Denmark.
- Diaz-Fierros T, F., Puerta, J., Suarez, J., Diaz-Fierros V, F. (2002) 'Contaminant loads of CSOs at the wastewater treatment plant of a city in NW Spain', *Urban Water*, 4(3), 291–299.
- Diehl, S., Farås, S. (2012) 'Fundamental nonlinearities of the reactor-settler interaction in the activated sludge process.', *Water Science & Technology*, 66(1), 28–35.
- Diehl, S., Jeppsson, U. (1998) 'A model of the settler coupled to the biological reactor', *Water Research*, 32(2), 331–342.
- Doyle, M.W., Ensign, S.H. (2009) 'Alternative reference frames in river system science', *BioScience*, 59(6), 499–510.
- Dubois, D., Prade, H. (1984) 'Criteria aggregation and ranking of alternatives in the framework of fuzzy set theory', *TIMS Studies in the Management Sciences*, 20, 209–240.
- DWA (1992a) *Standard ATV-DVWK-A 128E Standards for the Dimensioning and Design of Stormwater Structures in Combined Sewers*, German Association for Water, Wastewater and Waste.
- DWA (1992b) *Standard ATV-DVWK-A 131E Dimensioning of Single-Stage Activated Sludge Plants*, Deutsche Vereinigung für Wasserwirtschaft, Abwasser und Abfall e.V.
- DWA (2000) *Standard ATV-DVWK-A 134E Planning and Construction of Wastewater Pumping Stations*, German Association for Water, Wastewater and Waste: Hennef, Germany.
- DWA (2003) *Standard ATV-DVWK-A 198E Standardisation and Derivation of Dimensioning Values for Wastewater Facilities*, German Association for Water, Wastewater and Waste: Hennef, Germany.
- DWA (2006) *Standard DWA-A 118E Hydraulic Dimensioning and Verification of Drain and Sewer Systems*, German Association for Water, Wastewater and Waste: Hennef, Germany.
- DWA (2009) *Arbeitsblatt DWA-A 226 Grundsätze Für Die Abwasserbehandlung in Belebungsanlagen Mit Gemeinsamer Aerober Schlammstabilisierung Ab 1.000 Einwohnerwerte*, German Association for Water, Wastewater and Waste: Hennef, Germany.
- EC (1991) 'Council Directive 91/271/EEC of 21 March 1991 concerning urban wastewater treatment', *Official Journal of the European Communities*, 40(L135), 30.
- EC (2000) 'Directive 2000/60/EC of the European Parliament and of the Council of 23 October 2000 establishing a framework for Community action in the field of water policy.', *Official Journal of the European Communities*, 43(L327), 1–71.

References

- Egea, J.A., Vries, D., Alonso, A.A., Banga, J.R. (2007) 'Global Optimization for Integrated Design and Control of Computationally Expensive Process Models', *Industrial & Engineering Chemistry Research*, 46(26), 9148–9157.
- El-Din, A.G., Smith, D.W. (2002) 'A neural network model to predict the wastewater inflow incorporating rainfall events', *Water Research*, 36(5), 1115–1126.
- Elliott, A.H., Trowsdale, S.A. (2007) 'A review of models for low impact urban stormwater drainage', *Environmental Modelling & Software*, Special section: Advanced Technology for Environmental Modelling, 22(3), 394–405.
- Ellis, J.B. (2001) 'Sewer infiltration/exfiltration and interactions with sewer flows and groundwater quality', in *2nd International Conference Interactions between Sewers, Treatment Plants and Receiving Waters in Urban areas—Interurba II*, 19–22.
- Erbe, V., Risholt, L., Schilling, W., Londong, J. (2002) 'Integrated modelling for analysis and optimisation of wastewater systems – the Odenthal case', *Urban Water*, 4(1), 63–71.
- Esogbue, A.O., Kacprzyk, J. (1998) 'Fuzzy dynamic programming', in *Fuzzy Sets in Decision Analysis, Operations Research and Statistics*, Springer, 281–307.
- eWater (2011) *MUSIC by eWater, User Manual.*, eWater: Melbourne, Australia.
- Fiorelli, D., Schutz, G. (2009) 'Real-time control of a sewer network using a multi-goal objective function', in *17th Mediterranean Conference on Control and Automation, 2009. MED '09*, Presented at the 17th Mediterranean Conference on Control and Automation, 2009. MED '09, 676–681.
- Fiorelli, D., Schutz, G., Klepizewski, K., Regneri, M., Seiffert, S. (2013) 'Optimised real time operation of a sewer network using a multi-goal objective function', *Urban Water Journal*, 10(5), 342–353.
- Fletcher, R. (2013) *Practical Methods of Optimization*, John Wiley & Sons.
- Flores-Alsina, X., Comas, J., Roda, I.R., Poch, M., Gernaey, K.V., Jeppsson, U. (2009) 'Evaluation of plant-wide WWTP control strategies including the effects of filamentous bulking sludge', *Water Science & Technology*, 60(8), 2093–2103.
- Fradet, O., Pleau, M., Desbiens, A., Colas, H. (2010) 'Theoretical and field validation of solutions based on simplified hydraulic models for the real-time control of sewer networks', *NOVATECH 2010*.
- Freni, G., Mannina, G., Viviani, G. (2009) 'Uncertainty assessment of an integrated urban drainage model', *Journal of Hydrology*, 373(3–4), 392–404.
- Fronteau, C., Bauwens, W., Vanrolleghem, P.A. (1997) 'Integrated modelling: comparison of state variables, processes and parameters in sewer and wastewater treatment plant models', *Water Science & Technology*, 36(5), 373–380.
- Fuchs, L., Beeneken, T. (2005) 'Development and implementation of a real-time control strategy for the sewer system of the city of Vienna', *Water Science & Technology*, 52(5), 187–194.
- Fuchs, L., Beeneken, T., Sponemann, P., Scheffer, C. (1997) 'Model based real-time control of sewer system using fuzzy-logic', *Water Science and Technology*, 36(8-9), 343–347.
- Fu, G., Butler, D., Khu, S.-T. (2008) 'Multiple objective optimal control of integrated urban wastewater systems', *Environmental Modelling & Software*, 23(2), 225–234.
- Gaborit, E., Muschalla, D., Vallet, B., Vanrolleghem, P.A., Anctil, F. (2013) 'Improving the performance of stormwater detention basins by real-time control using rainfall forecasts', *Urban Water Journal*, 10(4), 230–246.
- García, C.E., Prett, D.M., Morari, M. (1989) 'Model predictive control: Theory and practice—A survey', *Automatica*, 25(3), 335–348.
- Garriga, J.L., Soroush, M. (2010) 'Model predictive control tuning methods: A review', *Industrial & Engineering Chemistry Research*, 49(8), 3505–3515.
- Gasperi, J., Gromaire, M.C., Kafi, M., Moillon, R., Chebbo, G. (2010) 'Contributions of wastewater, runoff and sewer deposit erosion to wet weather pollutant loads in combined sewer systems', *Water Research*, 44(20), 5875–5886.

- Gasperi, J., Kafi-Benyahia, M., Lorgeoux, C., Moilleron, R., Gromaire, M.-C., Chebbo, G. (2008) 'Wastewater quality and pollutant loads in combined sewers during dry weather periods', *Urban Water Journal*, 5(4), 305–314.
- Gelormino, M.S., Ricker, N.L. (1994) 'Model-predictive control of a combined sewer system', *International Journal of Control*, 59(3), 793–816.
- Gernaey, K.V., Alex, J., Benedetti, L., Copp, J., Jeppson, U., Nopens, I., Pons, M.N., Rieger, L., Rosen, C., Steyer, J.P., Vanrolleghem, P.A., Winkler, S. (2008) *Benchmark Simulation Model No. 1 (BSM1)* [online], available: http://apps.ensic.inpl-nancy.fr/benchmarkWWTP/Pdf/Description_BSM1_20080405.pdf [accessed 24 Jul 2014].
- Gernaey, K.V., Flores-Alsina, X., Rosen, C., Benedetti, L., Jeppsson, U. (2011) 'Dynamic influent pollutant disturbance scenario generation using a phenomenological modelling approach', *Environmental Modelling & Software*, 26(11), 1255–1267.
- Gernaey, K.V., van Loosdrecht, M.C., Henze, M., Lind, M., Jørgensen, S.B. (2004) 'Activated sludge wastewater treatment plant modelling and simulation: state of the art', *Environmental Modelling & Software*, 19(9), 763–783.
- Gernaey, K.V., Rosen, C., Jeppsson, U. (2006) 'WWTP dynamic disturbance modelling an essential module for long-term benchmarking development', *Water Science & Technology*, 53(4-5), 225–234.
- Giokas, D., Vlessidis, A., Angelidis, M., Tsimarakis, G., Karayannis, M. (2002) 'Systematic analysis of the operational response of activated sludge process to variable wastewater flows. A case study', *Clean Technologies and Environmental Policy*, 4(3), 183–190.
- Giraldo, J.M., Leirens, S., Díaz-Grenados, M.A., Rodríguez, J.P. (2010) 'Nonlinear optimization for improving the operation of sewer systems: the Bogotá Case Study. International Environmental Modelling and Software Society (iEMSs)', in *2010 International Congress on Environmental Modelling and Software Modelling for Environments Sake, Fifth Biennial Meeting, Ottawa, Canada*.
- Goovaerts, P. (2000) 'Geostatistical approaches for incorporating elevation into the spatial interpolation of rainfall', *Journal of hydrology*, 228(1), 113–129.
- Gretzschel, G., Schmitt, T., Hansen, J., Siekmann, K., Jakob, J. (2012) 'Schlammfäulung statt aerober Stabilisierung?', *WWT*, 2012(3), 27–33.
- Gromaire, M.C., Garnaud, S., Saad, M., Chebbo, G. (2001) 'Contribution of different sources to the pollution of wet weather flows in combined sewers', *Water Research*, 35(2), 521–533.
- Grum, M., Thornberg, D., Christensen, M.L., Shididi, S.A., Thirsing, C. (2011) 'Full-Scale Real Time Control Demonstration Project in Copenhagen's Largest Urban Drainage Catchments', in *Proceedings of the 12th International Conference on Urban Drainage*, Presented at the 12th International Conference on Urban Drainage, Porto Alegre, Brazil, available: <http://web.sbe.hw.ac.uk/staffprofiles/bdgsa/temp/12th%20ICUD/PDF/PAP005541.pdf> [accessed 1 Jun 2013].
- Grüne, L., Pannek, J. (2011) *Nonlinear Model Predictive Control: Theory and Algorithms*, Springer.
- Gujer, W., Henze, M., Mino, T., Loosdrecht, M. van (1999) 'Activated sludge model no. 3', *Water Science & Technology*, 39(1), 183–193.
- Han, H.-G., Qian, H.-H., Qiao, J.-F. (2014) 'Nonlinear multiobjective model-predictive control scheme for wastewater treatment process', *Journal of Process Control*, 24(3), 47–59.
- Han, H.-G., Qiao, J.-F., Chen, Q.-L. (2012) 'Model predictive control of dissolved oxygen concentration based on a self-organizing RBF neural network', *Control Engineering Practice*, 20(4), 465–476.
- Hansen, L.S., Borup, M., Møller, A., Mikkelsen, P.S. (2011) 'Flow Forecasting in Urban Drainage Systems using Deterministic Updating of Water Levels in Distributed Hydraulic Models', in *Proceedings of the 12th International Conference on Urban Drainage*, Presented at the 12th International Conference on Urban Drainage, Porto

References

- Alegre, Brazil, available:
<http://web.sbe.hw.ac.uk/staffprofiles/bdgsa/temp/12th%20ICUD/PDF/PAP005144.pdf>
[accessed 29 May 2013].
- Han, Y., Lau, S., Kayhanian, M., Stenstrom, M. (2006) 'Correlation analysis among highway stormwater pollutants and characteristics', *Water Science & Technology*, 53(2), 235–243.
- He, D., Du, W., Hu, J. (2011) 'Water Quality Dynamic Monitoring Technology and Application Based on Ion Selective Electrodes', in *Recent Developments in Mobile Communications - A Multidisciplinary Approach*.
- Heip, L., Van Assel, J., Swartenbroekx, P. (1997) 'Sewer flow quality modelling', *Water Science & Technology*, 36(5), 177–184.
- Henze, M. (1992) 'Characterization of Wastewater for Modelling of Activated Sludge Processes', *Water Science & Technology*, 25(6), 1–15.
- Henze, M., Grady, C.P.L., Gujer, W., Marais, G., Matsuo, T. (1987) *Activated Sludge Model No. 1*, IAWQ: London.
- Henze, M., Gujer, W., Mino, T., Matsuo, T., Wentzel, M.C., Van Loosdrecht, M. (1999) 'Activated sludge model no. 2d, ASM2d', *Water Science & Technology*, 39(1), 165–182.
- Herrera, J., Ibeas, A., de la Sen, M. (2013) 'Identification and control of integrative MIMO systems using pattern search algorithms: An application to irrigation channels', *Engineering Applications of Artificial Intelligence*, 26(1), 334–346.
- Heusch, S. (2011) *Modellprädiktive Abflusssteuerung Mit Hydrodynamischen Kanalnetzmodellen*, PhD thesis, Technische Universität Darmstadt.
- Heusch, S., Hanss, H., Ostrowski, M., Rosen, R., Sohr, A. (2012) 'Optimal Control of Sewer Networks Problem Description', in Martin, A., Klamroth, K., Lang, J., Leugering, G., Morsi, A., Oberlack, M., Ostrowski, M. and Rosen, R., eds., *Mathematical Optimization of Water Networks*, International Series of Numerical Mathematics, Springer Basel, 69–82.
- Holenda, B., Domokos, E., Rédey, Á., Fazakas, J. (2008) 'Dissolved oxygen control of the activated sludge wastewater treatment process using model predictive control', *Computers & Chemical Engineering*, 32(6), 1270–1278.
- Holenda, B., Pásztor, I., Kárpáti, A., Rédey, A. (2006) 'Comparison of one-dimensional secondary settling tank models', *E-Water, Journal of the European Water Association*.
- Hooke, R., Jeeves, T.A. (1961) "Direct Search" Solution of Numerical and Statistical Problems', *Journal of the ACM (JACM)*, 8(2), 212–229.
- Hoppe, H., Messmann, S., Giga, A., Gruening, H. (2011) 'A real-time control strategy for separation of highly polluted storm water based on UV-Vis online measurements – from theory to operation', *Water Science & Technology*, 63(10), 2287.
- Hou, S.-L., Ricker, N.L. (1992) 'Minimization of combined sewer overflows using fuzzy logic control', in , *IEEE International Conference on Fuzzy Systems, 1992*, Presented at the , IEEE International Conference on Fuzzy Systems, 1992, 1203–1210.
- Hvitved-Jacobsen, T., Vollertsen, J., Tanaka, N. (1999) 'Wastewater quality changes during transport in sewers — An integrated aerobic and anaerobic model concept for carbon and sulfur microbial transformations', *Water Science and Technology*, 39(2), 233–249.
- IFAK (2007) *SIMBA (Simulation of Biological Wastewater Systems): Manual and Reference.*, Institut für Automation und Kommunikation e. V.: Magdeburg, Germany.
- ifak (2009) *SIMBA 6.0 - Simulation of Wastewater Systems - Reference*, ifak system GmbH.
- Insel, G., Artan, N., Orhon, D. (2005) 'Effect of Aeration on Nutrient Removal Performance of Oxidation Ditch Systems', *Environmental Engineering Science*, 22(6), 802–815.
- Jeppsson, U. (1995) 'A simplified control-oriented model of the activated sludge process', *Mathematical Modelling of Systems*, 1(1), 3–16.

- Jeppsson, U., Pons, M.-N. (2004) 'The COST benchmark simulation model—current state and future perspective', *Control Engineering Practice*, Benchmarking Modelling and Control in Wastewater Treatment, 12(3), 299–304.
- Jeppsson, U., Pons, M.-N., Nopens, I., Alex, J., Copp, J.B., Gernaey, K.V., Rosen, C., Steyer, J.-P., Vanrolleghem, P.A. (2007) 'Benchmark simulation model no 2: general protocol and exploratory case studies', *Water Science & Technology*, 56(8), 67.
- Jiang, F., Leung, D.H., Li, S., Chen, G.-H., Okabe, S., van Loosdrecht, M.C.M. (2009) 'A biofilm model for prediction of pollutant transformation in sewers', *Water Research*, 43(13), 3187–3198.
- Joannis, C., Aumond, M., Dauphin, S., Ruban, G., Deguin, A., Bridoux, G. (1999) 'Modeling activated sludge mass transfer in a treatment plant', *Water Science & Technology*, 39(4), 29–36.
- Kacprzyk, J., Esogbue, A.O. (1996) 'Fuzzy dynamic programming: Main developments and applications', *Fuzzy Sets and Systems*, Fuzzy Optimization, 81(1), 31–45.
- Kafi, M., Gasperi, J., Moillon, R., Gromaire, M.C., Chebbo, G. (2008) 'Spatial variability of the characteristics of combined wet weather pollutant loads in Paris', *Water Research*, 42(3), 539–549.
- Kalker, T., van Goor, C., Roeleveld, P., Ruland, M., Babuska, R. (1999) 'Fuzzy control of aeration in an activated sludge wastewater treatment plant: design, simulation and evaluation', *Water Science & Technology*, 39(4), 71–78.
- Kaymak, U., Sousa, J.M. (2003) 'Weighted Constraint Aggregation in Fuzzy Optimization', *Constraints*, 8(1), 61–78.
- Kaymak, U., Sousa, J.M., Verbruggen, H.B. (1997) 'A comparative study of fuzzy and conventional criteria in model-based predictive control', in , *Proceedings of the Sixth IEEE International Conference on Fuzzy Systems, 1997*, Presented at the , Proceedings of the Sixth IEEE International Conference on Fuzzy Systems, 1997, 907–914 vol.2.
- Kim, H., McAvoy, T.J., Anderson, J.S., Hao, O.J. (2000) 'Control of an alternating aerobic–anoxic activated sludge system — Part 2: optimization using a linearized model', *Control Engineering Practice*, 8(3), 279–289.
- Kirpich, Z.P. (1940) 'Time of concentration of small agricultural watersheds', *Civil Engineering*, 10(6), 362.
- Kleidorfer, M., Deletic, A., Fletcher, T.D., Rauch, W. (2009) 'Impact of input data uncertainties on stormwater model parameters', *Water Science & Technology*, 60(6), 1545–1554.
- Klepiszewski, K., Schmitt, T. (2002) 'Comparison of conventional rule based flow control with control processes based on fuzzy logic in a combined sewer system', *Water Science & Technology*, 46(6-7), 77–84.
- Koch, G., Kühni, M., Rieger, L., Siegrist, H. (2001) 'Calibration and validation of an ASM3-based steady-state model for activated sludge systems—part II: prediction of phosphorus removal', *Water Research*, 35(9), 2246–2255.
- Kopecny, E., Lahoud, A., Moller, A., Bourgogne, P., Chang, J., Briat, P. (2000) 'Real time control of the sewer system of the «Louis Fargue» treatment plant catchment, Bordeaux, France', in *International Congress on Advanced Urban Drainage Management*, 23–25.
- Krebs, P. (1995) 'Success and shortcomings of clarifier modelling', *Water Science & Technology*, 31(2), 181–191.
- Krebs, P., Holzer, P., Huisman, J., Rauch, W. (1999) 'First flush of dissolved compounds', *Water Science & Technology*, 39(9), 55–62.
- Kroiss, H., Svardal, K. (2009) 'Energiebedarf von Abwasserreinigungsanlagen', *Österreichische Wasser- und Abfallwirtschaft*, 61(11-12), 170–177.
- Kutzner, R., Brombach, H., Geiger, W.F. (2007) 'Sewer solids separation by sedimentation – the problem of modeling, validation and transferability', *Water Science & Technology*, 55(4), 113.

References

- Lacour, C., Schütze, M. (2011) 'Real-time control of sewer systems using turbidity measurements', *Water Science & Technology*, 63(11), 2628.
- Laird, C.D., Biegler, L.T., van Bloemen Waanders, B.G., Bartlett, R.A. (2003) 'Time dependent contamination source determination for municipal water networks using large scale optimization', *Journal of Water Resources Planning and Management*, available: <http://www.cs.sandia.gov/~bartv/papers/fullspace.pdf> [accessed 9 Jan 2014].
- Langergraber, G., Rieger, L., Winkler, S., Alex, J., Wiese, J., Owerdieck, C., Ahnert, M., Simon, J., Maurer, M. (2004) 'A guideline for simulation studies of wastewater treatment plants', *Water Science & Technology*, 50(7), 131–138.
- Langeveld, J.G., Benedetti, L., de Klein, J.J.M., Nopens, I., Amerlinck, Y., van Nieuwenhuijzen, A., Flameling, T., van Zanten, O., Weijers, S. (2013) 'Impact-based integrated real-time control for improvement of the Dommel River water quality', *Urban Water Journal*, 10(5), 312–329.
- Lang, M., Li, P., Yan, X. (2013) 'Runoff concentration and load of nitrogen and phosphorus from a residential area in an intensive agricultural watershed', *Science of The Total Environment*, 458–460, 238–245.
- Lau, J., Butler, D., Schütze, M. (2002) 'Is combined sewer overflow spill frequency/volume a good indicator of receiving water quality impact?', *Urban Water*, 4(2), 181–189.
- Lee, J.H., Bang, K.W. (2000) 'Characterization of urban stormwater runoff', *Water Research*, 34(6), 1773–1780.
- Leirens, S., Giraldo, J.M., Negenborn, R.R., De Schutter, B. (2010) 'A pattern search method for improving the operation of sewer systems', in *In: Proceedings 12th LSS Symposium, Large Scale Systems: Theory and Applications*, Villeneuve, France.
- Leitão, R.C., van Haandel, A.C., Zeeman, G., Lettinga, G. (2006) 'The effects of operational and environmental variations on anaerobic wastewater treatment systems: A review', *Bioresource Technology*, 97(9), 1105–1118.
- Lewis, F.L., Vrable, D., Syrmos, V.L. (2012) *Optimal Control*, John Wiley & Sons.
- Lewis, R.M., Torczon, V., Trosset, M.W. (2000) 'Direct search methods: then and now', *Journal of Computational and Applied Mathematics*, 124(1–2), 191–207.
- Libralato, G., Volpi Ghirardini, A., Avezzi, F. (2012) 'To centralise or to decentralise: An overview of the most recent trends in wastewater treatment management', *Journal of Environmental Management*, 94(1), 61–68.
- Liguori, S., Rico-Ramirez, M.A., Schellart, A.N.A., Saul, A.J. (2012) 'Using probabilistic radar rainfall nowcasts and NWP forecasts for flow prediction in urban catchments', *Atmospheric Research*, 103, 80–95.
- Lijklema, L., Tyson, J.M., Lesouef, A. (1993) 'Interactions Between Sewers, Treatment Plants and Receiving Waters in Urban Areas: A Summary of the Interurba '92 Workshop Conclusions', *Water Science & Technology*, 27(12), 1–29.
- Linde-Jensen, J.J. (1993) 'Real Time Control in Part of Copenhagen', *Water Science & Technology*, 27(12), 209–212.
- Li, S.-Y., Zou, T., Yang, Y.-P. (2004) 'Finding the fuzzy satisfying solutions to constrained optimal control systems and application to robot path planning', *International Journal of General Systems*, 33(2-3), 321–337.
- Longhurst, R.D., Roberts, A.H.C., O'Connor, M.B. (2000) 'Farm dairy effluent: A review of published data on chemical and physical characteristics in New Zealand', *New Zealand Journal of Agricultural Research*, 43(1), 7–14.
- Löwe, R., Mikkelsen, P.S., Madsen, H. (2012) 'Forecast generation for real-time control of urban drainage systems using greybox modelling and radar rainfall', in *In: Proceedings of the 10th International Conference on Hydroinformatics*, Hamburg, Germany.
- Lukasse, L.J.S., Keesman, K.J. (1999) 'Optimised operation and design of alternating activated sludge processes for N-removal', *Water Research*, 33(11), 2651–2659.

- Makinia, J., Rosenwinkel, K.-H., Spering, V. (2005) 'Long-term simulation of the activated sludge process at the Hanover-Gümmerwald pilot WWTP', *Water Research*, 39(8), 1489–1502.
- Mallin, M.A., Johnson, V.L., Ensign, S.H. (2009) 'Comparative impacts of stormwater runoff on water quality of an urban, a suburban, and a rural stream', *Environmental Monitoring and Assessment*, 159(1-4), 475–491.
- Marinaki, M., Papageorgiou, M. (2005) *Optimal Real-Time Control of Sewer Networks*, Springer.
- Marler, R.T., Arora, J.S. (2004) 'Survey of multi-objective optimization methods for engineering', *Structural and multidisciplinary optimization*, 26(6), 369–395.
- Mattson, C.A., Messac, A. (2005) 'Pareto Frontier Based Concept Selection Under Uncertainty, with Visualization', *Optimization and Engineering*, 6(1), 85–115.
- Meirlaen, J. (2002) *Immission Based Real-Time Control of the Integrated Urban Wastewater System*, available: <https://biblio.ugent.be/publication/522030/file/1874292.pdf> [accessed 3 Mar 2014].
- Meirlaen, J., Van Assel, J., Vanrolleghem, P.A. (2002) 'Real time control of the integrated urban wastewater system using simultaneously simulating surrogate models', *Water Science & Technology*, 45(3), 109–116.
- Meirlaen, J., Huyghebaert, B., Sforzi, F., Benedetti, L., Vanrolleghem, P. (2001) 'Fast, simultaneous simulation of the integrated urban wastewater system using mechanistic surrogate models', *Water Science & Technology*, 43(7), 301–310.
- Mendonça, L.F., Sousa, J.M.C., Kaymak, U., Sá da Costa, J.M.G. (2006) 'Weighting goals and constraints in fuzzy predictive control', *Journal of Intelligent and Fuzzy Systems*, 17(5), 517–532.
- Michalska, H., Mayne, D.Q. (1989) 'Receding horizon control of nonlinear systems', in *Proceedings of the 28th IEEE Conference on Decision and Control*, IEEE: Tampa, FL, USA, 107–108.
- Miettinen, K. (1999) *Nonlinear Multiobjective Optimization*, Springer Science & Business Media.
- Miranda, R., Leitão, P.C., Coelho, H.S., Martins, H., Neves, R.R. (1999) 'Transport and mixing simulation along the continental shelf edge using a Lagrangian approach', *BOLETIN-INSTTUTO ESPANOL DE OCEANOGRAFIA*, 15(1/4), 39–60.
- Mitchell, G. (2005) *Aquacycle User Guide*, CRC for Catchment Hydrology: Melbourne, Australia.
- Morari, M., Lee, J.H. (1999) 'Model predictive control: past, present and future', *Computers & Chemical Engineering*, 23(4–5), 667–682.
- Muschalla, D. (2009) *Optimisation of Water Resources Systems Using Evolutionary Algorithms*, PhD thesis, Technische Universität Darmstadt.
- Negenborn, R.R., De Schutter, B., Hellendoorn, J. (2008) 'Multi-agent model predictive control for transportation networks: Serial versus parallel schemes', *Engineering Applications of Artificial Intelligence*, 21(3), 353–366.
- Nielsen, M., Bechmann, H., Henze, M. (2000) 'Modelling and test of aeration tank settling (ATS)', *Water Science & Technology*, 41(9), 179–184.
- Nyberg, U., Andersson, B., Aspegren, H. (1996) 'Real time control for minimizing effluent concentrations during storm water events', *Water Science & Technology*, 34(3-4), 127–134.
- O'Brien, M., Mack, J., Lennox, B., Lovett, D., Wall, A. (2011) 'Model predictive control of an activated sludge process: A case study', *Control Engineering Practice*, 19(1), 54–61.
- Obropta, C.C., Kardos, J.S. (2007) 'Review of Urban Stormwater Quality Models: Deterministic, Stochastic, and Hybrid Approaches1', *JAWRA Journal of the American Water Resources Association*, 43(6), 1508–1523.
- Ocampo-Martinez, C. (2010) *Model Predictive Control of Wastewater Systems*, Springer Science & Business Media.
- Olsson, G. (2012) 'ICA and me – A subjective review', *Water Research*, 46(6), 1585–1624.

References

- Olsson, G., Jeppsson, U. (2006) 'Plant-wide control: dream, necessity or reality?', *Water Science & Technology*, 53(3), 121–129.
- Ostace, G.S., Cristea, V.M., Agachi, P.S. (2010) 'Investigation of different control strategies for the BSM1 waste water treatment plant with reactive secondary settler model', in *Proceedings 20th European Symposium on Computer Aided Process Engineering*, Ischia, 1841–1846.
- Ostace, G.S., Cristea, V.M., Agachi, P.S. (2011) 'Cost reduction of the wastewater treatment plant operation by MPC based on modified ASM1 with two-step nitrification/denitrification model', *Computers & Chemical Engineering*, 35(11), 2469–2479.
- Pai, T.Y., Shyu, G.S., Chen, L., Lo, H.M., Chang, D.H., Lai, W.J., Yang, P.Y., Chen, C.Y., Liao, Y.C., Tseng, S.C. (2013) 'Modelling transportation and transformation of nitrogen compounds at different influent concentrations in sewer pipe', *Applied Mathematical Modelling*, 37(3), 1553–1563.
- Paulsen, O. (1987) *Kontinuierliche Simulation von Abflüssen und Stofffrachten in der Trennwässerung*, PhD thesis, Universität Hannover.
- Petersen, B., Gernaey, K., Henze, M., Vanrolleghem, P.A. (2003) 'Calibration of activated sludge models: A critical review of experimental designs', *Biotechnology for the environment: Wastewater treatment and modeling, waste gas handling*, 101–186.
- Petruck, A., Holtmeier, E., Redder, A., Teichgräber, B. (2003) 'Real time control of a combined sewer system using radar-measured precipitation - results of the pilot study', *Water Science & Technology*, 47(7-8), 365–370.
- Phatak, A., De Jong, S. (1997) 'The geometry of partial least squares', *Journal of Chemometrics*, 11(4), 311–338.
- Pierson, S.T., Cabrera, M.L., Evanylo, G.K., Kuykendall, H.A., Hoveland, C.S., McCann, M.A., West, L.T. (2001) 'Phosphorus and Ammonium Concentrations in Surface Runoff from Grasslands Fertilized with Broiler Litter', *Journal of Environment Quality*, 30(5), 1784.
- Pires, O.C., Palma, C., Costa, J.C., Moita, I., Alves, M.M., Ferreira, E.C. (2006) 'Knowledge-based fuzzy system for diagnosis and control of an integrated biological wastewater treatment process', *Water Science & Technology*, 53(4-5), 313.
- Pleau, M., Colas, H., Lavallée, P., Pelletier, G., Bonin, R. (2005) 'Global optimal real-time control of the Quebec urban drainage system', *Environmental Modelling & Software*, 20(4), 401–413.
- Pleau, M., Pelletier, G., Colas, H., Lavalle, P., Bonin, R. (2001) 'Global predictive real-time control of Quebec Urban Community's westerly sewer network', *Water Science & Technology*, 43(7), 123–130.
- Plósz, B.G., De Clercq, J., Nopens, I., Benedetti, L., Vanrolleghem, P.A. (2011) 'Shall we upgrade one-dimensional secondary settler models used in WWTP simulators? – An assessment of model structure uncertainty and its propagation', *Water Science & Technology*, 63(8), 1726.
- Plósz, B.G., Weiss, M., Printemps, C., Essemiani, K., Meinhold, J. (2007) 'One-dimensional modelling of the secondary clarifier-factors affecting simulation in the clarification zone and the assessment of the thickening flow dependence', *Water Research*, 41(15), 3359–3371.
- Precup, R.-E., Hellendoorn, H. (2011) 'A survey on industrial applications of fuzzy control', *Computers in Industry*, 62(3), 213–226.
- Pujol, R., Lienard, A. (1990) 'Qualitative and Quantitative Characterization of Waste Water for Small Communities', *Water Science & Technology*, 22(3-4), 253–260.
- Rabitz, H., Aliş, Ö.F., Shorter, J., Shim, K. (1999) 'Efficient input–output model representations', *Computer Physics Communications*, 117(1–2), 11–20.
- Ráduly, B., Gernaey, K.V., Capodaglio, A.G., Mikkelsen, P.S., Henze, M. (2007) 'Artificial neural networks for rapid WWTP performance evaluation: Methodology and case study', *Environmental Modelling & Software*, 22(8), 1208–1216.

- Rammacher, J., Hansen, J. (2000) 'Control of nutrient removal based on simple measurement values', *Water Science & Technology*, 41(1), 29–32.
- Rao, S.S. (2009) *Engineering Optimization: Theory and Practice*, John Wiley & Sons.
- Rauch, W., Bertrand-Krajewski, J., Krebs, P., Mark, O., Schilling, W., Schütze, M., Vanrolleghem, P.A. (2002) 'Deterministic modelling of integrated urban drainage systems', *Water Science & Technology*, 45(3), 81–94.
- Rauch, W., Harremoës, P. (1996) 'The importance of the treatment plant performance during rain to acute water pollution', *Water Science & Technology*, 34(3-4), 1–8.
- Rauch, W., Harremoës, P. (1999) 'Genetic algorithms in real time control applied to minimize transient pollution from urban wastewater systems', *Water Research*, 33(5), 1265–1277.
- Rauch, W., Seggelke, K., Brown, R., Krebs, P. (2005) 'Integrated Approaches in Urban Storm Drainage: Where Do We Stand?', *Environmental Management*, 35(4), 396–409.
- Regneri, M., Klepiszewski, K., Seiffert, S., Vanrolleghem, P.A., Ostrowski, M. (2012) 'Transport sewer model calibration by experimental generation of discrete discharges from individual CSO structures', in *In: Proceedings of the International Environmental Modelling and Software Society (iEMSs 2012)*, Leipzig, Germany, 3109–3116, available: http://www.iemss.org/sites/iemss2012/proceedings/I5_0753_Regneri_et_al.pdf [accessed 25 May 2014].
- Reynoso-Meza, G., Blasco, X., Sanchis, J., Martínez, M. (2014) 'Controller tuning using evolutionary multi-objective optimisation: Current trends and applications', *Control Engineering Practice*, 28, 58–73.
- Ribeiro, R.A. (1996) 'Fuzzy multiple attribute decision making: A review and new preference elicitation techniques', *Fuzzy Sets and Systems, Fuzzy Multiple Criteria Decision Making*, 78(2), 155–181.
- Rieger, L., Gillot, S., Langergraber, G., Ohtsuki, T., Shaw, A., Takács, I., Winkler, S. (2013) *Guidelines for Using Activated Sludge Models*, IWA Publishing: London.
- Rieger, L., Koch, G., Kühni, M., Gujer, W., Siegrist, H. (2001) 'The eawag bio-p module for activated sludge model no. 3', *Water Research*, 35(16), 3887–3903.
- Rieger, L., Thomann, M., Joss, A., Gujer, W., Siegrist, H. (2004) 'Computer-aided monitoring and operation of continuous measuring devices', *Water Science & Technology*, 50(11), 31–39.
- Rios, L.M., Sahinidis, N.V. (2012) 'Derivative-free optimization: a review of algorithms and comparison of software implementations', *Journal of Global Optimization*, 56(3), 1247–1293.
- Rodríguez, J.P., McIntyre, N., Díaz-Granados, M., Achleitner, S., Hochedlinger, M., Maksimović, Č. (2013) 'Generating time-series of dry weather loads to sewers', *Environmental Modelling & Software*, 43, 133–143.
- Rommelfanger, H. (1994) *Fuzzy Decision Support-Systeme*, Springer DE.
- Rosen, C., Olsson, G. (1998) 'Disturbance detection in wastewater treatment plants', *Water Science & Technology*, 37(12), 197–205.
- Rossi, L., Krejci, V., Rauch, W., Kreikenbaum, S., Fankhauser, R., Gujer, W. (2005) 'Stochastic modeling of total suspended solids (TSS) in urban areas during rain events', *Water Research*, 39(17), 4188–4196.
- Ruano, M.V., Ribes, J., Sin, G., Seco, A., Ferrer, J. (2010) 'A systematic approach for fine-tuning of fuzzy controllers applied to WWTPs', *Environmental Modelling & Software*, 25(5), 670–676.
- Saagi, R., Flores, X., Fu, G., Benedetti, L., Gernaey, K.V., Jeppsson, U., Butler, D. (2014) 'Benchmarking dry weather integrated control strategies using an extended BSM2 platform', in *In: Proceedings 13th International Conference on Urban Drainage (ICUD2014)*, Kuching, Malaysia.

References

- Sasikumar, K., Mujumdar, P. (1998) 'Fuzzy Optimization Model for Water Quality Management of a River System', *Journal of Water Resources Planning and Management*, 124(2), 79–88.
- Schaarup-Jensen, K., Johansen, C., Thorndahl, S.L. (2005) 'Uncertainties related to extreme event statistics of sewer system surcharge and overflow', in *In: Proceedings 10th International Conference on Urban Drainage*, 1–8.
- Schellart, A.N.A., Shepherd, W.J., Saul, A.J. (2012) 'Influence of rainfall estimation error and spatial variability on sewer flow prediction at a small urban scale', *Advances in Water Resources*, 45, 65–75.
- Schilling, W., Andersson, B., Nyberg, U., Aspegren, H., Rauch, W., Harremoës, P. (1996) 'Real time control of wastewater systems', *Journal of Hydraulic Research*, 34(6), 785–797.
- Schmitt-Heidereich (1995) *Vorfluterbelastung aus städtischen Einzugsgebieten unter Berücksichtigung von Unsicherheiten*, PhD thesis, Universität Karlsruhe.
- Schütze, M., Butler, D., Beck, B.M. (2002) *Modelling Simulation and Control of Urban Wastewater Processes*, Springer.
- Schütze, M., Butler, D., Beck, M. (1999) 'Optimisation of control strategies for the urban wastewater system - an integrated approach', *Water Science & Technology*, 39(9), 209–216.
- Schütze, M., Campisano, A., Colas, H., Schilling, W., Vanrolleghem, P.A. (2004) 'Real time control of urban wastewater systems—where do we stand today?', *Journal of Hydrology*, 299(3–4), 335–348.
- Schütze, M., Erbe, V., Haas, U., Scheer, M., Weyand, M. (2008) 'Sewer system real-time control supported by the M180 guideline document', *Urban Water Journal*, 5(1), 69–78.
- Schütze, M., Reussner, F., Alex, J. (2011) 'SWQM-A simple river water quality model for assessment of urban wastewater discharges', in *In: Proceedings 11th International Conference on Urban Drainage (11ICUD)*, 11–15.
- Seggelke, K., Fuchs, L., Tränckner, J., Krebs, P. (2008) 'Development of an integrated RTC system for full-scale implementation', in *Proceedings 11th International Conference on Urban Drainage*, Edinburgh, Scotland, UK.
- Seggelke, K., Löwe, R., Beeneken, T., Fuchs, L. (2013) 'Implementation of an integrated real-time control system of sewer system and waste water treatment plant in the city of Wilhelmshaven', *Urban Water Journal*, 10(5), 330–341.
- Seggelke, K., Rosenwinkel, K., Vanrolleghem, P.A., Krebs, P. (2005) 'Integrated operation of sewer system and WWTP by simulation-based control of the WWTP inflow', *Water Science & Technology*, 52(5), 195–203.
- Shen, W., Chen, X., Corriou, J.P. (2008) 'Application of model predictive control to the BSM1 benchmark of wastewater treatment process', *Computers & Chemical Engineering*, 32(12), 2849–2856.
- Shen, W., Chen, X., Pons, M.N., Corriou, J.P. (2009) 'Model predictive control for wastewater treatment process with feedforward compensation', *Chemical Engineering Journal*, 155(1–2), 161–174.
- Smets, I.Y., Haegebaert, J.V., Carrette, R., Van Impe, J.F. (2003) 'Linearization of the activated sludge model ASM1 for fast and reliable predictions', *Water Research*, 37(8), 1831–1851.
- Solvi, A., Benedetti, L., Gillé, S., Schosseler, P., Weidenhaupt, A., Vanrolleghem, P.A. (2005) 'Integrated urban catchment modelling for a sewer-treatment-river system', in *Proceedings 10th International Conference on Urban Drainage*, Copenhagen, Denmark.
- Soonthornnonda, P., Christensen, E.R. (2008) 'Source apportionment of pollutants and flows of combined sewer wastewater', *Water Research*, 42(8–9), 1989–1998.
- Sousa, J.M.C., Kaymak, U. (2002) *Fuzzy Decision Making in Modeling and Control*, World Scientific.

- Stamou, A.I., Giokas, D.L., Kim, Y., Paraskevas, P.A. (2008) 'Validation and application of a simple model for circular secondary settling tanks', *GLOBAL NEST JOURNAL*, 10(1), 62–72.
- Stare, A., Vrečko, D., Hvala, N., Strmčnik, S. (2007) 'Comparison of control strategies for nitrogen removal in an activated sludge process in terms of operating costs: A simulation study', *Water Research*, 41(9), 2004–2014.
- Suárez, J., Puertas, J. (2005) 'Determination of COD, BOD, and suspended solids loads during combined sewer overflow (CSO) events in some combined catchments in Spain', *Ecological Engineering*, 24(3), 199–217.
- Sztruhár, D., Sokáč, M., Holienčin, A., Markovič, A. (2002) 'Comprehensive assessment of combined sewer overflows in Slovakia', *Urban Water*, 4(3), 237–243.
- Takács, I., Patry, G.G., Nolasco, D. (1991) 'A dynamic model of the clarification-thickening process', *Water Research*, 25(10), 1263–1271.
- Tamaki, R.D. (1994) *Real-Time Fuzzy Logic Control of Combined Sewer Flows*, Master thesis.
- Tamura, H. (1990) *Large-Scale Systems Control and Decision Making*, CRC Press.
- Tchobanoglous, G., Burton, F.L., Stensel, H.D. (2004) *Wastewater Engineering: Treatment and Reuse*, McGraw-Hill Education.
- Thiessen, A.H. (1911) 'Precipitation Averages for Large Areas', *Monthly Weather Review*, 39(7), 1082–1089.
- Tomita, R.K., Park, S.W., Sotomayor, O.A.Z. (2002) 'Analysis of activated sludge process using multivariate statistical tools—a PCA approach', *Chemical Engineering Journal*, 90(3), 283–290.
- Tong, R.M., Beck, M.B., Latten, A. (1980) 'Fuzzy control of the activated sludge wastewater treatment process', *Automatica*, 16(6), 695–701.
- Tränckner, J., Franz, T., Seggelke, K., Krebs, P. (2007a) 'Dynamic optimisation of WWTP inflow to reduce total emission', *Water Science & Technology*, 56(10), 11–18.
- Tränckner, J., Franz, T., Seggelke, K., Krebs, P. (2007b) 'Integrated control of sewer and WWTP based on the assessment of treatment capacity', in *Proceedings NOVATECH 2007 - 6th International Conference on Sustainable Techniques and Strategies in Urban Water Management*, Lyon, France.
- Traoré, A., Grieu, S., Thiery, F., Polit, M., Colprim, J. (2006) 'Control of sludge height in a secondary settler using fuzzy algorithms', *Computers & Chemical Engineering*, 30(8), 1235–1242.
- Trivedi, H.K. (2009) 'Simultaneous Nitrification and Denitrification (SymBio® Process)', in DEE, L.K.W., PE, Shammas, N.K. and DEE, Y.-T.H., PE, eds., *Advanced Biological Treatment Processes*, Handbook of Environmental Engineering, Humana Press, 185–208.
- Tsai, Y.P., Ouyang, C.F., Chiang, W.L., Wu, M.Y. (1994) 'Construction of an on-line fuzzy controller for the dynamic activated sludge process', *Water Research*, 28(4), 913–921.
- Vaes, G., Willems, P., Berlamont, J. (2005) 'Areal rainfall correction coefficients for small urban catchments', *Atmospheric Research, Precipitation in Urban Areas 6th International Workshop on Precipitation in Urban Areas*, 77(1–4), 48–59.
- Valeo, C., Ho, C.L.I. (2004) 'Modelling urban snowmelt runoff', *Journal of Hydrology, Urban Hydrology*, 299(3–4), 237–251.
- Vallerio, M., Van Impe, J., Logist, F. (2014) 'Tuning of NMPC controllers via multi-objective optimisation', *Computers & Chemical Engineering*, 61, 38–50.
- Vanhooren, H., Meirlaen, J., Amerlinck, Y., Claeys, F., Vangheluwe, H., Vanrolleghem, P.A. (2003) 'WEST: Modelling biological wastewater treatment', *Journal of Hydroinformatics*, 5(1), 27–50.
- Vanrolleghem, P.A. (1995) 'Model-based control of wastewater treatment plants', in *Proceedings ESF Workshop Integrated Environmental Bioprocess Design*, Obernai, France.

References

- Vanrolleghem, P.A., Fronteau, C., Bauwens, W. (1996) 'Evaluation of design and operation of the sewage transport and treatment system by an EQO/EQS based analysis of the receiving water immission characteristics', in *Proceedings WEF Specialty Conference on Urban Wet Weather Pollution: Controlling Sewer Overflows and Stormwater Runoff*, 14–46.
- Vanrolleghem, P.A., Gillot, S. (2002) 'Robustness and economic measures as control benchmark performance criteria', *Water Science & Technology*, 45(4-5), 117–126.
- Vanrolleghem, P.A., Jeppsson, U., Carstensen, J., Carlsson, B., Olsson, G. (1996) 'Integration of wastewater treatment plant design and operation—a systematic approach using cost functions', *Water Science & Technology*, 34(3), 159–171.
- Vanrolleghem, P.A., Rosén, C., Zaher, U., Copp, J., Benedetti, L., Ayesa, E., Jeppsson, U. (2005) 'Continuity-based interfacing of models for wastewater systems described by Petersen matrices', *Water Science & Technology*, 52(1), 493–500.
- Vanrolleghem, P.A., Schilling, W., Rauch, W., Krebs, P., Alderink, H. (1999) 'Setting up measuring campaigns for integrated wastewater modelling', *Water science and technology*, 39(4), 257–268.
- Vega, P., Revollar, S., Francisco, M., Martín, J.M. (2014) 'Integration of set point optimization techniques into nonlinear MPC for improving the operation of WWTPs', *Computers & Chemical Engineering*, 68, 78–95.
- Venkatasubramanian, V., Rengaswamy, R., Yin, K., Kavuri, S.N. (2003) 'A review of process fault detection and diagnosis: Part I: Quantitative model-based methods', *Computers & chemical engineering*, 27(3), 293–311.
- Wagener, T., McIntyre, N., Lees, M.J., Wheater, H.S., Gupta, H.V. (2003) 'Towards reduced uncertainty in conceptual rainfall-runoff modelling: dynamic identifiability analysis', *Hydrological Processes*, 17(2), 455–476.
- Wahab, N.A., Katebi, R., Balderud, J. (2009) 'Multivariable PID control design for activated sludge process with nitrification and denitrification', *Biochemical Engineering Journal*, 45(3), 239–248.
- Watts, R., Svoronos, S., Koopman, B. (1996) 'One-Dimensional Clarifier Model with Sludge Blanket Heights', *Journal of Environmental Engineering*, 122(12), 1094–1100.
- Weijers, S.R. (2000) *Modelling, Identification and Control of Activated Sludge Plants for Nitrogen Removal*, PhD thesis, Technische Universiteit Eindhoven.
- Weinreich, G., Schilling, W., Birkely, A., Moland, T. (1997) 'Pollution based real time control strategies for combined sewer systems', *Water Science & Technology*, 36(8-9), 331–336.
- Weiß, G., Brombach, H., Haller, B. (2002) 'Infiltration and inflow in combined sewer systems: long-term analysis', *Water Science & Technology*, 45(7), 11–19.
- Van Wensen, J. (2001) *Hydrologische Gesamtbetrachtung eines Entwässerungssystems*, Prof. Dr.-Ing. F. Sieker: Hannover.
- Wetter, M., Wright, J. (2004) 'A comparison of deterministic and probabilistic optimization algorithms for nonsmooth simulation-based optimization', *Building and Environment*, 39(8), 989–999.
- Wiese, J., Simon, J., Schmitt, T.G. (2005) 'Integrated real-time control for a sequencing batch reactor plant and a combined sewer system', *Water Science & Technology*, 52(5), 179–186.
- Willems, P. (2008) 'Quantification and relative comparison of different types of uncertainties in sewer water quality modeling', *Water Research*, 42(13), 3539–3551.
- Wilson, J.D., Sawford, B.L. (1996) 'Review of Lagrangian stochastic models for trajectories in the turbulent atmosphere', *Boundary-layer meteorology*, 78(1-2), 191–210.
- Xi, Y.-G., Li, D.-W., Lin, S. (2013) 'Model Predictive Control — Status and Challenges', *Acta Automatica Sinica*, 39(3), 222–236.
- Yan, H., Luh, P.B. (1997) 'A fuzzy optimization-based method for integrated power system scheduling and inter-utility power transaction with uncertainties', *IEEE Transactions on Power Systems*, 12(2), 756–763.

- Yoo, C.K., Vanrolleghem, P.A., Lee, I.-B. (2003) 'Nonlinear modeling and adaptive monitoring with fuzzy and multivariate statistical methods in biological wastewater treatment plants', *Journal of Biotechnology*, 105(1–2), 135–163.
- Zacharof, A.I., Butler, D., Schütze, M., Beck, M.B. (2004) 'Screening for real-time control potential of urban wastewater systems', *Journal of Hydrology*, 299(3–4), 349–362.
- Zadeh, L.A. (1965) 'Fuzzy sets', *Information and control*, 8(3), 338–353.
- Zahraei, A., Hsu, K., Sorooshian, S., Gourley, J.J., Lakshmanan, V., Hong, Y., Bellerby, T. (2012) 'Quantitative Precipitation Nowcasting: A Lagrangian Pixel-Based Approach', *Atmospheric Research*, 118, 418–434.
- Zamora, C., Giraldo, J.M., Leirens, S. (2010) 'Model predictive control of water transportation networks', in *2010 IEEE ANDESCON*, Presented at the 2010 IEEE ANDESCON, 1–6.
- Zawilski, M., Brzezińska, A. (2009) 'Variability of COD and TKN fractions of combined wastewater', *Polish Journal of Environmental Studies*, 18(3), 501–505.
- Zhang, Y., Huang, W.D., Gou, Q.Z., Wang, G., Xie, R.H. (2009) 'Application of computational fluid dynamics in design of oxidation ditch', *Industrial Water & Wastewater*, 40(1), 49–53.
- Zhang, Z. (2007) 'Estimating Rain Derived Inflow and Infiltration for Rainfalls of Varying Characteristics', *Journal of Hydraulic Engineering*, 133(1), 98–105.
- Zhu, G., Peng, Y., Ma, B., Wang, Y., Yin, C. (2009) 'Optimization of anoxic/oxic step feeding activated sludge process with fuzzy control model for improving nitrogen removal', *Chemical Engineering Journal*, 151(1–3), 195–201.
- Zhu, G.-Y., Henson, M.A., Ogunnaike, B.A. (2000) 'A hybrid model predictive control strategy for nonlinear plant-wide control', *Journal of Process Control*, 10(5), 449–458.
- Zierolf, M.L., Polycarpou, M.M., Uber, J.G. (1998) 'Development and autocalibration of an input-output model of chlorine transport in drinking water distribution systems', *IEEE Transactions on Control Systems Technology*, 6(4), 543–553.
- Zimmermann, H.-J. (2001) *Fuzzy Set Theory-And Its Applications*, Springer.
- Zopounidis, C., Doumpos, M. (2002) 'Multicriteria classification and sorting methods: A literature review', *European Journal of Operational Research*, 138(2), 229–246.
- Zoppou, C. (2001) 'Review of urban storm water models', *Environmental Modelling & Software*, 16(3), 195–231.